School of Electrical Engineering and Computer Science
Faculty of Science and Engineering
Queensland University of Technology

Channel Tracking in SDMA-Based Multi-User MIMO-OFDM Communications Systems

Lakmali Nadisha Atapattu

Bachelor of Science (Computer Engineering) (Hons.)
(University of Peradeniya) – 2008

Thesis submitted in accordance with the regulations for the Degree of Doctor of Philosophy in the Faculty of Science and Engineering, Queensland University of Technology according to QUT requirements.

December, 2013
Principal Supervisor: Dr. Karla Ziri-Castro
Associate Supervisor: Dr. Dhammika Jayalath
Associate Supervisor: Dr. Hajime Suzuki (CSIRO)

Declaration

The work contained in this thesis has not been previously submitted for a degree or diploma at any higher education institution. To the best of my knowledge and belief, the thesis contains no material previously published or written by another person except where explicitly stated otherwise and due reference is made.

Signed: QUT Verified Signature **Date:** 03-12-2013

Copyright in Relation to This Thesis

[1] lakmali@qut.edu.au
[2] www.qut.edu.au

Abstract

Multiple-input multiple-output (MIMO) and orthogonal frequency division multiplexing (OFDM) stand as promising technologies to resolve bottlenecks in the traffic capacity of current and future high data rate wireless systems such as long-term evolution (LTE), Wi-Fi, and worldwide interoperability for microwave access (WiMAX). Recently, the expansion of MIMO systems to employ multiple users (multi-user MIMO) has been a key topic of interest, mainly motivated by the need to recognise the network capacity enhancements resulting from the use of MIMO technology. In Australia, the Commonwealth Scientific and Industrial Research Organisation (CSIRO) has proposed and implemented a novel and feasible system called the "Ngara wireless broadband access" system using space division multiple access (SDMA) to allow multiple users to employ the same frequency at the same time in MIMO-OFDM systems. In SDMA-based multi-user MIMO-OFDM, wireless broadband services with higher spectral efficiency can be enabled by employing multiple antennas at an access point to serve each mobile stations equipped with a single antenna.

Over the last fifteen years, multi-user MIMO-OFDM wireless communications have been the subject of extensive interest from both the academic and industrial communities. However, a realistic multi-user MIMO-OFDM transceiver design, with the ability to achieve channel capacity boundaries in practical channel conditions remains a primary problem. Specifically, the performance of multi-user MIMO-OFDM depends heavily on the accuracy of the estimation of channel state information (CSI) which is defined by the propagation environment of wireless systems. Practically, wireless channels experience multi-path propagation and time-variations which should be tracked recursively to accurately detect transmitted data at the receiver. Typically, CSI can be estimated by sending known symbols. However, this increases overheads if the channel changes significantly over time. Therefore, the design and implementation of an efficient SDMA-based multi-user MIMO-OFDM system still faces major challenges, in particular, the development of an efficient and accurate channel tracking method. Moreover, channel compensation has been identified as a key issue from the beginning of wireless communications, and the latest growth in this dominion has made the old issue more challenging. The exploitation of an equalizer which can track the changing channel with increased accuracy with the introduction of SDMA-based multi-user, multiple-antenna systems with OFDM transmission is more demanding.

To optimise the performance and ensure adequate planning of this point-to-multipoint wireless communication technology, this research has developed a novel, efficient and accurate algorithm for tracking CSI. A methodical approach has been used to derive an accurate channel tracking algorithm. The tracked channel estimation provides a significantly lower error vector magnitude (EVM) when used in SDMA-based multi-user MIMO-OFDM systems. For example, the EVM for the proposed novel method is up to 79% lower than for a training-based channel estimation method using a single training sequence. Therefore, the novel channel tracking method offers a significant advantage of using a reduced amount of frequency bandwidth when compared to the training-based channel estimation method. The results are shown for the improved performance of the channel tracking mechanism when the maximum Doppler frequency is less than 30 Hz and SNR is greater than 13 dB. There is an added cost of computational complexity. However, with the recent advancement in signal processing hardware makes the proposed methods practical. Moreover, the proposed method shows lower EVM values for lower maximum Doppler shifts (f_d). For example, when f_d is less than 30Hz, the EVM approximately remains under 0.2. Since the proposed method uses hard-decisions, the noise can be efficiently removed from the tracked channel estimation. This shows the significance of the proposed novel channel tracking method in SDMA-based multi-user MIMO-OFDM systems, offering a more efficient use of frequency bandwidth and performing accurate channel tracking for time-varying, frequency selective, multi-user, multi-path, MIMO channels.

The research has led to various publications to date, namely:

Journal publications

1. Atapattu, Lakmali, Ziri-Castro, Karla, Suzuki, Hajime, and Jayalath, Dhammika (2013) "Efficient Channel Tracking Algorithms in SDMA-Based Multi-User MIMO-OFDM Systems", IEEE Transaction on Wireless Communications. Submitted (Covered in Chapters 4 and 6)

2. Atapattu, Lakmali and Ziri-Castro, Karla (2013), "Effective Adaptive Equalization for SDMA-based Multi-User MIMO-OFDM Systems in Frequency Selective Channels", EURASIP Journal on Wireless Communications and Networking. Submitted (Covered in Chapter 5)

3. Atapattu, Lakmali and Ziri-Castro, Karla (2013), "Effective Channel Estimation in Multi-User MIMO-OFDM systems", European Journal on Scientific Research. Submitted (Covered in Chapter 4)

4. Atapattu, Lakmali and Ziri-Castro, Karla (2013), "Adaptive Equalization, Channel Estimation and Channel Tracking", European Journal on Scientific Research. Submitted (Covered in Chapter 3)

Conference publications

5. Atapattu, Lakmali, Munasinghe, Gayan, Ziri-Castro, Karla, Suzuki, Hajime and Jayalath, Dhammika (2012), "Linear adaptive equalization in multiuser MIMO-OFDM systems". In: Australasian Telecommunication Networks and Applications Conference (ATNAC), $7-9$ November 2012, Brisbane, Australia. (Covered in Chapter 5)

6. Ratnayake, Nisal Lahiru, Atapattu, Lakmali, Ziri-Castro, Karla and Jayalath, Dhammika (2010), "Efficient wireless broadband communications for rural area". In: 9^{th} Annual Symposium on Electromagnetic Compatibility (EMC), $8-10$ September 2010, Novotel St Kilda, Melbourne, Victoria. **This paper won the "Best Student Paper" award**. (Covered in Chapters 2)

Peer reviewed conference paper abstracts

7. Atapattu, Lakmali (2013), "A novel channel tracking and equalization methods in MU-MIMO-OFDM systems". In: IEEE International Symposium on a World of Wireless, Mobile and Multimedia Networks (WoWMoM 2013), $4-7$ June 2010, Madrid, Spain. (Covered in Chapters 4 and 6)

8. Atapattu, Lakmali Nadisha Kumari (2010), "Channel tracking algorithms for highly efficient wireless broadband communications in rural areas". In: IEEE International Symposium on a World of Wireless, Mobile and Multimedia Networks (WoWMoM 2010), $14-17$ June 2010, Montreal, QC, Canada. (Covered in Chapter 4)

Acknowledgements

This work evolved during my time as a PhD candidate at the Queensland University of Technology (QUT), Australia. I have received an immense amount of support from various people and organisations. First and foremost, I wish to express my earnest gratitude to my principal supervisor, Dr. Karla Ziri-Castro and my associate supervisor from the CSIRO, Dr. Hajime Suzuki, for offering me this precious opportunity, excellent guidance, great support and technical contributions in order for me to conduct my research. Without their indispensable assistance, the completion of this thesis would not have been possible. Also, I would like to express my sincere gratitude to my QUT associate supervisor, Dr. Dhammika Jayalath, for his unprecedented support and priceless advice given to me during my PhD journey. The time spent working with my supervisors has greatly shaped my professional identity and effectively made me the researcher I am today. For this I will always be grateful to them.

I gratefully acknowledge the CSIRO Ngara wireless broadband project team for making this research a reality. My heartfelt thanks goes to the QUT high performance computing (HPC) group for their support related to HPC operations. I also express my sincere thanks to the staff members of the QUT Science and Engineering Faculty research office of QUT, including Ms. Diane Kolomeitz and Ms. Elaine Reyes, for their support in creating a productive research environment.

I appreciatively acknowledge the financial support offered by the Queensland Government under the Smart Future Fellowship scheme by providing a fee-waiver scholarship and living allowance scholarship to carry out this research and the travelling expenses in relation to national and international conferences. I would also like to thank all academic and non-academic staff for the support given to me in a countless number of ways.

In closing, I would like to thank my parents for supporting and encouraging me in every possible way to achieve my goal.

Acronyms & Abbreviations

In alphabetical order,

ADC	analog-to-digital converter
AE	adaptive equalization
AP	access point
AWGN	additive white Gaussian noise
BC	broadcast channel
BER	bit error rate
BPSK	binary phase shift keying
BRAN	broadband radio access network
CDMA	code division multiple access
CIR	channel impulse response
CFR	channel frequency response
CP	cyclic prefix
CSI	channel state information
CSIRO	commonwealth scientific and industrial research organisation
DAB	digital audio broadcasting
DDCE	decision directed channel estimation
DFE	decision feedback equalizer
DVB	digital video broadcasting
EVM	error vector magnitude
FDM	frequency division multiplexing
FFT	fast Fourier transform
ICI	inter-carrier interference
IF	intermediate frequency
IFFT	inverse fast Fourier transform
ISI	inter-symbol interference
LDPC	low density parity check
LMS	least mean square
LoS	line-of-sight
LS	least squares
LTE	long term evolution
MAC	multiple access channel
MAI	multiple access interference

MIMO	multiple-input multiple-output
MLE	maximum likelihood estimator
MSE	mean squared error
MMSE	minimum mean square error
MS	mobile station
MU-MIMO	multi-user-MIMO
OFDM	orthogonal frequency division multiplexing
OFDMA	orthogonal frequency division multiple access
PDF	probability density function
PSK	phase-shift keying
PS	parallel-to-serial
PSA	pilot symbol aided
QAM	quadrature amplitude modulation
QPSK	quadrature phase-shift keying
RF	radio frequency
RLS	recursive least squares
RMS	root mean square
SEP	symbol error probability
SER	symbol error rate
SISO	single-input single-output
SDM	spatial division multiplexing
SDMA	space division multiple access
SEP	symbol error probability
SM	spatial multiplexing
SNR	signal-to-noise ratio
SP	serial-to-parallel
ST	space-time
STBC	space-time block coding
STS	space-time spreading
STTC	space-time trellis coding
Wi-Max	worldwide interoperability for microwave access
WLAN	wireless local area network
WMAN	wireless metropolitan area network
WRAN	wireless regional area network
ZF	zero-forcing

Variables & Notation

τ	excess delay
c	speed of light
cp	length of cyclic prefix
m	m^{th} mobile station
r	r^{th} receiver at the Access Point
f_d	maximum Doppler shift
q	order of feedback filter
u	discrete time instant
$\mathbf{H}$	channel matrix
$\mathbf{H_0}$	training-based initial channel estimation
$\hat{\mathbf{H}}$	tracked channel estimation
K	Rician K-factor
L	number of multi-paths
M	number of mobile stations
N	number of subcarriers, point FFT/IFFT
O	modulation order
P	order of the equalizer
Q	number of symbols in a group for tracking
R	number of receiver antennas at the Access Point
U	number of OFDM symbols
$\mathbf{x}$	transmitted signal vector
$\mathbf{y}$	received signal vector
$\mathbf{z}$	AWGN noise vector
μ	step size of LMS
λ	forgetting factor of RLS
ξ	MSE
$\mathbb{C}$	set of complex numbers
$\mathbb{E}[\cdot]$	mathematical expectation
$F(\cdot)$	Fourier transform
δ	Kronecker function
$\mathbf{H}^H$	Hermitian transpose of H
$\mathbf{A}^T$	transpose of A
a^*	complex conjugate of a

$\otimes$	convolutional operation
T_s	Symbol period

Content

List of Figures

List of Tables

Chapter 1

Introduction

1.1 Introduction

High-speed broadband Internet access is widely recognised as a catalyst to economic growth and social equity in Australia and around the world. The Australian Government has therefore commenced the construction of the National Broadband Network (NBN) to deliver the best and most cost effective infrastructure across Australia [10]. However, rural Australia's inherent dispersed population over a large geographical area makes delivery of efficient, well-maintained and cost-effective Internet access a challenging task. Therefore, the Commonwealth Scientific and Industrial Research Organisation (CSIRO) has proposed and implemented a novel and feasible system called the "Ngara wireless broadband access" system, which is an efficient multi-user single-antenna multiple-input multiple-output (MUSA-MIMO) wireless communications technology as a practical solution to provide cheaper and faster Internet services to rural areas in a spectrally efficient and cost-effective manner [11].

The advancement of multicarrier orthogonal frequency division multiplexing (OFDM) [12] technology with multiple-input multiple-output (MIMO) MIMO) [13] systems stand as promising technologies to address bottlenecks in the traffic capacity of current and future high data rate wireless communications systems like long-term evolution (LTE), Wi-Fi, and worldwide interoperability for microwave access (WiMAX) [14]. MIMO systems use multiple antennas at both the transmitter and receiver to create additional sub-channels in the spatial domain. Parallel channels are established over the same time and frequency. Therefore, higher capacity and reliability can be achieved without the need for increased transmission power or additional bandwidth [6]. OFDM converts a frequency selective channel into a parallel set of frequency flat channels by splitting the available spectrum into a number of overlapping but orthogonal narrowband subcarriers. Furthermore, it alleviates the inter-symbol interference (ISI) caused by multi-paths and offers comparatively

simpler implementations [15]. Overall, these performance strengthening advantages have made the combination of MIMO-OFDM the favoured method for several high data rate wireless technologies [14].

Recently, the extension of MIMO systems to accommodate multiple users (multi-user MIMO) has been a major matter of interest. It is mainly motivated by the necessity to identify the network capacity improvements resulting from the employment of MIMO arrangements. In multi-user MIMO-OFDM, wireless broadband services with higher spectral efficiency can be enabled by employing multiple antennas at an access point (AP) to serve mobile stations (MS) equipped with a single antenna or multiple antennas.

Standardised wireless local loop (WLL), wireless local area network (WLAN), wireless metropolitan area network (WMAN), and more recently wireless regional area network (WRAN) technologies have been considered to provide terrestrial fixed wireless multiple access for rural areas. However, these standard technologies achieve a spectrum efficiency of less than 6 bits/s/Hz/cell [16]. Therefore, to simultaneously serve every user in a cell with high data rates, either a wide frequency spectrum or an excess of access points would be required. Therefore, the CSIRO has proposed and implemented a novel and feasible system called the "Ngara wireless broadband access" system [17].

This system uses point-to-multi-point wireless communications technology with multiple users (multi-user MIMO) and has been implemented using OFDM. This system employs the space division multiple access (SDMA) technique to allow users to employ the same frequency at the same time. With this system, the AP is equipped with multiple antennas to serve sparsely distributed user terminals with a single antenna using the same bandwidth. This approach facilitates the allocation of a wide frequency bandwidth for each user, thus giving them access to faster data rates [18]. However, this novel system did not have a proper channel tracking algorithm. Therefore, our research aimed to develop a novel channel tracking algorithm that suit this novel system. Moreover, we received financial support from the Queensland Government under the Smart Future Fellowship Scheme to conduct this research. The present research is based on this Ngara wireless broadband access system and focuses on the case of six users with a 12 AP antenna system, as implemented in [19]. However, the proposed methods are applicable to a larger number of users and antennas.

The multiple paths in a channel represent the effect of multiple wavefronts. The channel is said to be time-varying, when the transmitter or the receiver is mobile or the channel is rapidly changing due to environmental conditions. Identifying the information about the channel is important in order to recover the transmitted

signal at the receiver under these channel conditions. This phenomenon is referred to as *channel estimation*. The removal of channel effects is referred to as *equalization*. Channel tracking performs an important task to track a time-varying channel even after the initial channel estimation. The motivation of the study presented in this thesis is to develop channel tracking algorithm that can suit the novel SDMA based multi-user MIMO-OFDM communication system developed by CSIRO. The next section presents an outline of the motivation of the thesis.

1.1.1 Motivation for the thesis

Multi-user MIMO-OFDM wireless communications have received immense interest from both the academic and industrial communities over the last fifteen years as shown in literature review in Chapter 2. However, the ability to attain channel capacity boundaries in realistic channel conditions remains a primary problem with realistic multi-user MIMO-OFDM transceiver designs. Channel state information (CSI) characterises the propagation environment of wireless systems [20]. The accuracy of the estimation of CSI is critical for the performance of multi-user MIMO-OFDM systems [21]. Typically, the estimation of CSI can be performed by transmitting known symbols [22]. However, this method adds overheads to the system if the channel changes drastically over time. Therefore, the design and implementation of the CSIRO's SDMA-based multi-user MIMO-OFDM system still faces key demands, particularly, the development of an efficient and accurate channel tracking algorithm. Moreover, the latest growth in multi-user wireless communications demands channel compensation [23]. The development of an adaptive equalizer which can compensate the channel impairments caused by multi-path propagation and time-variations in the channel with increased accuracy for the introduction of the SDMA-based multi-user MIMO-OFDM system is challenging.

1.1.2 Why does a channel need to be estimated and tracked?

In order to accomplish the maximum capacity and diversity gain in MIMO channels, optimisation difficulties such as power, rate adaptation, code design, joint detection, channel estimation and channel tracking should be addressed [24]. Those optimisation difficulties depend on the structure of the system. Therefore, channel estimation and tracking are significant for the implementation and design of reliable wireless communications. It is also independent of the other above mentioned problems and is a prerequisite to the implementation of solutions to the previously cited problems such as power, rate adaptation, code design and joint detection [24].

MIMO-OFDM communications systems need the knowledge of the CSI in order

to detect the transmitted symbols at the receiver [25]. In reality, temporal variations in the communications systems such as movement between transmitter and receiver cause rapid changes in the channel and multi-path propagation cause frequency selectivity in the channel. These effects in the propagation path exhibit a time-varying and frequency selective channel matrix. Therefore, the coefficients of the channel matrix have to be known at each time instance, if the channel changes, in order to detect the transmitted signals at the receiver. These coefficients are obtained by employing a suitable channel estimation scheme. The channel is estimated at the transmitter (by channel reciprocity or channel feedback, or other prediction methods) or at the receiver. In most two-way communications systems, the receiver will estimate the channel condition. A data block is transmitted and reconstructed at the receiver based on the channel estimated at the receiver. Moreover, the time-variations change the channel coefficients even after the initial estimation so, the time variation of the MIMO channel must be taken into account. Therefore, a channel tracking algorithm is essential to recursively update the estimated state of the channel.

The channel tracking methods are required to accurately estimate the channel so that the transmitter can communicate with the reciever to use CSI in order to improve the data rate. The receiver will negotiate with the transmitter about whether to decrease or increase the size of the constellation depending on the condition of the channel. If the channel is very noisy, the receiver will negotiate with the transmitter to decrease the size of the constellation so that the symbol error rate will still be satisfactory. If the channel is not noisy, then the receiver will negotiate with the transmitter to increase the size of the constellation and therefore the data rate can be improved for a less noisy channel.

The system's knowledge pertaining to the channel conditions encountered is crucial for achieving high capacity and the realisable integrity of communication systems [26]. Therefore, the provision of an accurate and efficient channel tracking approach is a critical feature in accomplishing high performance wireless systems. The need of equalization in OFDM dictates the need of channel tracking in time-varying channels.

Therefore, to optimise the performance and ensure adequate planning of this novel multi-user MIMO-OFDM wireless communications system, an accurate channel tracking algorithm needs to recursively track the state of the channel and obtain the CSI. Specifically, the main research questions that motivated this research are:

1. How can a time-varying channel model for an SDMA-based multi-user MIMO-OFDM system be created for the purpose of evaluating the proposed channel tracking algorithms?

2. How can the CSI for an SDMA-based time-varying multi-user MIMO-OFDM system be obtained?

3. How can SDMA-based multi-user MIMO-OFDM channels be adaptively equalized?

4. How can the SDMA-based multi-user MIMO-OFDM channel be recursively tracked?

5. How can the effect of time-variations in terms of error vector magnitude (EVM) be measured?

Therefore, the study presented in this thesis aimed to answer these research questions.

1.2 Objectives

To further improve the performance of the CSIRO MUSA-MIMO system, an algorithm that can track time-varying, frequency selective, multi-user, MIMO channels is required. Therefore, the research presented in this thesis arose the following objectives in order to detect the transmitted data at the receiver:

1. To create a time-varying channel model for SDMA-based multi-user MIMO-OFDM systems for characterising the time-varying, frequency selective channels for the purpose of evaluating the proposed channel tracking algorithms.

2. To obtain the time-varying, frequency selective CSI at the receiver for SDMA-based multi-user MIMO-OFDM systems.

3. To adaptively equalize SDMA-based time-varying, frequency selective, multi-user MIMO channels.

4. To recursively track the time-varying, frequency selective, multi-user MIMO channels.

5. To measure the effect of proposed channel tracking method in terms of the error vector magnitude (EVM) between the recovered symbols and the transmitted symbols.

1.3 Significance of the research

The proposed channel tracking method performs accurately by recursively estimating the time-varying, frequency selective, multi-user, MIMO channel with 79% lower EVM than for the training-based channel estimation method. Moreover, this method is a simple method that is developed to suit the design of the unique system developed by the CSIRO.

To the best of the author's knowledge, many of the channel estimation and tracking methods for multi-user MIMO found in the literature depend on the number of users. For example, when the number of users was increased, the performance of the methods were degraded [27, 28]. These methods perform well only when the number of users is limited. However, in realistic wireless communications systems, we cannot expect to limit the number of MSs in the system. The tracking method proposed can be extendable up to any number of users and we show the results for six as an example.

Most conventional channel estimation and tracking methods use more than 20% of the duration of OFDM transmission to send training sequences. For example, [27,28] incorporated 12 out of 60 symbols and 16 or 32 as training sequences in their channel estimation methods. However, the tracking method proposed in this thesis performed accurately with only one OFDM symbol per transmitter as the pilot sequence, saving valuable bandwidth in the system. Moreover, the training symbol incorporated in our method provides a full description of frequency selectivity characteristics in the channel.

Many adaptive equalization techniques [29] in the literature perform well only for a 2×2 MIMO system limiting the number of antennas, while our methods show performance for a 12×6 SDMA-based multi-user MIMO-OFDM system. Moreover, with the method presented in [29], the symbol error rate (SER) reached 10^{-3} only when the signal-to-noise ratio (SNR) is equal to 40 dB, while the adaptive equalization method proposed in the present research reached the same value of bit error rate (BER), when the SNR equals to 12 with a decision feedback equalizer (DFE). Therefore, the method proposed in this study performed well at low SNR values.

1.4 Contributions of the research

The main contributions of this thesis are as follows:

- The application of linear and DFE adaptive equalization methods that can compensate channel impairments like ISI and frequency selectivity effects in

SDMA-based multi-user MIMO-OFDM systems.
The proposed methods are combined with least mean square (LMS) and recursive least square (RLS) adaptive algorithms to provide low BER values in SDMA-based multi-user MIMO-OFDM systems.

- The development of a channel tracking algorithm that can recursively update channel variations in SDMA-based multi-user MIMO-OFDM systems.
  The proposed channel tracking algorithm performed efficiently and accurately with 79% lower EVM for time-varying, frequency selective multi-user MIMO channels than for the training-based channel estimation method with employing only one pilot symbol for each transmit-receiver pair. Therefore, efficient bandwidth can be saved by the proposed novel channel tracking method.

- The development of the novel channel tracking algorithm to suit CSIRO's unique SDMA-based multi-user MIMO-OFDM system.
  No other research has developed such a scheme to track the time-varying, frequency selective, multi-user, MIMO channels. To the best of the author's knowledge, this is the first time that a six-user, twelve-antenna multi-user MIMO-OFDM channel is tracked.

1.5 Thesis outline

The organisation of the remainder of this thesis is as follows:

- In **Chapter 2**, a detailed discussion on the principles and recent research efforts regarding fading channels, MIMO systems and OFDM systems is presented. This chapter is structured in four main sections. The first section sets out a brief outline of wireless communications, arranging the necessary background to understand the subsequent sections. The succeeding sections of this chapter present a comprehensive discussion and a literature review on widely used communications technologies such as OFDM and MIMO that help to mitigate the negative effects caused by multi-path fading and take advantage of the multi-path fading.

- **Chapter 3** provides a comprehensive literature review on the existing adaptive equalization techniques, channel estimation methods and channel tracking algorithms that are employed in MIMO-OFDM communications systems. The literature review is categorised in three main sections. First, the literature on adaptive equalization is presented by discussing three main areas: linear vs. non-linear (DFE) equalization methods, adaptive filters and adaptive

algorithms. Then, channel estimation is discussed in regard to uncertainty models for channel state information, channel estimation methods, multi-user channel estimation and channel estimators. Finally channel tracking is discussed. The literature review points out the existing gaps in knowledge, providing the base for preparing the scope, objectives and methodology of the present research.

- **Chapter 4** discusses the methodology carried out for performing the research in five phases. First, we report the construction of a time-varying, frequency selective, multi-user MIMO channel model to characterise the wireless propagation environment. Next, the development of an efficient mechanism for initial channel estimation exploiting a training sequence for each transmit-receiver pair is discussed. Then, the development of adaptive channel equalization methods for SDMA-based multi-user MIMO-OFDM systems is presented. Next, the development of a novel and efficient channel tracking algorithm for multi-user MIMO-OFDM systems is explained. Finally, the statistical analysis of the EVM between the recovered symbols ($\hat{X}$) and the transmitted symbols (X) is explained.

- **Chapter 5** discusses the adaptive equalization techniques developed for SDMA-based multi-user MIMO-OFDM systems. The overall performance of multi-user MIMO-OFDM systems is affected by the critical factors such as the ISI produced by multi-path propagation within time dispersive channels and frequency selectivity. The employment of appropriate equalization at the receiver can compensate these channel impairments. Therefore, this chapter reveals the system model developed for linear and DFE adaptive equalization in SDMA-based multi-user MIMO-OFDM systems. The proposed equalization mechanisms adaptively equalize the channel and compensate for channel impairments. To determine optimal performance, least mean square (LMS) and recursive least squares (RLS) adaptive algorithms as well as training sequence based equalization methods are used in the proposed adaptive equalizers.

- In **Chapter 6**, the novel and efficient channel tracking algorithm for time-varying and frequency selective channels in SDMA-based multi-user MIMO-OFDM systems is presented. A detailed analysis of the simulation results with error, channel matrix, Doppler shift and SNR are discussed. The results demonstrate that the proposed algorithm performed better than the training sequence based method in time-varying, frequency selective, multi-path channels in SDMA-based multi-user MIMO-OFDM systems. The results of the

statistical analysis on both of the magnitude error and variance of EVM are presented in this chapter.

- In **Chapter 7**, the research findings and deductions of this monograph are summarised and the conclusions of the thesis are provided. Directions in future research are suggested as well as extensions to which the results derived in the study presented in the thesis can be applied.

Chapter 2

Principles of Multi-Path Fading, MIMO and OFDM

2.1 Introduction

This chapter presents a detailed discussion of the principles and recent research efforts regarding fading channels, MIMO systems and OFDM systems. The chapter is set out in five main categories; background, OFDM, MIMO systems and multi-user MIMO. The first section provides a brief outline of wireless communications, establishing the necessary background to understand the following sections. The next sections of this chapter discuss widely-used communications technologies such as OFDM and MIMO that help to mitigate the negative effects caused by multi-path fading and, in fact, take advantage of multi-path fading. The final section presents multi-user MIMO technology.

2.2 Introduction to wireless communications

The understanding of radio propagation channels to design wireless communication systems effectively is imperative. Previously, the wireless medium was analysed as a limiting factor in designing reliable communications links. However, this pattern has been transformed into modern day communications systems over enormous research and successive insights, which have a tendency to explore the channel behaviour for better performances.

The term "Wireless communications" refers to the transfer of information using electromagnetic radiation from the transmitter to the receiver. The transmitted signal propagates through a physical medium that contains reflective surfaces or permeating obstacles. This causes multiple reflected signals of the same source to arrive at the receiver at different times. The material properties such as dielectric

constants, permeability, conductivity and thickness of the reflective surface directly influence the reflected signal. These propagation medium effects are characterised as an abstract entity called the *channel* [9]. The physical transmission medium is the defined as the channel.

This section provides a brief outline of wireless communications. This overview is intended to provide the necessary background to understand the research provided in the following chapters.

2.2.1 Fading

Communication in wireless channels is limited primarily by fading. In wireless systems, fading is primarily due to multi-path propagation or shadowing from obstacles. The transmitted signal arrives at the receiver through diverse angles and/or diverse time delays and/or diverse frequency shifts because of the scattering effect of electromagnetic waves in the environment. This arbitrary variation in signal level is known as multi-path fading. The signal experiences shadowing fading, when the surrounding obstacles block the dominant path of the wave propagation. The quality and consistency of wireless communication are significantly influenced by fading. Furthermore, the task of planning high data rate, highly reliable wireless communications systems is enormously challenging due to the restrictions created by inadequate power and scarce bandwidth.

It is important to take into account whether the observation of such fluctuations has been made over short distances or long distances. For a wireless channel, the first scenario explains rapid fluctuations in the envelope of the signal, whereas the second scenario presents a slowly varying, averaged view. Consequently, the former case is referred to as *small-scale fading* or *multi-path fading*, whereas the latter is called *large-scale fading* or *path loss* [9].

Large scale fading is explained by the gradual loss of received signal power with transmitter-receiver separation distance. The objective of the present research is to maximise channel estimation and channel tracking efficiencies. Therefore, we only needed to consider small-scale fading characteristics and the large-scale fading is not considered in this research. However, it is significant to address the different types of small-scale fading; both in terms of the signal dispersion and the time-variance of the channel (see Figure 2.1). A few important properties of wireless channels are briefly outlined below.

1. Doppler shift

   The *Doppler shift* (f_d) is the frequency offset experienced by each multi-path wave, due to the relative motion between the transmitter and the receiver.

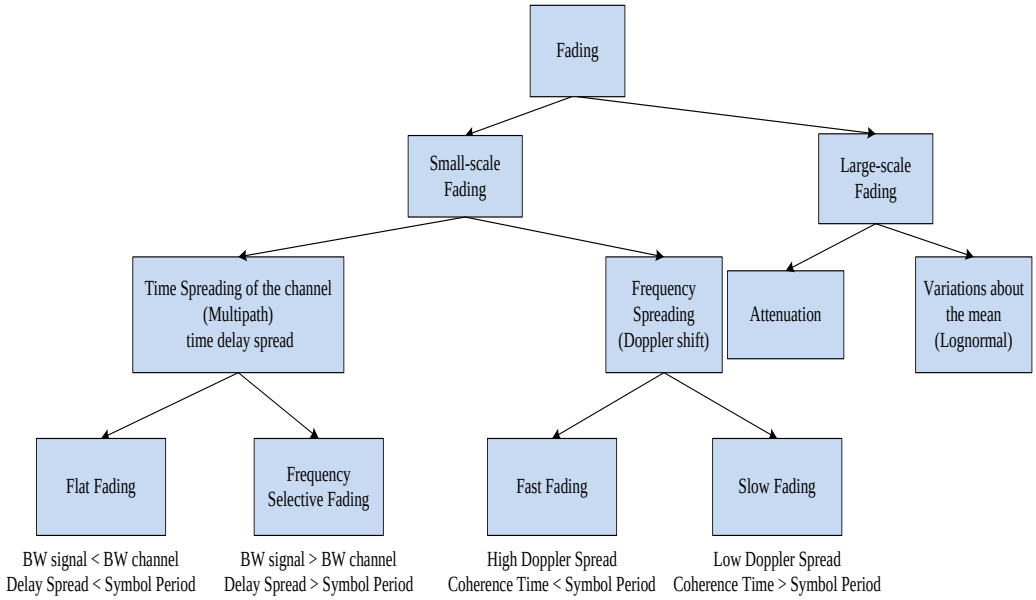

Figure 2.1: Types of fading channels.

It is directly proportional to the velocity and the direction of motion of the mobile with respect to the direction of arrival of the received multi-path wave. Accordingly, the Doppler shift can be expressed as:

$$f_d = \frac{v}{\lambda} \cos(\alpha) \tag{2.1}$$

$$= \frac{v f_c}{c} \cos(\alpha)$$

where v is the speed of the mobile, λ is the wavelength of the radio signal, α is the direction of motion of the mobile with respect to the direction of arrival of the multi-path, c is the speed of light ($3e8$ m/s) and f_c is the carrier frequency of the radio signal. In general, the Doppler shift will become time dependent if any form of acceleration or change of direction between the transmitter and receiver (e.g., driving in a curve), is introduced (Doppler spread is expalined below).

2. Coherence bandwidth

   A channel which passes all spectral components with approximately equal gain

and linear phase, is described as flat. The *coherence bandwidth*, B_c of a channel is a statistical measure of the range of frequencies over a flat channel. It is a significant parameter in the design of many wireless systems. Especially in OFDM systems, each subcarrier would be affected by a flat channel, if the subcarrier spacing is set to be less than coherence bandwidth. Therefore, simple one-tap equalization can be employed yielding a simpler OFDM system design.

3. Coherence time

   The coherence time, T_c, is the time domain equivalent of the Doppler spread. The time-varying nature of the channel can be characterized by T_c in the time domain. Moreover, T_c is the time for which the correlation of the channel responses reduces by 3 dB. For instance, to avoid the fast fading effect in the OFDM systems, the coherence time of the channel is required to be longer than the OFDM symbol length.

4. Fast fading channels

   In a *fast fading channel*, the channel impulse response (CIR) varies rapidly within the symbol duration. For such channels, the coherence time of the channel, T_c, is smaller than the symbol period of the transmitted signal, T_s, yielding frequency dispersion (or time-selective fading). This causes signal distortion. In the frequency domain, the mobility results in the frequency spread of the signal. It depends on the operating frequency and the relative speed between the transmitter and receiver, also known as Doppler spread. Therefore, a signal undergoes fast fading or time selective fading if: $T_s > T_c$ and $B_s < B_d$, where B_s is the bandwidth of the transmitted signal and B_d is the Doppler spread of the channel.

5. Slow fading channels

   The channel is said to be *slow fading*, if the CIR varies at a much slower rate than that of the transmitted baseband signal. Under such circumstances, the channel is said to be static over one or several bandwidth intervals. In the frequency domain, this implies that the Doppler spread, B_d of the channel is much less than the bandwidth of the baseband signal, B_s. Consequently, a signal experiences slow fading if: $T_s << T_c$ and $B_s >> B_d$.

6. Frequency selective channels

   The channel creates *frequency selective fading* on the received signal, if the channel has a constant-gain and a linear phase response over a bandwidth that is smaller than the bandwidth of the transmitted signal, B_s. In this case, the CIR possesses a multi-path delay spread which is greater than the mutual bandwidth of the transmitted message waveform. Consequently, the received signal will be distorted, as it includes multiple versions of the transmitted waveform which are attenuated (faded) and delayed in time. This leads to ISI. Moreover, the spectrum of the transmitted signal has a bandwidth which is greater than the coherence bandwidth B_c of the channel. Therefore, a signal experiences frequency selective fading if: $B_s >> B_c$ and $T_s < \sigma_\tau$, where σ_τ is the root mean square (RMS) value of the delay spread.

7. Flat fading channels

   The received signal experiences *flat fading* (or *frequency flat fading*), if the channel has a constant gain and a linear phase response over a bandwidth that is greater than the bandwidth of the transmitted signal. Since the bandwidth of the applied signal, B_s is narrow compared to the coherence bandwidth, B_c, or the flat fading bandwidth, the flat fading channel is sometimes referred to as the narrowband channel. Thus, a signal undergoes flat fading if: $B_s << B_c$ and $T_s > \sigma_\tau$ [9].

The delay spread of the signal is the maximum time delay that occurrs. It changes as the environment changes. In summary, when the delay spread is smaller than a symbol period, the distortion is called flat fading. The frequency selective fading occurs when the delay spread is larger than a symbol period. At deep fade frequencies, the channel does not allow any information to pass through. The fading occurs at selected frequencies, and is therefore called frequency selective fading.

2.2.2 Multi-path fading

Fading is caused, when the path followed by the propagation signal from the transmitter to the receiver involves either reflections or obstructions (see Figure 2.2(a)). For example, the link path changes in environments such as a moving car, indoor area, or a populated urban area with tall buildings. Here, a copy of the original signal arrives at the receiver from many different paths. Each of these rays has a slightly diverse delay and slightly diverse gain. The signal degrades as the

time delays cause phase shifts in the main signal component, resulting in multi-path fading.

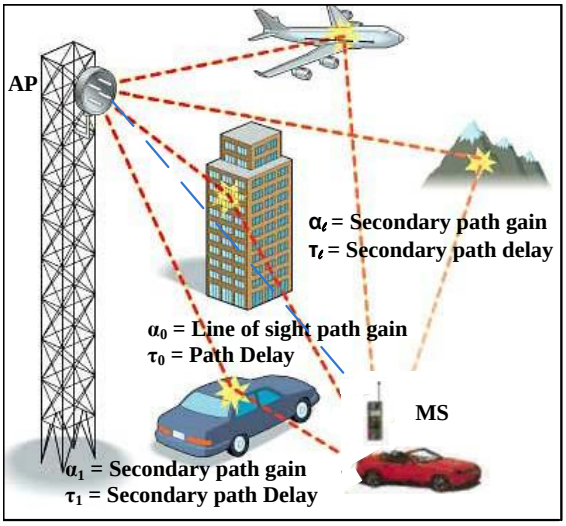

(a)

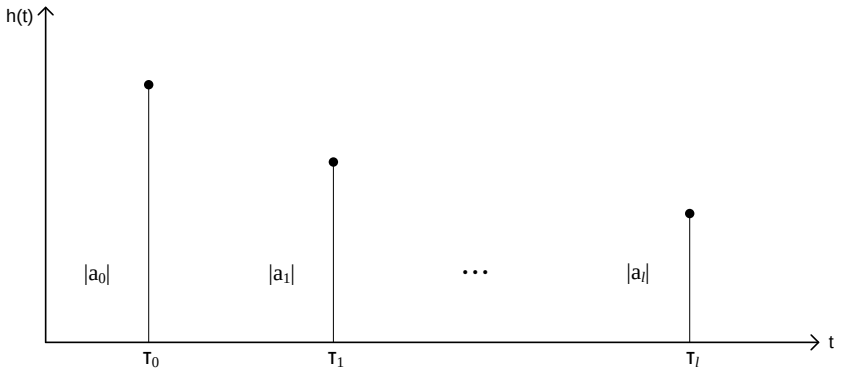

(b)

Figure 2.2: (a) Multi-path distortion (b) Graphical representation of the multi-path impulse response.

The impulse response of a multi-path channel can be expressed as:

$$\mathbf{h_c}(t) = \sum_{l=0}^{L-1} a_l \delta(t - \tau_l) \tag{2.2}$$

where a_l are complex path gains, τ_l are the normalised path delays relative to the line-of-sight (LoS) and L is the number of paths followed by the signal. Figure

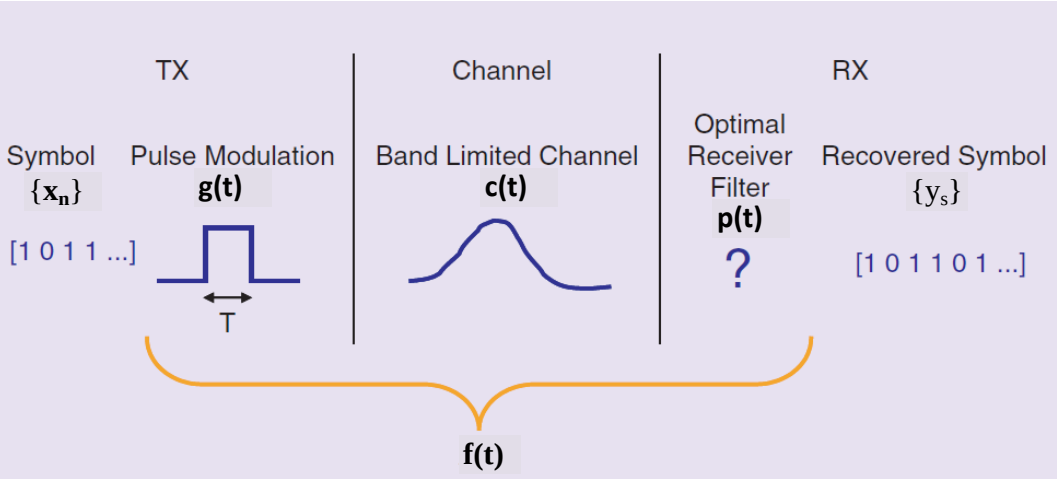

Figure 2.3: Communications channel with transmitter pulse modulation and receiver filter [1].

2.2(b) shows a representation of the multi-path impulse response.

In fading, the delayed reflected signals add to the main signal component thus, leading to either gains in the signal strength or deep fades. During deep fades, the receiver fails to detect the transmitted symbol. Rayleigh fading occurs, when there is no direct path (LoS) but only multi-path components in the received signal. If the LoS component is present, the channel fading is assumed to have a Rician distribution [30].

2.2.3 Inter-symbol interference (ISI)

ISI is the echoes from proceeding or succeeding symbols that are adding to or subtracting from the symbol being detected. It is the dispersion effect in the discrete time domain, where the transmitted data are considered as digital symbols with pulse modulation. Figure 2.3 illustrates a communication channel with transmitter pulse modulation and receiver filter. As shown for binary data, the discrete information-bearing symbol $\mathbf{x_n}$ is either "1" or "0" and the modulation pulse is a square pulse.

Without considering channel noise, the received signal can be expressed as: [20]

$$\mathbf{y}\,(t) = \sum_{n=0}^{\infty} \mathbf{x_n f}\,(t - nT) \tag{2.3}$$

where $f(t)$ is the overall response with the transmitter modulation, channel and receiver filter as depicted in Figure 2.3. In order to obtain the recovered symbol, $\mathbf{y}(t)$ is sampled at times $t = sT + \tau_0$, $\mathbf{s} = 0, 1,...$, where τ_0 is the propagation delay. We then have

$$\mathbf{y}\left(sT + \tau_0\right) = \mathbf{y_s} = \sum_{n=0}^{\infty} \mathbf{x_n f}\left(sT + \tau_0 - nT\right) \tag{2.4}$$

or equivalently,

$$\mathbf{y_s} = \sum_{n=0}^{\infty} \mathbf{x_n f_{s-n}} = \mathbf{f_0 x_s} + \sum_{n=0, n\neq s}^{\infty} \mathbf{x_n f_{s-n}} \tag{2.5}$$

The term $\mathbf{f_o x_s}$ indicates the desired information symbol at the s^{th} sampling instant and the term $\sum_{n=0,n\neq s}^{\infty} \mathbf{x_n f_{s-n}}$ indicates ISI.

The CIR is an impulse, $\delta\left(t\right)$, if the channel has infinite bandwidth. Due to the channel's bandwidth limitation, the CIR, $\mathbf{c}\left(t\right)$, is a spread pulse as depicted in Figure 2.3. The convolution of the modulating pulse $\mathbf{g}\left(t\right)$, with $\mathbf{c}\left(t\right)$, outcomes an impulse response whose pulse width is larger than T, the pulse width of $\mathbf{g}\left(t\right)$.

Generally, the receiver filter is designed as a match filter. If an equalizer has not been employed in the receiver filter, the overall impulse response will have a larger pulse width than T, as shown in the top scheme in Figure 2.4. The bottom scheme of the figure illustrates the transmission of four consecutive symbols of "1"s. If we look at the sampling instant sT, the recovered symbol is a summation of the desired symbol value labelled by point 0, which equals x_0 on curve C, plus the ISI resulting from neighbouring symbols, which are point 1 on curve B $(= x_1)$, point 2 on curve A $(= x_2)$, and point 3 on curve D $(= x_{-1})$. The ISI terms due to the prior symbols are called precursors and the ISI terms due to the subsequent symbols are called postcursors.

ISI occurs when the spread of the overall impulse response, $\mathbf{x}\left(t\right)$ is larger than the symbol period T_s. ISI creates uncertainty in the received data samples. The receiver gets a continuous signal whose samples can take any value, rather than receiving discrete levels that are transmitted. The receiver must then compose an estimate from the received symbols to detect the transmitted symbols.

The basic principles governing multi-path fading in wireless channels have been reviewed in this section. The most widely used transmission techniques that help mitigate the effects that arise due to multi-path fading in wireless channels are discussed next.

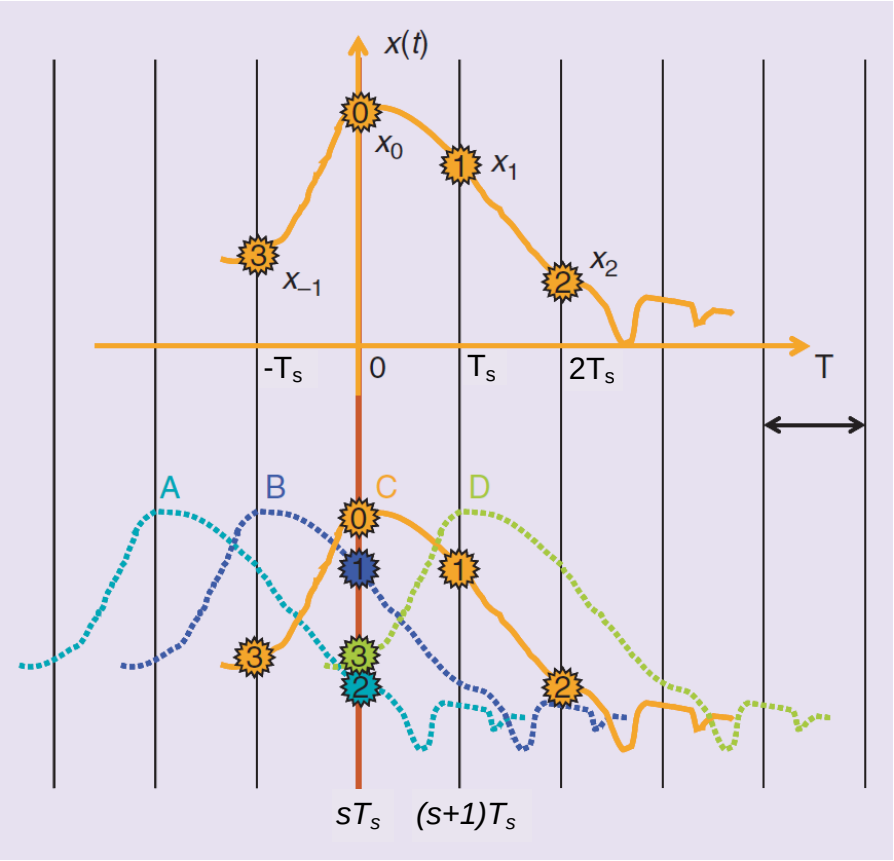

Figure 2.4: Illustration of ISI [1]

2.3 Orthogonal frequency division multiplexing (OFDM)

During the past several decades, wireless communications has benefitted from significant progress. It has become the key enabling method of ground-breaking consumer products. Significant scientific accomplishments are required to make sure that wireless devices have suitable architectures appropriate to support a broad variety of services brought to users, and to satisfy the requirements of a range of applications.

The necessities of high bandwidth applications and the large-scale deployment of wireless devices lead to new challenges in terms of the efficient use of the attainable spectral resources. Among the existing air-interface technologies, orthogonal frequency division multiplexing [31–33] shows numerous advantages and has attracted extensive attention.

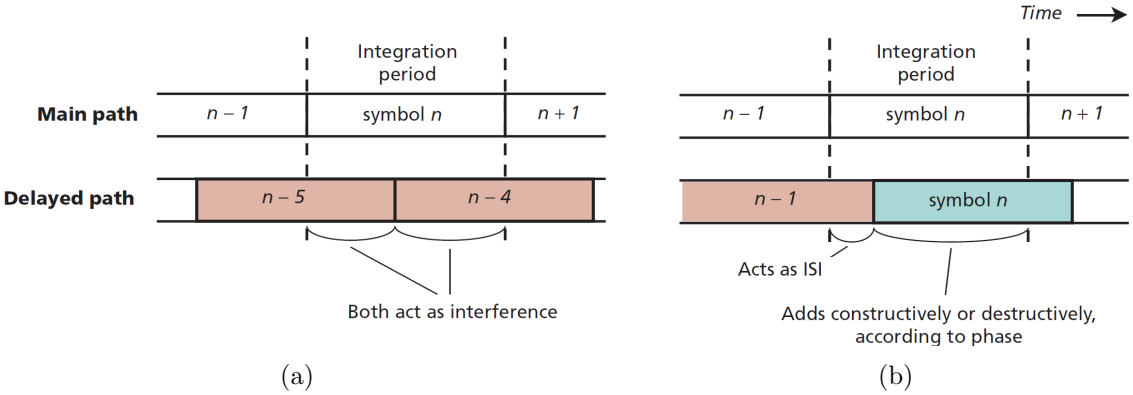

Figure 2.5: How a delayed component of multi-path fading causes ISI with (a) long delay (b) short delay [2].

OFDM deals with the problems of frequency selective fading. The delayed and reflected radio paths impose ISI on the neighbouring bits, when transmitting at a high data rate. The basic principle of OFDM was invented by Chang [34] and, over the years, a range of researchers have investigated this technology. In its early years, even though it is conceptually elegant, the use of OFDM has mostly been restricted to military purposes because of implementation difficulties. However, in recent years, a variety of applications such as digital audio broadcasting (DAB) [35], digital video broadcasting (DVB) [36, 37], WLANs [38], broadband radio access networks (BRANs) [39] and a range of high-rate applications [40] have been implemented using OFDM. These wide ranges of applications emphasise its significance.

2.3.1 Why use multiple carriers?

The employment of multiple carriers is pursued from the existence of multi-path. Assume a carrier is modulated with digital information. The carrier is transmitted with a particular phase and amplitude which is selected from the constellation employed, during each symbol. A number of bits of information are transmitted via each symbol. The number of bits is equal to the logarithm of the number of states in the constellation.

Let us consider that this transmitted symbol n has arrived to the receiver via two paths, having a relative delay between them. The receiver will try to demodulate the information sent via this symbol by observing all the received data relating to symbol n, that is the data received directly and via the delayed multi-path

component.

Figure 2.5 shows how two instances of the delay cause ISI. Figure 2.5(a) depicts an instance of a long delay which occurs when the relative delay is larger than one symbol period. Here, the signal received via the delayed path only take information which belongs to a preceding symbol or symbols. Therefore this signal acts entirely as ISI. Figure 2.5(b) illustrates an instance of a short delay which occurs when the relative delay is smaller than one symbol period. Here, a fraction of the signal received via the delayed path acts entirely as interference, as it only takes information which belongs to the preceding symbol. The remainder of the signal takes the information from the required symbol, adding constructively or destructively to the information of the main path.

This implies that, to have a considerable level of delayed signals, the symbol rate must decrease adequately. Therefore, the total delay spread which is the difference in the delay between the first and the last multi-path components will be only a modest division of the symbol period. Consequently, in the presence of multi-path propagation, the information that can be passed by a single carrier is restricted. This implies that if one carrier cannot carry the information rate required, the idea of splitting the high-rate data into many low-rate parallel sub streams, each passed on by its own carrier should be considered. This is a type of frequency division multiplexing (FDM), and is the first step towards OFDM.

2.3.2 OFDM fundamentals

OFDM is a combination of multiplexing and modulation techniques. It converts a wideband frequency selective channel to a set of parallel flat fading channels by splitting the wideband channel into narrow channels. The narrow band channels are first modulated by data and are then remultiplexed to create OFDM carriers. The subcarriers are orthogonal to each other. The basic principle of OFDM is the orthogonality of the subcarriers. The orthogonality allows simultaneous transmission on many subcarriers in a tight frequency space without causing interference to each other.

OFDM directly modulates the arriving symbol sequence onto the subcarriers not including the pulse shaping. As intuitively illustrated in Figure 2.6, rectangular pulses in the time domain have a sync signal response in the frequency domain and a sync signal response has spectral nulls at $f_c + / - 1/T_s$. Therefore, the carriers can be squeezed together as the subcarriers can be placed exactly at $1/T_s$.

As well as the same carrier ISI, *inter-carrier interference* (ICI) will also occur if the integration period spans for two symbols due to delayed paths, as illustrated in

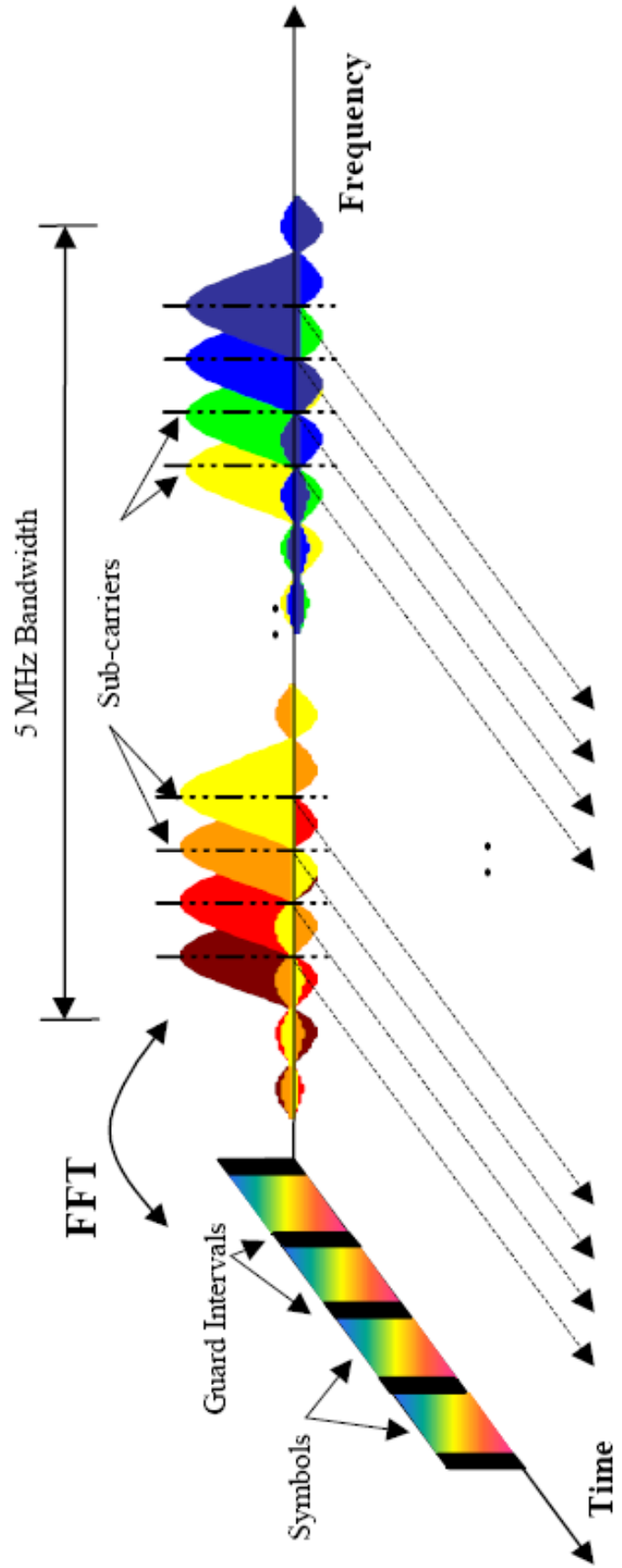

Figure 2.6: Orthogonal Frequency Division Multiplexing [3]

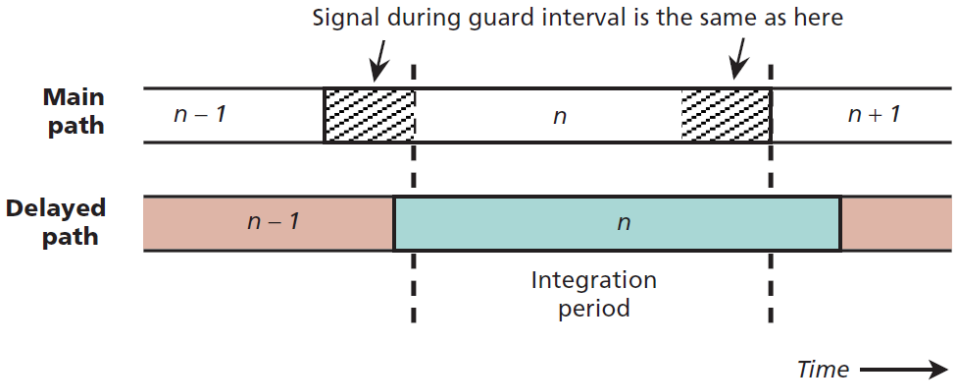

Figure 2.7: Addition of guard interval [2].

Figure 2.5. When the beat tones from other carriers alter in phase and/or amplitude during the symbol period, they no longer integrate to zero, hence ICI occurs. This can be avoided by adding a guard interval as depicted in Figure 2.7. It makes sure that all the integrated information comes from the same symbol and appears constant during the symbol period.

The symbol period is expanded so that it goes beyond the receiver integration period. The guard interval length is selected to match the the length in time within which significant muti-path component arrives. The segment inserted at the start of the symbol to fill the guard interval is identical to the segment of the same length at the end of the symbol. Hence, it is called the cyclic prefix. All the signal components within the integration period come from the same symbol, provided that the delay of any path with respect to the main multi-path component is less than the guard interval. Therefore, both ICI and ISI will only take place when the relative delay exceeds the guard interval.

2.3.3 OFDM systems

As illustrated in Figure 2.8 a serial data stream of a traffic channel is passed through a serial-to-parallel (SP) convertor, which divides the data-stream into K number of low-rate parallel sub-channels. OFDM employs a scheme of modulators with carrier frequencies $f_0, f_1, \ldots, f_k$. The data symbols of each sub-channel are applied to a separate modulator. The sub-channels are Δf apart and therefore the overall bandwidth W of K modulated subcarriers is $K\Delta f$. The symbol duration of each of the K sub-channels is expanded by a factor of K, where $K \leq 128$ is considered

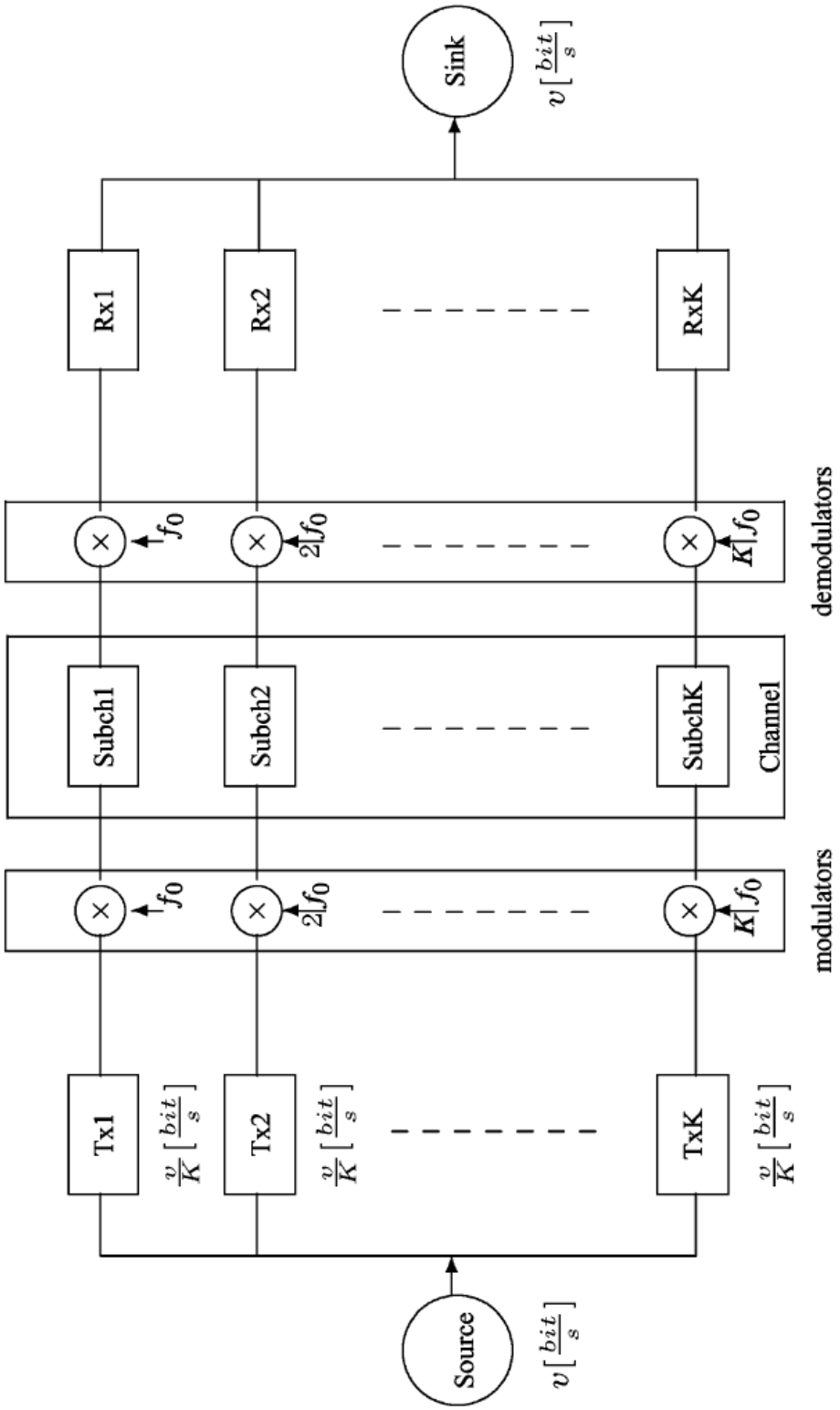

Figure 2.8: Schematic diagram of the orthogonal parallel modem [4]

in this thesis. Therefore, one significant benefit of this method is that usually, the signal of each subcarrier is likely to remain unaffected by the multi-path dispersion. Then, the OFDM signal is generated by combining these K modulated carriers. The SP convertor, is exploited to apply every K^{th} symbol to a modulator. This has the effect of interleaving the symbols passed to each modulator. Therefore, symbols s_0, s_k, s_{2k} are applied to the modulator whose carrier frequency is f_0. At the receiver end, the received OFDM signal is demultiplexed into K frequency bands and the K modulated signals are then demodulated. To recombine the baseband signals, they are passed through a parallel-to-serial (PS) converter and sent to the sink.

Since the symbol period T_s is extended, the delay spread of the channel becomes a considerably shorter division of a symbol period than that of a serial system. Therefore, the key benefit of the OFDM concept is that it is less responsive to ISI than the conventional serial system. Hence, only a few subcarriers are affected in a frequency selective fading environment. Instead of a whole symbol being knocked out, only a subset of $(1/K)$ bits are lost. With proper equalization this can be avoided.

We have to use K modulators and "square-root-Nyquist" filters at the transmitter and K demodulators and "square-root-Nyquist" filters at the receiver. Hence, the implementation complexity may seem to increase when compared to a conventional serial modem. This may look like a disadvantage. However, each sub-channel modulator is operated at a K-times lower symbol-rate. Therefore, the system may be analysed as a "parallelized low-speed implementation" of a high-speed serial modem.

As a further complexity alleviation technique, the fast Fourier transform (FFT) algorithm is employed to perform N-point inverse FFT (IFFT) and FFT at the transmitter and the receiver, respectively as depicted in Figure 2.9. First, a high data rate binary data stream $\mathbf{b}[\mathbf{n}]$ is passed through a serial-to-parallel converter. They are then, mapped into N complex points $\bar{\mathbf{x}}_\mathbf{i}$ by modulation, which corresponds to each one of the subcarriers. Next, the points $\bar{\mathbf{x}}_\mathbf{i}$ are converted into time domain by IFFT operation. The IFFT modulates the signals of a block of K sub-channels onto the subcarriers in a single step. To combat time dispersion and avoid ICI, cyclic prefix is added as illustrated in Figure 2.7. The resultant digital signal is then converted to analog and frequency up conversion is performed.

At the receiver, the received radio frequency (RF) signal is first down converted and transformed into a digital sequence after being sent through an analog-to-digital converter (ADC). The cyclic prefix is then removed by eliminating the guard band from each OFDM symbol. The rest of the symbols are sent through a serial-to-parallel converter and an N-point FFT is performed to obtain the frequency domain

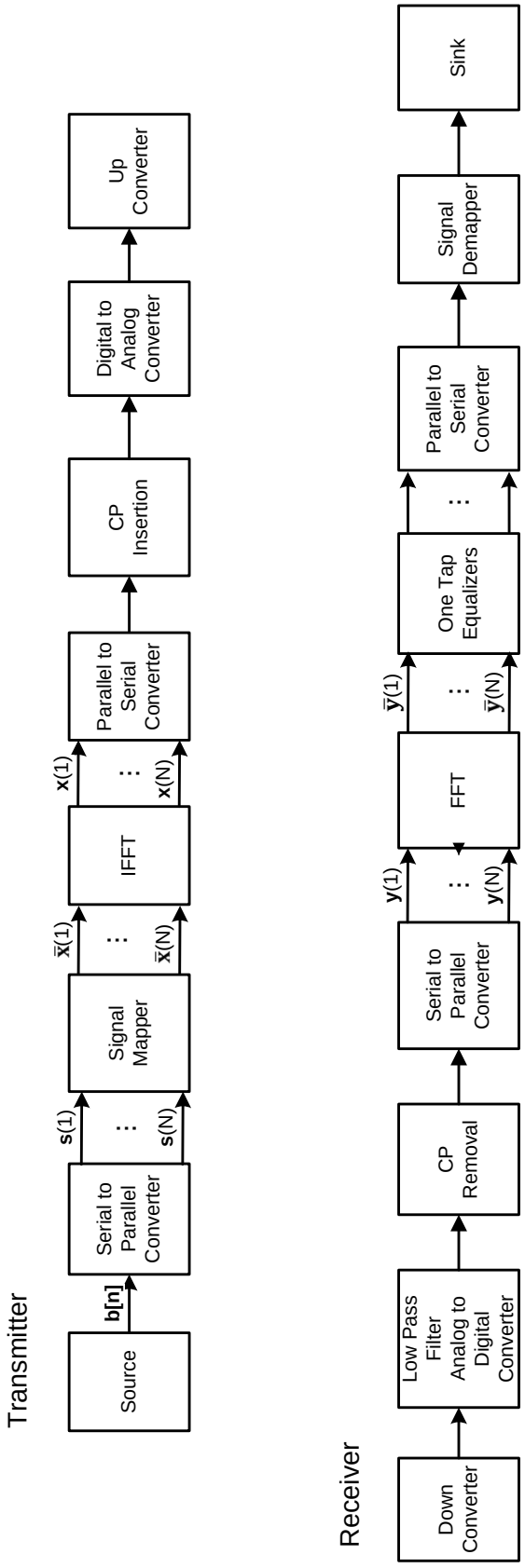

Figure 2.9: OFDM system

points. The resultant $\bar{\mathbf{y}}^{\mathbf{n}}$ ($\mathbf{n} = 1, 2, \ldots, N$) complex points are the complex baseband version of the N modulated subcarriers. Next, frequency domain one tap equalizers are exploited to compensate for the channel's dispersion occurs at certain subcarriers due to decomposition of the broadband channel into N sub-channels. Finally, the demodulation is performed and the data is sent to the sink.

2.3.4 Benefits of OFDM

OFDM offers important benefits over other commonly employed wireless transmission methods, such as direct-sequence spread spectrum (DSSS), frequency-hopping spread spectrum (FHSS) and single-carrier transmission methods. The main advantage of OFDM is the ability to transmit multiple symbols in parallel while increasing the spectral efficiency, as the radio channel is split into many narrowband, low-rate, and frequency flat subcarriers. Consequently, a simple multiple access technique has being developed, known as the orthogonal frequency division multiple access (OFDMA) technique to deliver the information of different users using separate subcarriers [41–44]. This leads to the transmission of a variety of media such as video, graphics, speech, text, or other data within the same radio link. However, the transmission depends on the precise types of services and their quality-of-service necessities.

OFDM offers simple implementation by employing FFT and IFFT. OFDM is suitable for high data rate communications over time-varying, frequency selective channels as it allows low complexity in transmission and reception. Moreover, the OFDM system is more immune to frequency selective fading than single carrier systems as the channel is spilt into narrowband flat fading subcarriers. Furthermore, OFDM is less responsive to ISI than the conventional serial system as it employs a cyclic prefix [45]. Employing channel coding in OFDM systems leads to coded OFDM (COFDM) [46, 47], which offers the recovery of symbols lost because of the frequency selectivity of the channel.

2.3.5 Major contributions on OFDM

This section presents a literature review on the key findings on OFDM systems. The major contributions found in the OFDM literature are summarised in Tables 2.1, 2.2, and 2.3.

Table 2.1: Major research contributions to OFDM (part 1) [4]

Year	Author(s)	Contribution
1966	Chang [34]	Proposal of the first OFDM system for dispersive fading channels
1967	Saltzberg [48]	Examination of a multi-carrier system using orthogonal quadrature amplitude modulation (QAM) of the carriers
1968	Chang and Gibby [49]	Theoretical analysis of the performance of an orthogonal multiplexing data transmission method
1970	Chang [50]	Issue of U.S patent on OFDM
1971	Weinstein and Ebert [51]	Application of discrete Fourier transform (DFT) on OFDM modems
1980	Hirosaki [52]	Design of a sub-channel based equalizer for an orthogonally multiplexed QAM system
	Peled and Ruiz [45]	Discussion of a decreased complexity frequency division data transmission technique with a cyclic prefix approach
	Keasler [53]	Patent of an OFDM modem in telephone networks
1981	Hirosaki [54]	Recommendation of an implementation of OFDM systems using DFT
1985	Cimini [55]	Examination of the viability of OFDM in mobile communications
1986	Hirosaki, Hasegawa, and Sabato [56]	Development of a groupband data modem employing an orthogonality multiplexed QAM method
1987	Alard and Lasalle [55]	Employment of OFDM in digital broadcasting
1989	Kalet [57]	Analysis of multitone QAM modems in linear channels
1990	Bingham [33]	In depth discussion of a range of aspects of early OFDM methods
1991	Cioffi [58]	Introduction of the American national standards institute (ANSI) asymmetric digital subscriber line (ADSL) standard
1993-1995	Warner [59], Moose [60] and Pollet [61]	Studies of time and frequency synchronisation in OFDM systems
1994-1996	Jones [62], Shepherd [63] and Wulich [64, 65]	Investigation of a range of coding and post processing methods intended to minimise the peak power of OFDM signal
1997	Li and Cimini [66, 67]	Exposure of the effect of clipping and filtering on OFDM systems
	Hara and Prasad [68]	Comparison of a range of techniques for combining CDMA and OFDM
1998	Li, Cimini and Sollenberger [69]	Design of a robust channel estimator using minimum mean square error (MMSE) in OFDM systems
	May, Rohling and Engels [46]	Performance analysis of Viterbi decoding using 64-differential amplitude phase-shift keying (PSK) and 16-ary QAM modulated OFDM signals
1999	Li and Sollenberger [70]	Study of parameter estimation based on a MMSE diversity combiner in adaptive antenna array aided OFDM systems
	Amour, Nix and Bull [71–73]	Design of OFDM equalization-based receiver and the proposal of a pre-FFT equalizer

Table 2.2: Major research contributions to OFDM (part 2) [4]

Year	Author(s)	Contribution
1999	Prasetyo and Aghvami [74, 75]	Simplification of the transmission frame structure to attain fast burst synchronisation in OFDM systems
	Cherriman, Keller and Hanzo [76]	Evaluation of packetization and packet acknowledgment method based on H.263 video codec in OFDM systems
	Wong *et al.* [77]	Proposal of a subcarrier, bit, and power allocation algorithm to reduce the total transmit power of multi-user OFDM systems
2000	Fazel and Fettweis [78]	Study of state-of-art works on OFDM
	Nee and Prasad [79]	OFDM in wireless multimedia communications
	Lee, Keller and Hanzo [80]	Study of enhanced turbo-coded OFDM receivers for DVB-T
	Keller and Hanzo [81]	Emphasis on the adaptive bit allocation and turbo coding in the framework of OFDM
	Lin, Cimini and Chuang [47]	Application of turbo coding in OFDM systems employing antenna diversity
	Keller and Hanzo [82]	Analysis of design tradeoffs of turbo-coded burst-by-burst adaptive OFDM wideband transceivers
2001-2002	Keller *et al.* [83]	Quantification of the effect of time-domain and frequency-domain synchronisation errors in the framework of OFDM system
	Lu and Wango [84–87]	Performance analysis of low density parity check (LDPC) based STC assisted OFDM systems
	Cherriman, Keller and Hanzo [77]	Proposal of various adaptive OFDM video systems for interactive communications over wireless channels
2003	Hanso, Mnster, Choi and Keller [31]	OFDM for broadband multi-user communications, WLANs and broadcasting
2004	Simeone, Bar-Ness, and Spagnolini [88]	Demonstration of subspace tracking algorithm employed for channel estimation in OFDM systems
	J. Zhang, Rohling, and P. Zhang [89]	Adoption of ICI self-cancellation scheme to combat the ICI caused by phase noise in OFDM systems
	Necker and Stber [90]	Design of an ML assisted blind channel estimation method for OFDM systems
	Doufexi *et al.* [91]	Emphasis on the benefits of employing sectorized antennas in WLANs
	Alsusa, Lee, and McLaughlin [92]	Proposal of multicarrier packet based multi-user systems with adaptive subcarrier-user allocation
2005	Williams *et al.* [93]	Design of pre-FFT synchronisation technique in OFDM systems

Table 2.3: Major research contributions to OFDM (part 3)

Year	Author(s)	Contribution
2007	Hanzo and Choi [94]	Review on adaptive high-speed downlink packet access (HSDPA) approach
2009	Fischer and Siegl [95]	Performance of analysis of peak-to-average power ratio reduction in single- and multi-antenna point-to-point OFDM systems
	Mileounis *et al.* [96]	Blind identification of Hammerstein channels employing QAM, PSK, and OFDM inputs
	Huang and Hwang [97]	Performance enhancement of active interference cancellation in OFDM cognitive radio
	Chen *et al.* [98]	Design of spectrum sensing algorithms for OFDM systems using pilot tones
	Talbot and Farhang-Boroujeny [98]	Proposal of time-varying carrier offset model in mobile OFDM systems
2010	Sun, Morelli, and Zhang [99]	Investigation of carrier frequency offsets tracking in the IEEE 802.16e uplink based on the least squares (LS) method
2011	K. Wu and J. Wu [100]	Suggestion of a low complexity DDCE algorithm in OFDM systems with transmit diversity
2012	Lu *et al.* [101]	Suggestion of a hard-decision directed frequency tracking method in OFDM systems for frequency selective channels
	Yu and Sadeghi [102]	Study of pilot based channel estimation methods for OFDM communications systems in time-varying frequency-selective channels

The principles of MIMO communications systems are discussed in the next section.

2.4 MIMO systems

The most important researcher in the field of communications theory is possibly Claude Shannon, at Bell Labs. His significant finding of the capacity formula, among many primary results in his renowned paper "A Mathematical Theory of Communication" [103], laid the foundation for a new field of research, known as information theory. Shannon proved that reliable communication between a transmitter and a receiver is feasible even in the presence of noise. Shannon obtained his celebrated formula on capacity, for the particular case of a unit-gain band-limited continuous channel in the presence of additive white Gaussian noise (AWGN):

$$C = Wlog_2\left(1 + \frac{P_T}{P_N}\right)[bits/s] \tag{2.6}$$

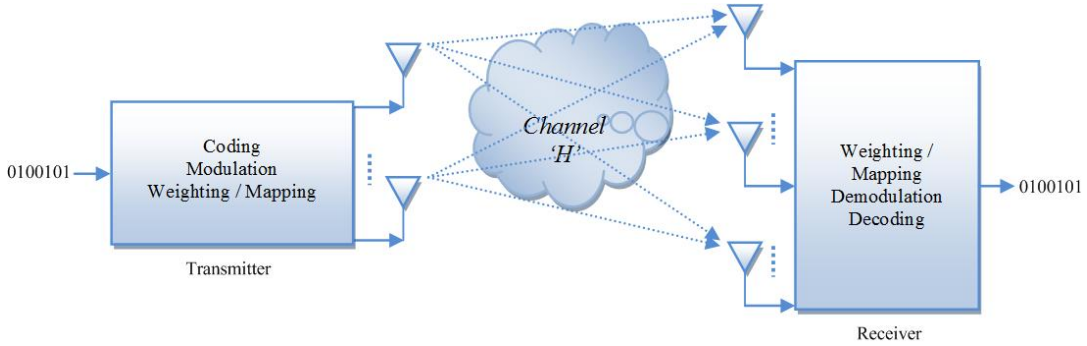

Figure 2.10: MIMO wireless communications system.

where W, P_T and P_N stand for the electromagnetic bandwidth available, the average transmitted power, and the noise power, respectively. However, W and the maximum radiated power are scarce since they are subject to fundamental physical and practical constraints as well as regulations.

One method to increase capacity is by increasing transmitted power. However, it is not economically feasible, as the spectral efficiency logarithmically depends on the transmitted power. It may also breach regulation power masks and result in nonlinearity in the power amplifier. Furthermore, the electromagnetic radiation can cause significant impact on people [104]. Another approach to increasing capacity would be to use a wider radio spectrum. However, it is very expensive as it is a scarce resource. Therefore, the design and implementation of wireless systems that can achieve increased data rates and better performance while exploiting existing frequency bands and channel conditions, are very challenging tasks.

MIMO communications and space-time processing is one of the most promising technologies to resolve the bottlenecks in the traffic capacity of current and future wireless networks. Foschini and Telatar showed in [13] and [105], that by deploying multiple antennas at both the transmitter and receiver, MIMO systems can increase the capacity without having to increase the transmission power or use a wider band when the channel experiences rich scattering. Moreover, due to its dominant performance-intensifying potential such as high capacity, increased diversity and interference suppression, it has rapidly progressed from the research arena to commercial availability within a decade [106].

The concept behind MIMO is to improve the data rate (bits/sec) or the quality of service (bit error rate or BER) of the communication for each user by combining the signals on the transmit antennas and receive antennas at two distinct ends [6]. In

particular, the capacity of a MIMO system can increase, linearly with the minimum over the number of inputs and outputs. The principles of MIMO communications systems are discussed next in more detail.

2.4.1 Principles of MIMO communications systems

An example of a MIMO wireless communication system is illustrated in Figure 2.10. A binary data stream is supplied to a basic transmitting block which includes the utilities of error control coding and mapping to complex modulation symbols (quadrature phase-shift keying (QPSK), M-ary QAM, etc.). Then, a number of separate symbol streams, which are collections of independent, partially redundant and fully redundant, are generated. Subsequently, each signal is mapped onto one of the multiple transmitter antennas. The signals are sent into the wireless channel following upward frequency conversion, filtering and amplification. Then, the signals are received by multiple receiver antennas and demodulation and demapping operations are executed to recover the original message [6].

2.4.2 MIMO channel

Since the MIMO system is employed with multiple antennas at both ends of the link, all the transmit and receive antenna pairs can be represented by the MIMO channel. A single-user communication system with M number of transmitter antennas and R number of receiver antennas is considered as shown in Figure 2.10. From a system level point of view, a linear time-variant MIMO channel can be represented by an $R \times M$ channel matrix [107]:

$$\mathbf{h}(t,\tau) = \begin{pmatrix} h_{11}(t,\tau) & h_{12}(t,\tau) & \cdots & h_{1M}(t,\tau) \\ h_{21}(t,\tau) & h_{22}(t,\tau) & \cdots & h_{2M}(t,\tau) \\ \vdots & \vdots & \ddots & \vdots \\ h_{R1}(t,\tau) & h_{R2}(t,\tau) & \cdots & h_{RM}(t,\tau) \end{pmatrix} \tag{2.7}$$

where τ denotes the excess delay and the elements, $h_{rm}(t,\tau)$ of the matrix $\mathbf{H}$ are complex random variables that represent the time-variant impulse response between the m^{th} transmit antenna and the r^{th} receiver antenna. There is no difference between the spatially separate antennas and diverse polarisations of the same antenna. Each element, $h_{rm}(t,\tau)$ needs to be substituted by a polar metric sub matrix if diverse polarised antennas are used. Therefore, the number of antennas used in the system will be increased [107].

The physical characteristics of the propagation environment directly affect each

sub-channel $h_{rm}(t,\tau)$. The signals from the transmitter to the receiver and vice versa are highly influenced by the quantity and complexity of the scattering mechanisms. Consequently, the $h_{rm}(t,\tau)$ signals have a complex variation, and it is essential to model them as stochastic signals [108].

Several assumptions are regularly made in the $h_{rm}(t,\tau)$ sub-channels considering the statistics. For example, that there are independently and identically distributed (i.i.d) complex Gaussian variables with zero mean; hence, a Rayleigh distribution is followed by their modulus and their phase is uniformly distributed. However, the statistical behaviour of the channel changes due to the presence of an LoS or a dominant reflected component. In such circumstances, other distributions such as Nakagami or Rice distributions better fit their behaviour [108].

The effects of the antennas such as the type, configuration and frequency filtering (bandwidth-dependent) are included in the channel matrix (2.7). Let $\mathbf{x}(t)$ and $\mathbf{y}(t)$ be the length-M transmit signal vector and length-R receive signal vector respectively:

$$\begin{aligned}\mathbf{x}(t) &= [x_1, x_2, \ldots, x_M]^T \\ \mathbf{y}(t) &= [y_1, y_2, \ldots, y_R]^T\end{aligned} \tag{2.8}$$

Then, the overall MIMO input-output relationship can be expressed as:

$$\mathbf{y}(t) = \int_{\tau} \mathbf{H}(t,\tau)\,\mathbf{x}(t-\tau)d\tau + \mathbf{z}(t) \tag{2.9}$$

where $\mathbf{z}(t)$ indicates the noise and the interference vector at the receiver. If the channel is *time-invariant*, then the channel matrix $\mathbf{H}(t,\tau) = \mathbf{H}(\tau)$. For linear, *time-invariant* and frequency flat channels;

$$\mathbf{y}(t) = \mathbf{H}\mathbf{x}(t) + \mathbf{z}(t) \tag{2.10}$$

Due to the fundamental mathematical nature of MIMO, where data is transmitted over a matrix rather than a vector channel, new and significant opportunities are produced beyond the added diversity or array gain benefits [6].

2.4.3 Benefits of MIMO technology

MIMO systems offer an impressive advance of both the capacity of the system and spectral efficiency when compared with single-input single-output (SISO) systems. The capacity of a wireless channel increases linearly as a function of the minimum of the number of the transmit or receiver antennas [109,110]. A significant reduction of the effects of fading can be achieved by the increased diversity and this is particularly

favorable, when the different channels fade independently.

The principal performance-enhancing potentials such as high capacity, increased diversity and interference suppression of MIMO systems arise from the *array gain*, *diversity gain*, *spatial multiplexing gain* and *interference reduction* [111]. Each of these leverages is discussed next.

1. Array gain

   The array gain is the increase in the average received signal-to-noise ratio (SNR) that results from a coherent combining effect of wireless signals at a receiver. It is obtained through processing at the transmitter and receiver. Depending on the number of transmitter and receiver antennas, transmit and receive array gain require channel knowledge at the transmitter and receiver, respectively. Although channel knowledge at the receiver is usually available, the CSI at the transmitter is more complex to obtain. The coverage and the range of a wireless network can be improved by the array gain, as it improves resistance to noise.

2. Diversity gain

   As explained earlier, the power of a signal fluctuates arbitrarily. This fading effect in wireless channels can be reduced by diversity techniques that rely on the transmission of the signal over multiple (ideally independent) fading paths in time, frequency or space. The diversity ensures that the receiver receives multiple copies of the same transmitted signal. If these copies are affected by independent fading conditions, the probability of fading all the copies at the same time decreases [6]. Therefore, the diversity helps to improve the quality of a wireless system. The most common diversity technique is spatial (or antenna) diversity [112] in MIMO systems, whereby multiple antennas are spatially separated and the receiver selects the best signal at a given time. As spatial diversity does not require transmission time or bandwidth expenditure, it is favored over time or frequency diversity. The number of paths is often referred to as diversity order. The probability that at least one of the paths is not experiencing a deep fade can be enhanced by increasing the diversity order. Therefore, the quality and reliability of the received signal is improved. A MIMO channel with N_T transmit antennas and N_R receiver antennas offers $N_T \times N_R$ independently fading links. Consequently, $N_T N_R{}^{th}$-order spatial diversity can be obtained.

3. Spatial multiplexing gain

Spatial multiplexing gain is the linear increase in capacity offered by MIMO channels without additional power or bandwidth [105]. It is a transmission scheme only possible in MIMO systems. This is realized by transmitting multiple, independent data streams from the individual antennas within the bandwidth operation. The receiver can split the different data streams under suitable channel conditions such as rich scattering, yielding a linear increase in capacity in the wireless network. The concept of spatial multiplexing is detailed in the section 2.4.4.

4. Interference reduction or avoidance

   Co-channel interference results from frequency reuse in wireless channels. With the aid of multiple antennas, the separation between the preferred signal and co-channel signals can be used to reduce interference. Although interference reduction requires knowledge of the channel of the desired signal, precise knowledge of the channel of the interferer may not be essential. Furthermore, the interference reduction can be executed at the transmitter, by decreasing the interference energy sent to the co-channel users, while transmitting the signal to the desired user. The multi-cell capacity can be enhanced by interference reduction as it allows for aggressive frequency reuse.

In general, due to conflicting demands on the spatial degrees of freedom (or number of antennas), it is not feasible to take advantage of all the leverages of MIMO technology simultaneously. The extent to which these conflicts are resolved can be determined by the signalling scheme and transceiver design [111].

2.4.4 Main types of MIMO systems

Recently, a variety of designs for smart antenna have become popular, which have established applications in various scenarios. Table 2.4 summarises the four most widely used MIMO types. These four MIMO designs are employed to achieve a range of design objectives. The spatial division multiplexing (SDM) [31, 113] technique is used to maximise the achievable multiplexing gain. SDM increases the throughput of a single user by employing the unique, antenna-specific CIRs of the array elements. SDMA arrangements [31] are closely related to the SDM technique. As opposed to SDM, it shares the total throughput among the supported users to maximise the number of supported users. The family of space-time block coding (STBC) [115] and space-time trellis coding (STTC) [119] techniques aim to maximise the possible diversity gain [118]. Finally, the objective of beamforming is to alleviate the effects of interfering users roaming in the vicinity of the preferred user [122]. Here the received signals of the users are angularly separable.

Table 2.4: Four main MIMO applications in wireless communications [4]

Space-division multiplexing (SDM) systems [113]	SDM systems use multiple antennas to increase the throughput of a wireless system in terms of the number of bits per symbol that can be sent by a specific user in a known bandwidth at a given integrity.
Space-division multiple access (SDMA) [31, 114]	SDMA supports multiple users within the same frequency band and/or time slot. It uses unique, user specific "spatial signatures", i.e. the CIRs of the individual users for distinguish among them. The CIRs need to be adequately dissimilar and precisely measured.
Spatial diversity (STBC [115–117], STTC [116, 118, 119]) and space-time spreading (STS) [120, 121]	In spatial diversity methods, such as space-time block or trellis codes [118] the multiple antennas are located as far apart as possible as opposed to the $\lambda/2-$spaced phased array elements of beamforming. Therefore, the transmitted signals of different antennas can experience independent fading, leading to maximum achievable diversity gain.
Beamforming [122]	Smart antennas using beamforming are used to lessen the effects of cochannel interference and to provide beamforming gain. To certain a spatially selective transceiver beam, $\lambda/2-$spaced antenna elements are used.

A. Space-division multiple access (SDMA)

In space-division multiple access (SDMA), the direction (angle) is used as another dimension in the signal space. The direction can be channelised and assigned to different users. This is usually performed by directional antennas, as depicted in Figure 2.11. Only if the angular separation between the users surpasses the angular resolution of the directional antenna, can the orthogonal channels be assigned to users. If directionality is acquired by employing an antenna array, the exact angular resolution needs a large array. However, this may be impractical for the AP and is indeed not viable in small user terminals. Practically, sectorised antenna arrays are exploited in implementing SDMA. In these arrays, the angular range of 360^o is divided into K sectors. There is high directional gain in each sector and small interference between sectors. For mobile stations, SDMA should be able to adapt as user angles change; or, if directionality is attained using sectorised antennas. So, when a user moves out of its initial sector, it should be handed off to a new sector. A more detailed discussion is presented later in Section 2.6.1.

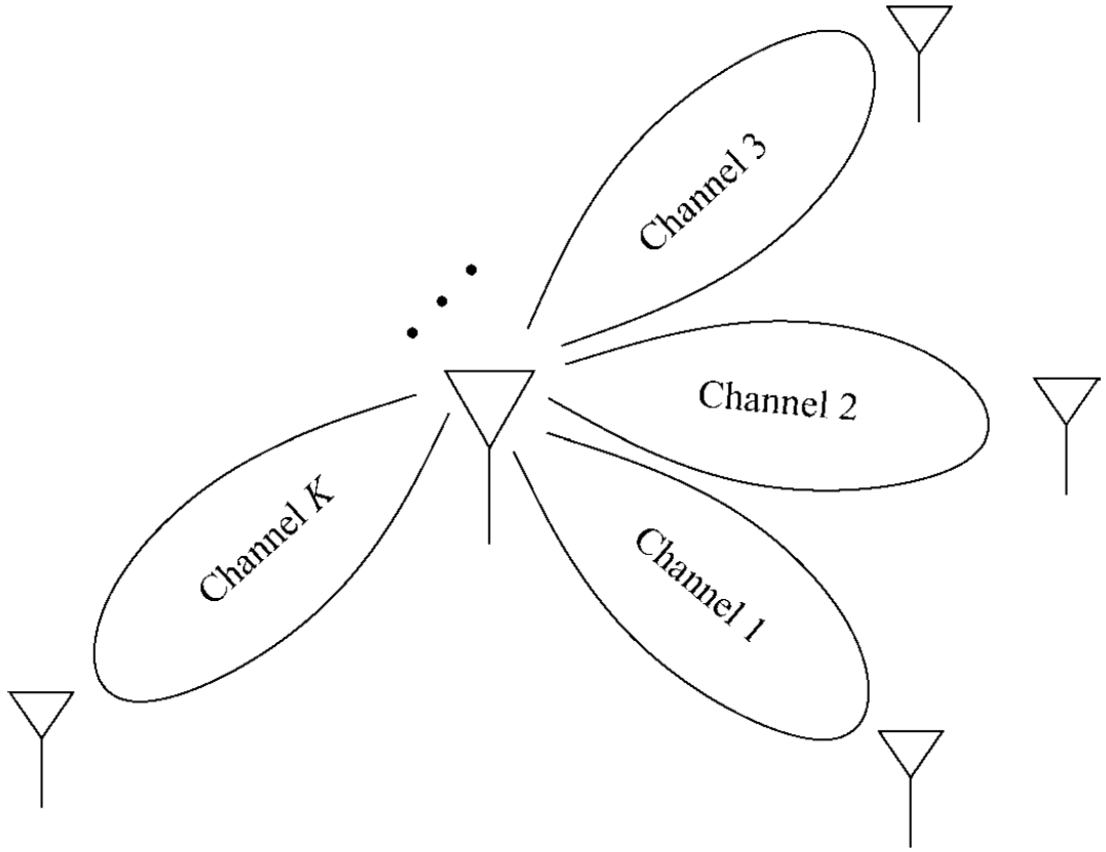

Figure 2.11: Space-division multiple access (SDMA) [5].

B. Spatial multiplexing (SM)

Spatial multiplexing, often referred to as V-BLAST (vertical-bell labs space-time architecture) in the literature [123, 124], is a transmission algorithm which is only possible in MIMO systems. This implementation approach can be considered as a special class of STBCs. SM transmits streams of independent data over different antennas, consequently offering a linear increase in the transmission rate for the same bandwidth, with no additional power expenditure required [6, 123].

The concept of SM is illustrated in Figure 2.12. First, at the transmitter a high-rate bit stream (left) is broken down into three independent-rate bit sequences. Then, they are transmitted simultaneously via multiple antennas. Hence, only one-third of the nominal spectrum is consumed and it leads to three-fold improvement in spectral efficiency. Since the signals use the same frequency spectrum, they are launched and mixed together in the wireless channel as expected. At the receiver, the mixing channel matrix is identified through training symbols. Subsequently, the

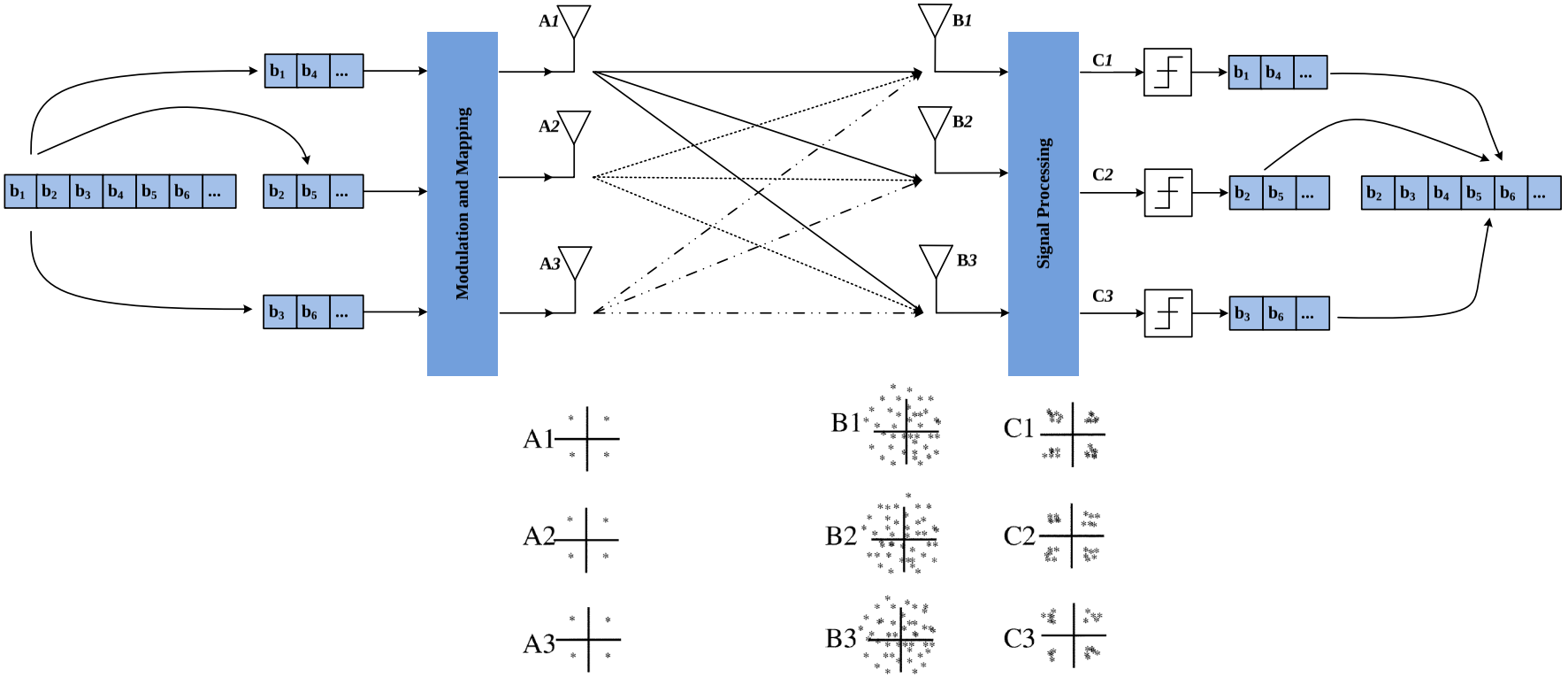

Figure 2.12: Spatial multiplexing for a three transmitter and three receiver antenna yielding three-fold spectrum efficiency improvement. Ai, Bi, and Ci show the signal constellation for the three inputs at the different phases of transmission and reception [6].

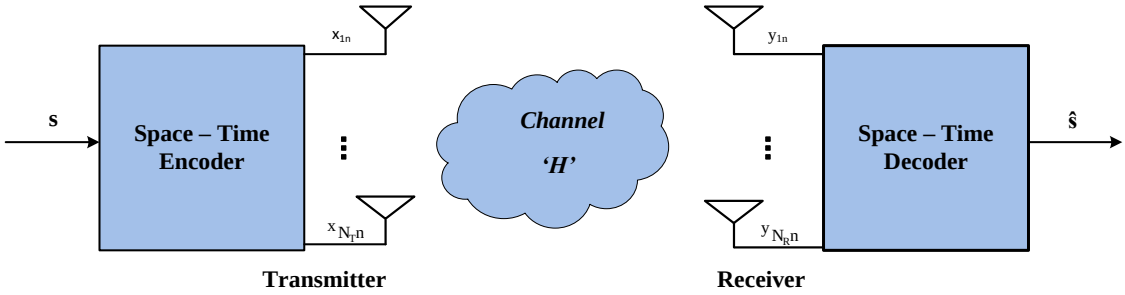

Figure 2.13: Generic space-time coding system.

individual bit streams are separated and estimated in the same way as the three unknowns are determined from a linear system of three equations.

A potential separation can only be achieved if the equations are independent. Each receiver antenna should be able to adequately see different channels and thus detect and merge the bit streams together to yield the unique high-rate signal. As proposed in [125], iterative versions of this detection algorithm can be employed to enhance performance.

C. Space-time coding

Space-time coding is a promising signalling technique that supports reliable communications over the shared air interface, by using multiple antennas at the transmitter and receiver. The data transmission in an ST system is carried out in two dimensions, the space dimension and the time dimension as the acronym ST implies. The space dimension is spanned by multiple transmit antennas while the time dimension is spanned by multiple time intervals over which multiple blocks are transmitted.

As depicted in Figure 2.13, an ST system employs an ST encoder at the transmitter and an ST decoder at the receiver. The ST encoder converts one-dimensional block transmissions into two-dimensional ST transmissions. Let S be the signal constellation to which the information symbols belong. It takes a block of $s \in S^{N_s \times 1}$ of N_s information symbols as inputs and outputs a space-time unique code matrix $\mathbf{X}$. The ST coding process can be viewed as a one-to-one mapping from s to X.

N_T transmitted signals corrupted by fading and additive noise are collected by each of the N_R antennas at the receiver. The ST decoder is employed at the receiver to recover $\mathbf{X}$ and s from $\mathbf{Y}$ which is the received signal. Similarly, the decoding process can be theoretically explained as a mapping from $\mathbf{Y}$ to $\mathbf{X}$ or s. However,

the implementation of ST systems highly depends on the availability of CSI [126].

2.4.5 Major research contributions on MIMO literature

This section presents a literature review of the key findings on MIMO systems. The major contributions reported in the MIMO literature are summarised in Tables 2.5 and 2.6.

Table 2.5: Major research contributions in MIMO (part 1) [4]

Year	Author(s)	Contribution
1984-1987	Winters [127–130]	Introduction of a mechanism to transmit information from multiple users over the same frequency/time channel using multiple antennas at both the transmitter and receiver
1985	Salz [131]	Investigation on optimization of joint transmitter and receiver employing MMSE principles
1992	Duel-Hallen [132]	Study of MMSE linear and decision feedback equalizers (DFEs) for MIMO systems with ISI
1993	Cheng and Verdu [133]	Study of capacity region of a two-user Gaussian multi-access channel with lSI
1994	Winters, Salz and Gitlin [134]	Examination of the impact of spatial diversity on the capacity of communications systems
	Yang and Roy [135, 136]	Investigation of optimisation of joint transmitter and receiver for MIMO transmission systems with decision feedback
	Winters and Salz [137]	Study of upper bounds on the BER of optimum combining in wireless communications systems with multiple cochannel interferers
1996	Raleigh nd Cioffi [109, 110]	Derivation of a model for the MIMO, dispersive, spatially selective wireless communications channel
	Foschini [113]	Invention of the Bell laboratories layered space-time (BLAST) architecture for wireless communication in a fading environment when employing multiple antennas at the transmitter and the receiver
1998	Tarokh, Seshadri and Calderbank [119]	Introduction of STTC technique
	Alamouti [115]	Introduction of STBC technique
	Winters [138]	Study of the diversity gain of transmit diversity to offer diversity advantage to a receiver in a Rayleigh fading environment
	Foschini and Gans [13]	Theoretical and numerical estimation of the limits of bandwidth proficient deliverance of high bit rate digital signals in wireless communications systems when multi-element arrays (MEAs) are employed
1999	Telatar [105]	Investigation of the use of MIMO systems for single user communications over additive Gaussian channels
	Foschini *et al.*	Investigation of a simplified, highly spectrally efficient space-time communications processing method

Table 2.6: Major research contributions in MIMO (part 2) [4]; from year 2007 onwards information is added by the author

Year	Author(s)	Contribution
2000	Lu and Wang [139]	Study of the applications of multi-user detection methods to STC system
2002	Kung, Wu, and Zhang [140]	Analysis on the design of Bezout space-time precoders and equalizers for MIMO channels
2003	Petre *et al.* [141]	Design of an ST block coded, single-carrier block transmission, direct-sequence-CDMA transceiver
2004	Zhang *et al.* [142]	Introduction of an MIMO model of single frequency network structure
	Zhu and Murch [143]	Proposal of a layered space-frequency equalization architecture for a single-carrier MIMO system over frequency-selective channels
2005	McKayand Collings [144]	Derivation of capacity and coded bit-error rate performance of MIMO with bit-interleaved coded modulation ZF receivers
2007	Balakumar, Shahbazpanahi, and Kirubarajan [145]	Investigation of channel tracking in MIMO systems for time-varying channels
2008	Koike-Akino and Toshiaki [146]	Investigation on a recursive least squares (RLS) channel estimation method in MIMO mobile communications for fast fading channels
2009	Kho and Taylor [147]	Development of a sequence-based MIMO receiver including channel estimation and tracking for frequency selective channels
2010	Chen and Su [148]	Proposal of iterative methods in estimating static and time-variant channels in MIMO systems
2011	Arablouei and Dogancay [149]	Development of a modified RLS method enhancing the tracking capability for channel estimation in MIMO systems
2012	Rupp [150]	Proposal of a robust design of adaptive equalizers

2.5 MIMO-OFDM

An immense amount of research interest has recently been concentrated on the modulation techniques that exhibit a high potential to satisfy the challenging requirements such as high data rates, imposed by the rapidly evolving wireless communications applications including wireless multimedia, wireless Internet access, and future-generation mobile communication systems. OFDM is a promising digital modulation scheme to simplify the equalization in frequency selective channels and provide simpler implementations [33, 55]. As detailed in the previous section, MIMO communications technology, can achieve significant increases in the channel capacity [6, 25, 111, 123]. Therefore, the combination of OFDM with MIMO communications,

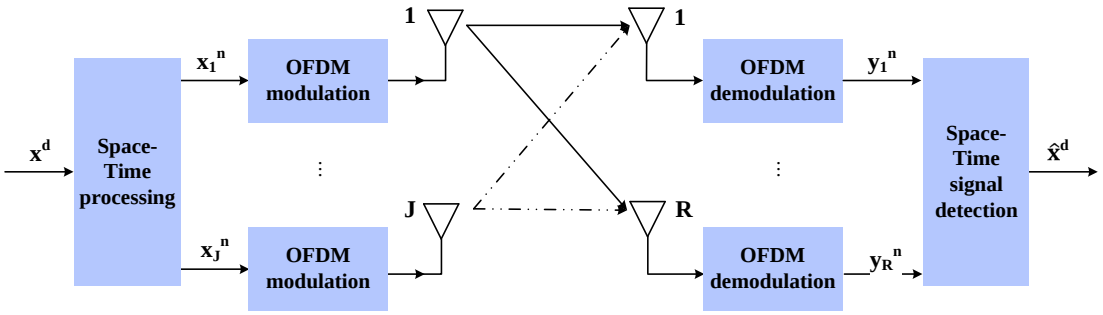

Figure 2.14: MIMO-OFDM system.

which is MIMO-OFDM systems, can realise high-performance transmissions [14, 25, 111, 151, 152]. Although, multi-path propagation causes frequency selectivity in broadband wireless channels, most MIMO systems are used for channels with flat fading. Therefore, the MIMO-OFDM technique has initially been proposed to use OFDM to alleviate ISI in MIMO systems and found to be a propitious selection for high data rate wireless broadband communications.

The capability of OFDM systems to cope with highly time-variant wireless channel characteristics explains the rapid employment of OFDM systems in the latest wireless communications systems. However, as stated in [26], systems knowledge pertaining to the channel conditions encountered is crucial in achieving high capacity and the realisable integrity of communication systems. Therefore, the provision of an accurate and efficient channel estimation approach is a critical feature in accomplishing high performance wireless systems.

2.5.1 MIMO-OFDM system

Figure 2.14 shows a MIMO-OFDM system with J transmit antennas and R receiver antennas. The module space-time processing performs the space-time methods developed for flat fading channels. It actually, processes the signals of the space-frequency domain in MIMO-OFDM, although it is called space-time processing [15]. The transmitted data stream or symbol $\mathbf{x^d}$ is converted into J sub-streams $\mathbf{x_j^n}$ via a simple multiplexing method or STC in the ST processing module. Then, OFDM modulation is performed and the data is transmitted through J different antennas. If the cyclic prefix is long enough and a multi-path wireless channel is considered, the demodulated received signal at each receiver antenna $\mathbf{r}$ ($\mathbf{r} = i, \ldots, R$) will be a superposition of those from different transmit antennas $\mathbf{j}$ ($\mathbf{j} = 1, \ldots, J$). It can be

expressed as [153]:

$$\mathbf{y_r^n} = \sum_{j=1}^{J} \mathbf{H}_{r,j}{}^{n} \mathbf{x_j^n} + \mathbf{z_r^n}, (\mathbf{n} = 1, 2, \ldots, N) \tag{2.11}$$

where $\mathbf{H_{r,j}^n}$ is the frequency response of the channel between the j^{th} transmitter and r^{th} receiver antenna at AP observed on the n^{th} OFDM subcarrier, $\mathbf{z_r^n}$ is the impact of channel noise at the n^{th} subcarrier of the r^{th} receiver antenna, which is typically independent from n or r, Gaussian with zero mean and N is the number of OFDM subcarriers. Equation (2.11) can also be expressed in matrix form as:

$$\mathbf{Y}^n = \mathbf{H}^n \mathbf{X}^n + \mathbf{Z}^n \tag{2.12}$$

where$\mathbf{Y}^n$, $\mathbf{H}^n$, $\mathbf{X}^n$ and $\mathbf{Z}^n$ are the received signal vector, channel matrix, transmitted signal vector and noise vector at the n^{th} subcarrier in the frequency domain, respectively and are defined as:

$$\begin{aligned}
\mathbf{Y}^n &= [Y_1^n, Y_2{}^n, \ldots, Y_R{}^n]^T \\
\mathbf{X}^n &= [X_1^n, X_2{}^n, \ldots, X_J{}^n]^T \\
\mathbf{Z}^n &= [Z_1^n, Z_2{}^n, \ldots, Z_R{}^n]^T \\
\mathbf{H}^n &= \begin{pmatrix} H_{11}^n & \cdots & H_{1J}^n \\ \vdots & \ddots & \vdots \\ H_{R1}^n & \cdots & H_{RJ}^n \end{pmatrix}
\end{aligned} \tag{2.13}$$

2.5.2 Major contributions in MIMO-OFDM literature

This section presents a literature review of the key findings on MIMO-OFDM systems. The major contributions found in the MIMO-OFDM literature are summarised in Tables 2.7 and2.8.

2.6 Multi-user MIMO technology

Wireless MIMO systems have attracted attention from both the academic and the industrial communities. Recently, the expansion of MIMO systems to employ multiple users (multi-user diversity) has been a topic of key interest, mainly motivated by the need of recognising the network capacity enhancements resulting from the use of MIMO technology. As explained above (Section 2.4), MIMO systems deploy

Table 2.7: Major research contributions in MIMO-OFDM (part 1) [4]

Year	Author(s)	Contribution
1999	Li, Seshadri, and Ariyavisitakul [153]	Investigation of channel estimation for OFDM systems with transmitter diversity using space-time coding
2001	Blum *et al.* [154]	Study of improved STC methods for MIMO-OFDM systems
2002	Li [155]	Proposal to improve the performance and reduce the complexity of channel parameter estimation in MIMO-OFDM systems by designing an optimum training sequence and simplified channel estimation method
	Bolcskei, Gesbert, and Paulraj [156]	Study of capacity behaviour of OFDM-based spatial multiplexing systems for the case where the CSI is unknown at the transmitter and known at the receiver
	Sampath *et al.* [14]	The first MIMO-OFDM system field tests to substantiate the performance of the MIMO-OFDM communications system
	Piechocki *et al.* [157]	Performance evaluation of SM and space-frequency coded modulation techniques
	Doufexi *et al.* [158]	Evaluation of performance in outdoor MIMO-OFDM channels using ST processing methods
2003	Bolcskei, Borgmann, and Paulraj [159]	Study of the impact of the propagation environment on the performance of space-frequency coded MIMO-OFDM systems
	Barhumi, Leus, and Moonen [160]	Proposal of an LS channel estimation scheme for MIMO-OFDM systems using pilot tones
	Cai,Song and Li [160]	Study of Doppler spread estimation in Rayleigh fading channels for mobile MIMO-OFDM systems
	Leus, and Moonen [161]	Development of a tone-by-tone based equalizer for MIMO-OFDM systems
	Piechocki *et al.* [162]	Development of a joint detection and channel estimation technique for ST coded MIMO-OFDM systems
2004	Stber *et al.* [25]	Summary of a variety of research challenges in MIMO-OFDM system implementation
	Shin, H. Lee and C. Lee [163]	Suggestion of a cyclic combo-type training structure for channel estimation while reducing mean squared error (MSE) at edge subcarriers in MIMO-OFDM
	Butler and Collings [164]	Proposal of an approximate log-likelihood decoding technique based on a zero-forcing MIMO-OFDM receiver with bit-interleaved coded modulation
	Zeng and Ng [165]	Suggestion of a subspace-based blind method for channel estimation for multi-user MIMO-OFDM uplink system
	Baek *et al.* [166]	Discussion of a time-domain semi-blind channel estimation method in MIMO-OFDM systems
2005	Yang [167]	Review of the state of the art techniques in MIMO-OFDM physical layer

Table 2.8: Major research contributions in MIMO-OFDM (part 2) [4]; from year 2007 onwards information is added by the author

Year	Author(s)	Contribution
2005	Ma *et al.* [168]	Design of pilot symbol based modulation for carrier frequency offset (CFO) and channel estimation in OFDM transmissions over MIMO frequency-selective fading channels
	Kim *et al.* [169]	Suggestion of a joint data detection and channel estimation algorithm employing QR decomposition-M algorithm and Kalman filter
	Qiao *et al.* [170]	Proposal of an iterative LS channel estimation algorithm in MIMO OFDM systems
2006	Bolcskei [171]	Overview of a variety of aspects in MIMO-OFDM technology
	Cicerone, Simeone, and Spagnolini [172]	Investigation of advantages of using a priori information about the multi-path channel on the performance of channel estimation in MIMO-OFDM systems
	Kashima, Fukawa, and Suzuki [173]	Suggestions of maximum a posteriori probability (MAP) receivers for MIMO-OFDM communications with a channel coding
2007	Jiang and Hanzo [4]	State of the study of multi-user MIMO-OFDM systems
	Zamiri-Jafarian and Pasupathy [170]	Design of an improved LS based channel estimation method by employing the noise correlation in MIMO-OFDM systems
2010	Lui *et al.* [174]	Design of a minimum-complexity channel estimation method for MIMO-OFDM systems
2011	Yoon and Moon *et al.* [175]	Development of a soft decision driven sequential channel estimation algorithm for pipelined turbo receivers in MIMO-OFDM systems
2012	Chen, Yang and Liao [176]	Suggestion of a channel estimation algorithm employing a Takagi-Sugeno (T-S) fuzzy-based Kalman filter under the time varying velocity of the mobile station in a MIMO-OFDM system

multiple antennas at the transmitter and receiver to use the new dimension known as *space*. The exploitation of this new dimension in communications can be addressed in two scenarios. In the single user setting, all the spatial dimensions (antennas) are allocated to one user to achieve higher rates, where as all the antennas are shared among several users in the multi-user scenario. The latter is referred to as multi-user MIMO (MU-MIMO) system. Since channel gains change over time due to fading and mobility, this system only selects the users with good instantaneous channel conditions for the signal transmission.

Standardised wireless local loop (WLL), wireless local area network (WLAN), wireless metropolitan area network (WMAN), and more recently wireless regional area network (WRAN) technologies have been considered to provide terrestrial fixed

wireless multiple access for rural areas. However, these standard technologies achieve a spectrum efficiency of less than 6 bits/s/Hz/cell [16]. Therefore, to simultaneously serve every user in a cell with high data rates, either a wide frequency spectrum or an excess of access points would be required.

With multi-user MIMO, the AP is equipped with multiple antennas to serve sparsely distributed user terminals with a single antenna using the same bandwidth. This approach facilitates the allocation of a wider bandwidth for each user, thus giving them access to faster data rates. Suzuki et al. [18,19], show that the spectrum efficiency can be enhanced linearly as a function of the number of antenna elements at the AP. This can be delivered without increasing the total transmitted power and, in predominantly LoS environments. A uniform circular array at the AP and a low-complexity zero-forcing (ZF) pre-coding based downlink are used to achieve this task [18]. MU-MIMO transmission techniques can achieve high data rates with the use of advanced signal processing and coding. The next generation of cellular systems supports spectral efficiencies in the 10's of bits/sec/Hz [177,178], by employing high-rate data-oriented downlink schemes with MU-MIMO transmission technology. These methods are implemented in the "Ngara wireless broadband access" solution [17] and are the basis for the research presented in this thesis.

There are two communication problems to be considered: downlink, that is the communication from the access point to multiple users, such as when a user downloads data from the Internet, and uplink, that is the communication from the user terminals to the same AP such as when users upload data to an Internet host. In single-user MIMO channels, the advantage of MIMO processing is achieved from the correlation of processing among all the transmitters or receivers. No correlation between the users is a common assumption in the multi-user channels [179].

As shown in Figure 2.15, for the uplink, the challenge is the processing done by the access point to separate the signals transmitted by the users, by employing techniques such as MUD and array processing. By employing an adaptive transmission and efficient resource-allocation scheme in the multi-user MIMO-OFDM system, the performance of the uplink can be considerably enhanced. Centrally, the AP decides not only the optimal bit loading and subcarrier allocation, but also the transmit antenna selection from multiple users based on the CSI of the system, in uplink scenarios [180]. In this thesis, our focus is on the uplink channel signal processing. In practice, the corresponding downlink channel processing needs to be implemented. For time division duplex systems, channel reciprocity may be utilised to derive the downlink channel from the uplink channel (which may be tracked or predicted). However, this is out of the scope of this thesis and is left for future works.

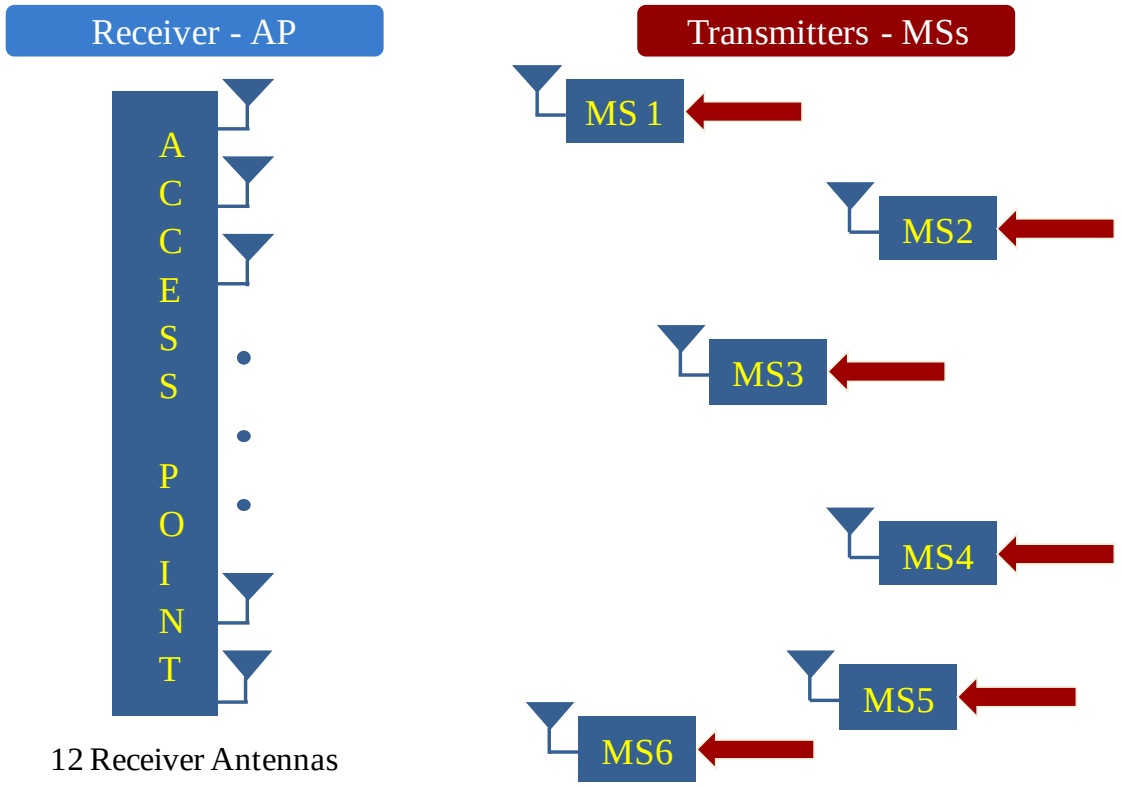

Figure 2.15: Illustration of the uplink of the multi-user MIMO system.

2.6.1 SDMA-based MIMO OFDM systems

As explained above (Section 2.4.4), SDMA is a sub-category of MIMO systems. Recently, the SDMA-based methods [31,181,182] have attracted considerable interest and SDMA has become one of the most capable mechanisms to resolve the capacity dilemma of wireless communications systems. SDMA enables multiple users to simultaneously share the same frequency bandwidth in diverse geographical areas. Specifically, this method uses a spatial dimension called the spatial signature which makes it feasible to recognize the individual users, even though they can be in the same time/frequency/code domains. This yields increased capacity of the system. The concept of the SDMA is illustrated in Figure 2.16. Here, a P-element receiver antenna array is exploited to support each MS having a single transmitter antenna, so that all MS can simultaneously communicate with the AP. As the transmit antennas belong to different users, the transmissions of the multiple transmit antennas cannot be coordinated and therefore, the SDMA technique can be considered as an explicit division of the group of MIMO systems. The main benefits of SDMA techniques

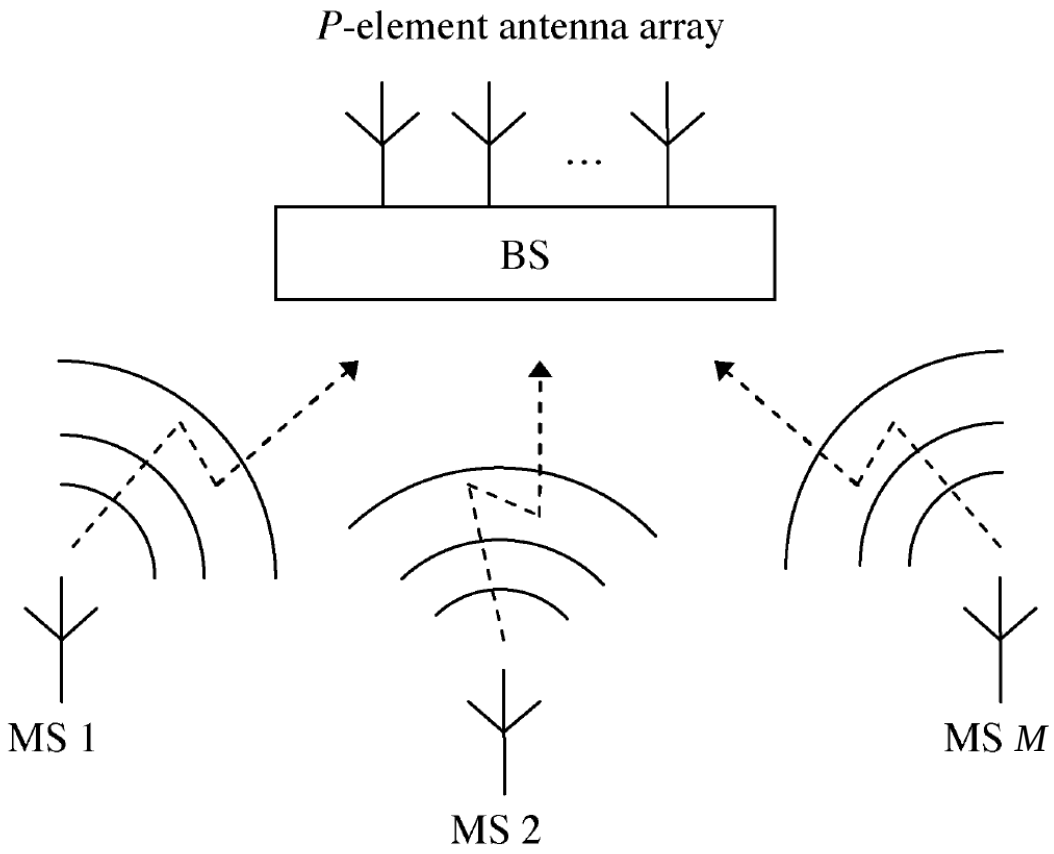

Figure 2.16: Schematic diagram of an SDMA system using a P-element receiver antenna array for communicating M number of MSs.

are as follows [4]:

- Range extension: Since an antenna array is exploited, the coverage area of high-reliability reception can be considerably larger than that of any single-antenna based systems. The number of cells essential for covering a specified geographical area can be significantly decreased with SDMA systems. For instance, a gain of ten can be achieved by a 10-element array, which usually doubles the radius of the cell and, therefore, quadruples the coverage area.

- Multi-path mitigation: As explained previously, with the advantages of MIMO architecture, SDMA systems effectively mitigate the negative effects of multi-path propagations. Additionally, by using efficient receiver diversity methods some precise cases of the multi-path propagation can even be used for improving the signals of desired users.

- Capacity increase: In theory, SDMA can be integrated with any existing multiple access technique while achieving a significant increase in capacity with only a limited amount of complexity. For example, by incorporating SDMA with a conventional time division multiple access (TDMA) technique, the same time slots can be shared by two or more users, yielding a doubled or higher capacity of the overall system.

- Interference suppression: The unique and user-specific CIRs of the desired user can be exploited in order to significantly reduce the interference caused by other systems and by users in other cells. Therefore, MAI is not considered in the study presented in this thesis.

- Compatibility: SDMA system are compatible with the majority of existing modulation methods, carrier frequencies and other provisions. Moreover, antenna types and different array geometries can be used to readily implement the SDMA technique.

The combination of SDMA and OFDM forms the SDMA-OFDM system [31, 181, 183, 184] which takes advantage of both SDMA and OFDM. This communications system has attracted more research interest [184–187] recently. SDMA supports multiple users within the same frequency band and/or time slot. It uses unique, user specific 'spatial signatures", i.e. the CIRs of the individual users to distinguish among them. The CIRs need to be adequately dissimilar and precisely measured. Therefore, the developed time-varying channel model is random and different for each mobile station. The challenge in SDMA-based multi-user MIMO-OFDM systems is that it does not have a suitable channel tracking algorithm that can update time-varying, frequency selective MIMO channels. In this thesis, this issue is addressed.

2.7 Chapter summary

In summary, this chapter provided a detailed overview of multi-path fading and MIMO-OFDM wireless communications systems, assembling the necessary background to the findings of the present research. It also presented a thorough literature review on the fundamentals and recent advances of OFDM, MIMO and MIMO-OFDM systems explaining the basic theoretical concepts and advantages of these technologies. The next chapter presents a comprehensive literature review on adaptive equalization, channel estimation and channel tracking.

Chapter 3

Fundamentals on Adaptive Equalization, Channel Estimation and Channel Tracking

3.1 Introduction

In a typical multi-user environment, a signal transmitted from an MS to an AP is subjected to a range of impairments. Communication in wireless channels is limited primarily by multi-path fading which introduces ISI. Moreover, the delay spread of the signal, which is the maximum time delay occurred, will change as the environment changes. When the delay spread is smaller than a symbol period, the distortion is called flat fading. The frequency selective fading occurs when the delay spread is larger than a symbol period. Information transfer is severely limited at the deep fade frequencies. The fading occurs at selected frequencies, and is therefore called frequency selective fading. On the other hand, the signal quality suffers from the time-varying fading by the introduction of a random amplitude and a phase shift to the transmitted signal. The channel is said to be time-varying, when the transmitter or the receiver is mobile or the channel is rapidly changing due to environmental conditions. Figure 3.1 shows an example of a simulated time-varying, frequency selective mobile OFDM communications channel where the subcarrier index is in the frequency domain and the OFDM symbols represent the time domain.

Identifying the information about the channel is necessary to recover the transmitted signal at the receiver. This process is known as *channel estimation*. The removal of the channel effects is referred to as *equalization* [31]. It is significant to keep a track of the activity in the channel by generating updates of the channel estimates. This process is called *channel tracking*.

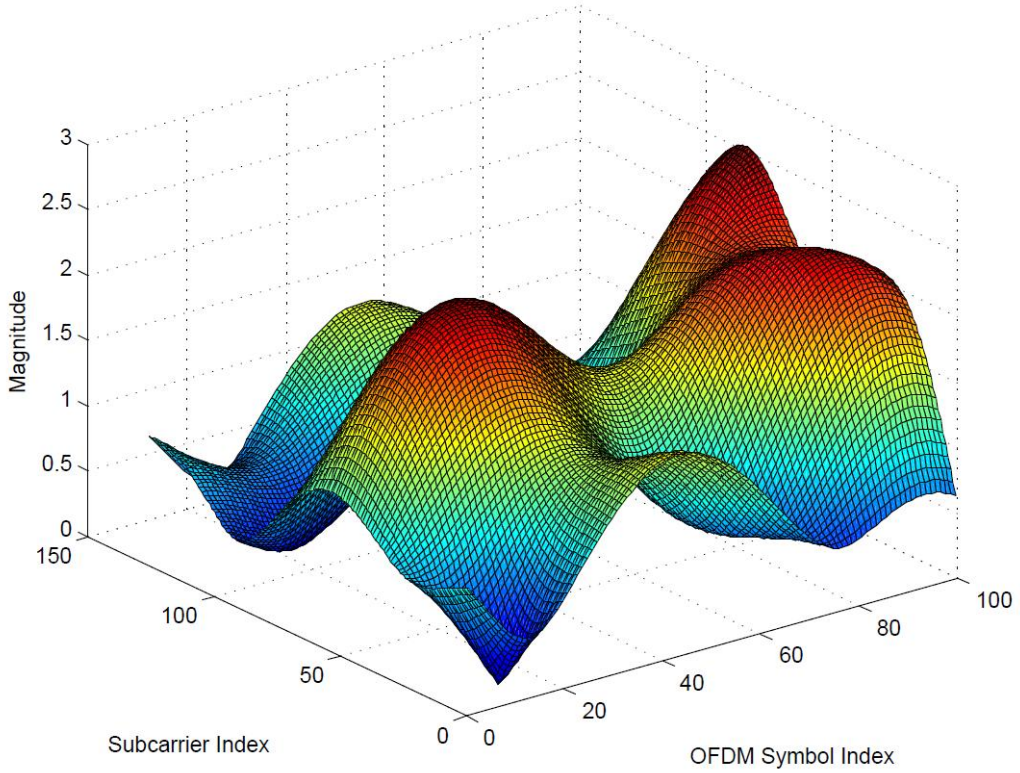

Figure 3.1: OFDM simulated time-varying, frequency selective channel.

Channel estimation and tracking algorithms for SDMA-based MIMO-OFDM systems have a strong influence on the development of new wireless systems because CSI is needed to detect the transmitted symbols at the receiver especially when the channel is time-varying. This chapter provides a comprehensive review of the literature on recent and relevant channel estimation and tracking algorithms developed for MIMO-OFDM systems. The chapter performs a key role in the literature survey discussing channel equalization, estimation and tracking. The outline of this chapter is shown in Figure 3.2.

3.2 Adaptive equalization (AE)

Digital signal processing (DSP) based equalization has been widely recognised in a variety of applications in voice, data and video communications using different transmission media. The function of an equalization scheme at the receiver is to compensate for impairments of the transmission channel like the ISI produced by

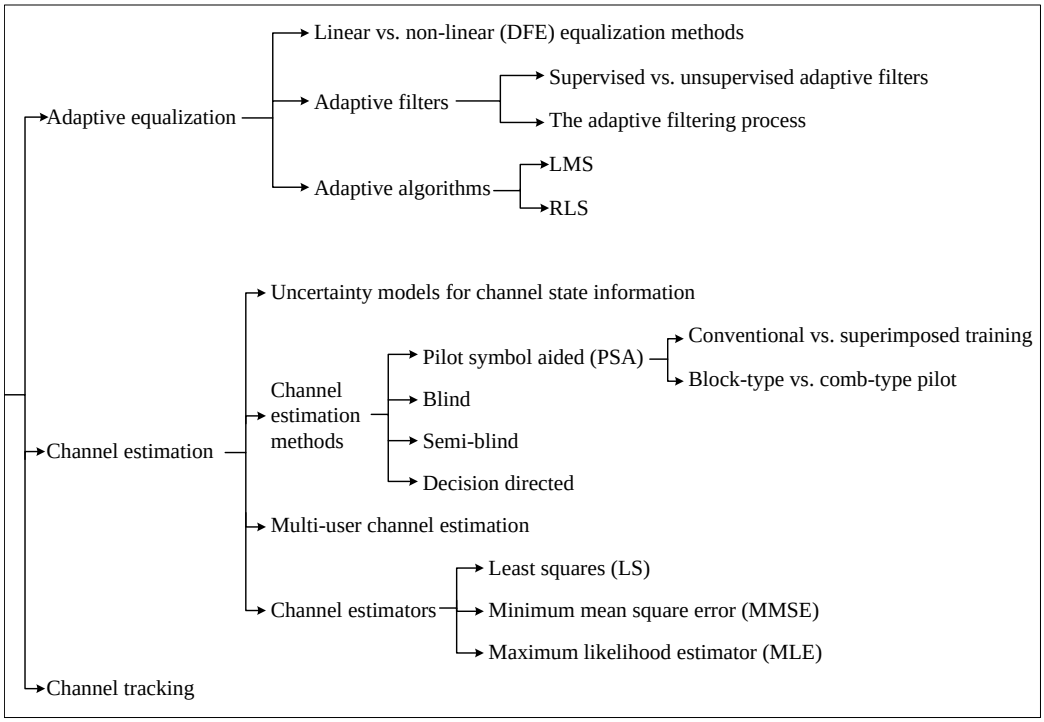

Figure 3.2: Outline of Chapter 3.

multi-paths within time-dispersive channels. It improves link performance in hostile environments.

The channels are characterised by a channel transfer function in which particular frequency components of transmitted signals are uniquely attenuated and uniquely delayed. The channel coefficients and their statistics are generally unknown and time-varying. The temporal variations change the channel coefficients even after the initial estimation. The equalizer must track or recursively update the time-varying channel characteristics and, therefore, is called an *adaptive equalizer*.

3.2.1 Linear and non-linear equalization methods

The two main types of AE are *linear* and *non-linear* which are determined by how the AE output is used for successive control (feedback) of the AE. The linear equalizers do not employ a feedback path to adopt the equalizer and therefore provide simpler implementations. The non-linear equalizers such as the DFE are widely employed in wireless applications where the channel distortions are too critical for a linear equalizer to manage. The non-linear DFE is significant because when an information symbol has been detected and decided on, the ISI that it

causes on future symbols can be estimated and subtracted out before detection of successive symbols [9].

A low complexity DFE was designed in [188] to decrease the effects of variations in the channel. In that study, a small matrix of main CSI was used to recursively compute the inversion of the matrix while considerably reducing complexity. Consequently, it was suggested that the method was suitable for consumer terminals. However, their research did not take multi-user scenarios in MIMO channels into account.

In [189], Gupta and Saini presented an STBC structure in MIMO-OFDM systems. They investigated the BER performance of STBC along with different equalizers such as ZF, DFE and ML in the frequency domain and then suggested the optimum equalization method. The simulations were performed for 2×1 and 2×2 transmit-receive antennas in both frequency selective and flat channels. They stated that their proposed method achieved simple implementation and complexity. However, it could not attain multi-path diversity nor a high data rate.

An AE operates in two modes: training and tracking [9]. First, the AE coefficients need to be trained in order to adapt to a proper value of minimum BER detection. This operation can be performed using three methods: the training sequence, blind, and semi-blind. The training data consists either of pilot symbols that are repeatedly multiplexed into the data stream, or of a training data block at the beginning of each packet, for packet transmission [24]. This method is widely used in current wireless communications systems as it shows high accuracy and low complexity. However, it introduces an overhead to the communication system and therefore, reduces spectrum efficiency. The equalizer is called 'blind' if the training sequences are not used. It depends on the structural properties of the received data. Although, it is bandwidth efficient, it requires the accumulation of a large amount of data. Semi-blind equalization, on the other hand, is based on a limited amount of pilot data in conjunction with blind algorithms. The semi-blind methods have three advantages over blind methods: the uncertainties inherent to blind methods can be resolved, convergence speeds are enhanced; and a more effective and robust tracking of time-varying channels is accomplished [190]. In addition, to compensate for the channel distortions, the AE uses an adaptive algorithm to evaluate the channel and adjust the filter coefficients recursively. A detailed description of the process of linear and DFE adaptive equalizers can be found in Chapter 5 (Section 4.4).

The MIMO channels are tracked mostly using an adaptive filter. The adaptive filtering process and the most widely used adaptive filters in the channel tracking process are discussed next in detail.

3.2.2 Adaptive filters

An *adaptive filter* is a self-learning system that incorporates a recursive algorithm. The recursive algorithm is used to adjust the filter parameters or coefficients in an environment where the knowledge of relevant statistics is unavailable. When the signal entered into the filter continues, the adaptive filter coefficients adjust themselves to achieve the desired result such as identifying the response of an unknown system. Adaptive filters can be classified into two main groups: *linear* and *non-linear* adaptive filters. The former computes an estimate as a linear function of the available observations while the latter does not use a linear combination of the observations for the estimation.

A. Supervised versus unsupervised adaptive filters

Adaptive filters can also be categorised into *supervised* and *unsupervised* adaptive filters. The supervised adaptive filter uses a training sequence to obtain different realisations of a desired response of a particular input signal vector. Then, it compares the desired response and the actual response of the filter to obtain an error signal. Next, this error signal and the input signal vector are used to adjust the filter parameters. The parameter adjusting process is performed step by step until a steady-state condition is found.

The unsupervised adaptive filters do not use a desired response to perform filter parameter adjustments. Such a filter performs its function by specifying a set of rules in its design to analyse the input-output mapping with the precise required properties. The unsupervised adaptive filters are often referred to in the literature as blind adaptation or blind de-convolution filters.

B. An adaptive filtering process

The adaptive filter performs in two basic processes: a filtering process and an adaptive process. The filtering process first calculates the output of the filter, $\mathbf{y}(u)$, in response to an input signal, $\mathbf{x}(u)$. Then, it produces an estimation error, $\mathbf{e}(u)$, by comparing this output with a desired response, $\mathbf{d}(u)$, defined as:

$$\mathbf{e}(u) = \mathbf{d}(u) - \mathbf{y}(u) \tag{3.1}$$

The adaptive process then continuously adjusts the filter coefficients according to the estimation error, so that filter output, $\mathbf{y}(u)$ becomes as close as possible to a desired signal, $\mathbf{d}(u)$. As shown in Figure 3.3, the combination of these two processes working together constitutes a feedback loop.

When signal and noise spectral characteristics are unknown and time-varying, the

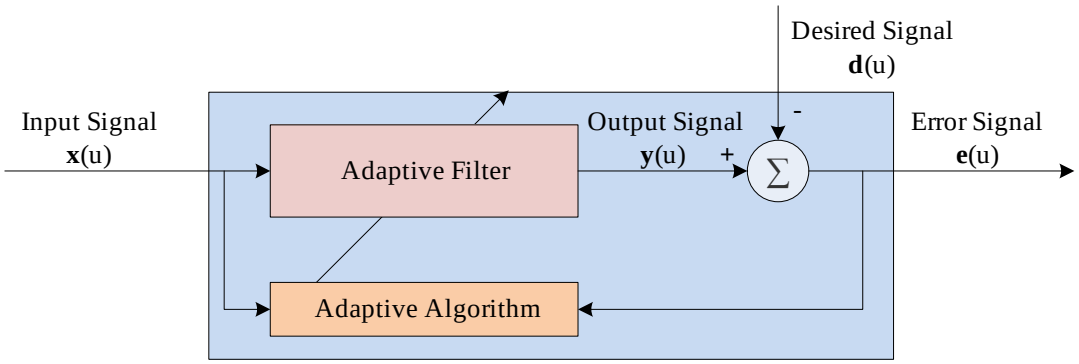

Figure 3.3: Block diagram of an adaptive filter.

adaptive filters adapt their frequency response appropriately. They are characterised by the filter structure and the coefficient update algorithm.

In [191], Liang et al. discussed a channel estimation method using adaptive filters in MIMO-OFDM systems. The proposed method estimated and tracked the time-varying channel coefficients by using pilot symbols and adaptive filters. Furthermore, prior knowledge of the channel statistics was not required. They verified that the proposed method using adaptive filters performed better than another method based on an LS algorithm. Moreover, they showed that the channel estimation using an LMS filter had lower computational complexity than that using an RLS filter. On the other hand, the channel estimation method using the RLS filter demonstrated better performance and faster convergence than using the LMS filter. Therefore, they concluded that a more suitable channel estimation method can be selected using different filters according to its characteristics. The most widely used adaptive algorithms in the MIMO communication system are discussed next.

3.2.3 Adaptive algorithms

A. Least mean square (LMS) algorithm

In 1959, Widrow and Hoff developed the ubiquitous LMS algorithm which was the first algorithm used to design a linear adaptive filter [192]. Since then, it has become one of the most widely used algorithms in adaptive filtering. The LMS algorithm is a stochastic gradient algorithm since it uses the gradient vector of the filter tap weights to converge to the optimal Wiener solution. It is widely used in adaptive signal processing due to its computational simplicity, simpler implementations, and

robust performance. Furthermore, it does not require measurements of the relevant correlation functions and matrix inversion. However, the LMS algorithm does not converge quickly and it is sensitive to the eigenvalue spread (i.e., the ratio of the largest eigenvalue to the smallest eigenvalue) of the correlation matrix of the input signal vector. The simplicity achieved in this algorithm has made it the benchmark, against which all other adaptive filtering algorithms are judged [193].

The LMS [194] adaptive algorithm is widely employed in MIMO equalization. In [194], Yapici and Yilmaz discussed the iterative channel estimation and tracking problem for time-varying frequency-flat fading MIMO systems. They employed the pilot symbol aided (PSA) technique to jointly estimate and track the time-varying multi-antenna channel. The MMSE filtering was used to further improve the error performance. Moreover, the computational complexity resulting from the MMSE filtering was reduced by introducing a low-complexity two-way LMS algorithm based on the forward-backward operation of the conventional forward only LMS algorithm. They showed that the two-way LMS had a near optimal error performance and better channel tracking potential than the conventional LMS algorithm with no significant complexity added. However, they does not consider the multi-user scenario or OFDM transmission system in their method.

B. Recursive least squares (RLS) algorithm

The LMS algorithm achieves simplicity of implementation by exploiting instantaneous estimates of the autocorrelation matrix of the input signal vector, and the cross-correlation vector between the input vector and the desired response. On the other hand, the RLS algorithm uses continuously updated estimates of these two measures, which go back to the beginning of the adaptive process [195]. Therefore, simulations for the proposed SDMA-based multi-user MIMO-OFDM adaptive equalizer, are conducted with LMS and RLS adaptive algorithms using the training sequence AE coefficients training method to achieve optimal performance through a comparative analysis. A more detailed discussion of the LMS and RLS AE is provided in Chapter 5 (Sections 4.4.3 and 4.4.4), respectively.

In [29], Mohammadi et al. derived a channel estimation method for a MIMO-OFDM receiver. First, they obtained an optimum training sequence based on the calculated MSE for the LS channel estimation. Then, adaptive channel estimation methods based on LMS and RLS were proposed, exploiting the training sequences derived to estimate the channel for a system which sends out independent data streams from the transmitter antennas. All sub-channel coefficients between a receiver antenna and all transmitters were estimated by these methods and the performance was computed by comparing LMS and RLS algorithms with the LS

algorithm. However, they did not consider the multi-user scenario in MIMO-OFDM systems and they simulated the performance only for a 2×2 MIMO system limiting the number of antennas, while our methods show performance for a 12×6 SDMA-based multi-user MIMO-OFDM system. Moreover, with their method, the BER reached 10^{-3} only when the SNR was equal to 40 dB, while the equalization method proposed in the present research reaches the same value of BER, when the SNR equals to 12 with a DFE. In the next sections, the literature on channel estimation and tracking is reviewed.

3.3 Channel estimation

3.3.1 Uncertainty models for channel state information

Time-variations of the channel and multi-path fading cause detrimental effects in wireless communications systems. In a typical communication system, the received power experiences deep fades within the time-frame related to receiver movements. Therefore, the communications system has to be able to reduce the fading effects, in order to achieve efficient transmission. If the current CSI is known in advance, the transceiver can re-allocate internal resources in a better way or alter the transmission scheme in anticipation of the future conditions. This can be achieved by predicting the CSI.

The full knowledge of the CSI is the knowledge required for the multi-user MIMO, for example, obtainable by sending and processing the training sequence, albeit corrupted by the noise. However, in most practical scenarios, the full knowledge of the CSI is never known *a priori*. Moreover, the channel estimate is not perfect due to noise, and the finite number of pilot symbols in a frame. In most typical communication setups, channel estimation of the CSI is executed at the receiver, using known pilot symbols and then employed in decoding if it is precise. Therefore, the performance depends on the quality of the channel estimate. The quality of the CSI can be classified into three different conditions, depending on the knowledge of the CSI at the receiver:

- Perfect CSI: The most commonly assumed situation is that perfect CSI is available at the receiver. The receiver has complete knowledge of the instantaneous channel realisation. Under these conditions, the detection of symbols is referred to as coherent detection.

- Imperfect CSI: The receiver may possess inaccurate knowledge about the parameters describing the channel. For example, the receiver may be informed

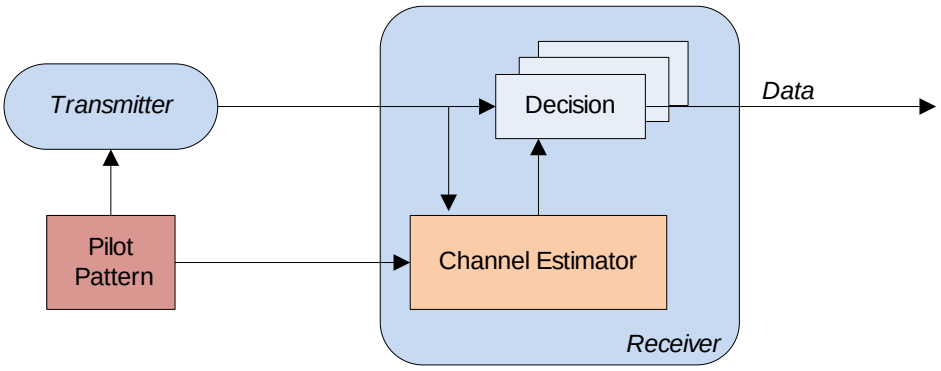

Figure 3.4: Pilot symbol aided estimation [7].

of the estimated channel matrix $\hat{\mathbf{H}} \neq \mathbf{H}$, with corresponding covariance error matrix $\mathbf{C}$. In that case the channel model that can be used is one in which the channel is a random matrix $\mathbf{H} \approx \mathbf{C}$.

- No CSI: The receiver may not possess any information about the values of the CSI, or its statistics. Under these conditions, the detection of symbols is referred to as non-coherent detection.

3.3.2 Channel estimation methods

The channel estimation methods can be categorised into four main groups: pilot-aided, blind, semi-blind and decision-directed. Pilot-aided algorithm schemes use a set of known symbols interleaved with data in order to acquire the channel estimate. Blind techniques, on the other hand, do not require any training data and use the statistical or structural properties of the signals. The semi-blind algorithm is a hybrid method that combines the blind estimation phenomenon with a limited amount of pilot data. The use of earlier estimations of the channel to detect data and apply it to estimate the channel in the last snapshot is called decision directing. These channel estimation methods are discussed in detail in the following sections.

A. Pilot symbol aided (PSA) channel estimation

Recently, there has been a growing interest in pilot symbol aided (PSA) MIMO channel estimation. The PSA channel estimation methods employ a pilot symbol or training sequence, known to the receiver, that is used to obtain an initial estimation of the channel parameters, timing, and frequency offset. These symbols are interleaved among the transmitted signal frame and sent through the channel.

Then, the channel is estimated using the received signal and the known pilot sequence, at the receiver (see Figure 3.4). PSA estimation algorithms are widely used in contemporary wireless communication systems, as they show high accuracy and relatively low computational complexity. However, they introduce overheads to the communication system by transmitting known pilot symbols and thus, reduce the spectrum efficiency.

Carvers in [196], invented the widely used pilot symbol aided modulation (PSAM) and presented an analytical approach to the design of pilot-assisted transmission (PAT) techniques. Tong et.al, in [197] presented an overview of the PAT system and discussed the channel estimation design criteria for recent wireless communication systems. However, to the author's knowledge, they did not analyse the channel estimation using PSAM for the particular case of multi-user in SDMA-based MIMO-OFDM systems.

Hassibi and Hochwald in [198] discussed how training affects the capacity of a multi-antenna fading channel without considering OFDM transmission. In particular, too little training leads to improperly learned channels and too much training yields no time left for data transmission before the channel changes. Therefore, they computed a lower bound on the channel capacity and maximised the bound as a function of the received SNR, fading coherence time, and number of transmitter antennas. Moreover, they gained the optimal number of pilot symbols showing the smallest training interval length that promised meaningful estimates of the channel matrix. Furthermore, they showed that the training-based schemes can be optimal at high SNR of 18 dB, but sub-optimal at low SNR of 6 dB.

In [199], Baek and Seo presented efficient pilot patterns and channel estimations for a high-rate MIMO-OFDM system. They proposed pilot patterns by using a basic orthogonal property of a unitary matrix and then used this orthogonal property to propose channel frequency response (CFR) and CIR estimations. They considered independent and suitably distributed two space-frequency coding encoders on multi-input single-output (MISO) OFDM systems of DVB-T2 to compare the results. The performance of the proposed channel estimation methods provided a low symbol error rate (SER) of 10^{-4} at an SNR of 25 dB when compared with the MISO-OFDM system channel estimation.

The pilot based channel estimation can be subclassified into four main categories. These are conventional pilot symbol versus superimposed training and the block-type versus comb-type pilot channel estimation, which are discussed as follows:

I. Conventional pilot symbol versus superimposed training

The PSA method can again be divided into two approaches, namely, the conven-

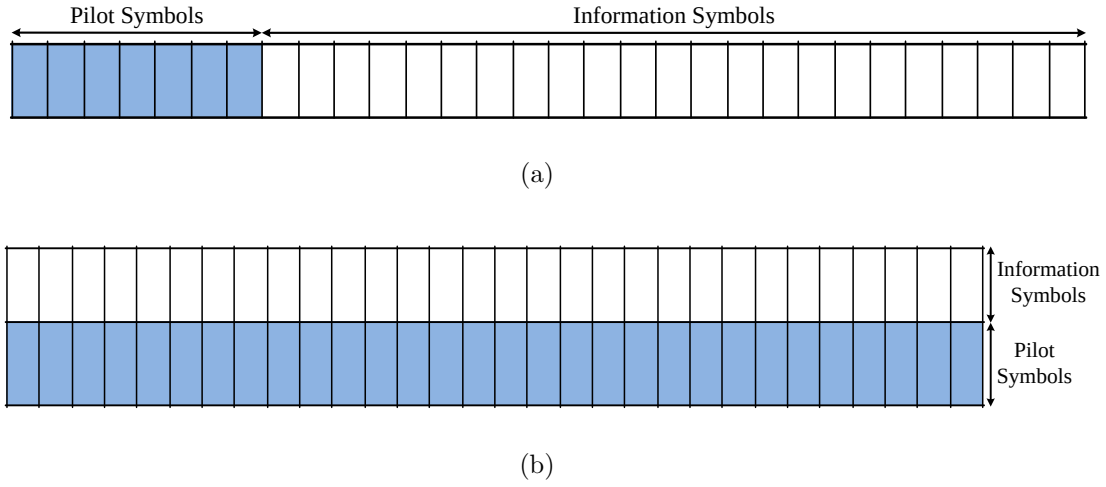

Figure 3.5: Schematic representation of channel estimation: (a) conventional pilot symbol, (b) superimposed training.

tional pilot symbol-aided and superimposed training. The difference between the conventional PSA and superimposed training channel estimation schemes are illustrated in Figure 3.5. The superimposed training scheme has recently gained research interest in channel estimation. In this method, the pilot signal is superimposed on the information signal. The complete transmitted frame can still be used to transmit information symbols. Therefore, the superimposed training scheme is more bandwidth efficient than the conventional pilot PSA scheme. However, the major drawback of this method is that some useful power, which could have been allocated for the transmitting information signal, is wasted in transmitting the superimposed training sequence. Moreover, this method is relatively more complex in decoupling the information/training signal at the receiver and orthogonal vulnerability of precoding and training matrices occurs.

II. Block-type versus comb-type pilot channel estimation

For OFDM systems, the channel estimation using the PSA approach can be further categorised into two methods: the *block-type* and *comb-type* pilot channel estimation [8]. In the block-type pilot channel estimation scheme, the pilot tones are inserted into all the subcarriers in an OFDM symbol, periodically (see Figure 3.6(a)). In this case, the coherence time of the channel must be much larger than the period of pilot insertion. This method assumes a slow fading channel condition to have

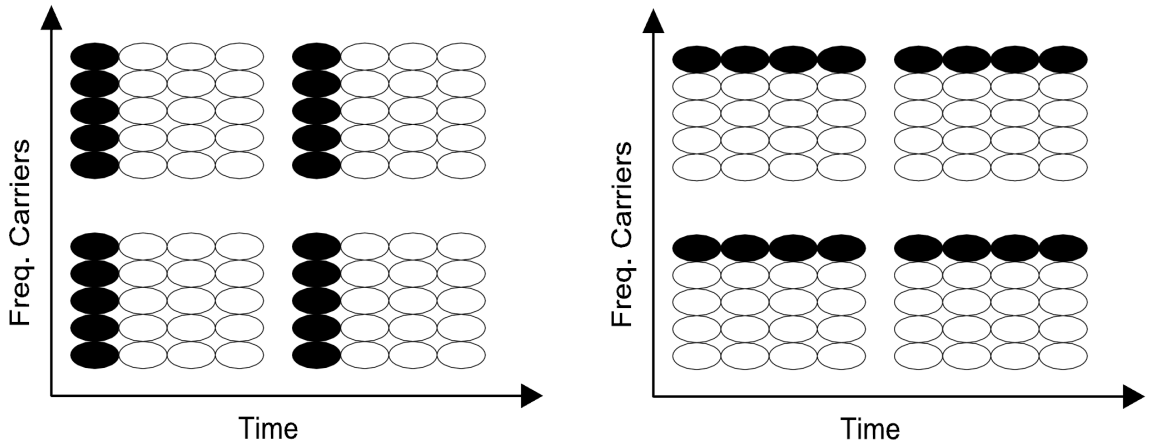

Figure 3.6: Pilot arrangements (a) block type (b) comb type [8].

an accurate channel estimation. In general, the estimation of the channel for this block-type pilot arrangement can be based on the channel estimators, LS [200] or MMSE [201], which will be discussed in detail later.

In the comb-type pilot channel estimation, the pilot tones are inserted into a number of subcarriers over the transmission time and use this estimation for a specific number of succeeding symbols (see Figure 3.6(b)). The total number of subcarriers is much larger than the number of pilot-inserted subcarriers. This method has been established in order to satisfy the need for equalizing when the channel changes even in one OFDM block. This method possesses algorithms to estimate the channel at pilot frequencies and to interpolate the channel. Moreover, the comb-type channel estimation can be based on LS, MMSE or LMS channel estimators. Usually, interpolation is used to estimate the CSI over the whole channel bandwidth, as the channel estimation is performed only for a certain number of subcarriers [202, 203].

Coleri et al., in [204] investigated the channel estimation methods for OFDM systems based on block-type and comb-type pilot arrangements. They studied channel estimation at pilot frequencies based on LS and LMS algorithms. A decision feedback equalizer was implemented for all OFDM subcarriers followed by periodic block-type pilots. Moreover, they evaluated the performances of all modulation schemes by measuring the BER with the 16-ary QAM, QPSK, differential-QPSK and BPSK as modulation schemes. Furthermore, multi-path Rayleigh fading and

auto-regressive based fading channels were used as channel models. Coleri et.al, argued that the comb-type pilot channel estimation with low-pass interpolation performed the best among all the channel estimation algorithms.

For OFDM systems, Liu et al., in [205] discussed a channel estimation algorithm based on the PSA method called as regression least square support vector machine (RLS-SVM). By obtaining the frequency responses of the positions of the pilot frequencies and the frequency responses between the carriers, they predicted the frequency responses of the positions of the subsequent OFDM sub-carriers by applying the RLS-SVM algorithm for the frequency selective multi-path Rayleigh fading channel model. They argued that, at the same transmission rate, the number of pilot frequencies in the RLS-SVM algorithm is less than in traditional algorithms. They stated that, therefore the RLS-SVM was far better than the others at the same SNR as the number of pilots decreased and the transmission efficiency improved. However, they did not analyse how the channel could be estimated for MIMO-OFDM systems or for the multi-user scenario of such a system. Therefore, multi-user MIMO communications based on OFDM systems seems to be an open area for the development of efficient channel estimation and tracking algorithms. The next sub-section discusses channel estimation using PSA for time-varying channel conditions.

Time-varying channel estimation using PSA

OFDM systems show performance degradation under time varying channels. The OFDM symbol duration should be increased as the delay spread increases. Consequently, OFDM systems become more vulnerable to time-variations, yielding inter-carrier interference (ICI). However, to improve the performance in high delay and Doppler spread environments, the ICI must be diminished. In slow time-varying environments, the variation in channel within each OFDM symbol is negligible, where by the channel is said to be quasistatic. This allows the independent estimation and equalization of fading in each subcarrier [206]. The estimation of quasistatic channels for MIMO-OFDM systems is investigated in [207, 208].

Hu et al., in [209] investigated the time-varying channel estimation methods for MIMO-OFDM systems based on pilot sequences. However, they assumed that the channel varied in a linear fashion during a block period. The CIR was expressed as a function of the middle impulse response and the slope of the channel variation. Consequently, they first estimated the middle CIR of the current OFDM symbol and then estimated the slope. Hu et al. demonstrated that the proposed estimation scheme performed well, while the use of the optimal pilot tones enhanced the channel estimation. However, the case of the time-varying effects on an SDMA-based multi-

user MIMO-OFDM channel estimation was not investigated.

In [210], Gao et al. investigated frequency-domain channel estimation in uplink MIMO OFDM access (OFDMA) systems for time-varying channels. They used training sequences to estimate the channel and showed that the proposed channel estimation method considerably outperformed the RLS channel estimation at the high SNR range. Moreover, to improve the accuracy of channel estimation they incorporated channel interpolation by using the correlation between adjoining subcarriers. With a training overhead of only 5%, this method attains a BER performance that was close to the case with perfect CSI.

B. Blind channel estimation

The term "blindness" means that the receiver has no knowledge of the transmitted sequence and the CIR. The statistical or structural properties of communication signals, such as cyclo-stationarity, high-order statistics, or the finite-alphabet property are used to perform channel estimation, equalization or demodulation. In general, training sequences are used to estimate the channel in static or slowly varying propagation environments. However, the PSAM method is not desirable in fast varying environments as the pilot overhead consumes a considerable amount of bandwidth. Therefore, the need for higher data rates inspires the search for blind channel estimation methods.

In OFDM systems, in general, up to 25% of the transmitted data are occupied by the cyclic prefix (CP). Moreover, if training sequences are employed in channel estimation and synchronisation processes, those may involve an additional 15% to 20% of the remaining data. Since it is more bandwidth-efficient, the blind channel estimation for MIMO-OFDM has been a recent active area of research. However, the main drawback of many blind estimation methods is that they become impractical over time-varying channels, since they require the accumulation of a large amount of received data.

Most existing blind estimation techniques for CP-based OFDM systems can be categorised into two types: *subspace-based* and *non-subspace-based* [211]. Non-subspace-based methods exploit the finite-alphabet property of transmitted symbols. Thus, it involves considerable computational complexity mainly when the size of the constellation is large. On the other hand, the subspace-based methods do not require any knowledge on the symbol constellations. However, it requires the statistical calculation of the received blocks and, thus, leads to slower convergence than the methods exploiting finite constellations.

Yatawatta et al., in [212] proposed a blind channel estimation method for multi-user MIMO-OFDM systems. A linear non-redundant block precoding scheme was

used at the input of the OFDM system. The precoding spread the OFDM symbols of each user over all the subcarriers. Simultaneously, it established a structure for the transmitted symbols, which was exploited at the receiver to estimate the channel in a blind approach. The proposed channel estimation scheme showed simple computations and did not introduce any redundancy in the precoding scheme.

C. Semi-blind channel estimation

Semi-blind algorithms are based on a limited amount of pilot data in conjunction with blind algorithms. As explained previously, semi-blind methods have three advantages over blind methods: the uncertainties inherent to blind methods can be resolved; convergence speeds are enhanced; and more effective and robust tracking of time-varying channels is accomplished.

Zhou et al., in [213], demonstrated a semi-blind channel estimator based on the finite-alphabet property of information symbols for multi-user OFDM systems. The proposed method used a limited amount of training and was used for PSK transmission. They stated that this algorithm could be applied both in CP-based OFDM and zero-padded OFDM transmissions. The proposed method improved the symbol recovery in zero padding OFDM systems. However, it led to modifications in the transmitter and complex equalization. Moreover, this scheme did not consider multi-antenna transmission with multi-user scenarios.

Chen and Zhou, in [214], presented a superimposed periodic pilot scheme by using only a first-order statistic to estimate the channel for OFDM systems. Since this scheme did not require dedicated slots for training, it was considered to be a semi-blind approach. They concluded that the proposed method performed simple channel estimation as well as equalization, without any loss of spectral efficiency. However, they implemented this scheme for mobile wireless propagation and they did not consider the multi-antenna specifications or multi-user scenario in their channel estimator.

In [215], Xu et al., presented a semi-blind channel estimation method for MIMO-OFDM systems. This method was based on both independent component analysis (ICA) and pilot carriers. For the initial estimation of the channel, pilot carrier were used. Then, those initial channel estimations were used as *a priori* information in the algorithm of ICA. Next, convolutional encoding between data carriers and pilot carriers was performed in order to correct the ordering and scaling of the estimated sources. They showed that the proposed method reached a BER of 10^{-5} at an SNR of 11 dB.

D. Decision-directed channel estimation (DDCE)

The statistical properties of the communications channel and the received information symbols are used to estimate the CSI in the decision-directed channel estimation method. The main advantage of this scheme is that the complete transmission session can be used to send information symbols since independent pilot symbols are not required. Therefore, it is ideally bandwidth-efficient in theory. However, this channel estimation scheme possesses some critical disadvantages. It is impractical to implement the DDCE in real-time communications systems as the computations are based on second-order statistics of the channel and the received signal is highly complicated. Moreover, the DDCE methods are only suitable for slowly varying channels where the channel statistics do not change over a long period as this scheme often relies on time averaging. Furthermore, it is well known that all DDCE algorithms have very poor performance in fast fading communication channels. Because of the high computational cost and constraints to some data and channel assumptions, DDCE methods, therefore, have limited use in practice [216].

For MIMO-OFDM systems, the number of transmit antennas that can be used in LS channel estimation is restricted by the ratio of the number of subcarriers and the number of significant CIR-related taps. Therefore, to allow for more complex situations in terms of the number of transmit antennas and users supported, Munster and Hanzo in [114] investigated a parallel-interference-cancellation-assisted DDCE for OFDM systems supporting multiple users employing multiple transmit antennas at the AP.

In [217], K. Wu and J. Wu proposed a low complexity DDCE method in transmit-diversity OFDM systems. To decouple the data, the correlation of subcarrier channel coefficients was used so that the proposed method can cancel the inter-antenna interference (IAI) for separating the estimation of each channel response. They also used the recent estimate of the channel response to eliminate the residual IAI. At an SNR of 20 dB the accuracy in channel estimation is dominated. However, their system incorporated a 2×2 transceiver with only a single user. Ganesh and Kumari, in [218] presented a survey of channel estimation mechanisms in MIMO-OFDM systems explaining three of the channel estimation methods (training-based, blind, semi-blind) and their performance.

3.3.3 Multi-user channel estimation

Most of the earlier works on MIMO-OFDM channel estimation are based on single-user MIMO channels [219]. However, in practical wireless communications systems, the multi-user communications should be addressed. The AP must be able to

simultaneously detect the signals from all the active users. Consequently, in [220], Gomma et al. used linear LS channel estimates to separate the users spatially at the AP in multi-user MIMO-OFDM systems. To achieve the full benefits of this method, the precise estimation of the multi-user channels is essential.

In [28], the multi-user channel estimation methods using pilot symbols for STBC-OFDM were experimentally investigated. LS and MMSE techniques were used for the estimation of multi-user channels. In a slowly faded quasistatic channel environment, it was shown that the estimated channel closely approximated the actual channel. Moreover, when the number of users was increased, the proposed methods degraded in performance. However, these methods incorporated 12 out of 60 symbols as training sequences, increasing the overhead to the communications system. Moreover, this method only performed well when the number of users was limited. The tracking method proposed in the present thesis does not depend on the number of users and performed accurately even with only one training symbol for SDMA-based multi-user MIMO-OFDM quasistatic channels.

In [221], Zhang et al. considered multiple users communicating over fading channels demonstrating a range of different characteristics such as time-variance and time-invariance. Since a high number of independent transmitterreceiver pairs had different statistical characteristics and had to be concurrently estimated for each subcarrier, channel estimation was relatively challenging in that case. They proposed a joint CIR and noise-variance estimation method for the uplink of SDMA based multi-user MIMO OFDMsystems. It was based on the expectation-conditional maximisation (ECM) algorithm. They showed that for SNR $>$ 9 dB, the proposed method was able to reach the Cramer-Rao lower bound (CRLB) in time-invariant scenarios.

In [27], Yang et al. addressed a pilot-assisted LS channel estimation method for the uplink of multi-user MIMO-OFDM systems. They developed channel estimation methods for centralised and decentralised multi-user scenarios. However, when the number of users increased, the MSE increased. In addition, they employed 16 or 32 symbols as pilots, increasing the overhead of the communications system. The tracking method we proposed in the present study employ only one OFDM symbol as the pilot sequence, saving valuable bandwidth in communications systems.

3.3.4 Channel estimators

A. Least squares (LS) channel estimator

Pilot-based channel estimation for MIMO-OFDM systems mainly focuses on LS channel estimators. It is the simplest approach to PSA channel estimation in OFDM

systems and no *a priori* information is assumed to be known about the statistics of the channel taps. However, it shows poor accuracy as it is performed on a frame by frame basis with no filtering of the estimate. The LS channel estimation h_{LS} for block-type pilots in the frequency domain can be expressed as:

$$h_{LS} = yx^{-1} \tag{3.2}$$

where y is the transmitted pilot symbol and x is the received pilot symbol. In [172], Cicerone et al. investigated the advantages of using *a priori* information about the construction of the multi-path fading channel on the performance of channel estimation in MIMO-OFDM systems. First, they derived a lower bound for the channel-estimation error for MIMO-OFDM systems and then designed an efficient estimator that works closer to the derived limit. Moreover, they stated that the fast-varying fading amplitudes are possible to track by using the LS algorithm. However, they did not consider the performance of the LS channel estimator in multi-user MIMO-OFDM systems.

In [222], Hidayat et al. investigated channel estimation for SM in MIMO-OFDM systems employing pilot symbols. The initial channel estimation was performed using the LS method. ZF algorithms were employed to detect and separate the received signal. They showed that at an SNR of 25 dB the normalised MSE of the channel reached 5×10^{-5} and the BER reached 3×10^{-4}. However, they stated that the channel estimation would be better by having an increased SNR.

B. Minimum mean square error (MMSE) channel estimator

The MMSE assumes the CIR as a random vector. In the MMSE estimator, the average is taken not only over the observed data as in the maximum likelihood estimator (MLE) but also over the probability density function (PDF) of the CIR. Therefore, the MMSE takes full advantage of the correlation of the CFR at different times and frequencies. Regarding all the CIR realisations, it is stated that the MMSE has the minimum MSE on average, in [223]. Moreover, MMSE performs better than MLE as it possesses prior information on the CIR.

In [224], Krouma et al. presented a low-rank MMSE channel estimator for a 2×2 MIMO-OFDM system in slowly fading channel environments. They performed a comparison with LS and MMSE estimators in both SISO and MIMO-OFDM systems with an SER. They have showed that a low computational complexity can be achieved by decreasing the rank of the auto-covariance of the channel matrix. Moreover, they showed that the proposed estimator offered a sound trade-off between complexity and performance.

C. Maximum likelihood estimator (MLE)

MLE does not require information on the channel statistics or the operating SNR [225]. It assumes that the CIR is a deterministic but unknown vector. Consequently, the MSE in the MLE is recognised as an average over the observed data. The CRLB provides a lower bound on the MSE matrix for random parameters. Since the MLE achieves the CRLB, it is the minimum-variance unbiased estimator. Further improvement in MSE is not possible as long as the CIR is assumed as a deterministic quantity and the estimator is unbiased. Moreover, MLE can be based on both pilot-assisted and blind channel estimation.

Morelli and Mengali, in [223], compared MLE and MMSE channel estimators for OFDM systems. The MLE is simpler to implement as it does not require knowledge of the channel statistics and the operating SNR. It is the main advantage of MLE over the MMSE estimator. Conversely, under certain operating conditions, the MMSE estimator shows better accuracy as it uses prior information about the channel. In particular, they found that: i) the channel estimates at the edges of the bandwidth were worse than those in the middle, ii) the MMSE estimator performed better than MLE at low SNR, and iii) at intermediate and high SNRs, the two techniques exhibited comparable performance, provided that the number of pilot tones was sufficiently greater than the duration of the CIRs. Otherwise, the MMSE estimator is better.

In [189], Du et al. proposed two iterative ML-based channel estimation methods for the uplink of OFDM systems in time-varying environments. First, they modeled the uplink multi-path fading channel in order to estimate the unknown channel coefficients. The proposed iterative ML-based method estimates the discrete-time channel coefficients based on the system model. Then, a second-order Taylor series expansion was employed to simplify the problem of channel estimation. A perturbation technique was used to analyse the MSE performance. Next, an enhanced iterative ML channel estimation algorithm based on a convergence analysis was presented, employing a successive over-relaxation technique. They showed that the simulated MSE performance agreed with the results gained from the theoretical analysis. However, these proposed methods did not consider MIMO systems.

The ML estimator for the tracking of MIMO channels, is presented in [226]. This algorithm was derived, first, by extracting the equations for ML estimation of a time-invariant channel and then by extending it to a time-variant channel. As a result, this algorithm did not possess desirable performance for time-varying channels. Vosoughi et al. evaluated the performance analysis of MLE and modified its structure in [227]. For time-varying flat fading MIMO channels, Karami and Shiva have proposed a tracking algorithm based on the ML algorithm in [228].

However, these algorithms depended on the channel model and hence the precise channel model must be known.

3.4 Channel tracking

Several channel tracking methods have been previously proposed for wireless communications. Molnar et al. [229] developed a method and apparatus for channel tracking using pulse-shaping information to track the medium (channel) response of the fading. For a received baseband signal to produce a filtered waveform, information symbol values were pre-filtered employing the pulse shape information. They exploited this waveform as a reference signal to estimate the medium response. This estimation was used to detect unknown information symbols using a coherent detector. The channel tracking module tracked the medium response of a fading, dispersive channel by processing the received data symbols. However, they only considered a single-user, single antenna scenario with single-carrier transmission.

In [230], Tu and Champagne presented a blind recursive algorithm in precoded MIMO-OFDM systems for tracking fast time-varying wireless channels. Typically, subspace-based tracking is used for slowly time-varying channels only. The proposed method could gather data from both the time and frequency domain due to the frequency correlation of the wireless channels and could accelerate the update of the necessary second-order statistics. A new channel estimate was obtained after each such update by recalculating the subspace information exploiting the orthogonal iteration. This method was evaluated in the case of the spatial channel model suburban macro of a third-generation partnership project (3GPP). In this system, an MS is allowed to move in any direction with a speed of up to 100 km/h, equivalent to a maximum Doppler shift of about 230 Hz in this scenario. They showed that when the SNR (per symbol) was $\geq$ 20 dB, the normalised MSE of the channel estimates converged to a level of -30 dB within less than five OFDM symbols.

Yakhnich [231] implemented a channel tracking method to update channel estimates on blocks of samples during the reception of a message. When the new sample data arrived, the channel tracking was performed by using the weighted RLS algorithm which recursively updated the coefficients of the channel model. This method updated the CSI once per sample block by applying a exponential weighting factor. Yakhnich selected the block length to be short enough to achieve preferable tracking performance while being adequately long enough to lessen the overhead caused by preliminary decisions and updating precalculated tables in the equalizer. Moreover, this method was implemented in both hardware and software. However, this technique was implemented only in single carrier SISO systems without taking

MIMO-OFDM communications into account.

Hyosung et al. [232] proposed a decision-directed channel tracking method to track doubly selective slow-varying, multi-user, MIMO channel estimates by using the complex exponential basis expansion model (CE-BEM) and Kalman filtering based on the decisions from a DFE. However, this method was designed for single-carrier MIMO systems without considering OFDM transmission. Moreover, a channel estimation algorithm was proposed by Hijazi et al. [233] to track fast time-varying environments in MIMO-OFDM systems. They also employed the basis expansion model (BEM) and Kalman filter for tracking. The function of channel estimation depended on the coefficients of a physical propagation channel or equivalent discrete time channel taps. A BEM was used to approximate the channel and to manage fast variations of the channels within a transmission block. This method did not exploit the multi-user scenarios.

Gifford et al., in [234] presented a low overhead channel tracking algorithm for mobile MIMO-OFDM communication systems. They used the PSA channel estimation in conjunction with adaptive decision feedback LMS, RLS and Kalman filter in their proposed algorithm. Moreover, the geometric wideband time-varying channel model (GWTCM) with Rayleigh fading channels was considered. However, the channel tracking algorithms for multi-user scenarios in SDMA-based MIMO-OFDM systems were not considered.

Schmidt et al. [235] studied the principles of channel estimation in the frequency domain for wireless OFDM systems and presented a low complexity channel tracking method for OFDM systems. They used hard-decisions to update the channel estimates in an indoor environment. To re-estimate the coefficients of the channel and to generate additional training symbols they re-modulated the received decided data. However, they only considered the SISO transmission with single- user scenarios. Therefore, in the present study, we present a novel channel tracking method for SDMA-based multi-user MIMO-OFDM systems under time-varying, frequency selective MIMO channel conditions.

3.5 Chapter summary

The comprehensive literature review revealed the existing adaptive equalization mechanisms, channel estimation methods and channel tracking algorithms that are employed in MIMO-OFDM systems. However, channel estimation, equalization and tracking algorithms for SDMA-based multi-user MIMO-OFDM communications systems are more demanding in the latest wireless communications systems. Therefore, the literature survey indicates the existing gaps in knowledge, providing the

foundation for formulating the scope, objectives and methodology of the present research.

Chapter 4

Estimating the Time-Varying Channel

4.1 Introduction

This chapter elaborates on the methodology undertaken to perform this research. The research for this project can be subdivided into five phases:
Phase 1: Construction of a SDMA-based time-varying, frequency selective, multi-user, MIMO channel model
Phase 2: Derivation of an efficient method for initial channel estimation
Phase 3: Development of adaptive channel equalizers for SDMA-based multi-user MIMO-OFDM systems
Phase 4: Development of a novel and efficient channel tracking algorithm for SDMA-based multi-user MIMO-OFDM systems
Phase 5: Statistical analysis of the error vector magnitude (EVM) between the recovered symbols ($\hat{\mathbf{X}}$) and the transmitted symbols ($\mathbf{X}$)

The following sections provide a detailed discussion of each of these phases.

4.2 Construction of a time-varying, frequency selective, multi-user, MIMO channel model

This section discusses the mathematical model of the SDMA-based multi-user MIMO-OFDM channel and provides an overview of how it is implemented and simulated.

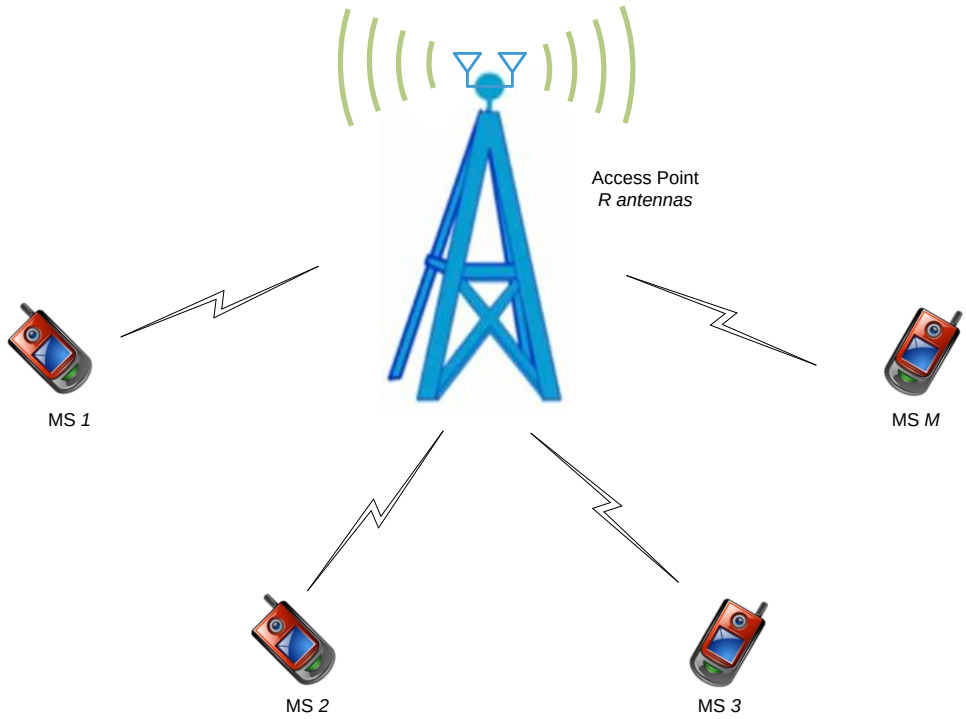

Figure 4.1: Multi-user MIMO communications system with a single antenna at the MS.

4.2.1 Channel model

In an SDMA-based multi-user MIMO-OFDM system, wireless broadband services with higher spectral efficiency can be enabled by employing multiple antennas at an AP to serve each MSs equipped with a single antenna or multiple antennas. Typically, the case of an MS using a single antenna is considered as illustrated in Figure 4.1 as it is generally easier and more cost effective to implement than the multiple antennas case.

As shown in Figure 4.1, communication resources such as time, frequency and spatial stream are allocated to M number of MSs. The AP and each MS are equipped with R antennas and a single antenna, respectively. The end-to-end communication between the MSs and the AP can be considered as an $M \times R$ MIMO system for the downlink and an $R \times M$ MIMO system for the uplink. The uplink and downlink channels in multi-user MIMO systems are referred to as a multiple access channel (MAC) and broadcast channel (BC), respectively. In this thesis, our

focus is on the uplink channel signal processing. In practice, the processing of the corresponding downlink channel needs to be implemented. For time division duplex systems, channel reciprocity may be utilised to derive the downlink channel from the uplink channel (which may be tracked or predicted). However, this is out of the scope of this thesis and is left for future work.

4.2.2 Multiple access channel model for a SDMA-based multi-user MIMO system

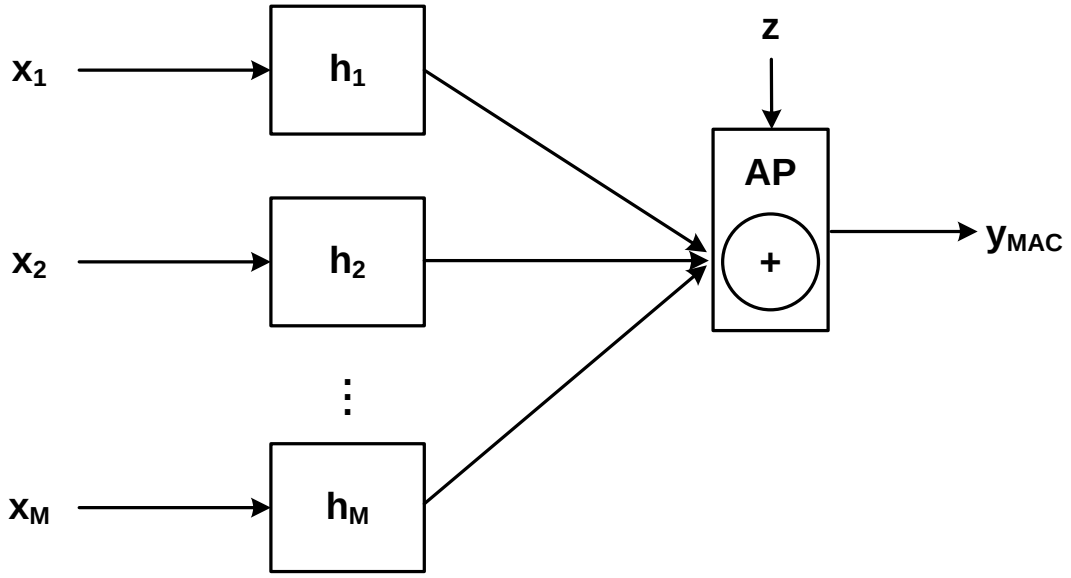

Figure 4.2: Multiple access channel (MAC): Uplink channel model for a multi-user MIMO system.

The CIR can be represented as an input-output relationship between the transmit and receive antenna pairs. The uplink channel for M independent MSs can be exemplified as in Figure 4.2. The received signal $\mathbf{y}_{MAC} \in \mathbb{C}^{R\times 1}$ at the AP can be expressed as:

$$\begin{aligned} \mathbf{y}_{MAC} &= \mathbf{h}_1\mathbf{x}_1 + \mathbf{h}_2\mathbf{x}_2 + \cdots + \mathbf{h}_M\mathbf{x}_M + \mathbf{z} \\ &= [\mathbf{h}_1\mathbf{h}_2\cdots\mathbf{h}_M]\begin{bmatrix}\mathbf{x}_1\\ \vdots \\ \mathbf{x}_M\end{bmatrix} + \mathbf{z} = \mathbf{H}\begin{bmatrix}\mathbf{x}_1\\ \vdots \\ \mathbf{x}_M\end{bmatrix} + \mathbf{z} \end{aligned} \tag{4.1}$$

where $\mathbf{x}_m \in \mathbb{C}$ is the transmit signal from the m^{th} mobile station, $\mathbf{m} = 1, 2, \cdots M$, $\mathbf{H} \in \mathbb{C}^{R \times M}$ and $\mathbf{h}_m$ is the channel gain between the m^{th} MS and the AP and $\mathbf{z} \in \mathbb{C}^{R \times 1}$ is the additive white Gaussian noise (AWGN).

4.2.2.1 Response of a time-varying channel

The CIR of a time-varying channel between a transmitter and receiver is modelled by L propagation paths and can be written as:

$$h(t, \tau) = \sum_{l=1}^{L} a_l(t)\, \delta(\tau - \tau_l(t)) \tag{4.2}$$

where $h(t, \tau)$ is the response at time instant t for an impulse signal transmitted at time $t - \tau$, $\sum_{l=1}^{L} a_l(t)$ are the channel coefficients at time instant t, and τ is the excess delay [3]. The corresponding CFR can be stated as:

$$h(f, t) = \int_{-\infty}^{\infty} h(t, \tau) \exp\{-j2\pi f \tau\}\, d\tau \tag{4.3}$$

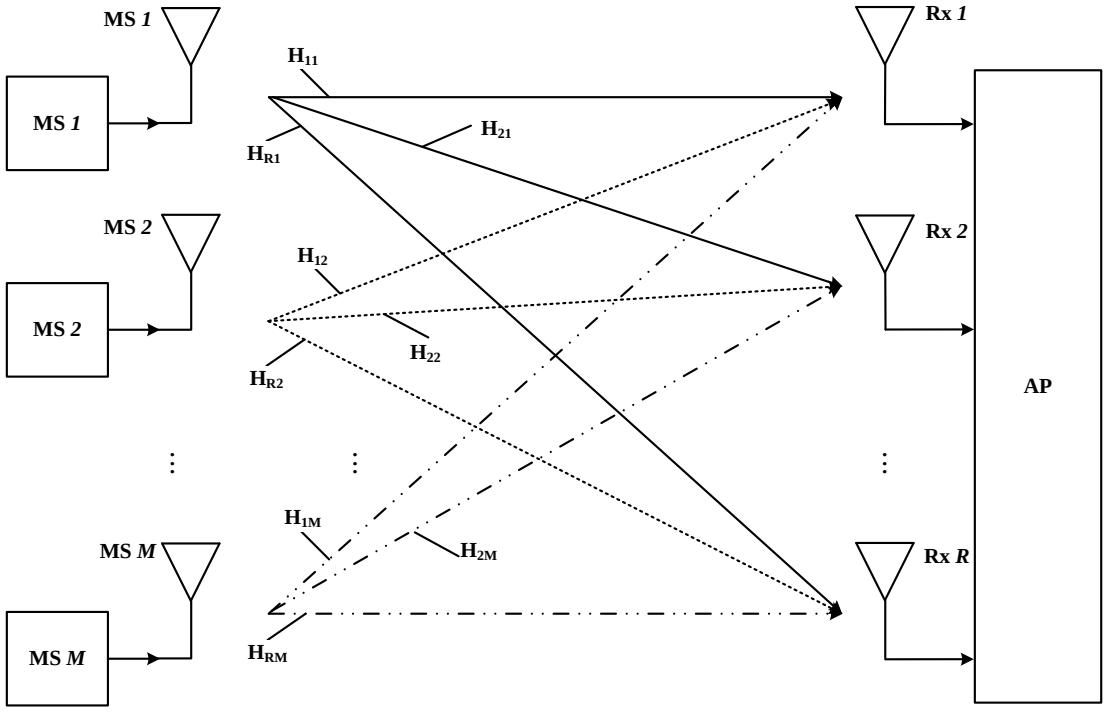

Figure 4.3: Multi-user MIMO channel.

A multi-user communications system with M number of transmitters (MSs) and R number of receiver antennas at the AP is considered, as shown in Figure 4.3. Since the multi-user MIMO uplink system is employed with multiple antennas at the receiver and a single antenna at the MS, all transmit and receive antenna pairs can be represented by a MIMO channel. From a system-level point of view, a linear time-variant uplink multi-user MIMO channel can be represented by an $R \times M$ channel matrix:

$$\mathbf{h}(t,\tau) = \begin{pmatrix} h_{11}(t,\tau) & h_{12}(t,\tau) & \cdots & h_{1M}(t,\tau) \\ h_{21}(t,\tau) & h_{22}(t,\tau) & \cdots & h_{2M}(t,\tau) \\ \vdots & \vdots & \ddots & \vdots \\ h_{R1}(t,\tau) & h_{R2}(t,\tau) & \cdots & h_{RM}(t,\tau) \end{pmatrix} \tag{4.4}$$

where the elements, $h_{rm}(t,\tau)$, of the matrix $\mathbf{h}$ are complex random variables that represent the time-variant impulse response between the m^{th} MS antenna and the r^{th} receiver antenna at the AP. The physical characteristics of the propagation environment directly affect each sub-channel $h_{rm}(t,\tau)$.

4.2.3 Construction of the channel model

Figure 4.4 illustrates two simulated OFDM time-varying, frequency selective channels between the first MS and the first AP antenna for maximum Doppler shifts (f_d) of 10 Hz and 70 Hz respectively. The subcarrier index shows the variations in frequency domain (frequency selectivity) and the symbol index shows the variations in the time domain. The frequency selectivity is due to multi-path propagation. The time-variations occur due to changes in the relative position/movement between the transmitter and the receiver. The time-variations are more noticeable in Figure 4.4(b) than Figure 4.4(a). The dynamic range of the magnitude of the channel when f_d is 10 Hz is 1.1081 with a minimum of 0.1879 and a maximum of 1.2959, while the dynamic range of the magnitude of the channel when f_d is 70 Hz is 1.7107 with a minimum of 0.0188 and a maximum of 1.7296. Therefore, the magnitude of the channel for f_d is 70 Hz has a higher dynamic range of 0.6026 than that of f_d is 10 Hz, when the subcarrier index (frequency) changes from 1 to 128 and the symbol index (time) changes from 1 to 96. This implies that when f_d is higher (i.e., the MS travels at a higher speed) the channels experience higher variations in time and frequency.

Figure 4.5 elaborates on how fast the channel varies with time [236], as it shows the time-varying channel between the first MS and the first receiver antenna at the AP of the first subcarrier. Figures 4.5(a) and 4.5(b) illustrate the time-varying

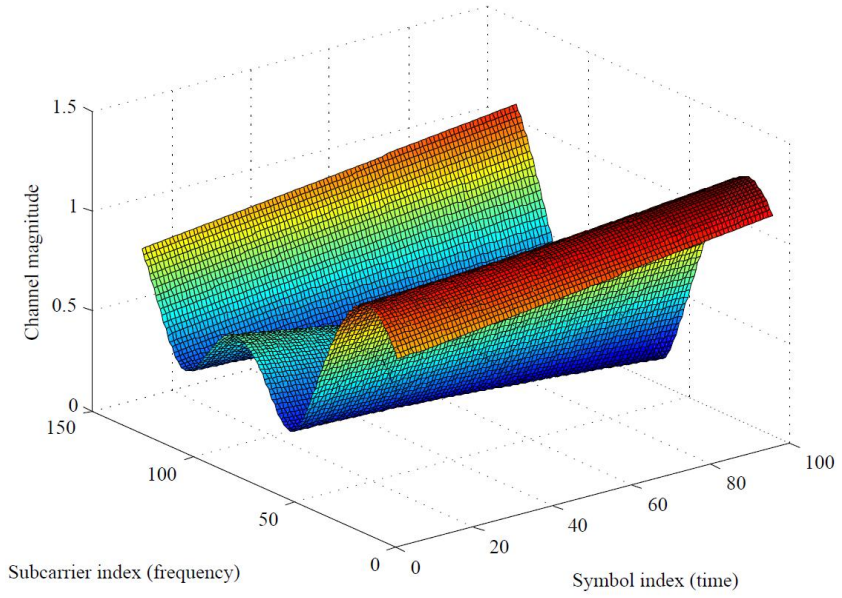

(a)

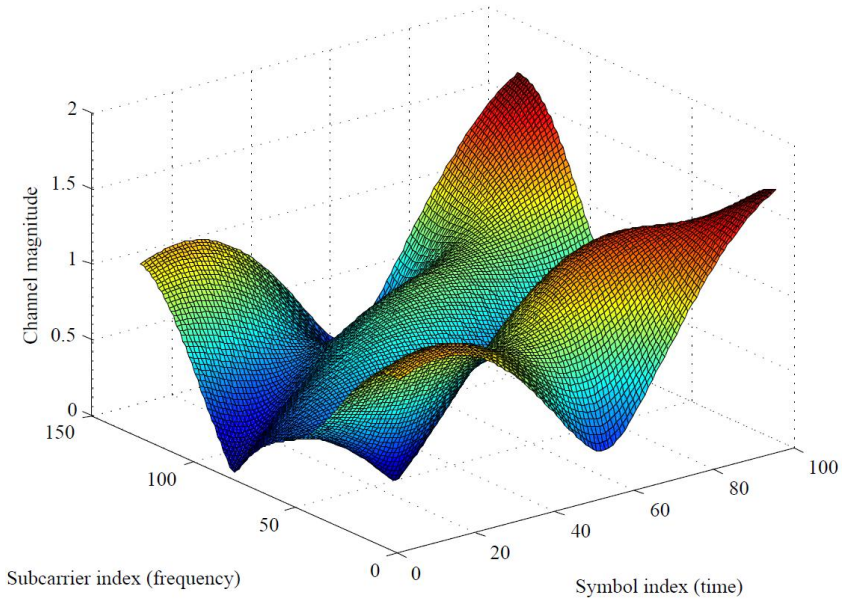

(b)

Figure 4.4: Simulated channel frequency response (a) $f_d = 10$ Hz (b) $f_d = 70$ Hz.

channels for $f_d = 10$ and $f_d = 70$, respectively. The dynamic range of the magnitude of the channel when f_d is 10 Hz is 0.2205 with a minimum of 0.9367 and a maximum

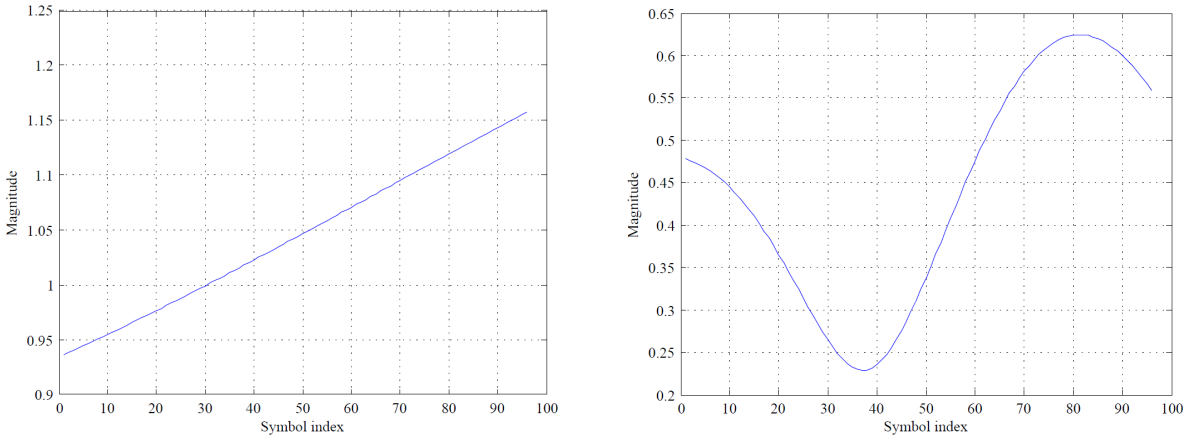

(a) (b)

Figure 4.5: Time-varying channels (a) $f_d = 10$ Hz (b) $f_d = 70$ Hz.

of 1.1572, while the dynamic range of the magnitude of the channel when f_d is 70 Hz is 1.4202 with a minimum of 0.3085 and a maximum of 1.7287. Therefore, the magnitude of the channel for f_d is 70 Hz has a higher dynamic range of 1.1997 than that of f_d is 10 Hz, when the symbol index (time) changes from 1 to 96. This implies that when f_d is higher, the channels experience a higher variation in time.

Figures 4.6(a) and 4.6(b) depict the frequency selective channels between the first MS and the first receiver antenna at the AP for the first symbol for $f_d = 10$ and $f_d = 70$, respectively. The dynamic range of the magnitude of the channel when f_d is 10 Hz is 0.8049 with a minimum of 0.3326 and a maximum of 1.1374, while the dynamic range of the magnitude of the channel when f_d is 70 Hz is 1.1162 with a minimum of 0.0286 and a maximum of 1.1448. Therefore, the magnitude of the channel for f_d is 10 Hz has a higher dynamic range of 0.3113 than that of f_d is 70 Hz, when the frequency index changes from 1 to 128.

The simulations are performed using Matlab. First, a channel object is created to generate frequency selective fading channels that model each separate path as an independent Rayleigh/Rician fading process. There are L separate fading paths and each path had its own corresponding average power gain and delay. Three distinct paths are chosen to create each power delay profile. Average path gains in dB were set to a vector of the form $[0 \quad g \quad g-1]$ where g is randomly generated using Rayleigh distribution. The channel experiences frequency flat fading when $L = 1$, while a frequency selective fading occurred for $L > 1$. Several values of L

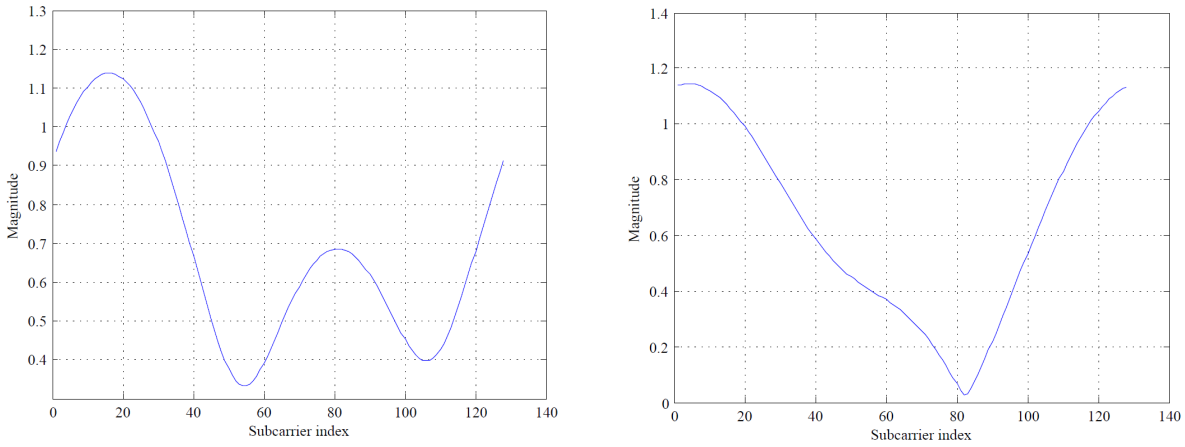

(a) (b)

Figure 4.6: Frequency selective channels (a) $f_d = 10$ Hz (b) $f_d = 70$ Hz.

are simulated and $L = 3$ is selected as a trade-off to allow channel tracking and frequency selectivity at the same time. The Rician K-factor is the ratio between the power of the direct path and the power in the other, scattered, paths. It is typically between 1 and 10 and is normally expressed linearly, not in dB. When the K-factor is 0, Rayleigh fading occurs. The channel object is created as a Rayleigh fading channel that acted on a signal sampled at 10 kHz or $10,000$ samples per second.

A vector of average path gains, in dB, a vector of path delays, in seconds, and the maximum Doppler shift (f_d), in Hz, are given as parameters to create the channel object. The average path gains specified the average power gain of each fading path, which is a large negative dB value in real propagation conditions. However, average path gains between -20 dB and 0 dB are usually employed in computer simulations [237]. The average path gains are produced as Rayleigh distributed random numbers for each creation of the channel object. The path gains are normalised to make sure that the total power of the expected values of the path gains is 1.

In this thesis, we assumed that the access point (receiver) has knowledge of all the spatial parameters such as angle of arrival, angle of departure, cluster spread. In generating MIMO channels for multiple users, number of multi-paths are set to 3, maximum Doppler shift is fixed to 10 Hz unless otherwise mentioned, sample time is fixed to 10 kHz, the vector of path delays is fixed to $[0 \quad 1.1e-4 \quad 2.1e-4]$ and the number of OFDM symbols is set to 100. Average path gains in dB were set

to a vector of the form $[0 \quad g \quad g-1]$ where g is randomly generated using Rayleigh distribution. Therefore, the average path gains are different for each mobile station.

The delay of the first path is usually set to zero, which corresponds to the first propagation path. To follow reflected paths, a delay of 1 μs corresponds to a 300 m difference in path length. There could be up to a number of kilometres of difference between the longest and the shortest path in some outdoor multipath propagation environments [237]. In this study, the path delays are set to a vector of $[0 \quad 1.1e-4 \quad 2.1e-4]$ in seconds. The last path is 63 km longer than the shortest path, and therefore arrived 0.21 ms later. In indoor propagation conditions, the delays of succeeding paths are typically between 1 ns and 100 ns while in outdoor propagation conditions, the delays of succeeding paths are typically between 100 ns and 10 μs [237]. For example, an area bounded by mountains can be represented by a very large set of delays in this range of 0 to 102.3 μs [238].

The maximum Doppler shift is calculated according to Equation (2.1). Slow variations in time are resulted by a smaller f_d (a few hertz to a fraction of a hertz) and faster variations are created by a large f_d. At a frequency of operation of 700 MHz, an example of a typical long term evolution (LTE) carrier frequency, an f_d of 10 Hz is equivalent to a mobile speed of 15.4 km/h and an f_d of 70 Hz will represent a mobile travelling at a speed of 108 km/h. A signal from a moving pedestrian may experience an f_d of about 3 Hz, while a signal from a moving car on a freeway may experience an f_d of about 65 Hz. The channel object models the channel as static (i.e., fading does not change with time), if either $f_d = 0$ or f_d is not defined during the creation of the channel object.

Time-varying conditions are created by filtering the OFDM symbols through the channel object. Then, multiple different channels are created for each channel between multiple users and multiple antennas at the AP. Since our focus is on the case with six users with 12 AP antenna system, as implemented in [19], the number of MSs is set to $M = 6$ and the number of antennas at the AP is set to $R = 12$ in the simulations. Figure 4.4 is plotted for a Rayleigh fading channel with 100 channel realisations. The number of OFDM symbols used in the simulations is set to 96 and the number of OFDM subcarriers is set to 128.

Figure 4.7 shows the CIR of the multi-path channel and the band-limited channel response. The multi-path response is indicated by stems, each related to one multi-path component. The paths with the shortest and the largest delays are shown in red and blue, respectively. The green curve represents the band-limited channel response which is the result of convolving the multi-path impulse response, with a sinc pulse of period, T (the sample period of the input signal). The channel filter response sampled at rate $1/T$ is represented by the solid green circles.

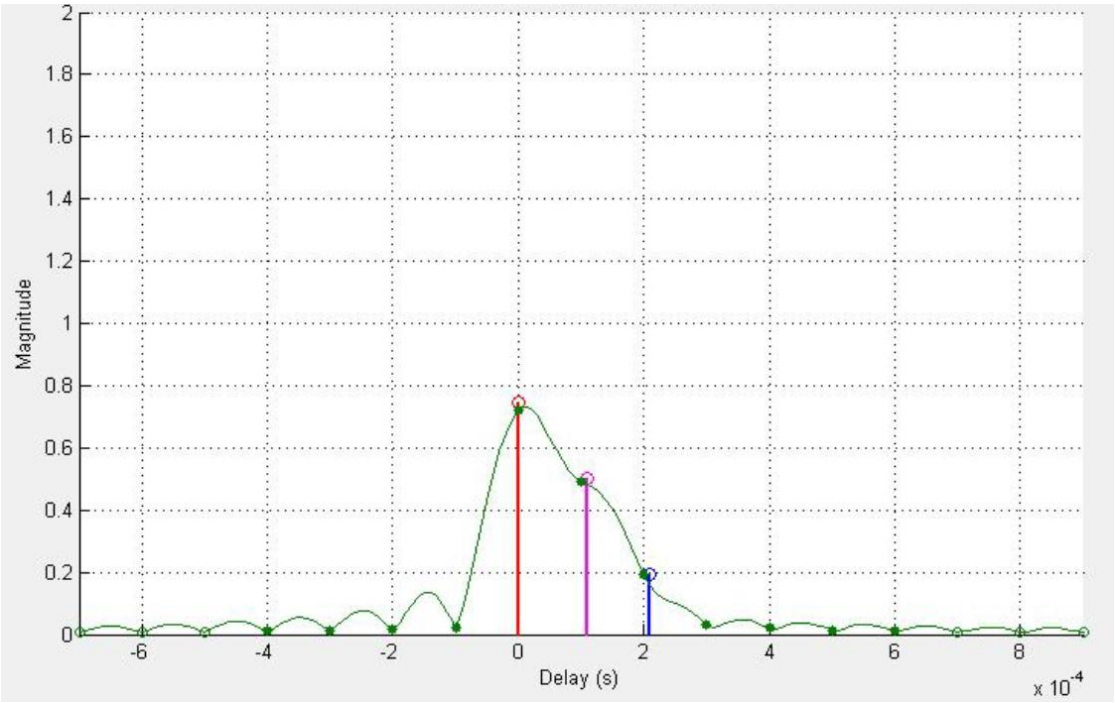

Figure 4.7: Channel impulse response (CIR) and the band-limited response.

The progression of the magnitude impulse response over time is shown by Figure 4.8 for f_d of 10 Hz and 70 Hz, respectively. The last 10 snapshots of the band-limited impulse response of the channel are shown and the darkest green curve represents the current response. The time of the channel snapshot relative to the current response time is represented by the time offset. The range of the delay spread of the channel for $f_d = 10$ Hz is from -0.2 ms to 0.3 ms and the range of the delay spread of the channel for $f_d = 70$ Hz is from -0.4 ms to 0.6 ms. It can be clearly seen that there are more time-variations when $f_d = 70$ Hz than that of $f_d = 10$ Hz.

Figure 4.9 exemplifies the magnitudes of the simulated uplink frequency selective channel model for all MSs and receiver antenna combinations for $f_d = 10$ Hz. The figure shows the magnitude of the channel in dB, averaged over all time symbols versus the OFDM subcarriers (frequency). It can be seen that almost all the channels experience frequency selectivity. For example, the channel between the MS 4 and the receiver antenna 10 faced a deep fade. The dynamic range of magnitude for this specific channel is 0.8677 with a minimum of 0.0252 and a maximum of 0.8929 of in dB.

In this thesis, the CSIRO's system is used as a reference model. However, there

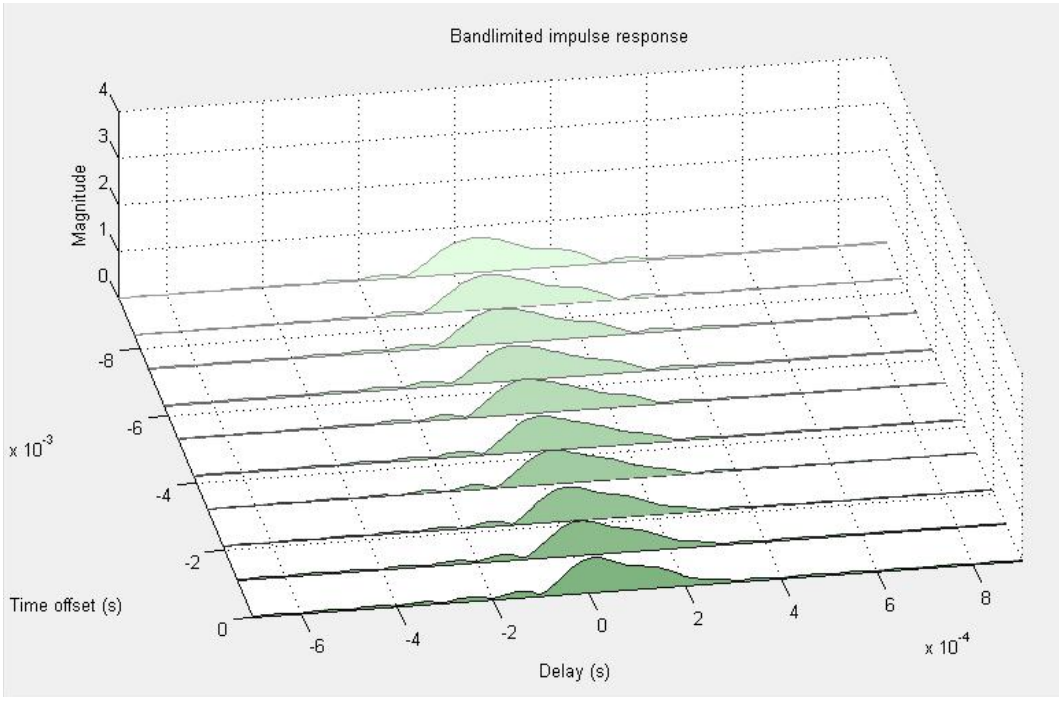

(a)

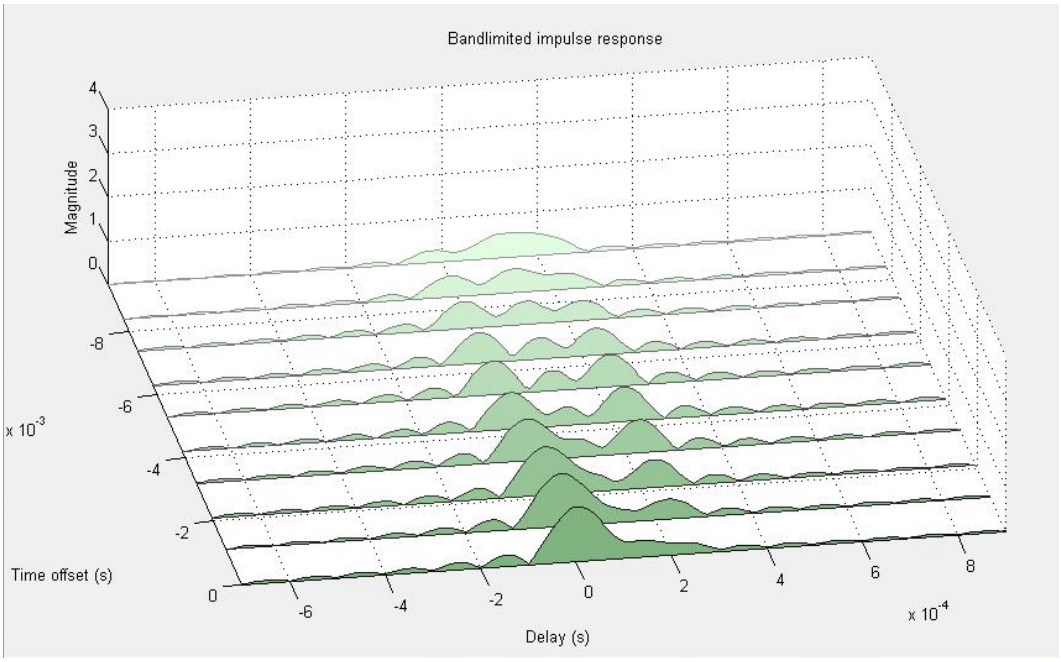

(b)

Figure 4.8: Impulse response waterfall plot of the multi-path channels (a) $f_d = 10$ Hz (b) $f_d = 70$ Hz.

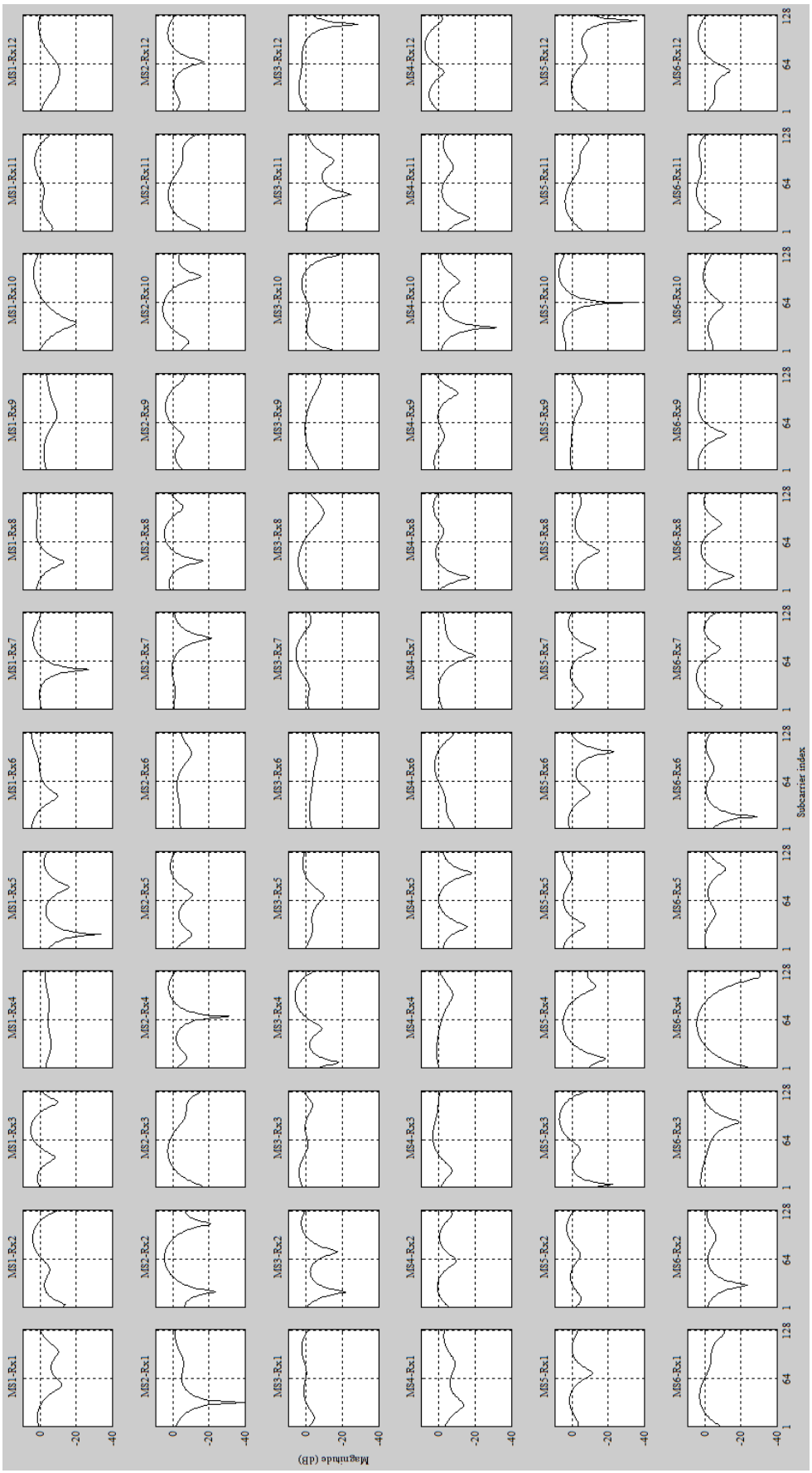

Figure 4.9: Magnitude of the uplink of the frequency selective multi-user MIMO channel with $f_d = 10$ Hz

are some differences between the parameters in simulations and the actual CSIRO system, For example, the number of OFDM subcarriers used in the simulations are 128 whereas that of CSIROs system is 1705. Therefore, a fair comparison between simulation results in this thesis and experimental data from CSIRO test bed measurements is not possible in most cases.

Figure 4.10 and Figure 4.11 exemplify the simulated uplink time-varying channel model for all MSs and receiver antenna combinations for $f_d = 10$ Hz and $f_d = 70$ Hz, respectively. The figures are illustrated for the magnitudes of the channel in dB, averaged over all OFDM subcarriers versus all time symbols. As expected, there are more variations when $f_d = 70$ Hz than that of $f_d = 10$ Hz. It can be seen that almost all the channels experienced variations in time, especially when $f_d = 70$ Hz. For example, for the channel between the MS 4 and the receiver antenna 10, the dynamic range of magnitude when $f_d = 10$ is 0.2353 with a minimum of 0.2426 and a maximum of 0.478 of in dB and the dynamic range of magnitude when $f_d = 70$ is 0.7840 with a minimum of 0.0660 and a maximum of 0.85 of in dB.

4.3 Derivation of an efficient method for initial channel estimation

SDMA-based MIMO-OFDM communications systems need the knowledge of the CSI. The channel coefficients of the channel matrix have to be known, in order to detect the transmitted signals at the receiver. These coefficients are obtained by employing a suitable channel estimation scheme. In this study, the training sequences that are known to both the transmitter and receiver are employed in the adaptive channel equalization methods and the channel tracking method to estimate the channel initially.

4.3.1 OFDM packet format

The OFDM packet format for transmit antenna 1 (MS 1) containing training and data is depicted in Figure 4.12. The training sequence is at the front end of the packet followed by F number of OFDM frames. Ideally, the training period, R_T should be minimised and the number of OFDM frames could be increased to lessen the training sequence overhead effect on communications systems.

The adaptive equalization methods requires training sequences to equalize the received signal. The first 20 transmitted data symbols are used as the known training symbols in the adaptive equalization method at the receiver.

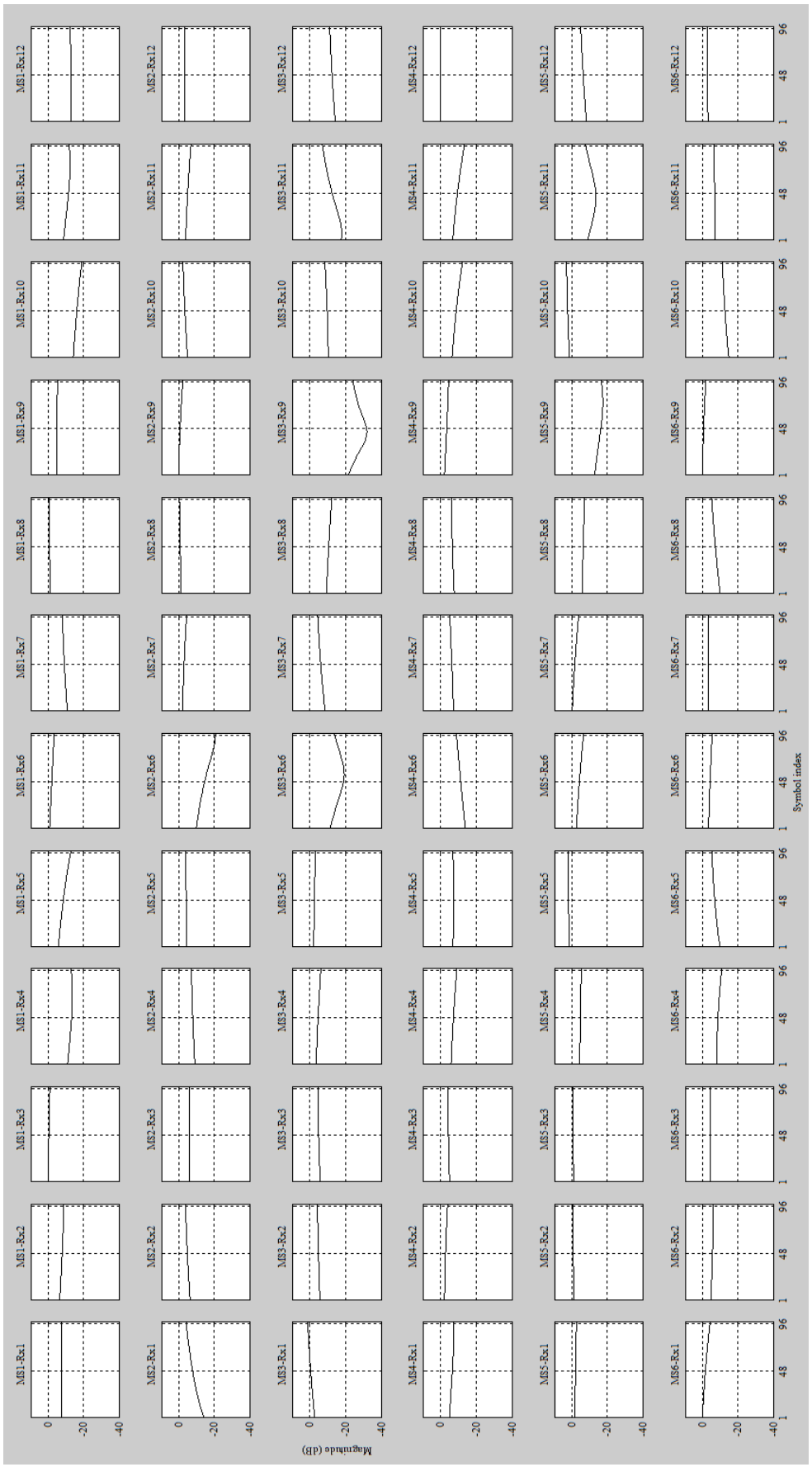

Figure 4.10: Magnitude of the uplink of the time-varying multi-user MIMO channel with $f_d = 10$ Hz

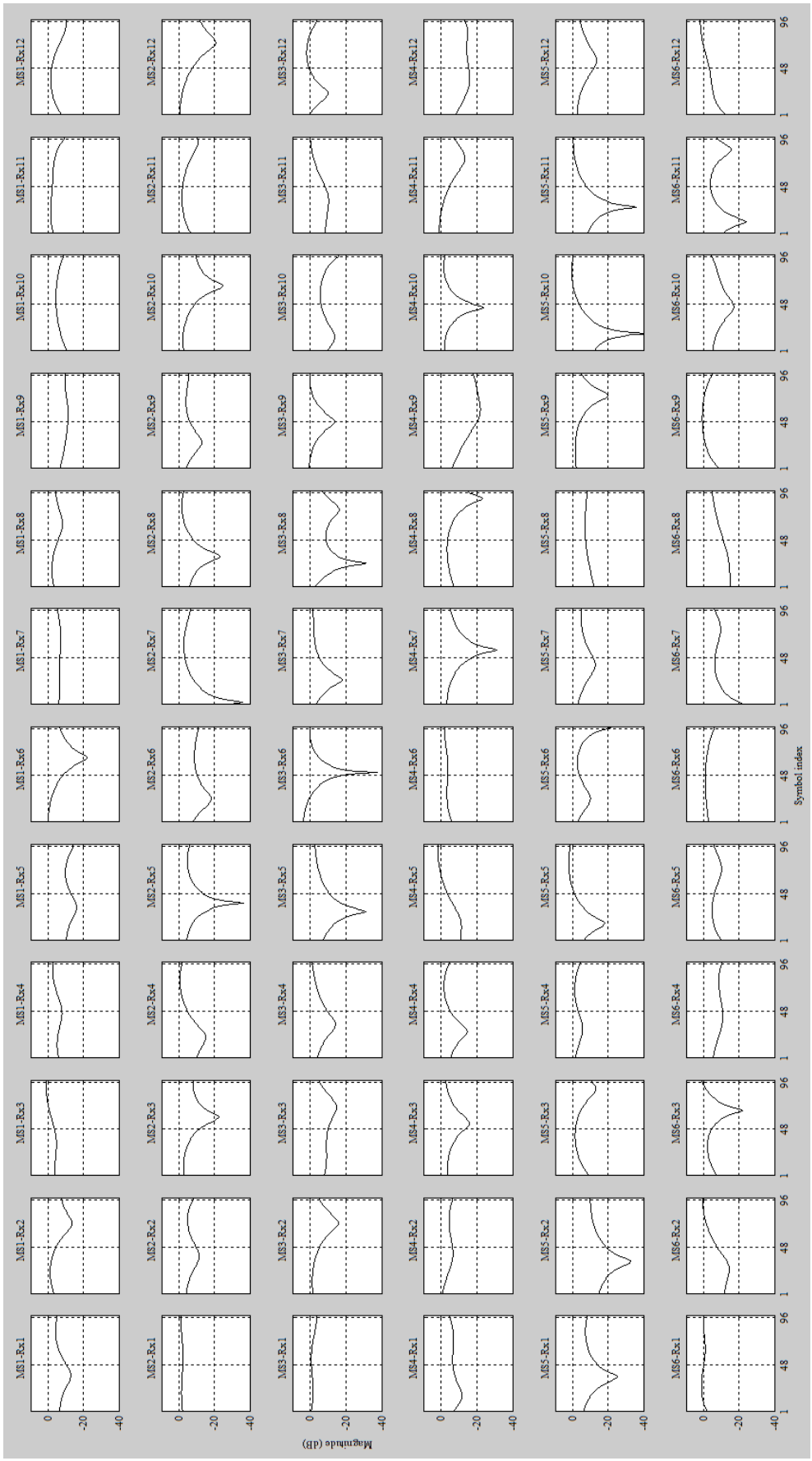

Figure 4.11: Magnitude of the uplink of the time-varying multi-user MIMO channel with $f_d = 70$ Hz

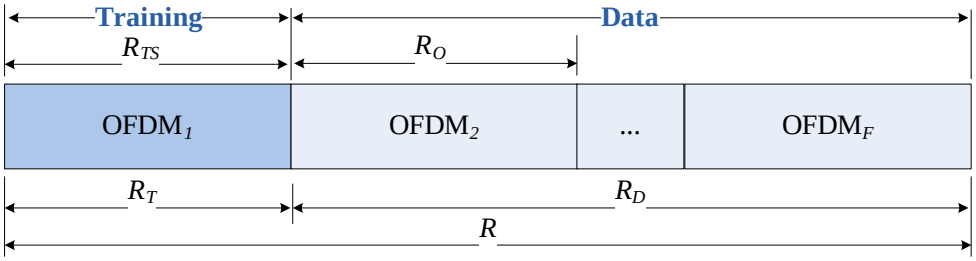

Figure 4.12: OFDM packet format.

4.3.2 Initial channel estimation

The channel tracking method incorporates an initial channel estimation method and it is performed using training sequences for multiple users. In the novel channel tracking method (as explained later in Chapter 6), only the first data symbol of each transmitter is used as the known training symbol in the initial channel estimation method. The training symbol incorporates AWGN noise at each receiver antenna at the AP.

Let $\mathbf{y_0}$ be the received training symbols at the AP and $\mathbf{x_0}$ be the transmitted training symbol as defined in Section 4.2.2. Then, the initial channel estimation is:

$$\hat{\mathbf{H}}_\mathbf{0} = \mathbf{y_0}(\mathbf{x_0})^{-1} = \mathbf{H_0} + \mathbf{z_0}(\mathbf{x_0})^{-1} \tag{4.5}$$

The actual channel ($\mathbf{H_0}$) plus a noise term ($Z_0(X_0)^{-1}$) can be found by using Equation (4.5). The noise term is the channel estimation error (E).

4.4 Development of adaptive channel equalizers for SDMA-based multi-user MIMO-OFDM systems

Multi-path fading in band-limited (frequency selective), time dispersive channels creates ISI deforming the transmitted signal which creates error bits at the receiver. ISI is one of the main barriers in high-data rate communication over mobile radio channels. Therefore, equalization is performed at the receiver to battle ISI [239]. Typically, the mobile radio channels are time-varying and random. The time-varying characteristics of the channel must be tracked by the equalizers and therefore these

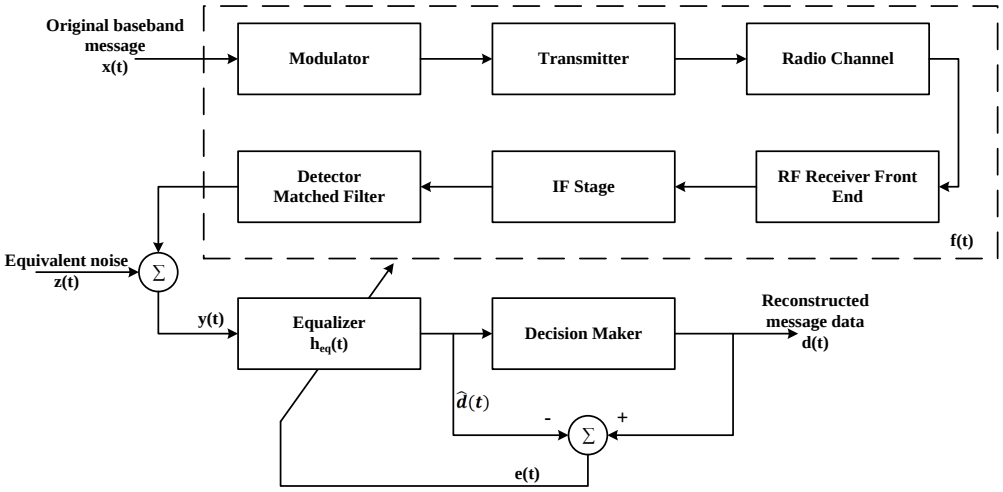

Figure 4.13: Schematic diagram of a simplified communications system with an adaptive equalizer at the receiver [9].

are called adaptive equalizers (AE).

As mentioned earlier, an AE operates in two modes: training and tracking. First, a fixed-length training sequence known to the receiver is transmitted by the MS so that the equalizer at the AP can converge to a suitable setting. The user data is transmitted immediately following the training sequence. To compensate for channel changes, the AE at the AP uses a recursive algorithm to assess the channel and estimate the tap weights of the AE. The tap weights are near the optimal values, when the training sequence is finished, so that the AE is ready for receiving the user data. The characteristics of the changing channel are tracked by the AE, when the user data are received. Consequently, the AE continuously changes its tap weights over time. Typically, the implementation of an equalizer takes place at baseband or intermediate frequency (IF) in a receiver. The channel response, demodulated signal and the adaptive equalizer algorithms are normally implemented and simulated at the baseband as the baseband complex envelope expression can be used to characterise the bandpass waveform [9].

Figure 4.13 presents a schematic diagram of a communications system with an AE at the receiver. Let $\mathbf{x}(t)$ be the original message signal and $\mathbf{f}(t)$ be the combined complex baseband impulse response of the transmitter, channel, and the RF/IF sections of the receiver. Then, the signal received as the input of equalizer can be represented as:

$$\mathbf{y}(t) = \mathbf{x}(t) \otimes \mathbf{f}^*(t) + \mathbf{z}(t) \tag{4.6}$$

where $\otimes$ is the convolutional operation, $\mathbf{f}^*(t)$ is the complex conjugate of $\mathbf{f}(t)$ and $\mathbf{z}(t)$ is the baseband noise at the input of the equalizer. Let $\mathbf{h}_{eq}(t)$ be the impulse response of the equalizer. Then, the output of the equalizer can be expressed as:

$$\hat{\mathbf{d}}(t) = x(t) \otimes \mathbf{f}^*(t) \otimes \mathbf{h}_{eq}(t) + \mathbf{z}(t) \otimes \mathbf{h}_{eq}(t) \tag{4.7}$$

$$= \mathbf{x}(t) \otimes \mathbf{g}(t) + \mathbf{z}(t) \otimes \mathbf{h}_{eq}(t)$$

where $\mathbf{g}(t)$ is the combined impulse response of the transmitter, channel, RF/IF sections of the receiver, and the equalizer. The complex baseband impulse response of a transversal filter equalizer can be expressed as:

$$\mathbf{h}_{eq}(t) = \sum_u \mathbf{w}_u \delta\left(t - uT\right) \tag{4.8}$$

where $\mathbf{w}_u$ are the equalizer's complex filter coefficients. The original source data $\mathbf{x}(t)$ is the desired output of the equalizer. If $\mathbf{z}(t) = 0$ then, with the aim of forcing $\hat{\mathbf{d}}(t) = \mathbf{x}(t)$ in Equation (4.7), $\mathbf{g}(t)$ has to be equal to:

$$\mathbf{g}(t) = \mathbf{f}^*(t) \otimes \mathbf{h}_{eq}(t) = \delta(t) \tag{4.9}$$

The objective of equalization is to ensure Equation (4.9). In the frequency domain, this equation can be represented as:

$$\mathbf{H}_{eq}(f)\mathbf{F}^*(-f) = 1 \tag{4.10}$$

where $\mathbf{H}_{eq}(f)$, $\mathbf{F}^*(-f)$ are the Fourier transform of $\mathbf{h}_{eq}(t)$ and $\mathbf{f}^*(t)$, respectively. As can be seen from Equation (4.10), an equalizer is in fact an inverse filter of the channel. The equalizer improves the frequency components that have small amplitudes, if the channel is frequency selective. To offer a flat, composite, received frequency response and a linear phase response, the equalizer attenuates the strong frequency components in the received frequency spectrum. To track the channel variations in a time-varying channel, an adaptive equalizer is designed to approximately satisfy Equation (4.10).

4.4.1 Process of a linear adaptive equalizer

An adaptive equalizer is a time-varying filter, so that the filter coefficients must continuously be retuned. Figure 4.14 illustrates the process of a linear adaptive equalizer, where u denotes the discrete time index or the OFDM symbol index and there is only a single input ${\mathbf{y}_{u,r}}^n$ at any time instant. As depicted in Chapter

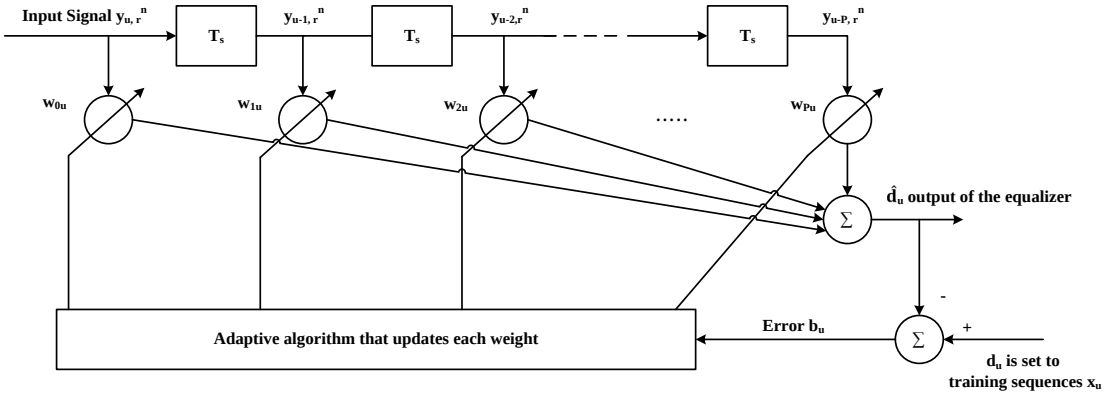

Figure 4.14: Linear adaptive equalizer during training.

5 (Figure 5.1) and Figure 4.13, the value of $\mathbf{y}_{u,r}{}^{n}$ depends on two criteria: the instantaneous state of the radio channel and the specific value of the noise. n denotes that the received symbols are taken OFDM carrier-wise after being sent through the FFT module. The adaptive equalizer shown in Figure 4.14 is referred to as a transversal filter and has P delay elements, $P+1$ taps and $P+1$ tunable complex multipliers referred to as weights. The physical location in the delay line structure describes the weights of the filter and u symbolises that the weights vary with time. The adaptive algorithm employed in the equalizer continuously updates these weights on a sample-by-sample basis (i.e., whenever u increases by 1).

Error signal $\mathbf{b}_u$ controls the adaptive algorithm and it is derived by comparing the output of the equalizer, $\hat{\mathbf{d}}_u$, with a training sequence $\mathbf{d}_u$ (an exact replica of the transmitted signal $\mathbf{x}_u$). The adaptive algorithm, then employs $\mathbf{b}_u$ to minimise a cost function and updates the equalizer coefficients in a way that iteratively decreases the cost function. For instance, the filter coefficients of the equalizer are updated by the LMS algorithm by searching the optimum or near-optimum filter weights as follows:

$$New \quad weights = Previous \quad weights + (constant) \times (Previous \quad error) \quad (4.11)$$

$$\times (Current \quad input \quad vector)$$

where

$$Previous \quad error = Previous \quad desired \quad output - Previous \quad actual \quad output \quad (4.12)$$

and the constant is adjusted by the adaptive algorithm for controlling the variations between the filter coefficients on succeeding iterations.

The most frequently used cost function is the mean square error (MSE) between the desired signal and the output of the equalizer [240]. It is indicated by $E[\mathbf{b}(u)\mathbf{b}^*(u)]$. The adaptive algorithm at the equalizer calculates and minimises the cost function, by detecting the training sequence. It derives the filter coefficients until the subsequent training sequence is transmitted.

Since the input of the equalizer, ${\mathbf{y}_{u,r}}^n$ which is the output of the FFT module at time instant u on the receiver antenna r at the OFDM subcarrier n can be taken separately and inserted to separate equalizers the study of the process of an equalizer can be simplified by letting the input of the equalizer be $\mathbf{y}_u$ where

$$\mathbf{y}_u = \begin{bmatrix} y_u & y_{u-1} & \dots & y_{u-P} \end{bmatrix}^T \tag{4.13}$$

The output of the equalizer can be expressed as:

$$\hat{\mathbf{d}}_u = \sum_{p=0}^{P} \mathbf{w}_{pu}\mathbf{y}_{u-p} \tag{4.14}$$

where $\mathbf{w}_u$ is the vector of filter weights and can be expressed as:

$$\mathbf{w}_u = \begin{bmatrix} w_{0u} & w_{1u} & w_{2u} & \dots & w_{Pu} \end{bmatrix}^T \tag{4.15}$$

By using Equations (4.13) and (4.15), Equation (4.14) can be written in vector notations as:

$$\hat{\mathbf{d}}_u = \mathbf{y}_u^T\mathbf{w}_u = \mathbf{w}_u^T\mathbf{y}_u \tag{4.16}$$

When the desired output of the equalizer is known (i.e, $D_u = X_u$), the error signal B_u is given by:

$$\mathbf{b}_u = \mathbf{d}_u - \hat{\mathbf{d}}_u = \mathbf{x}_u - \hat{\mathbf{d}}_u \tag{4.17}$$

and substituting $\hat{\mathbf{d}}_u$ from Equation (4.16):

$$\mathbf{b}_u = \mathbf{x}_u - \mathbf{y}_u^T\mathbf{w}_u = \mathbf{x}_u - \mathbf{w}_u^T\mathbf{y}_u \tag{4.18}$$

Equation (4.18) is squared in order to calculate MSE $|\mathbf{b}_u|^2$, at time instant u:

$$|\mathbf{b}_u|^2 = \mathbf{x}_u^2 + \mathbf{w}_u^T\mathbf{y}_u\mathbf{y}_u^T\mathbf{w}_u - 2\mathbf{x}_u\mathbf{y}_u^T\mathbf{w}_u \tag{4.19}$$

The expected value of $|\mathbf{b}_u|^2$ over u (which amounts to calculating a time average

practically) yields:

$$E\left[|\mathbf{b}_u|^2\right] = E\left[\mathbf{x}_u^2\right] + \mathbf{w}_u^T E\left[\mathbf{y}_u \mathbf{y}_u^T\right] \mathbf{w}_u - 2E\left[\mathbf{x}_u \mathbf{y}_u^T\right] \mathbf{w}_u \tag{4.20}$$

Notice that the time average does not include the filter coefficients w_u as, for convenience, they are assumed to be converged to an optimum value and are not time-varying.

Equation (4.20) would be insignificant to simplify if $\mathbf{x}_u$ and $\mathbf{y}_u$ are independent. However, in general, this is not true as the input signal vector should be correlated with the desired output signal vector of the equalizer. If not, the desired signal would not be easily extracted by the equalizer. As an alternative, the cross correlation vector $\mathbf{v}$ between the desired response and the input signal can be expressed as:

$$\mathbf{v} = E\left[\mathbf{x}_u \mathbf{y}_u\right] = E[\mathbf{x}_u \mathbf{y}_u \quad \mathbf{x}_u \mathbf{y}_{u-1} \quad \mathbf{x}_u \mathbf{y}_{u-2} \quad \dots \quad \mathbf{x}_u \mathbf{y}_{u-P}]^T \tag{4.21}$$

and the input correlation matrix or the input covariance matrix can be defined as $(P+1)\times(P+1)$ square matrix $\mathbf{A}$ where

$$\mathbf{A} = E\left[\mathbf{y}_u \mathbf{y}_u^*\right] = \begin{pmatrix} \mathbf{y}_u^2 & \mathbf{y}_u \mathbf{y}_{u-1} & \mathbf{y}_u \mathbf{y}_{u-2} & \cdots & \mathbf{y}_u \mathbf{y}_{u-P} \\ \mathbf{y}_{u-1} \mathbf{y}_u & \mathbf{y}_{u-1}^2 & \mathbf{y}_{u-1} \mathbf{y}_{u-2} & \cdots & \mathbf{y}_{u-1} \mathbf{y}_{u-P} \\ \vdots & \vdots & \vdots & \ddots & \vdots \\ \mathbf{y}_{u-P} \mathbf{y}_u & \mathbf{y}_{u-P} \mathbf{y}_{u-1} & \mathbf{y}_{u-P} \mathbf{y}_{u-2} & \cdots & \mathbf{y}_{u-P}^2 \end{pmatrix} \tag{4.22}$$

The mean square values of each input sample is contained in the main diagonal of A and the cross terms indicate the autocorrelation terms resultant from the delayed samples of the input signal.

If $\mathbf{y}_u$ and $\mathbf{x}_u$ are static, then the components of $\mathbf{A}$ and $\mathbf{v}$ are the second order statistics which are not time-varying. Equation (4.20) can be rewritten by employing Equations (4.21) and (4.22) as:

$$MSE = \xi = E\left[\mathbf{x}_u^2\right] + \mathbf{w}^T \mathbf{A} \mathbf{w} - 2\mathbf{v}^T \mathbf{w} \tag{4.23}$$

The equalizer can be adaptively tuned by minimizing Equation (4.23) in terms of the weight vector $\mathbf{w}_u$ so that the equalizer can provide a flat spectral response (with minimum ISI) in the received signal and minimising the MSE yields an optimal solution for $\mathbf{w}_u$.

As can be seen from Figure 4.13, the channel noise is included in the received signal. Since the noise $\mathbf{z}(t)$ is present, an equalizer cannot realise prefect performance. Therefore, there will always be some residual ISI with some tracking error. In practice, noise makes Equation (4.9) difficult to realise. Consequently, a flat

instantaneous combined frequency response will be hard to attain.

Minimising the MSE has a propensity to reduce BER. This can be elaborated upon with a simple intuitive justification. Suppose the error signal $\mathbf{b}_u$ is Gaussian distributed with zero mean. Then, $E\left[|\mathbf{b}_u|^2\right]$ is the variance or the power of the error signal. There is less possibility of disturbing the output signal $\mathbf{d}_u$, if the variance is minimised and the decision device has more possibility to detect $\mathbf{d}_u$ as the transmitted signal $\mathbf{x}_u$. Therefore, in this research BER is analyzed for a range of SNR values.

4.4.2 DFE adaptive equalizer

When the channel distortions are too severe for a linear equalizer to maintain, nonlinear equalizers like DFE are employed. If there are deep spectral nulls in the passband of the channels then, linear equalizers do not execute well. The linear equalizers put too much gain in the locality of the spectral null while attempting to compensate for the distortions. Consequently, the noise present in those frequencies will be enhanced.

The nonlinear equalizer DFE is significant because when an information symbol has been detected and decided on, the ISI that it causes on future symbols can be estimated and subtracted out before the detection of successive symbols [9]. Figure 4.15 illustrates a DFE adaptive equalizer during training. The signals are the same as for the linear adaptive equalizer. The detected output is fed back to the equalizer as a decision feedback path after the initial training sequence is used to generate the initial equalized signal. The error signal B_u controls both the set of feed forward and the feedback weights. P and Q are the order of the feed forward and feedback filters, respectively. The output of the equalizer can be represented as:

$$\hat{\mathbf{d}}_u = \sum_{p=1}^{P} \mathbf{w}_p^* \mathbf{y}_{u-p} + \sum_{q=1}^{Q} \mathbf{f}_q \mathbf{d}_{u-q} \tag{4.24}$$

where $\mathbf{w}_u$ and $\mathbf{y}_u$ are tap gains and input of the forward filter, respectively. As mentioned earlier, since the input of the equalizer, $\mathbf{y}_{u,r}{}^n$ which is the output of the FFT module at time instant u on the receiver antenna r at the OFDM subcarrier n can be taken separately and inserted to separate equalizers the study of the process of an equalizer can be simplified by letting the input of the equalizer be $\mathbf{y}_u$. $\mathbf{f}_u$ and $\mathbf{d}_q$ are the tap gains and input of the feedback filter, respectively. $\mathbf{d}_q$ $(q < u)$ is the previous decision made on the detected symbol. Next, the previous decisions $d_{u-1}, d_{u-2}, \ldots$ with d_u are fed back to the equalizer. Then, using Equation (4.24), $\hat{\mathbf{d}}_{u+1}$ is obtained.

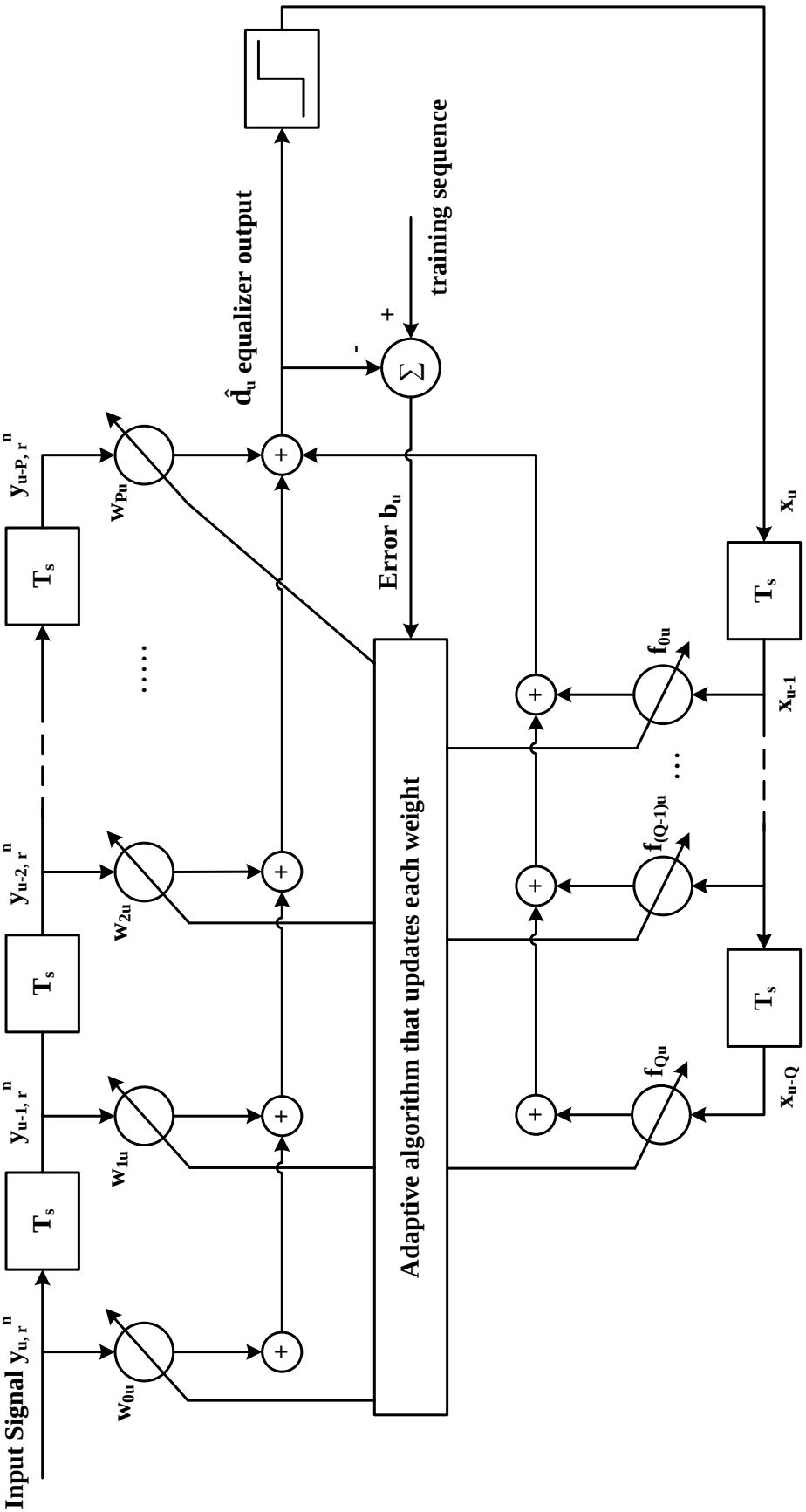

Figure 4.15: Decision feedback adaptive equalizer during training

4.4.3 Least mean square (LMS) algorithm

LMS uses the minimisation of the MSE between the desired output and the actual output of the equalizer. Let us consider Figure 4.14. The error signal B_u can be expressed as:

$$\mathbf{b}_u = \mathbf{d}_u - \hat{\mathbf{d}}_u = \mathbf{x}_u - \hat{\mathbf{d}}_u \tag{4.25}$$

and from Equation (4.16):

$$\mathbf{b}_u = \mathbf{x}_u - \mathbf{y}_u^T \mathbf{w}_u = \mathbf{x}_u - \mathbf{w}_u^T \mathbf{y}_u \tag{4.26}$$

To calculate MSE $|\mathbf{b}_u|^2$, at time instant u, Equation (4.26) is squared to acquire:

$$\xi = E\left[\mathbf{x}_u^* \mathbf{x}_u\right] \tag{4.27}$$

The LMS algorithm seeks to minimise the MSE obtained in Equation (4.27). For a precise channel condition, the error signal $\mathbf{b}_u$ depends on the tap gain vector $\mathbf{w}_P$. This implies that the MSE of an equalizer is a function of the tap gain vector and lets the cost function $\mathbf{J}(\mathbf{w}_P)$ be the MSE as a function of $\mathbf{w}_P$. Considering the derivation in Section 4.4.1 and so as to minimize the MSE, it is necessary to make the derivative of Equation (4.28) to zero.

$$\frac{d}{d\mathbf{w}_P}\mathbf{J}\left(\mathbf{w}_P\right) = -2\mathbf{v}_P + 2\,\mathbf{A}_{PP}\mathbf{w}_P = 0 \tag{4.28}$$

Simplifying Equation (4.28):

$$\mathbf{A}_{PP}\hat{\mathbf{w}}_P = \mathbf{v}_P \tag{4.29}$$

Since the error is minimised and is made orthogonal (normal) to the projection of the desired signal $\mathbf{x}_u$, Equation (4.29) is called the normal equation. When Equation (4.29) is fulfilled, the MMSE of the equalizer can be expressed as:

$$\mathbf{J}_{opt} = J(\hat{\mathbf{w}}_P) = E\left[\mathbf{x}_u \mathbf{x}_u^*\right] - 2\mathbf{v}_P^T \hat{\mathbf{w}}_P \tag{4.30}$$

To acquire the optimal tap gain vector $\hat{\mathbf{w}}_P$, the normal Equation in (4.29) must be solved iteratively while the equalizer converges to an adequately small value of $\mathbf{J}_{opt}$. Practically, the MMSE is executed recursively by employing the *stochastic gradient algorithm* proposed by Widrow [241]. This method is commonly referred to as the LMS algorithm. It needs only $2P + 1$ operations per iteration and therefore, is the simplest equalization algorithm. Let the parameter i be the sequence of iterations

and LMS is calculated iteratively by:

$$\hat{\mathbf{d}}_u(i) = \mathbf{w}_P^T(i)\mathbf{y}_P(i)$$

$$\mathbf{b}_u(i) = \mathbf{d}_u(i) - \hat{\mathbf{d}}_u(i) \tag{4.31}$$

$$\mathbf{w}_P(i+1) = \mathbf{w}_P(i) - \mu\mathbf{b}_u^*(i)\mathbf{Y}_P(i)$$

where the number of delay phases in the equalizer is denoted by P and μ is the step size of the LMS algorithm. It controls the convergence and the stability of the algorithm.

The ratio of signal to distortion is maximised by LMS at its outputs within the limitations of the filter length of the equalizer. The equalizer will not be able to lessen the distortion, if an input signal of the equalizer has a time dispersion characteristic that is larger than the equalizers propagation delay. Since only one variable, the step size μ, controls the rate of adaptation, the convergence rate of the LMS algorithm is not fast. To avoid the adaptation becoming unsteady, the value of μ is selected from

$$0 < \mu < \frac{2}{\left(\sum_{p=1}^{P} \gamma_p\right)} \tag{4.32}$$

where γ_p is the p^{th} eigenvalue of the covariance matrix $\mathbf{A}_{PP}$

4.4.4 Recursive least squares (RLS) Algorithm

The gradient based-LMS algorithm is very slow due to its convergence rate. This is severe specifically when the eigenvalues of the input covariance matrix $\mathbf{A}_{PP}$ have a very large spread, i.e., $\gamma_{\max} \setminus \gamma_{\min} >> 1$. In order to attain faster convergence, complex algorithms which consist of extra variables are employed. The method of least squares is used to develop rapid converging algorithms, rather than using the statistical technique employed in the LMS algorithm. This means that the fast convergence relies on error measures that are represented in the time average of the actual received signal rather than of a statistical average. This results in a powerful, although complex, adaptive signal processing approach termed as *recursive least squares* (RLS) [195]. It extensively enhances the convergence rate of adaptive equalizers.

The definition of the least square error derived from the time average can be expressed as [242]:

$$\mathbf{J}(i) = \sum_{u=1}^{i} \lambda^{i-u}\mathbf{b}^*(u,i)\,\mathbf{b}(u,i) \tag{4.33}$$

where λ is the weighting factor and it should be closer to but less than 1, $\mathbf{b}^*(u,i)$ is the complex conjugate of $\mathbf{b}(u,i)$ and it can be expressed as:

$$\mathbf{b}(u,i) = \mathbf{x}(u) - \mathbf{y}_P^T(u)\mathbf{w}_P(i) \quad 0 \leq u \leq i \tag{4.34}$$

and

$$\mathbf{y}_P(u) = [y(u), y(u-1), \ldots, y(u-P+1)]^T \tag{4.35}$$

where $\mathbf{y}_P(u)$ is the input vector at time instant u, and $\mathbf{w}_P(i)$ is the new tap gain vector at time instant i. Consequently, the error signal employing the recent tap gain at time instant i for testing the previous data at time instant u is $\mathbf{b}(u,i)$, and the cumulative squared error of the recent tap gains on the previous data is $J(i)$.

By minimising the cumulative squared error $\mathbf{J}(i)$, the RLS solution attempts to find the tap gain vector of the equalizer $\mathbf{w}_P(i)$. All the old data are used to test the recent tap gains. The variable λ is a data weighting factor which is also called the forgetting factor. In non-stationary conditions, λ weights the new data more heavily in the calculations; therefore, $\mathbf{J}(i)$ has a propensity to forget the previous data.

The gradient of $\mathbf{J}(i)$ is made zero for acquiring the minimum of least squares error $\mathbf{J}(i)$:

$$\frac{d}{dw_P}\mathbf{J}(i) = 0 \tag{4.36}$$

By using Equations (4.34), (4.35), and (4.36), we can derive [243]

$$\mathbf{A}_{PP}(i)\hat{\mathbf{w}}_P(i) = \mathbf{v}_P(i) \tag{4.37}$$

where $\hat{\mathbf{w}}_P(i)$ denotes the optimal tap gain vector of the RLS equalizer,

$$\mathbf{A}_{PP}(i) = \sum_{u=1}^{i} \lambda^{i-u}\mathbf{y}_P^*(u)\mathbf{y}_P^T(u) \tag{4.38}$$

$$\mathbf{v}_P(i) = \sum_{u=1}^{i} \lambda^{i-u}\mathbf{x}^*(u)\mathbf{y}_P(u) \tag{4.39}$$

where $\mathbf{A}_{PP}(i)$ is the deterministic correlation matrix of the input data of the equalizer $\mathbf{y}_P(u)$ and $\mathbf{v}_P(i)$ is the deterministic cross-correlation vector between the input vector of the equalizer $\mathbf{y}_P(u)$ and the desired output $\mathbf{d}_u$, where $\mathbf{d}_u = \mathbf{x}_u$. To calculate the weight vector of the equalizer, $\hat{\mathbf{w}}_P$, by employing Equation (4.37), it is necessary to calculate $\mathbf{A}_{PP}^{-1}(i)$. It is feasible to acquire a recursive equation stating

$\mathbf{A}_{PP}(i)$ in terms of $\mathbf{A}_{PP}(i-1)$ by using the definition in Equation (4.38).

$$\mathbf{A}_{PP}(i) = \lambda \mathbf{A}_{PP}(i-1) + \mathbf{y}_P(i)\mathbf{y}_P^T(i) \tag{4.40}$$

Note that the three terms in Equation (4.40) are all $P \times P$ matrices. Therefore, for deriving a recursive update for $\mathbf{A}_{PP}^{-1}(i)$ in terms of the earlier inverse, $\mathbf{A}_{PP}^{-1}(i-1)$, a matrix inverse lemma can be employed [9].

$$\mathbf{A}_{PP}^{-1}(i) = \frac{1}{\lambda}\left[\mathbf{A}_{PP}^{-1}(i-1) - \frac{\mathbf{A}_{PP}^{-1}(i-1)\mathbf{y}_P(i)\mathbf{y}_P^T(i)\mathbf{A}_{PP}^{-1}(i-1)}{\lambda + \alpha(i)}\right] \tag{4.41}$$

where

$$\alpha(i) = \mathbf{y}_P^T(i)\mathbf{A}_{PP}^{-1}(i-1)\mathbf{y}_P(i) \tag{4.42}$$

Therefore, using these recursive equations, the RLS minimisation can be expressed in terms of the following weight update equations:

$$\mathbf{w}_P(i) = \mathbf{w}_P(i-1) + \kappa_P(i)\mathbf{b}^*(i, i-1) \tag{4.43}$$

where

$$\kappa_P(i) = \frac{\mathbf{A}_{PP}^{-1}(i-1)\mathbf{y}_P(i)}{\lambda + \alpha(i)} \tag{4.44}$$

A summary of the RLS algorithm can be written as follows:

1. Initialise $w(0) = \kappa(0) = x(0)$, $\mathbf{A}^{-1}(0) = \delta I_{PP}$, where I_{PP} is an $P \times P$ identity matrix and δ is a large positive constant.

2. Compute the following equations recursively:

$$\hat{\mathbf{d}}(i) = \mathbf{w}^T(i-1)\mathbf{y}(i) \tag{4.45}$$

$$\hat{\mathbf{b}}(i) = \mathbf{x}(i) - \hat{\mathbf{d}}(i) \tag{4.46}$$

$$\kappa(i) = \frac{\mathbf{A}^{-1}(i-1)\mathbf{y}(i)}{\lambda + \mathbf{y}^T(i)\mathbf{A}^{-1}(i-1)\mathbf{y}(i)} \tag{4.47}$$

$$\mathbf{A}^{-1}(i) = \frac{1}{\lambda}\left[\mathbf{A}^{-1}(i-1) - \kappa(i)\mathbf{y}^T(i)\mathbf{A}^{-1}(i-1)\right] \tag{4.48}$$

$$\mathbf{w}(i) = \mathbf{w}(i-1) + \kappa(i)\mathbf{b}^*(i) \tag{4.49}$$

Chapter 5 (Section 5.2) provides a discussion about the system model developed with the proposed linear and DFE adaptive equalizers.

4.5 Development of a novel and efficient channel tracking algorithm for SDMA-based multi-user MIMO-OFDM systems

This section discusses the system model developed to perform the novel channel tracking method in the uplink of SDMA-based multi-user MIMO-OFDM systems.

4.5.1 System model

A block diagram of the uplink of an SDMA-based multi-user MIMO-OFDM system with channel tracking in the frequency domain is shown in Figure 4.16. The process in the transmitter is the same as the one described for the development of the adaptive equalizers. The same time-varying, frequency selective channel model described in Section 4.2.3 is used in the simulations.

At the receiving end, the signals received by R antennas in the AP are forwarded through FFT OFDM demodulators to obtain the frequency domain points. The resultant $\mathbf{y}^n$ $(\mathbf{n} = 1, 2, \ldots, N)$ complex points are the complex baseband version of the N modulated subcarriers and can be expressed as:

$$\mathbf{y} = \mathbf{H}\mathbf{x} + \mathbf{z} \tag{4.50}$$

where $\mathbf{z}$ is the Additive White Gaussian Noise.

4.5.1.1 Zero-forcing detection

To reduce the computational complexity, transmitted data are detected using the zero-forcing technique. First, zero-forcing is executed at the AP, using the initial channel estimates to detect the transmitted data on a symbol-by-symbol basis:

$$\mathbf{W} = \left(\hat{\mathbf{H}}_\mathbf{0}\hat{\mathbf{H}}_0^H\right)^{-1}\hat{\mathbf{H}}_\mathbf{0}^H$$

$$\mathbf{W}\hat{\mathbf{H}}_0 = \mathbf{I} \tag{4.51}$$

where $\{\cdots\}^H$ is the Hermitian Transpose, $\mathbf{I}$ is the identity matrix and $\hat{\mathbf{H}}_0$ is the initial estimate of the channel. The first detection after the initial channel estimation can be expressed as:

$$\mathbf{W}\mathbf{y} = \mathbf{W}\mathbf{H}\hat{\mathbf{x}} + \mathbf{W}\mathbf{z}$$

$$\mathbf{W}\mathbf{y} = \mathbf{W}\left[\hat{\mathbf{H}}_0 + \mathbf{\Delta H} - \mathbf{e}\right]\hat{\mathbf{x}} + \mathbf{W}\mathbf{z}$$

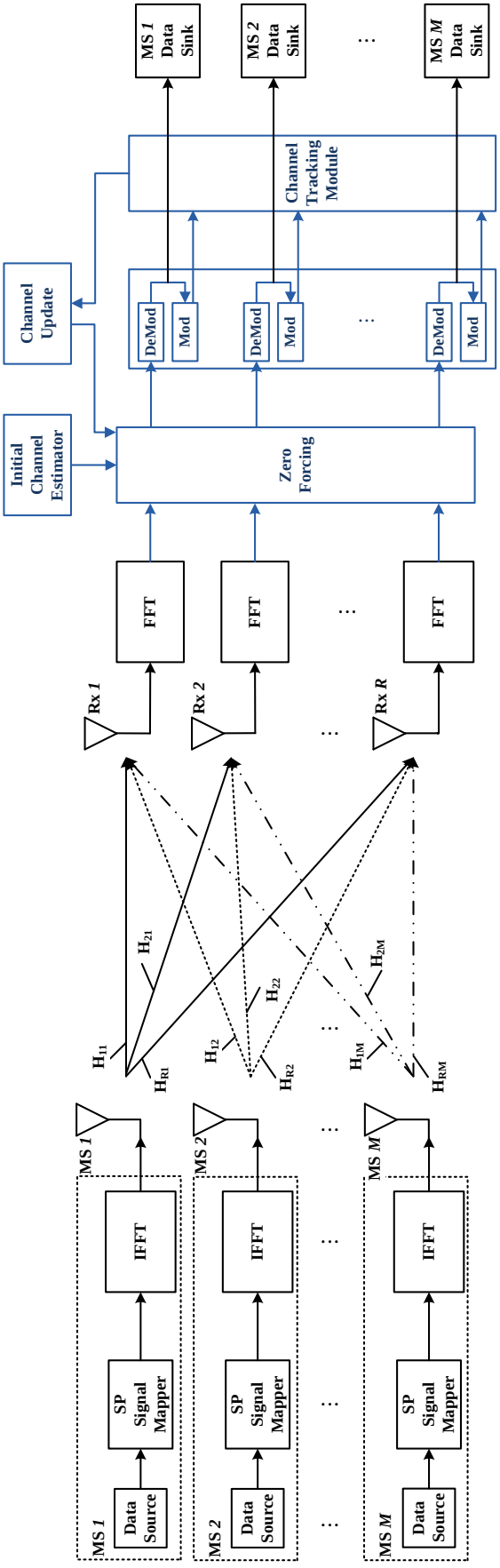

Figure 4.16: Uplink of an SDMA-based multi-user MIMO-OFDM transceiver model with channel tracking

$$\mathbf{Wy} = \left[\mathbf{W}\hat{\mathbf{H}}_\mathbf{0}\right]\hat{\mathbf{x}} + \mathbf{W}\boldsymbol{\Delta}\mathbf{H}\hat{\mathbf{x}} - \mathbf{We}\hat{\mathbf{x}} + \mathbf{Wz} \tag{4.52}$$

$$\mathbf{Wy} = \hat{\mathbf{x}} + \mathbf{W}\boldsymbol{\Delta}\mathbf{H}\hat{\mathbf{x}} + \mathbf{W}(\mathbf{z} - \mathbf{e}\hat{\mathbf{x}})$$

$$\boldsymbol{\Delta}\mathbf{H} = \mathbf{H} - \hat{\mathbf{H}}_\mathbf{0} + \mathbf{e}$$

where $\boldsymbol{\Delta}\mathbf{H}$ is the difference between the actual channel ($\mathbf{H}$) at time equals first detection, after initial channel estimation, and the estimated channel at initial channel estimation time. $\boldsymbol{\Delta}\mathbf{H}$ includes the estimation error ($\mathbf{e}$) plus the change in the channel due to the relative movement between the transmitter and the receiver. Multiple access interference (MAI) arises from the inaccuracy of channel estimation. Consequently, the recovered data $\hat{\mathbf{X}}$ can be obtained with zero-forcing.

4.5.2 Why quadrature amplitude modulation (QAM)?

In the simulations, 16-ary QAM are used as the preferred modulation scheme. In a phase-shift keying (PSK) system, the signal points are all spread on a circle. The distance between the signal points is decreased as the order of the PSK system increases. Consequently, the error rate increases. This means that when we send more bits together, we will have more points on a circle, leading to a higher error rate. The M-ary quadrature amplitude modulation (M-ary QAM) system provides a solution to this problem by modulating independent messages over the amplitudes of orthogonal carriers. The signal constellation can be extended to a higher level of signal constellation (e.g. 64-ary QAM, 256-ary QAM). The advantage of having a large constellation is that we can send a large number of bits together and therefore, increase the transmission data rate. However, if a PSK system is employed for a transmitter with a fixed transmission power, the symbol error probability (SEP) increases because the distance between signal points is decreased due to a dense constellation.

The modulation schemes require only one carrier with a fixed carrier frequency. Each OFDM subcarrier corresponds to one bit and if the PSK or QAM modulation is combined with OFDM, each subcarrier corresponds to more than one bit. The M-ary QAM system is preferred due to constellation being less dense than in a PSK system. Moreover, for both systems, the bandwidth will be reduced if the bit rate is kept the same and the bit rate will be increased if the bandwidth is kept the same. Therefore, the 16-ary QAM modulation scheme is employed in the system model developed in this study as it provided a less dense constellation than in a PSK modulation scheme.

4.6 Statistical analysis of the error vector magnitude

This section describes the statistical analysis of the EVM conducted in this study. EVM measurements can offer a significant amount of insight into the performance of digitally modulated signals. The types of degradations that exist in a signal can be identified with the appropriate use of EVM and related measurements and even can help in identifying their sources. It provides a measure of signal quality that is both simple and quantitative figure-of-merit for digitally modulated signals that can be applied in practical digital RF communications system designs. The employment of EVM measurements is increasing rapidly in acceptance. EVM has already been applied in standards such as global system for mobile (GSM) communications, the North American digital cellular (NADC) system and the personal handy-phone system (PHS). Therefore, it is useful to carry out a statistical analysis of EVM especially as lower EVM values lead to better performance.

4.6.1 Error vector magnitude (EVM)

The error vector magnitude as depicted in Figure 4.17 is a measure of the difference between the reference signal and the measured signal. This difference is referred to as the error vector. In the simulations in this study, the EVM is calculated by comparing the recovered symbols ($\hat{\mathbf{X}}$) with the actual transmitted symbols ($\mathbf{X}$).

4.6.2 Statistical analysis of the EVM

The statistical analysis is executed by carrying out the following steps:

1. The EVM is computed to obtain the magnitude and the complex numbers for different maximum Doppler shift values in a range of 1, 10, 20 and 30 Hz.

   The EVM values are computed for both the initial channel estimation and channel tracking algorithm. A specific range of maximum Doppler values is selected by observing the performance of the channel tracking algorithm with different f_ds. The computed EVM is simulated for 100 realisations for all the MSs, all the OFDM symbols and all the OFDM subcarriers.

2. The variance of the EVM is computed.

   The real and imaginary components of the variance of the EVM are computed separately.

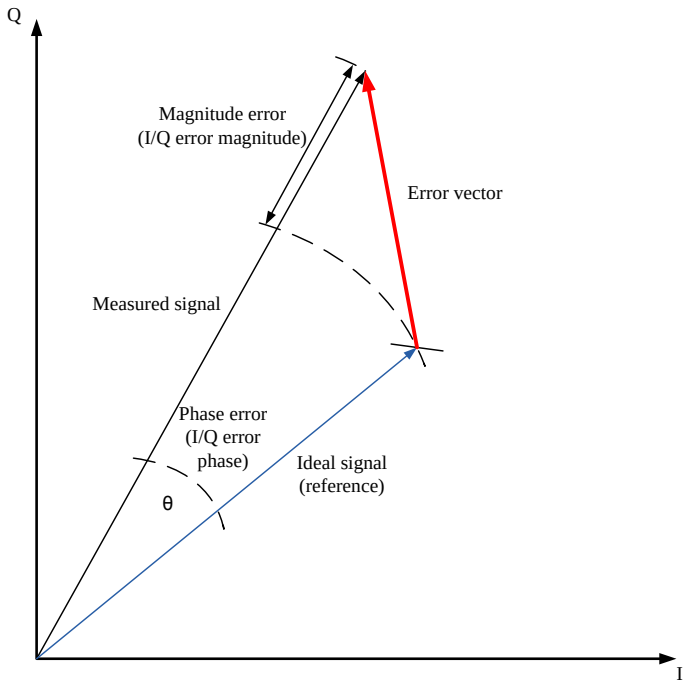

Figure 4.17: Error Vector Magnitude.

3. The variance of EVM for each of the below mentioned variables with the all OFDM symbols are characterised.

   A separate analysis of variance of EVM is conducted for different OFDM subcarriers, for different MSs, and different f_ds.

4. The EVM is characterised by finding its distribution.

4.7 Chapter summary

The methodology undertaken for conducting the research is discussed in this chapter. The research for this project is conducted in five phases. First, the construction of a time-varying, frequency selective, multi-user, MIMO channel model is performed. Then, an efficient method for initial channel estimation is derived employing a training sequence. Next, adaptive channel equalization methods for SDMA-based multi-user MIMO-OFDM systems are developed. After that, the development of a novel and efficient channel tracking algorithm for multi-user MIMO-OFDM systems is performed. Finally, statistical analysis of the EVM between the recovered symbols

($\hat{\mathbf{X}}$) and the transmitted symbols ($\mathbf{X}$) is carried out.

The next chapters discuss the adaptive equalization methods and the novel channel tracking algorithm.

Chapter 5

Adaptive Equalization in SDMA-Based Multi-User MIMO-OFDM Systems

5.1 Introduction

Linear and decision feedback adaptive channel equalization using the LMS algorithm and the RLS algorithm for multi-user MIMO-OFDM wireless communications systems are discussed in this chapter. The contribution of this chapter resides on the application of adaptive equalization techniques to multi-user MIMO-OFDM systems using SDMA for the first time. Moreover, this contribution consists of applying these techniques for static, frequency selective, SDMA-based multi-user MIMO-OFDM channels. The proposed equalization methods adaptively compensated the channel impairments caused by multi-path propagation and time-variations in the propagation environment. Simulations for the proposed adaptive equalizer are conducted using a training sequence method to determine optimal performance through a comparative analysis of LMS, RLS and without adaptive equalization. The results shows an improvement of 0.49 in BER (at an SNR of 16 dB) when using DFE adaptive equalization with RLS algorithm compared to the case in which no equalization is employed. In general, adaptive equalization using LMS and RLS algorithms is shown to be significantly beneficial for SDMA-based multi-user MIMO-OFDM systems.

The next sections present a theoretical framework for adaptive equalization and the simulation results obtained for static, frequency selective multi-user MIMO channels using linear and DFE adaptive equalization in the uplink of SDMA-based multi-user MIMO-OFDM systems.

5.2 Adaptive equalization in SDMA-based multi-user MIMO-OFDM systems

This section discusses the system model developed to perform adaptive equalization in the uplink of SDMA-based multi-user MIMO-OFDM systems.

5.2.1 System model

A block diagram of an uplink of an SDMA-based multi-user MIMO-OFDM system with adaptive equalization in frequency domain is shown in Figure 5.1. As a complexity alleviation technique in OFDM, the fast Fourier transform (FFT) algorithm is employed to perform N-point inverse FFT (IFFT) and FFT at the transmitter and the receiver, respectively. At the transmitter, a binary data stream from each MS M is passed through a serial to parallel (SP) converter and subsequently mapped onto blocks of data symbol constellation points. Binary phase shift keying (BPSK) modulation is used in the simulations. Then, inverse FFT is performed to generate OFDM subcarriers. There are $M \times N$-element signal constellation blocks. The signal from the m^{th} transmitter ($\mathbf{m} = 1, 2, \ldots, M$) can be expressed as:

$$\mathbf{x}_{u,m} = [x_{um}{}^{1}, x_{um}{}^{2}, \ldots, x_{um}{}^{N}]^{T} \tag{5.1}$$

where the index u is the current time instant and T is the transpose of the vector.

The outputs of the modulators are then transmitted by a single antenna at the MS through the unknown frequency selective channel model. It is assumed that all MSs are synchronised. At the receiving end, the signals received by R antennas in the AP are forwarded through FFT OFDM demodulators to obtain the frequency domain points. The resultant $\mathbf{y}^{n}$ ($\mathbf{n} = 1, 2, \ldots, N$) complex points are the complex baseband version of the N modulated subcarriers. The outputs of the demodulators are then sent through the proposed frequency domain linear adaptive equalizers to equalize the unknown channel to compensate for the channel's dispersion that occurred at different subcarriers as depicted in Figure 5.1.

The inputs to the n^{th} equalizer in the m^{th} MS bin are the complex samples at the output of the FFT demodulators and can be expressed as:

$$\mathbf{y}^{\mathbf{n}}_{\mathbf{u,r}} = \sum_{m=1}^{M} \mathbf{H}^{\mathbf{n}}_{\mathbf{rm}} \mathbf{x}_{\mathbf{um}}{}^{\mathbf{n}} + \mathbf{z}^{\mathbf{n}}_{\mathbf{ur}}, (\mathbf{n} = 1, 2, \ldots, N) \tag{5.2}$$

where $\mathbf{H}_{\mathbf{rm}}{}^{n}$ is the gain of the channel between the m^{th} MS and r^{th} receiver antenna at AP observed on the n^{th} OFDM subcarrier and $\mathbf{z}^{\mathbf{n}}_{\mathbf{ur}}$ is the additive white Gaussian

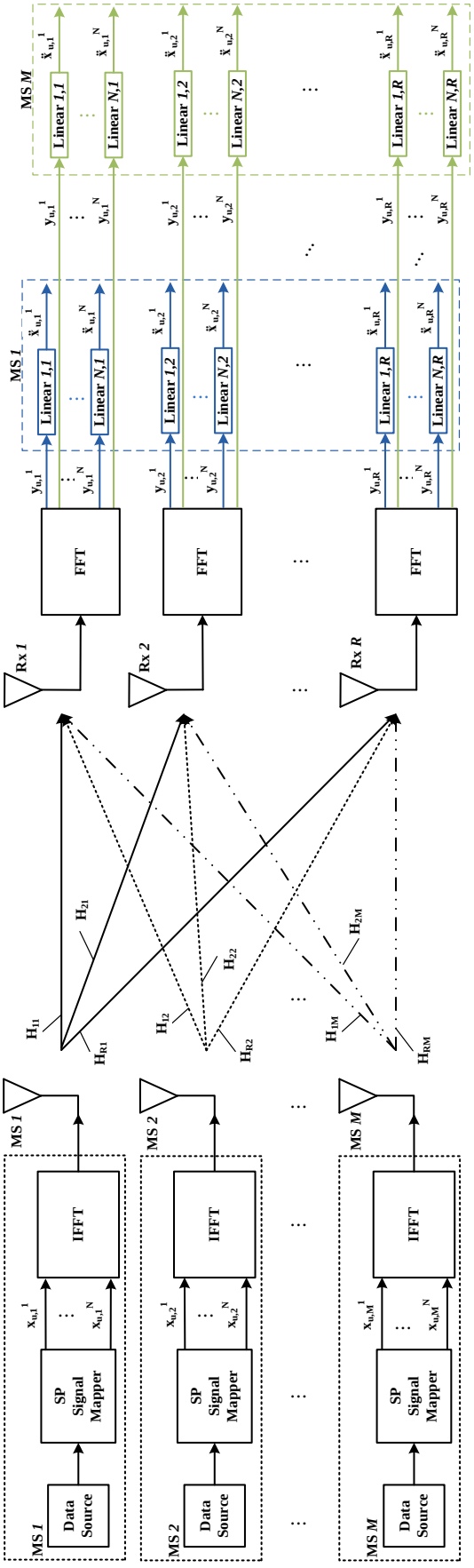

Figure 5.1: Uplink of SDMA-based multi-user MIMO-OFDM transceiver model with linear adaptive equalization

noise sample at the output of the n^{th} FFT bin of the r^{th} receiver antenna at the u^{th} time instant.

Since the subcarriers are mutually orthogonal, we could consider each output of the FFT module separately. There are $N \times R$ linear adaptive equalizers in each of the m bins. In the equalizer, the received symbols are equailized and detected. If we apply the following vector notation:

$$\begin{aligned}
\mathbf{y_u^n} &= [y_{u,1}^n, {y_{u,2}}^n, \ldots, {y_{u,R}}^n]^T \\
\mathbf{x_u^n} &= [x_{u,1}^n, {x_{u,2}}^n, \ldots, {x_{u,M}}^n]^T \\
\mathbf{z_u^n} &= [z_{u,1}^n, {z_{u,2}}^n, \ldots, {z_{u,R}}^n]^T \\
\mathbf{H^n} &= \begin{pmatrix} H_{11}^n & \cdots & H_{1M}^n \\ \vdots & \ddots & \vdots \\ H_{R1}^n & \cdots & H_{RM}^n \end{pmatrix}
\end{aligned} \tag{5.3}$$

we can express the outputs of the n^{th} bin of the FFT demodulator as:

$$\mathbf{y_u}^\mathbf{n} = \mathbf{H^n x_u^n} + \mathbf{z_u^n}, (\mathbf{n} = 1, 2, \ldots, N) \tag{5.4}$$

From our linear adaptive equalization method, the transmitted data block $\mathbf{x_u^n}$ could be found on the basis of the received sample vector $\mathbf{y_u^n}$ that is observed at the outputs of the n^{th} bin of R FFT OFDM demodulators. We jointly processed the output samples from a given m^{th} bin by averaging the detected symbols over R antennas and then, demodulated the resultant signal to calculate the BER. The delay (D) introduced by the reference tap in the equalizer is compensated by truncating the demodulated signal by D number of symbols. LMS and RLS adaptive algorithms can be used to adjust the coefficients of the equalizer in an environment where the knowledge of relevant statistics is unavailable.

Figure 5.2 illustrates the process of a linear adaptive equalizer. The adaptive algorithm LMS is controlled by error signal $\mathbf{b_u}$. The error signal is derived by comparing the output of the equalizer $\hat{\mathbf{d}}_\mathbf{u}$, with a training sequence $\mathbf{x_u}$. The adaptive algorithm, then uses $\mathbf{b_u}$ to minimize a cost function and updates the equalizer coefficients in a way that iteratively decreases the cost function. The filter coefficients of the equalizer are updated by the LMS algorithm as follows:

$$\mathbf{w_{u+1}} = \mathbf{w_u} + \mu \mathbf{b_u} \mathbf{y_{u,r}}^\mathbf{n} \tag{5.5}$$

where $\mathbf{y_{u,r}^n}$ is the input vector of time delayed input values, the tap weights of equalizer are $\mathbf{w_u} = [w_{0u}, w_{1u}, \ldots, w_{pu}]^T$ at time instant u and P is the order of the

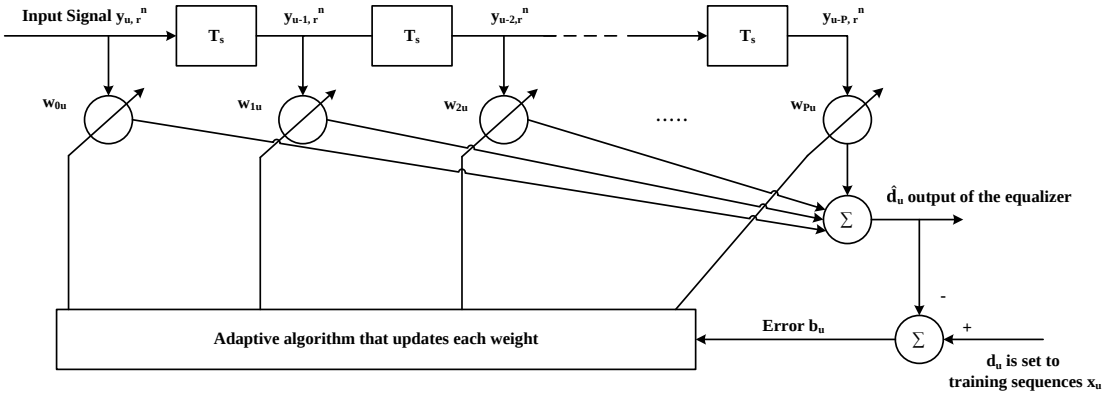

Figure 5.2: Linear adaptive equalizer during training.

equalizer. These coefficients contain information from channel characterization. The parameter μ is the step size which is a small positive constant and it controls the influence of the updating factor. In RLS, the cost function can be minimised as follows:

$$\xi(u) = \sum_{i=1}^{u} \lambda^{u-i} |\mathbf{b}(i)|^2 \tag{5.6}$$

where λ is the forgetting factor which is a positive constant close to, but less than 1.

Figure 5.3 shows the proposed DFE adaptive equalization method for the uplink of an SDMA-based multi-user MIMO-OFDM system. Architecture similar to the one used for linear equalization is employed to perform decision feedback equalization at the AP. A detailed description of the process of the linear and DFE adaptive equalizers can be found in Chapter 4 (Section 4.4).

5.3 Simulation results and discussion

The improvements achieved by the proposed linear and decision feedback adaptive equalization methods for the uplink of SDMA-based multi-user MIMO-OFDM systems using the LMS and the RLS adaptive algorithms for static, frequency selective multi-user MIMO channels are discussed in this section. Computer simulations are performed using Matlab. The simulations are conducted for two types of channels: a) two path, static, multi-user MIMO, frequency selective fading channels, and b) three path, multi-user MIMO, frequency selective fading channels. BPSK modulation is used for all the simulations with 100 iterations for BER. The simulations are

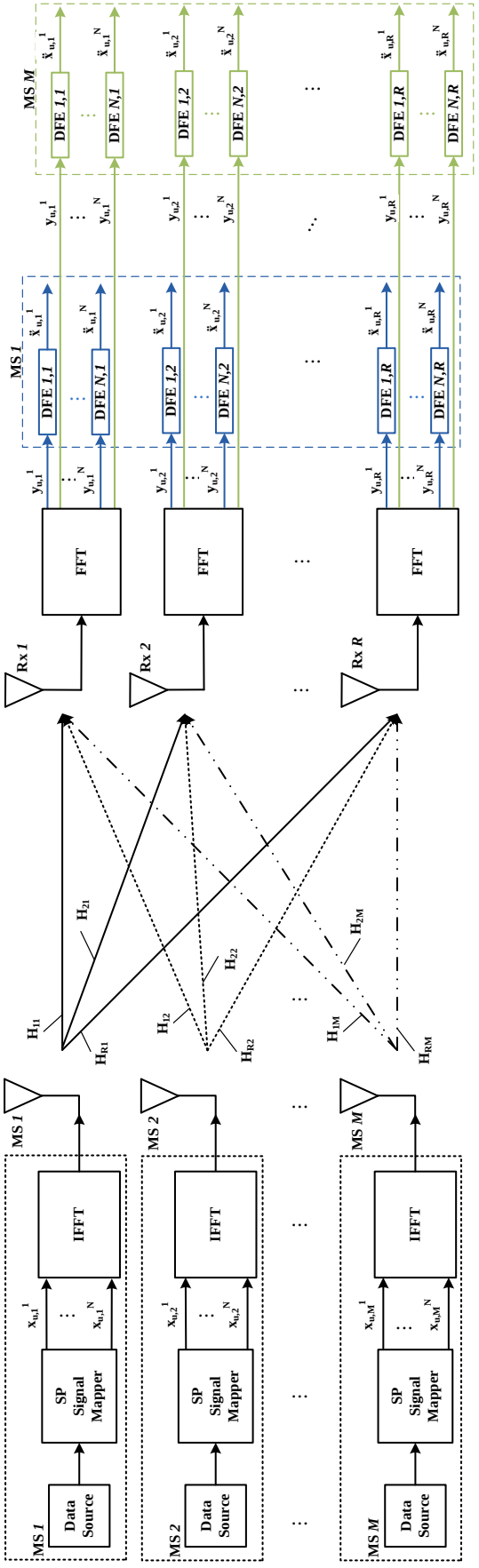

Figure 5.3: Uplink of an SDMA-based multi-user MIMO-OFDM transceiver model with decision feedback adaptive equalization

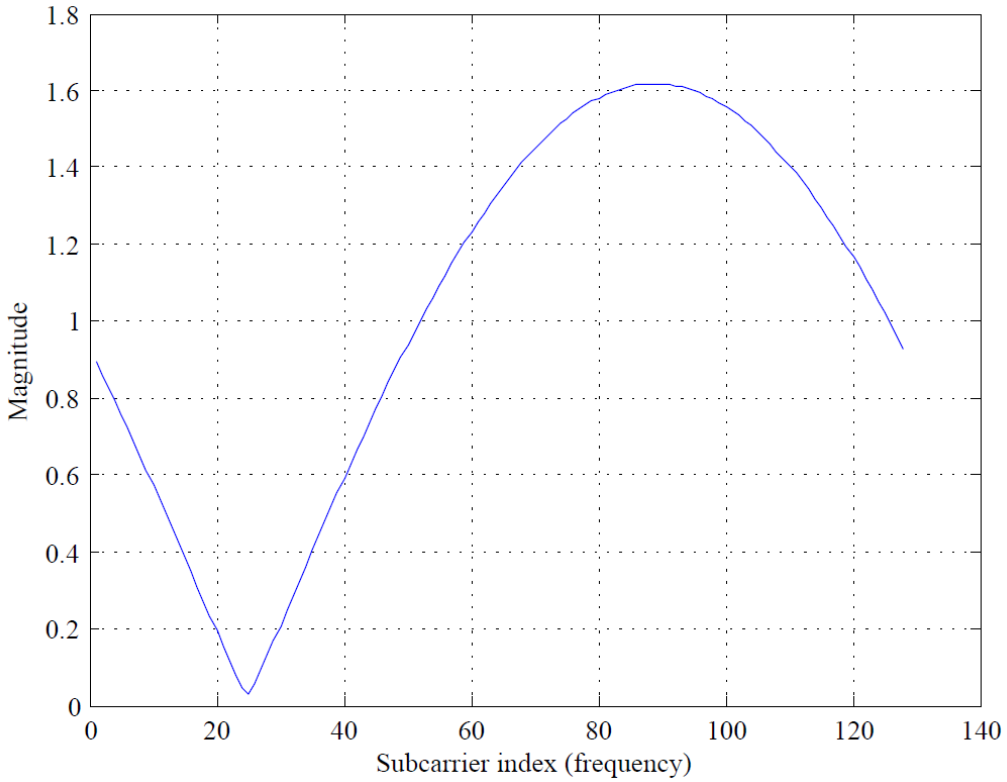

Figure 5.4: Static, frequency selective channel.

performed for 96 OFDM symbols (time index, $U = 96$), the number of subcarriers is $N = 128$, the number of MS is $M = 6$, and the number of receiver antennas at the AP is $R = 12$. The step size (μ) of the LMS is empirically fixed to 0.03 to allow a faster convergence and the forgetting factor (λ) of the RLS algorithm is fixed to 0.99 since $\lambda < 1$ implies the filter will have less memory and therefore will adapt to a time-varying channel more efficiently.

5.3.1 Linear adaptive equalization in SDMA-based multi-user MIMO-OFDM systems

The simulations conducted for the static, frequency selective multi-user MIMO channels with linear adaptive equalization are discussed in this section. The simulated CFR is depicted in Figure 5.4 with 128 OFDM subcarriers in the frequency domain. The time variations are not considered in this simulation, hence the channel is described as static or non-stationary. The dynamic range of the magnitude of the channel is 1.586 with a minimum of 0.0317 and a maximum of 1.618. Although the

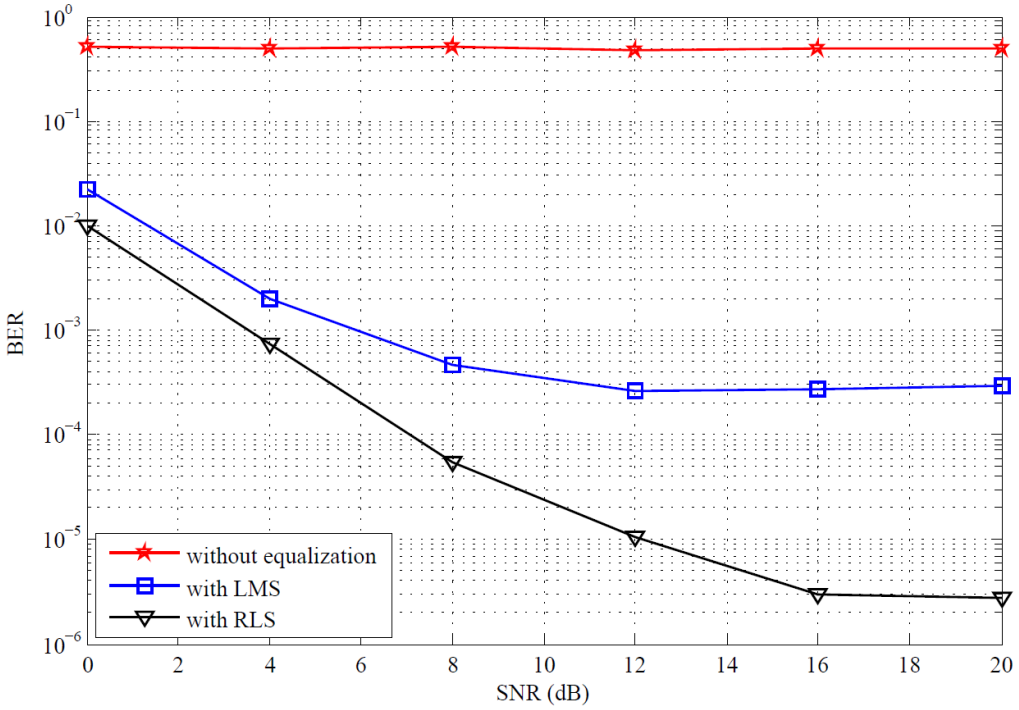

Figure 5.5: BER versus SNR for linear AE with LMS, RLS and without equalization for static, frequency selective, multi-user MIMO channels.

multi-user MIMO channel is static in time, it is frequency selective. Therefore, the effect we are discussing in this section is the effect of adaptive equalization in static, frequency selective, multi-user MIMO channels. The function of the equalizers is to compensate the impairments of the channel.

Figure 5.5 shows the simulation results for BER with LMS, RLS adaptive algorithms and without equalization. The BER values are averaged over the BER iterations and the number of MS. Linear adaptive equalization using LMS and RLS provided a significantly lower BER when used in multi-user MIMO-OFDM systems. For example, at an SNR of 16 dB, the average BER without equalization is 4.9×10^{-1} while the average BER with LMS is 2.8×10^{-4}. Similarly, at an SNR of 16 dB, the average BER with RLS is 2.95×10^{-6}. In general, these results demonstrate the significant effect AE is able to achieve in SDMA-based multi-user MIMO-OFDM systems. As expected, the RLS BER results shows a better performance than the LMS algorithm results, due to the adaptive property of RLS algorithms which continuously update the estimates of the autocorrelation matrix of the input signal vector and the cross-correlation vector between the input vector and the desired

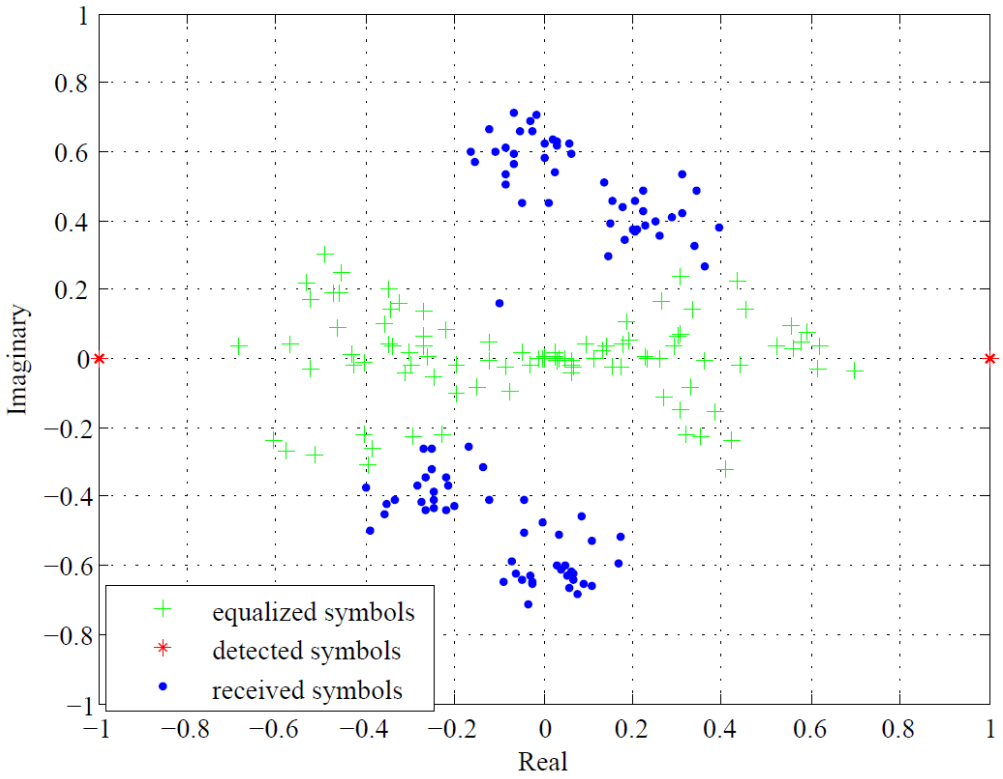

Figure 5.6: Signal constellation with LMS for static, frequency selective, multi-user MIMO channels.

response of the filter. For example, at an average BER of 10^{-3}, the required SNR with RLS is 3 dB lower than that of LMS. Moreover, the error floor for the LMS reduces dramatically from 3×10^{-4} to 3×10^{-6} by using RLS. There is an error floor for LMS and RLS because when SNR increases the error between the desired signal and the output signal of the adaptive filter decreases (see Figure 3.3). The filter coefficients converge to a minimum BER value by using adaptive algorithms such as LMS and RLS as there is no need to adjust filter coefficients as SNR increases. Therefore, the RLS algorithm performs better than the LMS algorithm with linear AE for the uplink of the multi-user MIMO-OFDM systems.

Signal constellations of equalized symbols, received symbols and detected symbols with LMS for the first subcarrier and for the first user at the first receiver antenna are shown in Figure 5.6. The standard deviation of the equalized symbols is 0.128 while that of the received symbols is 0.518, which is 0.39 higher than the standard deviation of the equalized symbols on the imaginary axis. This shows that the received symbols has a higher standard deviation after passing through the static,

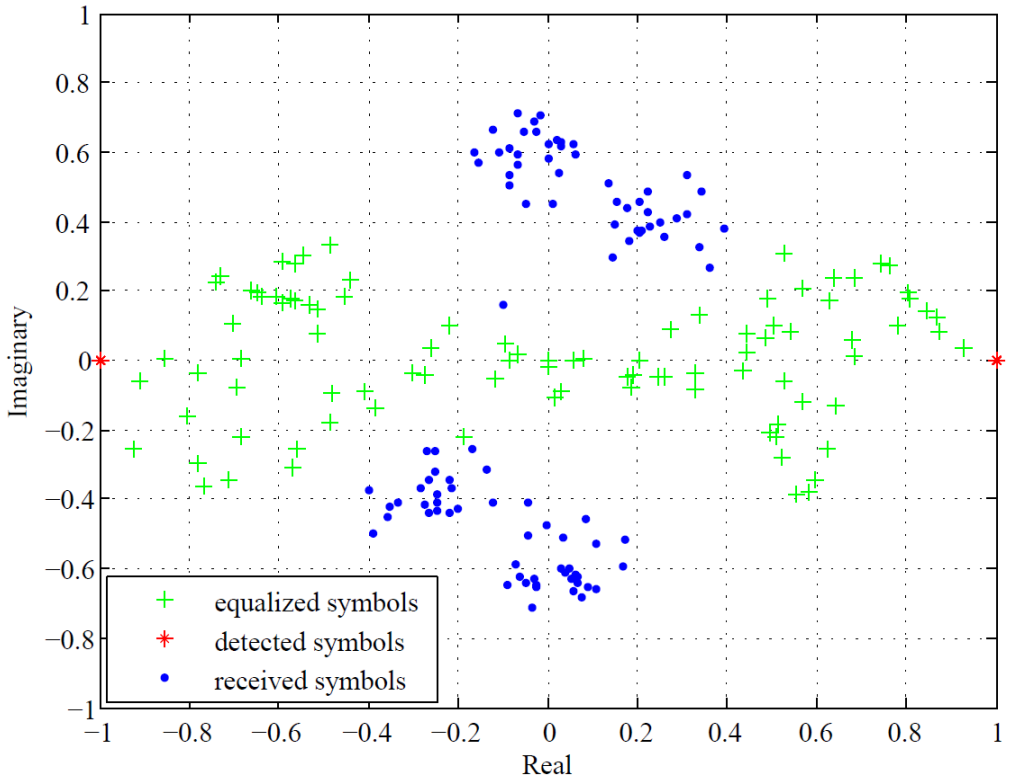

Figure 5.7: Signal constellation with RLS for static, frequency selective, multi-user MIMO channels.

frequency selective, multi-user MIMO channels. In addition, the equalizer with LMS lessened the effects of channel impairments as can be seen from the equalized symbols.

The signal constellations of the equalized symbols, received symbols and detected symbols with RLS for the first subcarrier and for the first user at the first receiver antenna are shown in Figure 5.7. The standard deviation of the equalized symbols is 0.196 while that of received symbols is 0.518, which is 0.322 higher than the standard deviation of the equalized symbols on the imaginary axis. This shows that the received symbols has a higher standard deviation after passing through the static, frequency selective, multi-user MIMO channels. Additionaly, the equalizer with RLS lessened the effects of channel impairments as can be seen from the equalized symbols.

The performance of the RLS adaptive algorithm in terms of the forgetting factor in linear adaptive equalization is analysed and the results are depicted in Figure 5.8. It can be seen that the BER reduces as the SNR increases with a minimum

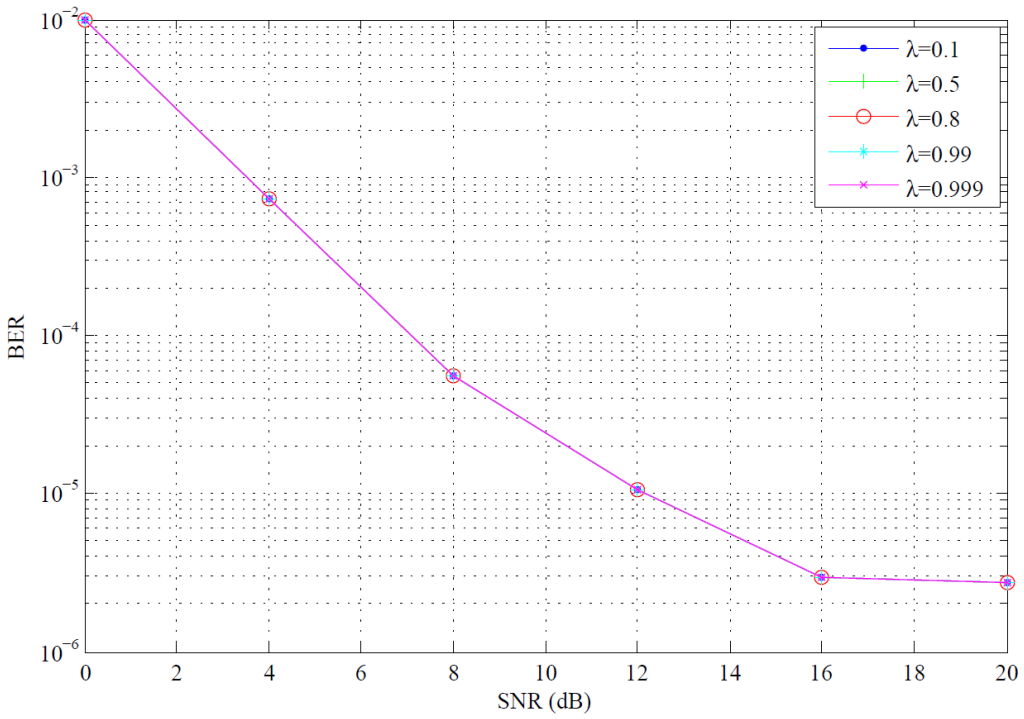

Figure 5.8: BER versus SNR for linear AE with different forgetting factors (λ) for RLS adaptive algorithm.

BER of 2.76×10^{-6} and a maximum of 9.7×10^{-3}. Moreover, there is no apparent difference in BER for different forgetting factors (λs) as the SNR increases. This implies that the linear adaptive equalization in static, frequency selective multi-user MIMO channels does not depend on the forgetting factor, λ. This is because the channel is static and the algorithm does not have to adapt any channel variations.

The next section presents the simulation results obtained using DFE adaptive equalization for static, frequency selective, multi-user MIMO channels in SDMA-based multi-user MIMO-OFDM systems.

5.3.2 Decision feedback adaptive equalization in SDMA-based multi-user MIMO-OFDM systems

The simulations conducted for the static, frequency selective multi-user MIMO channels with DFE adaptive equalization is discussed in this section. Figure 5.4 depicts the simulated CFR with 128 OFDM subcarriers in the frequency domain. The channel is called static as time variations are not considered in these simulations.

The performance of the DFE adaptive equalizer in terms of BER versus SNR in

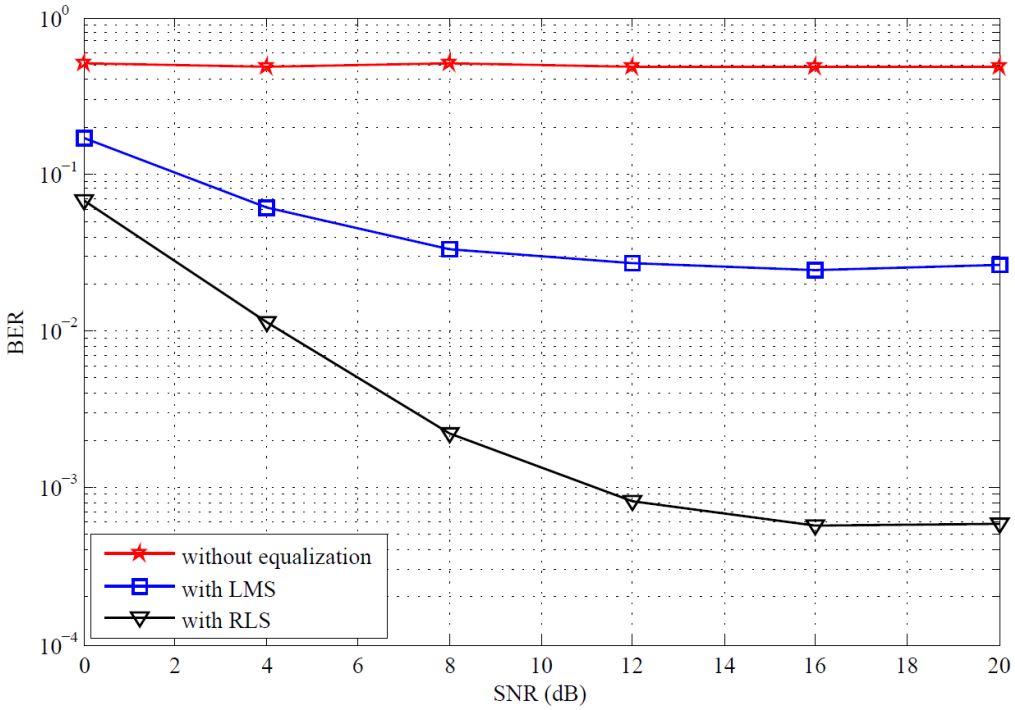

Figure 5.9: BER versus SNR for DFE with LMS, RLS and without equalization for static, frequency selective SDMA-based multi-user MIMO-OFDM channels.

(dB) is illustrated in Figure 5.9. It shows the performance with LMS, RLS adaptive algorithms and without equalization. The BER values are averaged over the BER iterations and the number of MS. A significantly lower BER can be achieved by the DFE adaptive equalization using LMS and RLS in SDMA-based multi-user MIMO-OFDM systems. For example, at an SNR of 16 dB, the average BER without equalization is 4.9×10^{-1} while the average BER with LMS is 2.4×10^{-2}. Similarly, at an SNR of 16 dB, the average BER with RLS is 5.7×10^{-4}. Generally, these results shows the important effect of DFE adaptive equalization is able to attain in SDMA-based multi-user MIMO-OFDM systems. As expected, the RLS BER results demonstrated better performance than the LMS algorithm results, as explained in the previous section. For example, RLS achieved an average BER of 10^{-3}. The error floor for LMS reduces dramatically from 2.4×10^{-2} to 5.7×10^{-4} by using RLS. Consequently, the RLS algorithm performs better than the LMS algorithm with DFE for the uplink of the SDMA-based multi-user MIMO-OFDM systems.

When compared with the DFE AE, the linear AE shows lower BER values. As argued in [9], the DFE AE is employed when the channel conditions are too severe

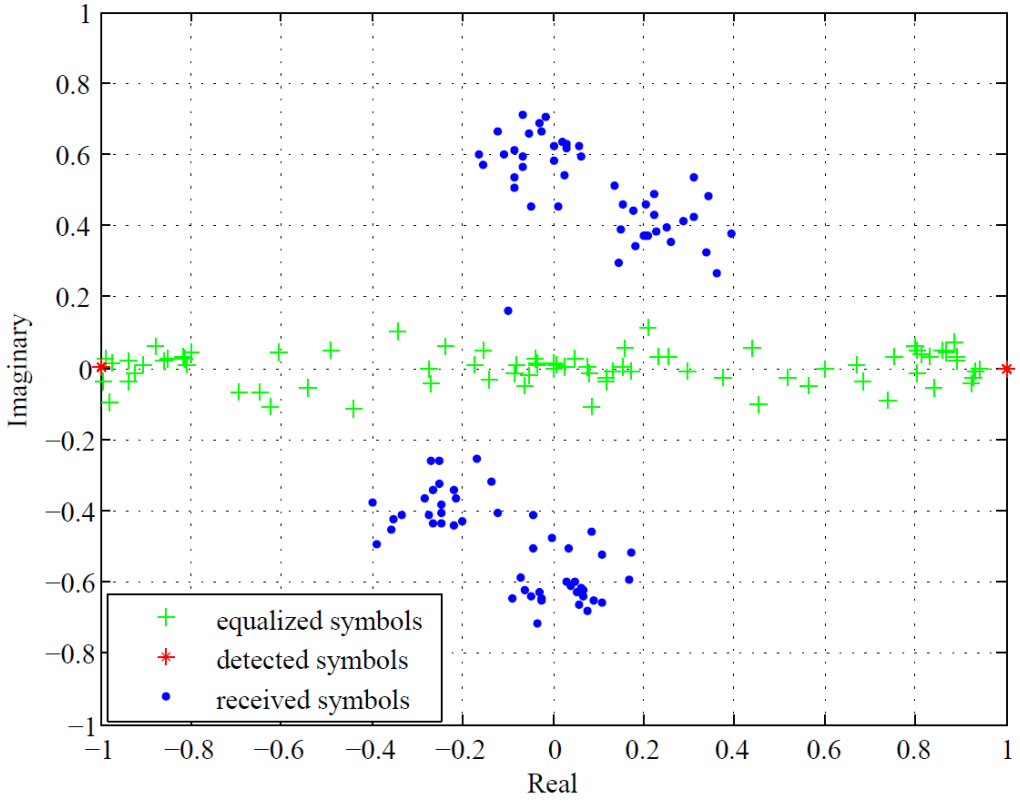

Figure 5.10: Signal constellation with LMS.

for a linear equalizer to manage and linear AE performs well for static channels. Now, our simulations have proven that linear AE performs better than the DFE AE for the SDMA-based multi-user MIMO-OFDM systems.

Figure 5.10 depicts the signal constellations of the equalized symbols, received symbols and detected symbols with LMS. The results are shown for the first subcarrier and for the first user at the first receiver antenna. The standard deviation of the equalized symbols is 0.046 while that of the received symbols is 0.518, which is 0.472 higher than the standard deviation of the equalized symbols on the imaginary axis. This demonstrates a higher standard deviation for the received symbols after passing through the static, frequency selective channel and the equalizer with LMS reduces the effect of channel impairments as can be seen from the equalized symbols. Furthermore, the output of the equalizer, namely, the detected symbols are at the precise demodulation points for BPSK.

Figure 5.11 illustrates the signal constellations of the equalized symbols, received symbols and detected symbols with RLS algorithm. The results are presented

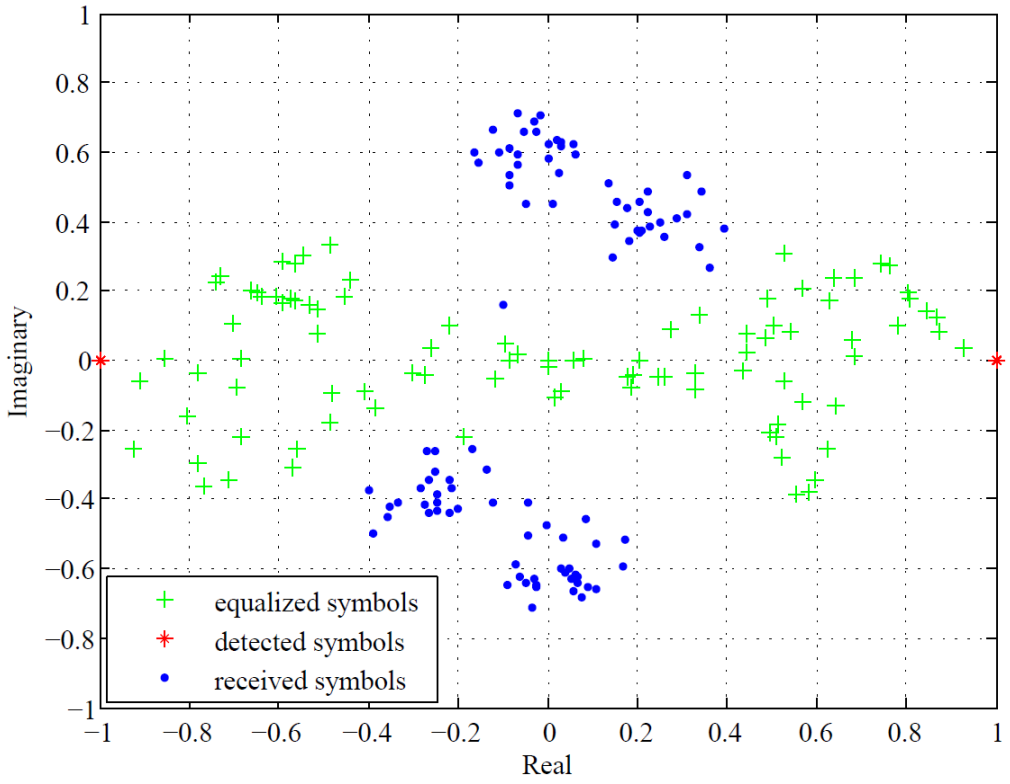

Figure 5.11: Signal constellation with RLS.

for the first subcarrier and for the first user at the first receiver antenna. The standard deviation of the equalized symbols is 0.18 while that of received symbols is 0.518, which is 0.338 higher than the standard deviation of the equalized symbols on the imaginary axis. This demonstrates a higher standard deviation for the received symbols after passing through the static, frequency selective channel and the equalizer with LMS diminished the effect of channel impairments as can be seen from the equalized symbols.

Figure 5.12 depicts the performance of the RLS adaptive algorithm in terms of the forgetting factor with DFE AE. It can be observed that the BER decreases as the SNR increases with a minimum of 6.9×10^{-4} and a maximum of 5.9×10^{-2}. Furthermore, as the SNR increases, there is no obvious difference in BER for the different forgetting factors (λs). This implies that the DFE adaptive equalization in static, frequency selective multi-user MIMO channels does not depend on the forgetting factor λ as the RLS algorithm does not have to adapt to any channel variations.

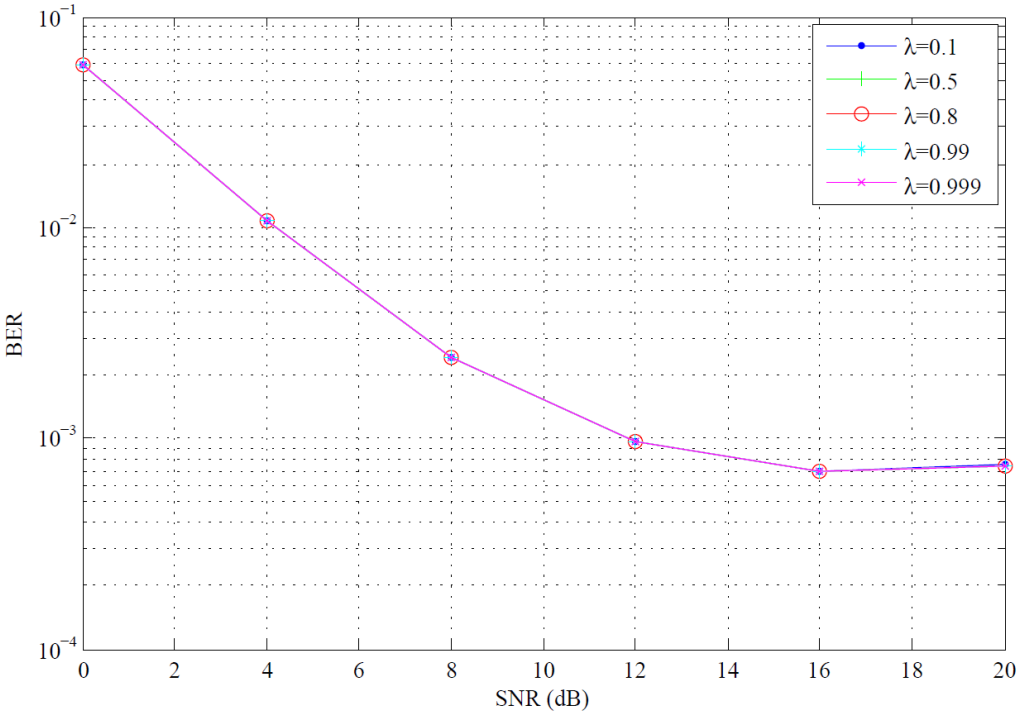

Figure 5.12: BER versus SNR for DFE AE with different forgetting factors (λ) for RLS adaptive algorithm.

5.4 Chapter summary

The critical factors that determine the overall performance of multi-user MIMO-OFDM systems are the ISI produced by multi-path fading within time-dispersive channels and frequency selectivity. These channel impairments could be compensated by appropriate equalization at the receiver. This chapter presented linear and DFE adaptive equalization methods for SDMA-based multi-user MIMO-OFDM systems. The proposed equalization methods adaptively equalized the channel and compensated for channel impairments. LMS and RLS adaptive algorithms as well as training sequence-based equalization methods are employed in the proposed AE to determine optimal performance. Average BER results for an SDMA-based multi-user MIMO-OFDM system employing 6 MSs and 12 receiving antennas at the AP using BPSK at an SNR of 16 dB shows a lower BER when using DFE AE, with BER equal to 2.4×10^{-2} for LMS and 5.7×10^{-4} for RLS algorithms, in comparison with a 4.9×10^{-1} BER when AE is not used. This implies that the RLS algorithm performs better than the LMS algorithm for the uplink of the multi-user

MIMO-OFDM systems. Moreover, it shows the significant effects the adaptive equalization can provide to SDMA-based multi-user MIMO-OFDM systems.

Since these adaptive equalization methods perform in a point-to-point basis, a novel channel tracking method is developed to track and estimate a time-varying frequency selective, multi-user MIMO channels. The development of the channel tracking algorithm is discussed in the next chapter.

Chapter 6

Novel and Efficient Channel Tracking in SDMA-Based Multi-User MIMO-OFDM Systems

6.1 Introduction

A novel and efficient channel tracking method for SDMA-based multi-user MIMO-OFDM wireless broadband communications systems is discussed in this chapter. This channel tracking method recursively updates the channel estimation for a time-varying, frequency selective, multi-antenna, multi-user, multi-path channel. The initial channel estimation is performed using training sequences for multiple users and transmitted data are detected using zero-forcing to reduce the computational complexity as discussed in Chapter 4. Simulations for the proposed tracking method are conducted to determine optimal performance through a comparative analysis. In general, channel tracking using detected data symbols is shown to be significantly beneficial for SDMA-based multi-user MIMO-OFDM systems. For example, the mean EVM for the proposed novel method is up to 79% lower than a training-based channel estimation method using a single-training sequence. This novel method offers a more efficient use of bandwidth, as it can perform accurate channel tracking with a single-training sequence, offering a reduction in bandwidth usage when compared to traditional training-based channel tracking methods.

6.2 Novel Channel tracking for SDMA-based multi-user MIMO-OFDM systems

This section discusses the proposed novel method of channel tracking in SDMA-based multi-user MIMO-OFDM systems. We focus on the case of six users with a 12 AP antenna system, as implemented in [19]. For channel tracking, first, zero-forcing is performed using initially estimated channel with the preamble to recover the subsequent twelve OFDM symbols. Then, hard-decision decoding is performed on the recovered data. A hard-decision receiver would operate to find the reference constellation that is closer to the recovered constellation. Then, modulation is performed on the hard-decisions to generate hard-decision data symbols. 16-ary QAM modulation is used in simulations. Figure 6.1 shows an example of the signal constellation of received data symbols versus hard-decision data symbols. The received data symbols are spread around the constellation points following a noise-like pattern.

Figure 6.2 shows a flow chart for the proposed channel tracking algorithm. As explained, in Section 4.3.2, a single-training symbol of each transmitter is used as the known training symbol in the initial channel estimation method to obtain the initial channel estimate, $\mathbf{H_0}$ according to Equation (4.5) . Then, this initial channel estimate $\mathbf{H_0}$ is used to perform zero-forcing at the AP to recover data $\hat{\mathbf{X}}$ as explained in Chapter 4 (Section 4.5.1.1). For channel tracking, the zero-forcing process is performed in groups of 12 symbols as $\hat{\mathbf{X}}$ should be an invertible matrix. Next, this recovered data $\hat{\mathbf{X}}$ is demodulated to obtain hard-decision received data bits and again modulated to obtain hard-decision received data symbols as illustrated in Figure 6.2 and in Figure 4.16 in Chapter 4.

Next, in the tracking module, the channel estimates, including noise, are updated using the modulated data symbols $\hat{\mathbf{x}}$ as follows:

$$\mathbf{Y}_{HD} = \mathbf{H_i}\hat{\mathbf{X}} \tag{6.1}$$

$$\mathbf{Y}_{HD}\left(\hat{\mathbf{X}}\right)^{-1} = \mathbf{H_i}\hat{\mathbf{X}}\left(\hat{\mathbf{X}}\right)^{-1} \tag{6.2}$$

$$\mathbf{Y}_{HD}\left(\hat{\mathbf{X}}\right)^{-1} = \hat{\mathbf{H}}_\mathbf{i} \tag{6.3}$$

The received data ($\mathbf{Y} \in \mathbb{C}^{R\times Q}$) with modulated data ($\hat{\mathbf{X}} \in \mathbb{C}^{U\times Q}$), the channel ($\mathbf{H} \in \mathbb{C}^{R\times U}$) and the AWGN ($\mathbf{z} \in \mathbb{C}^{R\times 1}$) are represented in Equation (6.1). Q is the number of symbols in one group for channel tracking. Q is set to 12 symbols as $\hat{\mathbf{X}}$ should be invertible. Then, the received data are multiplied by the inverse of the modulated data symbols as expressed in Equation (6.2). Ultimately, the tracked

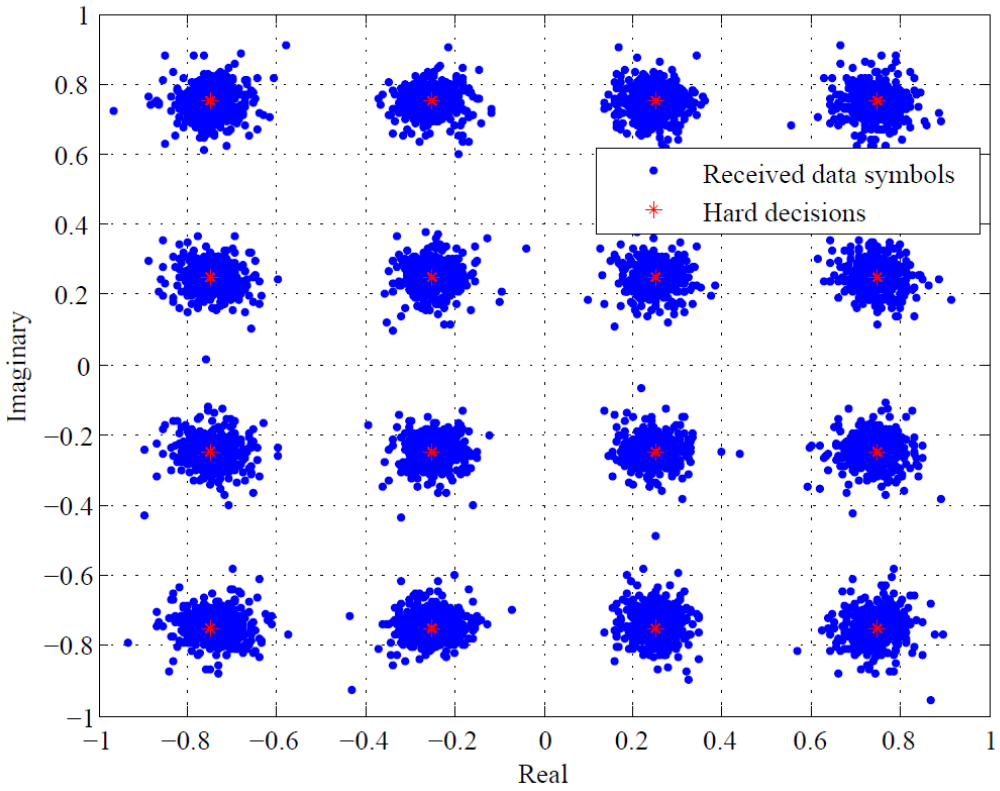

Figure 6.1: Signal constellation of received data and hard-decisions of 6×12 SDMA-based multi-user MIMO-OFDM uplink simulated transmission.

channel states ($\hat{\mathbf{H}}_\mathbf{i}$ ($\mathbf{i} = 1, 2, \ldots, 8$)) can be found by Equation (6.3). There are 8 groups of 12 symbols, as the simulations are conducted for 96 OFDM symbols.

Then, the updated (newly estimated) channel state $\hat{\mathbf{H}}_\mathbf{i}$ is used to produce a new updated channel response at the channel update module as shown in Figure 4.16 in Chapter 4 and in Figure 6.2. The previously estimated channel is replaced with the tracked channel estimate at the channel update module. Noise is removed by the hard-decision process as shown in Figure 6.1. The received data symbols in blue are spread around a constellation point, while the hard-decision data symbols in red are exactly at the constellation points, which we selected in the hard-decision process. Then, zero-forcing is performed as described in Chapter 4 (Section 4.5.1.1) using the updated channel response and recursively demodulated, modulated and tracked for all the OFDM symbols as illustrated in Figure 4.16 in Chapter 4 and in Figure 6.2.

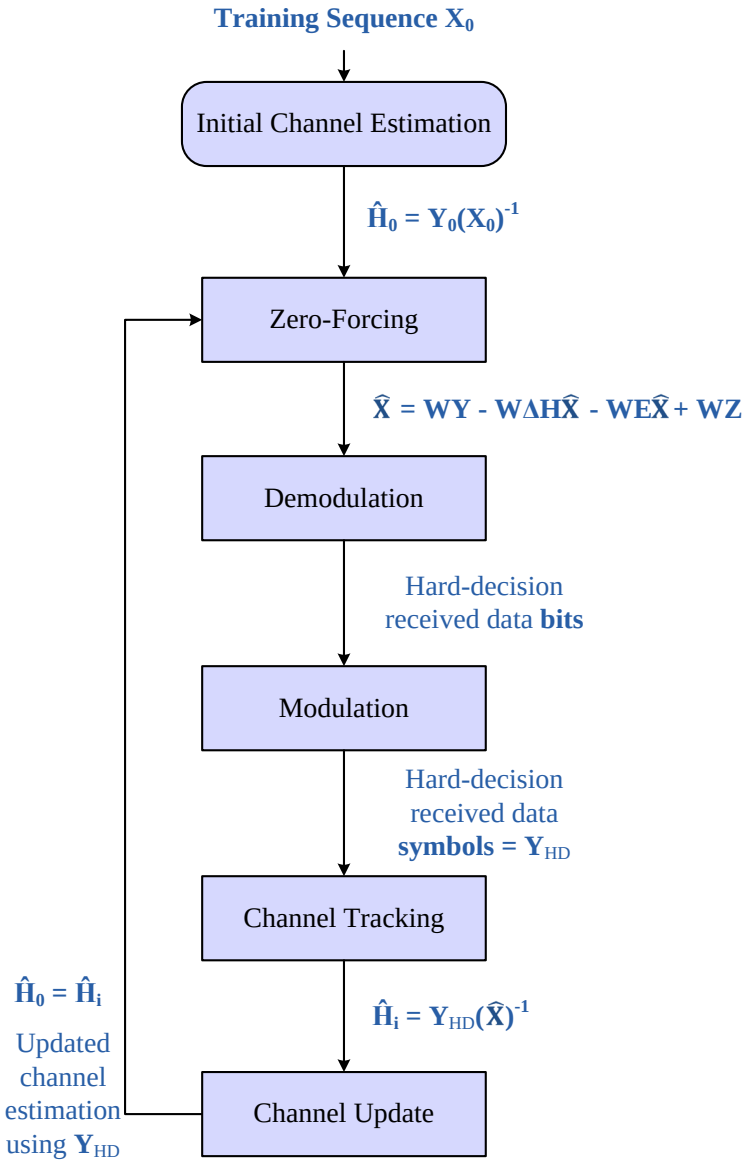

Figure 6.2: Channel tracking algorithm.

6.3 Simulation results and discussion

Computer simulations are performed using Matlab in order to show the improvements achieved by the novel channel tracking mechanism for uplink communications in SDMA-based multi-user MIMO-OFDM systems. Three path MIMO frequency selective fading channels are generated with 100 channel realisations and 16-ary QAM modulation. The simulations are performed for 96 OFDM symbols (time

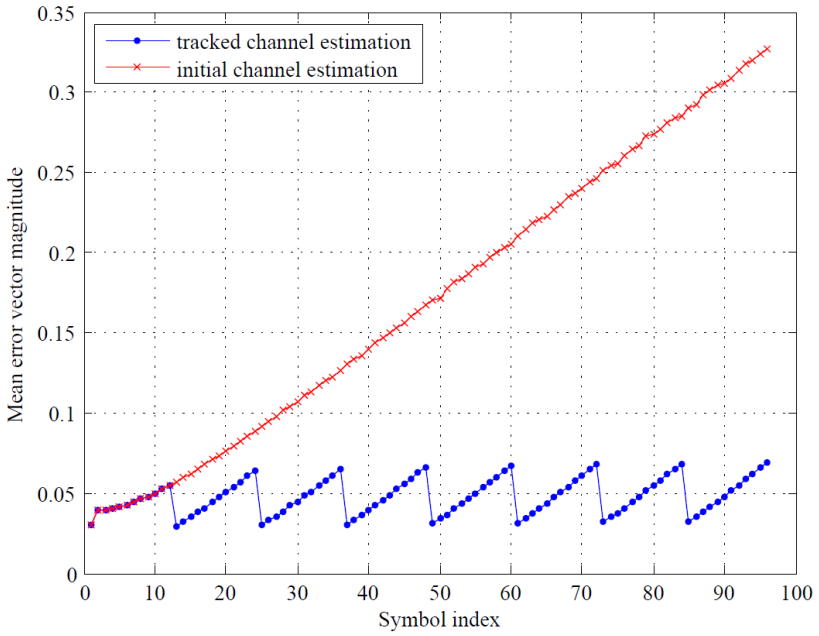

Figure 6.3: Mean error vector magnitude versus OFDM symbol index for the fourth mobile station (MS4).

index, $U = 96$), the number of subcarriers is 128 ($N = 128$), the number of MSs is 6 ($M = 6$), and the number of receiver antennas at the AP is 12 ($R = 12$). The SNR is set to 30 dB and the maximum Doppler shift is set to 10 Hz for the simulations unless otherwise stated. The channel model constructed in Section 4.2.3 is used in all the simulations unless otherwise stated. The simulations and analysis conducted are discussed in the following sub-sections.

6.3.1 Error analysis

This section provides a detailed analysis of the error produced by comparing the recovered symbols ($\hat{X}$) with the actual transmitted symbols (X), as explained in Chapter 4 (Section 4.6.1).

Figure 6.3 shows the simulation results for mean EVM versus OFDM symbols of the fourth MS with initial channel estimation and with the proposed channel tracking method. EVM is averaged over all channel realisations and all subcarriers. Usage of the tracked channel estimates provided a significantly lower mean EVM. For example, at OFDM symbol 96, the maximum mean EVM for the initial channel estimates is 0.33 while the mean EVM for the tracked channel estimates is 0.069, which is 0.258 (79%) lower than the mean EVM with the initial channel estimates.

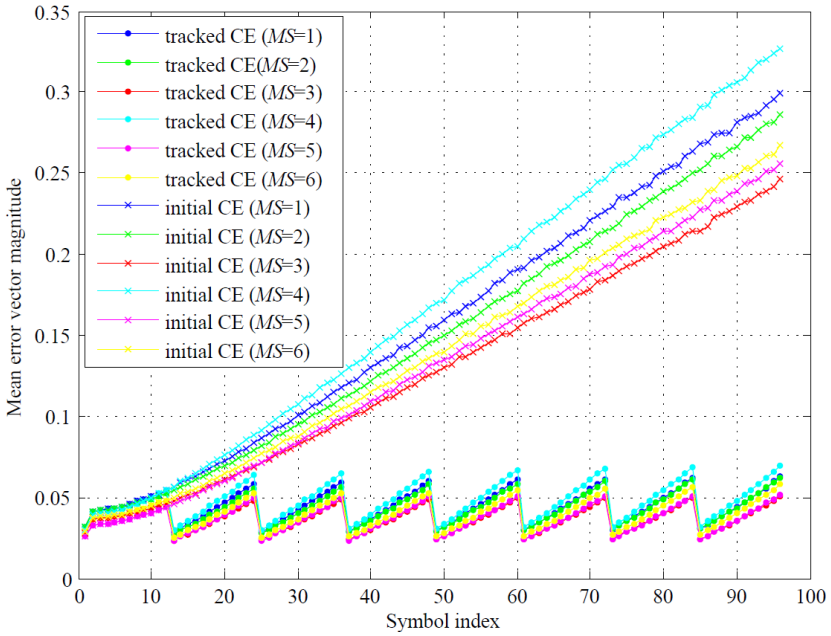

Figure 6.4: Mean Error Vector Magnitude versus OFDM symbol index for all six mobile stations.

Mean EVM is the same at the beginning for both methods. However, mean EVM increases linearly as a function of the number of OFDM symbols when the initial channel estimates are employed. This implies that, more training sequences should be incorporated to reduce the mean EVM as the symbol index increases. However, this increases the overhead in the communications system that consumes a considerable amount of bandwidth. With tracked channel estimates, the mean EVM remains at an average of 0.0478 for all OFDM symbols, which is significantly lower than the use of initial channel estimates, and tracking algorithm does not require the use of additional training sequences.The EVM returns to its minimum value every 12 symbols when the channel is updated. Therefore, we can see a pattern in mean EVM for tracked channel estimates as shown in Figure 6.3. This shows the significant effect in terms of efficient use of bandwidth that this novel channel tracking method can achieve in SDMA-based multi-user MIMO-OFDM systems.

Figure 6.4 shows the simulation results for mean EVM versus OFDM symbols for all the MSs with initial channel estimation and with tracked channel estimates. It can be seen that the mean EVM increases linearly as a function of the symbol index with the initial channel estimation method for all the MSs. However, the mean EVM varies around an average of 0.0414 and with a standard deviation of 0.0046

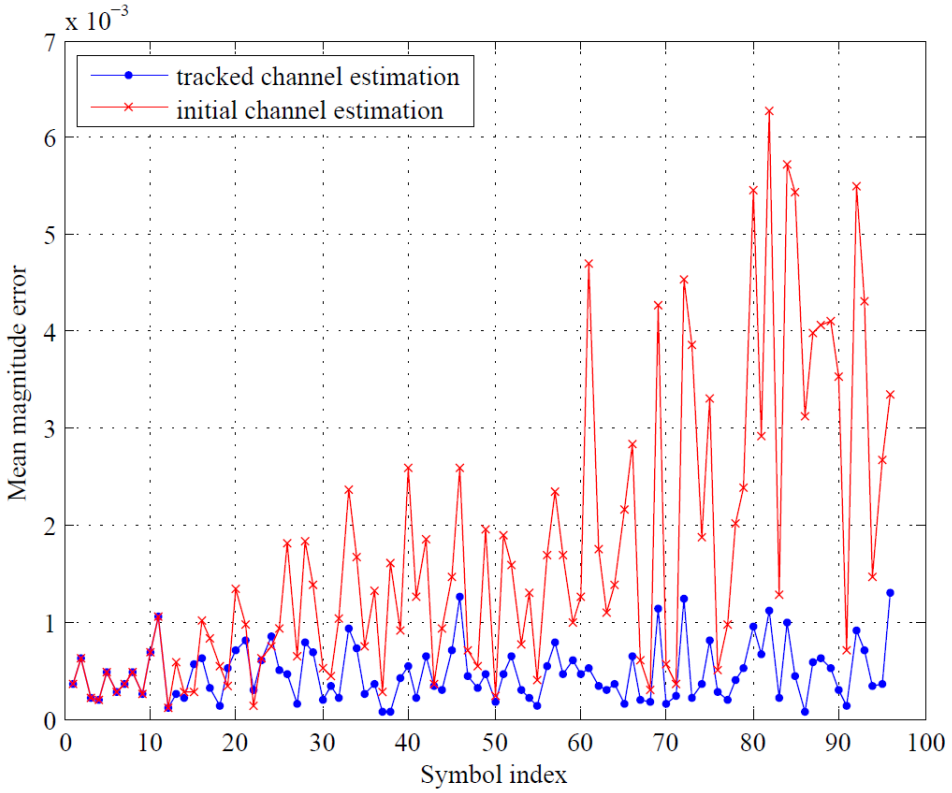

Figure 6.5: Mean magnitude error versus OFDM symbol index for the fourth mobile station.

for all the OFDM symbols and for all the MSs with the tracking method, as the channel is updated for every 12 symbols. As explained in Section 6.2, the channel is tracked for every 12 symbols, since the recovered data matrix $\hat{X}$ should be an invertible matrix. Since the received path gains for each MS is random, there is a small variation of mean EVM among MSs with a standard deviation of 0.0308 and 0.0071 for the initial channel estimation method and the channel tracking method, respectively, for the OFDM symbol 96.

Figure 6.5 depicts the simulation results for the magnitude error versus OFDM symbols for the fourth MS showing initial channel estimation and tracked channel estimates. It can be seen that the magnitude error increases when the symbol index increases for the initial channel estimation method with a mean of 1.6×10^{-3} and a standard deviation of 1.2×10^{-3}. However, it remains in a small range of values closer to 0 with a mean of 4.9×10^{-4} and a standard deviation of 2.9×10^{-4} for tracked channel estimates. The magnitude error is the same for the first 12 symbols for both methods, as the tracking method incorporates the initial channel estimates

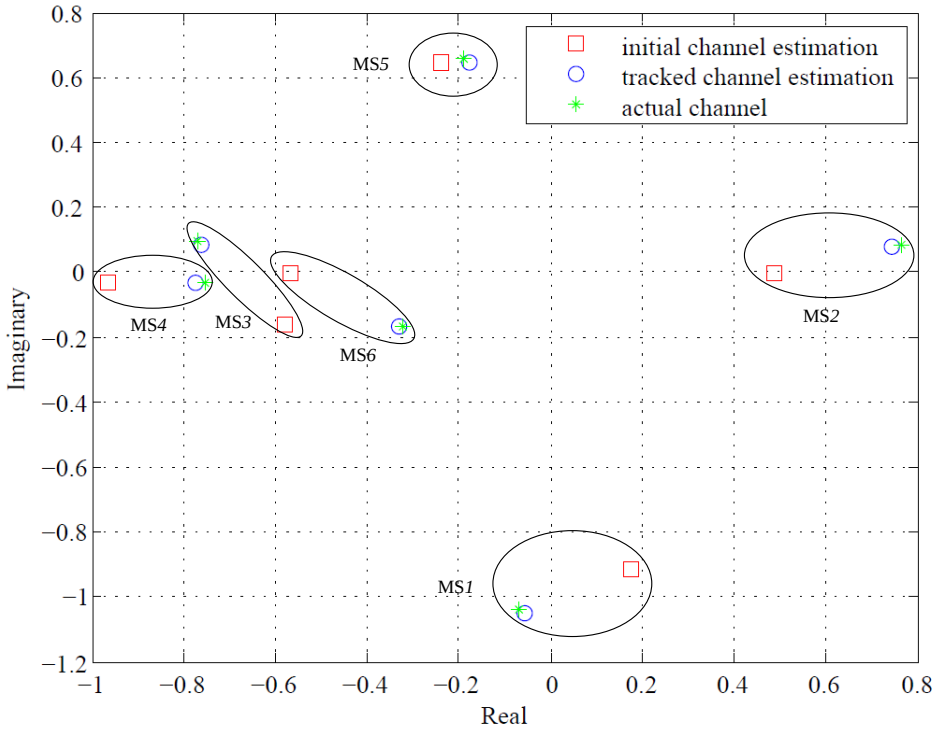

Figure 6.6: Sample signal constellation for actual channel, tracked channel and initial channel estimation for each mobile station at OFDM symbol 48.

for the first 12 symbols. This section discussed a detailed analysis on the errors produced by comparing the recovered symbols ($\hat{\mathbf{X}}$) with the actual transmitted symbols ($\mathbf{X}$).

6.3.2 Channel matrix analysis

This section provides a detailed analysis on the channel matrices obtained using the proposed channel tracking method and the training-based initial channel estimation method.

The collection of all possible signal points in the signal space is called the signal constellation. It is much easier to identify the distance between the signal points when using the signal space representation. The distance is closely related to the symbol error rate of a given constellation. Figure 6.6 illustrates a sample comparison of the signal constellation between the actual channel, the tracked channel estimates and the initial channel estimates for all the MSs at OFDM symbol 48. These

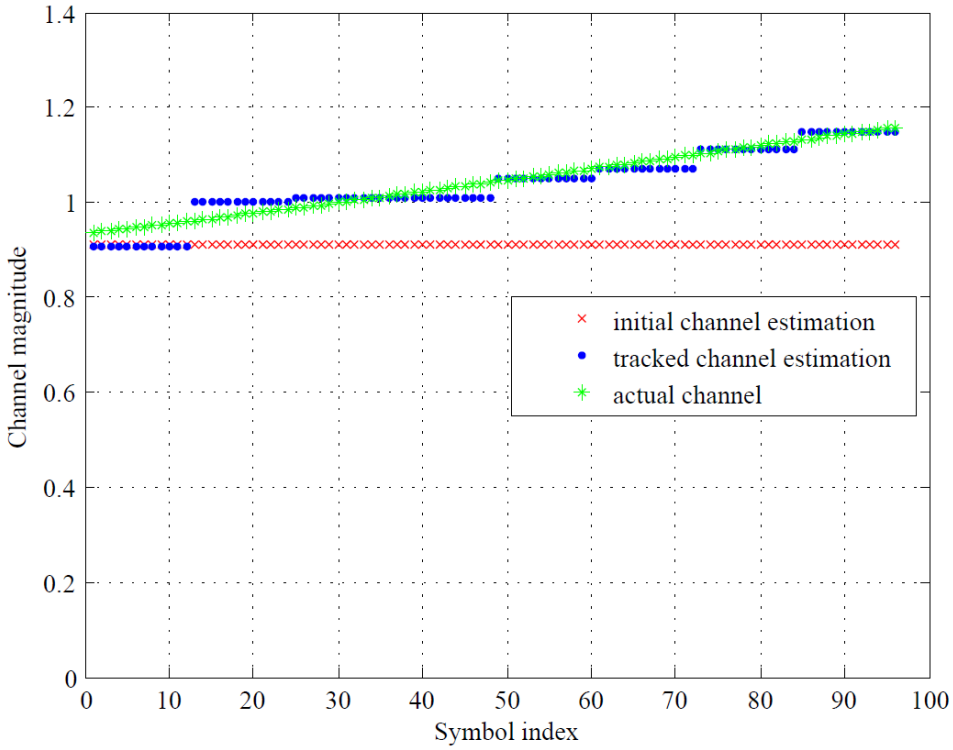

Figure 6.7: Magnitude of the tracked channel, the initial channel estimation and the actual channel.

simulation results represent the channels between all the MSs and first receiver antenna at the AP for the first subcarrier. These results show that the proposed method estimates the actual channel more accurately than the initial training-based channel estimation method. For example, the root mean square (RMS) error for the fourth MS is 0.2424 for the initial channel estimation method and 0.0557 for the channel tracking method which is 23% lower RMS error. This implies that the proposed tracking method tracks the actual channel matrix more accurately than the initial channel estimation method.

Figure 6.7 illustrates a comparison of the actual channel, the tracked channel and the initial channel estimation for the MS1 and the first receiver antenna at the AP. Results are shown for the first OFDM subcarrier. It shows that the tracked channel accurately approximates the actual time-varying channel for all the OFDM symbols. For example, the RMS error is 0.0145 for the channel tracking method and 0.0938 for the initial channel estimation method. Therefore, the RMS error of the channel tracking method is 0.0793 lower than that of the initial channel estimation method.

Moreover, the initial training-based method estimates a constant channel state for all the OFDM symbols. The proposed channel tracking method is able to adapt to channel variations effectively.

Comparisons of magnitudes of all the time-varying channels between all the MSs and the receiver antenna pairs with $f_d = 10$ Hz for the tracked channel estimation, the initial channel estimation and the actual channel are illustrated in Figure 6.8. The tracked channel estimates (blue curves) closely follow the actual channel (green curves) for most of the multi-user MIMO channels. Table 6.1 shows the goodness of fit calculated for the actual channel matrix with the tracked channel estimation and the estimated channel illustrated in Figure 6.8. If the value of goodness of fit is negative, then it is a bad fit and if it is closer to 1, then the fit is perfect. It can be seen that the goodness of fit values are always negative for the initial training-based channel and the goodness fit values of the tracked channel estimates almost have either a positive value or it is closer to 1. The mean value of the goodness of fit of the whole channel matrix is 0.5647 for the tracked channel matrix and -1.0921 for the initial training-based channel estimation. Therefore, the tracked channel approximates the actual channel better than the initial channel estimation.

The performance comparison of the mean magnitudes of the actual frequency selective channel between MS4 and receiver antenna 10 at the AP with $f_d = 10$ Hz for the tracked channel estimation and the initial channel estimation is exemplified in Figure 6.9. The performance is shown by averaging the results over all symbols. The goodness of fit values for the tracked channel and the initial channel estimate are 0.9678 and 0.4158, respectively. Therefore, at $f_d = 10$ Hz, the channel tracking method works with 97% accuracy, while the training-based initial channel estimation method shows poor performance in estimating the actual channel comparatively. The initial channel estimation suffered from not only channel variations but also from the channel estimation errors due to noise. The tracking method is actually eliminating/reducing the effects of channel estimation error due to noise. The Table 6.2 shows the dynamic ranges of the magnitude of the channels depicted in Figure 6.9. The difference of the dynamic ranges between the actual channel and the tracked channel estimation is 0.8507, which is smaller than the difference of the dynamic range between the actual channel and the initial channel estimation (1.4110).

The comparison between the mean magnitude of all the frequency selective channels with $f_d = 10$ Hz for the tracked channel estimation, the initial channel estimation and the actual channel is illustrated in Figure 6.10. Table 6.3 shows the goodness of fit values of the actual frequency selective channel with the tracked channel and the initially estimated channel for all the channel pairs between the

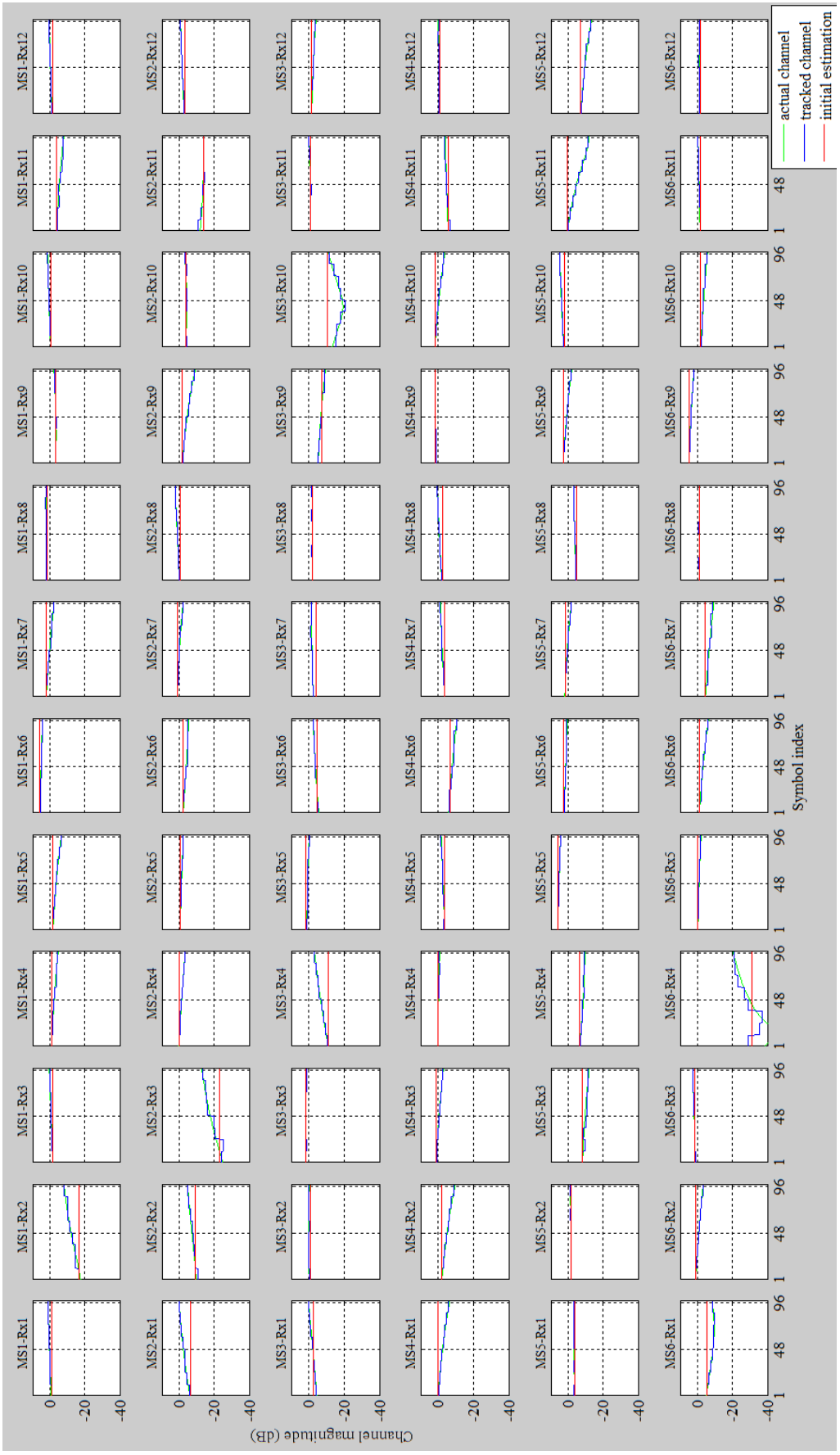

Figure 6.8: Performance comparison of magnitudes of all the time-varying channels between all the MSs and receiver antenna pairs with $f_d = 10$ Hz for the tracked channel estimation, the initial channel estimation and the actual channel

Table 6.1: Goodness of fit of the actual time-varying channel with the tracked channel and the initially estimated channel

		Receiver Antennas												Mean
		1	2	3	4	5	6	7	8	9	10	11	12	
MS1	Tracked	0.6077	0.7628	0.7065	0.7823	0.8305	0.8270	0.8342	-0.0233	0.5979	0.7099	0.7677	0.8035	0.6839
	Initial	-0.9463	-2.0739	-0.0614	-0.9360	-1.3251	-0.1223	-0.6839	-0.0058	-1.1856	-2.4171	-1.4776	-1.4751	-1.0592
MS2	Tracked	0.8519	0.7602	0.7229	0.7944	0.7967	0.7819	0.8305	0.8427	0.8272	0.3713	-0.2232	0.7981	0.6795
	Initial	-1.5303	-0.7894	-0.3736	-1.0553	-1.6911	-1.5137	-0.8354	-0.7351	-1.1529	-2.6590	-3.4963	-0.7078	-1.3783
MS3	Tracked	0.7473	-0.6046	-0.5612	0.8162	0.7345	0.7849	0.6702	-0.7172	0.6621	0.5024	0.7007	0.7265	0.3718
	Initial	-0.7330	-1.8559	-0.1755	-0.9225	-0.1123	-1.5734	-1.8697	-1.9862	-0.5952	-0.1696	-0.0494	-0.2726	-0.8596
MS4	Tracked	0.8350	0.8438	0.8088	0.5528	0.7361	0.7836	0.7884	0.8364	0.4199	0.8521	0.5051	0.6265	0.7157
	Initial	-0.4446	-0.4894	-0.5288	-0.0190	-1.2077	-0.7092	-2.4231	-1.0485	-0.0042	-0.5407	-0.2117	-2.0376	-0.8054
MS5	Tracked	-0.9339	-0.9937	0.5920	0.5614	0.7979	0.8063	0.8497	0.6594	0.8330	0.7229	0.8678	0.7400	0.4586
	Initial	-0.5480	-3.9631	-0.8241	-2.2163	-0.4004	-1.4629	-0.9445	-0.6163	-0.7489	-1.0300	-0.7538	-1.1895	-1.2248
MS6	Tracked	0.7508	0.8072	0.7171	0.3170	0.7493	0.8201	0.7305	-0.1197	0.8451	0.7756	0.6041	-1.2514	0.4788
	Initial	-1.3649	-0.9157	-1.3047	-0.1672	-0.9923	-0.7743	-1.5166	-2.5653	-0.7172	-0.7324	-1.5281	-2.1320	-1.2259
Mean	Tracked	0.4765	0.2626	0.4977	0.6374	0.7742	0.8006	0.7839	0.2464	0.6975	0.6557	0.537	0.4072	0.5647
	Initial	-0.9278	-1.6812	-0.5447	-0.886	-0.9548	-1.026	-1.3789	-1.1595	-0.734	-1.2581	-1.2528	-1.3024	-1.0921

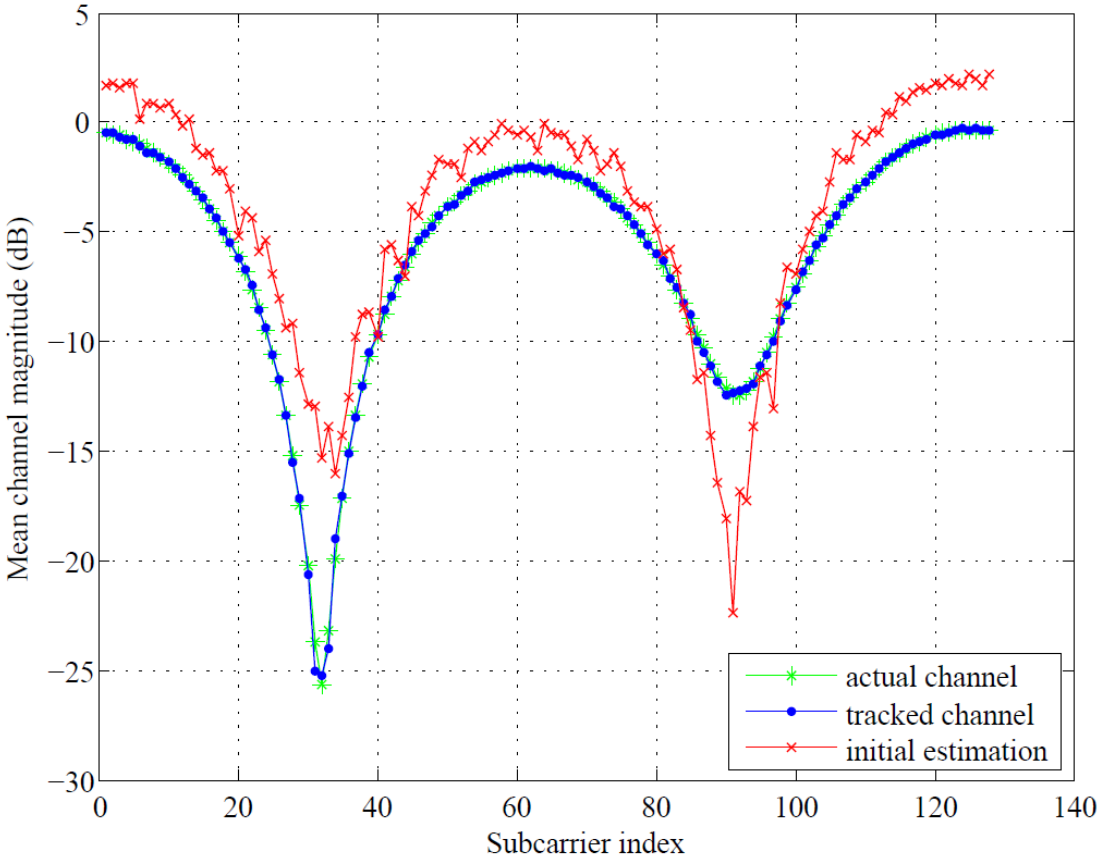

Figure 6.9: Sample performance comparison of mean channel magnitude of the actual frequency selective channel between MS4 and receiver antenna 10 at the AP with $f_d = 10$ Hz for the tracked channel estimation and the initial channel estimation.

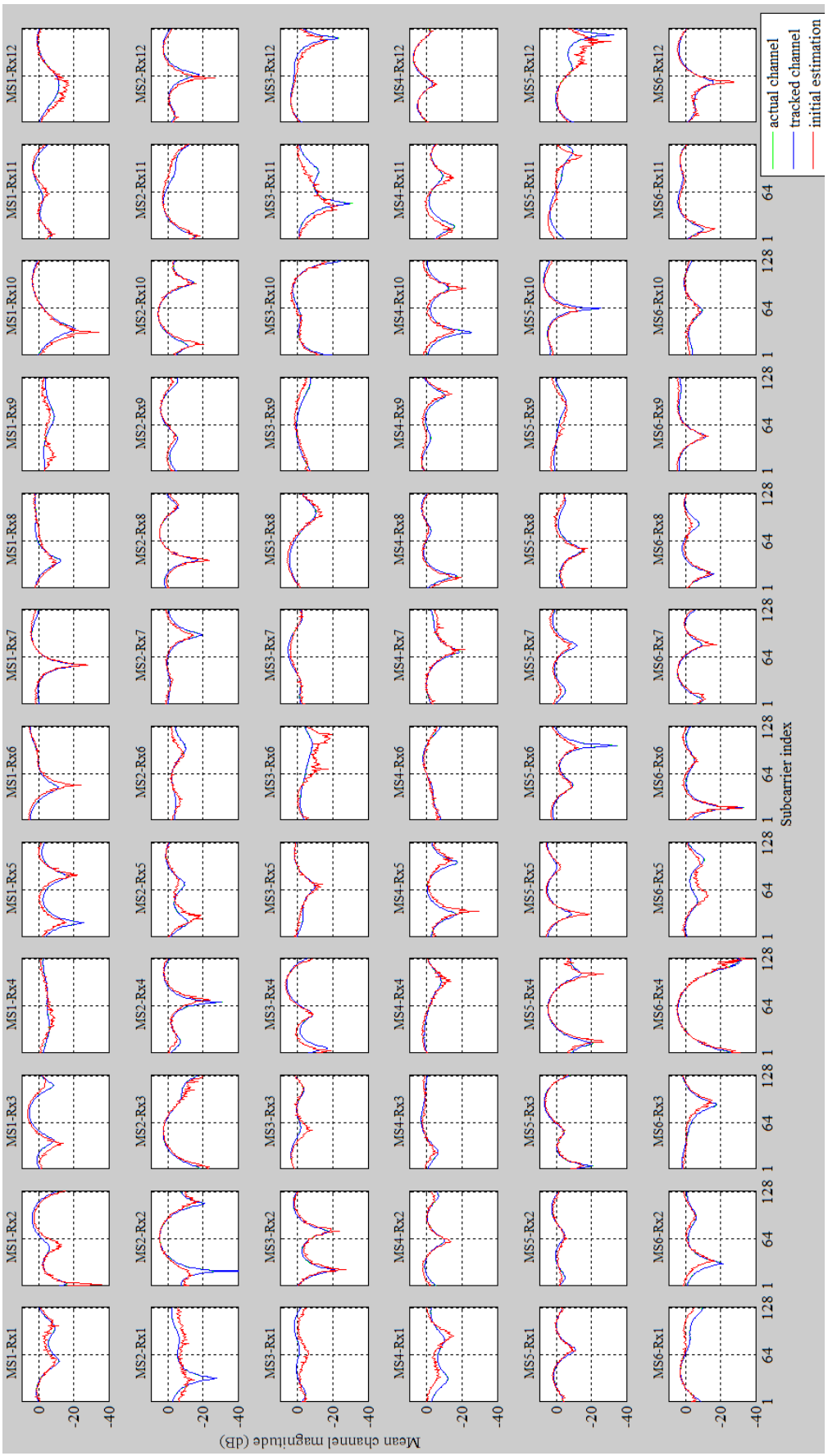

Figure 6.10: Mean magnitude of frequency selective channels for the tracked channel estimation and the initial channel estimation with $f_d = 10$ Hz

Table 6.2: Dynamic ranges of the channel tracking method and the initial channel estimation method in dB for the frequency selective channel

Method/Channel	Minimum	Maximum	Dynamic range
Actual channel	-0.3419	-25.6378	25.2959
Tracked channel estimation	-0.2762	-26.4228	26.1466
Initial channel estimation	2.1503	-21.7346	23.8849

MSs and the receiver antennas at the AP as depicted in Figure 6.10. As explained above, the goodness of fit values implies a perfect fit, when the corresponding value is closer to 1 and a bad fit, when it is negative. The majority of goodness of fit values for the tracked channel are closer to 1 with a minimum of 0.9262 and a maximum of 0.9898. A lower value of goodness of fit is shown for the training-based channel estimation method with a minimum of -0.8008 and a maximum of 0.8366, when it is compared with the novel tracking method. The mean value of the goodness of fit of the whole channel matrix is 0.9746 for the tracked channel matrix and 0.4594 for the initial training-based channel estimation. Moreover, at $f_d = 10$ Hz, the channel tracking method performs with higher accuracy (the blue curves overlaps the green curves). The initial channel estimates deviated from the actual frequency selective channel and shows a noise-like pattern for some OFDM subcarriers.

Figure 6.11(a) depicts an example of a Rician fading channel between the first MS and the first receiver antenna at the AP with k= 100 (20 dB) and $f_d = 10$ Hz. The dynamic range of the channel is from 0.4016 to 0.8406 having a maximum difference of 0.439. A sample of the performance of channel tracking method for the Rayleigh and Rician channels with different K-factors is shown in Figure 6.11(b). There is no considerable variation of the performance of the channel tracking method with the K-factor. This implies that the proposed technique does not depend on the Rician K-factor. However, the mean EVM for $K = 100$ is slightly lower than for the other K-factors. This is due to having a reduced multi-path propagation scenario (higher K-factors), which increases the correlation between the MIMO sub-channels, therefore reducing the channel capacity and deteriorating the performance of the system. This is independent of the channel tracking method. The dynamic range of mean EVM for MS 4 is ranges from 0.0255 to 0.0533 having a maximum difference of 0.0278.

For illustration purposes, Figure 6.12 compares the channel frequency response of the actual channel between the MS4 and the receiver antenna 10 with CFRs

Table 6.3: Goodness of fit of the actual frequency selective channel with the tracked channel and the initially estimated channel

		Receiver Antennas												Mean
		1	2	3	4	5	6	7	8	9	10	11	12	
MS1	Tracked	0.9735	0.9834	0.9855	0.9492	0.9654	0.9872	0.9696	0.9823	0.9507	0.9761	0.9751	0.9796	0.9731
	Initial	0.5849	0.4174	0.4064	-0.2563	0.4336	0.5450	0.7748	0.6460	-0.2235	0.6587	0.4280	0.5037	0.4099
MS2	Tracked	0.9524	0.9572	0.9770	0.9645	0.9785	0.9518	0.9765	0.9875	0.9825	0.9831	0.9796	0.9841	0.9729
	Initial	0.1757	0.4933	0.6377	0.5120	0.1414	0.1073	0.6378	0.7566	0.5214	0.6932	0.5836	0.5341	0.4828
MS3	Tracked	0.9662	0.9819	0.9802	0.9896	0.9764	0.9623	0.9858	0.9862	0.9695	0.9784	0.9492	0.9838	0.9758
	Initial	-0.6027	0.6360	0.2954	0.5558	0.6617	-0.8008	0.7274	0.7623	0.3037	0.7369	0.2935	0.5834	0.3460
MS4	Tracked	0.9596	0.9755	0.9796	0.9826	0.9695	0.9781	0.9797	0.9863	0.9808	0.9678	0.9665	0.9898	0.9763
	Initial	-0.1802	0.5451	0.4728	0.6443	0.3019	0.7119	0.7384	0.6494	0.5115	0.4158	0.2753	0.8366	0.4936
MS5	Tracked	0.9747	0.9762	0.9792	0.9767	0.9861	0.9563	0.9820	0.9742	0.9768	0.9875	0.9813	0.9599	0.9759
	Initial	0.7495	0.5944	0.8250	0.5922	0.5572	0.3809	0.4830	0.6196	0.2784	0.5956	0.2639	0.0760	0.5013
MS6	Tracked	0.9775	0.9739	0.9802	0.9565	0.9719	0.9262	0.9851	0.9771	0.9872	0.9752	0.9847	0.9848	0.9734
	Initial	0.2583	0.3517	0.5859	0.7449	-0.0638	0.5620	0.7047	0.5830	0.7664	0.5872	0.5671	0.6247	0.5227
Mean	Tracked	0.9673	0.9747	0.9803	0.9698	0.9746	0.9603	0.9798	0.9823	0.9746	0.978	0.9727	0.9803	0.9746
	Initial	0.1642	0.5063	0.5372	0.4655	0.3387	0.251	0.6777	0.6695	0.3596	0.6146	0.4019	0.5264	0.4594

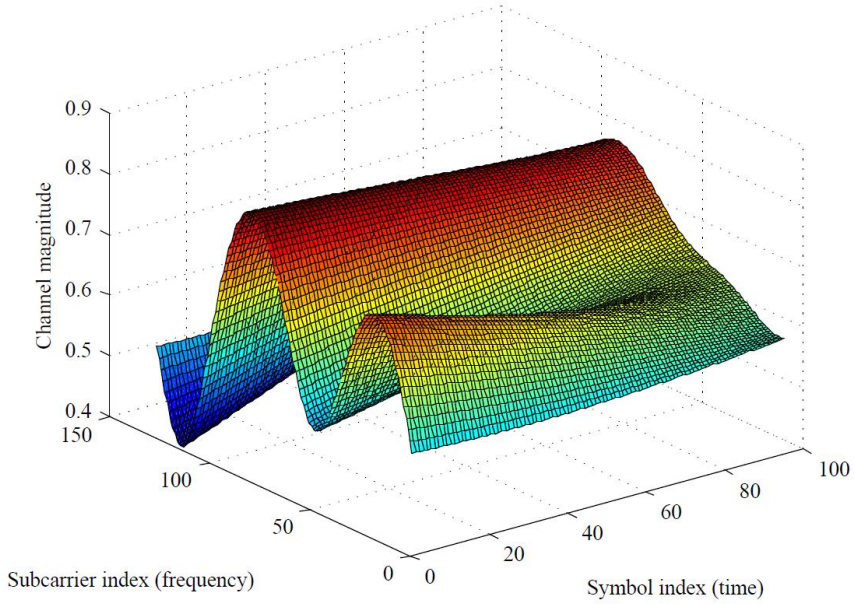

(a)

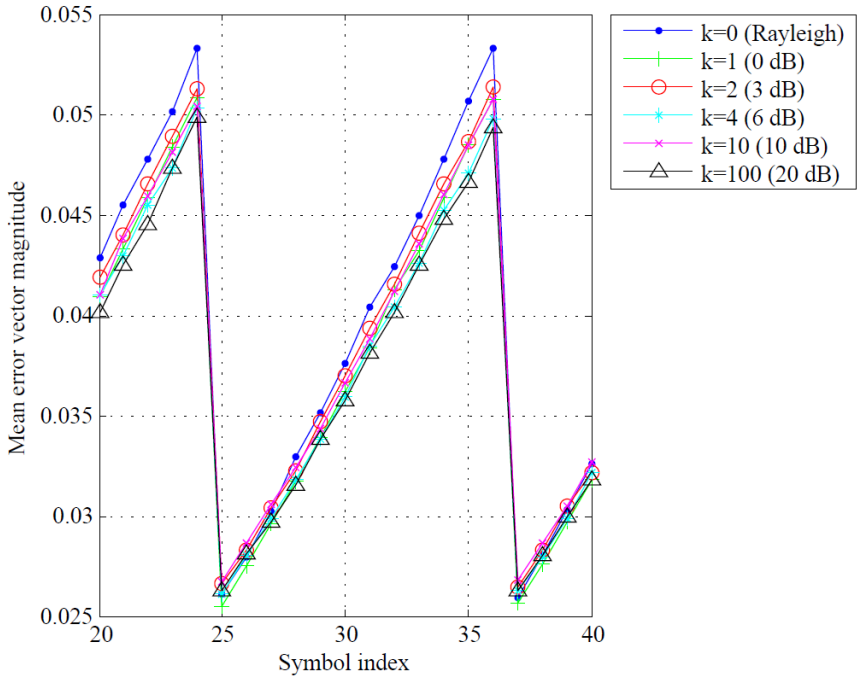

(b)

Figure 6.11: (a) Simulated Rician fading channel with k= 100 (20 dB) (b) Performance of channel tracking for different K-factors of MS4.

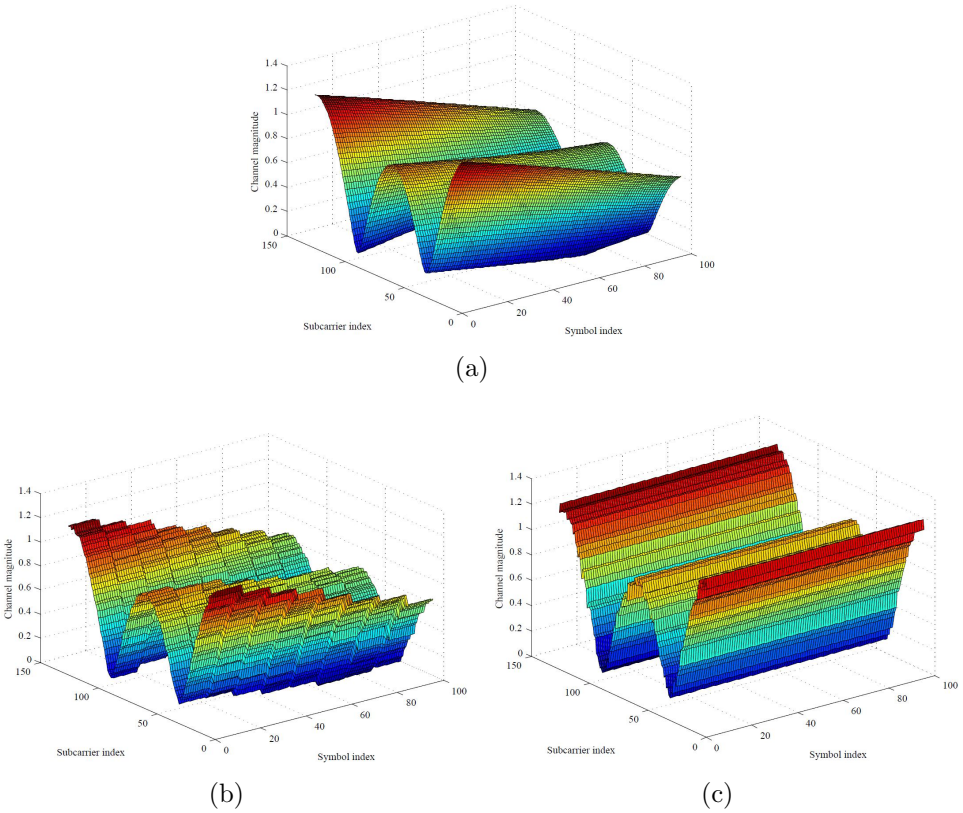

Figure 6.12: Illustration of (a) the actual time-varying, frequency selective channel and the channel frequency responses obtained by (b) channel tracking method (c) initial channel estimation method.

obtained by the proposed channel tracking method and the initial training-based channel estimation method. Despite both the channel tracking method and the initial channel estimation method provide a reasonably good fit in the frequency domain, the advantage of the tracking method is more noticeable in the time domain where the tracking method is able to follow the decreasing trend against time presented in the actual channel. In this section, a detailed analysis of the channel tracking method in terms of the CFR was discussed.

6.3.3 Doppler shift analysis

This section provides a detailed analysis of the performance of the proposed channel tracking method and the training-based initial channel estimation method for different maximum Doppler shifts (f_d).

The performance in terms of mean EVM for different maximum Doppler shifts ranging from $f_d = 1$ Hz to $f_d = 70$ Hz using the tracked channel estimation are illustrated in Figure 6.13. At a frequency of operation of 700 MHz, typical long term evolution (LTE) frequency, an f_d of 10 Hz is equivalent to a mobile speed of 15.4 km/h and f_d of 70 Hz will represent a mobile travelling at a speed of 108 km/h. The results are shown for EVM of the first user averaged over all the subcarriers and all EVM iterations. The maximum mean EVM is 0.0391, 0.0541, 0.1242, and 0.2872 when $f_d = 1$ Hz, $f_d = 10$ Hz, $f_d = 20$ Hz and $f_d = 30$ Hz, respectively. Therefore, the performance of channel tracking is better when $f_d <= 30$ Hz. Figure 6.14 exemplifies the signal constellations of the received data and the hard-decision symbols for $f_d = 1$ Hz, $f_d = 20$ Hz, $f_d = 30$ Hz and $f_d = 40$ Hz. From Figure 6.14, it can be seen that when f_d increases, the received data constellations merge with the neighbouring symbols and cause errors in the hard-decision process. Because of that, the channel tracking method does not work effectively at f_ds larger than 30 Hz, as the mean EVM increases as f_d increases. Since, the tracking method incorporates the channel estimated by using training symbols during the first 12 symbols, it shows a very low mean EVM at the beginning of the OFDM symbol index (during the first 12 symbols) for all the f_ds.

The performance comparisons in terms of the mean EVM for different maximum Doppler shifts ranging from $f_d = 1$ Hz to $f_d = 70$ Hz using the training-based initial channel estimation are illustrated in Figure 6.15(a). The results are shown for the EVM of the first user averaged over all the subcarriers and all EVM iterations. The maximum mean EVM for $f_d = 1$ Hz, $f_d = 10$ Hz, $f_d = 20$ Hz and $f_d = 30$ Hz are 0.0477, 0.2747, 0.5265, and 0.7608, respectively. A comparison of the performance of the tracking method and the initial channel estimation method in terms of mean EVM and f_d is depicted in Figure 6.15(b). The maximum mean EVM of the tracking method is 0.0086, 0.2206, 0.4022, and 0.4736 when $f_d = 1$ Hz, $f_d = 10$ Hz, $f_d = 20$ Hz and $f_d = 30$ Hz, respectively and these values are lower than that of the initial channel estimation method by a maximum of 80% at $f_d = 10$ Hz. The mean EVM increases as the f_d increases for both methods. Therefore, both methods are affected by higher Doppler shifts. However, the channe tracking method kept a maximum mean EVM 80% lower than the initial estimation method at $f_d = 10$ Hz. At these higher f_ds the mean EVM for both methods increase with time. However, the channel tracking method can provide a lower mean EVM i.e of 22% at $f_d = 70$ Hz.

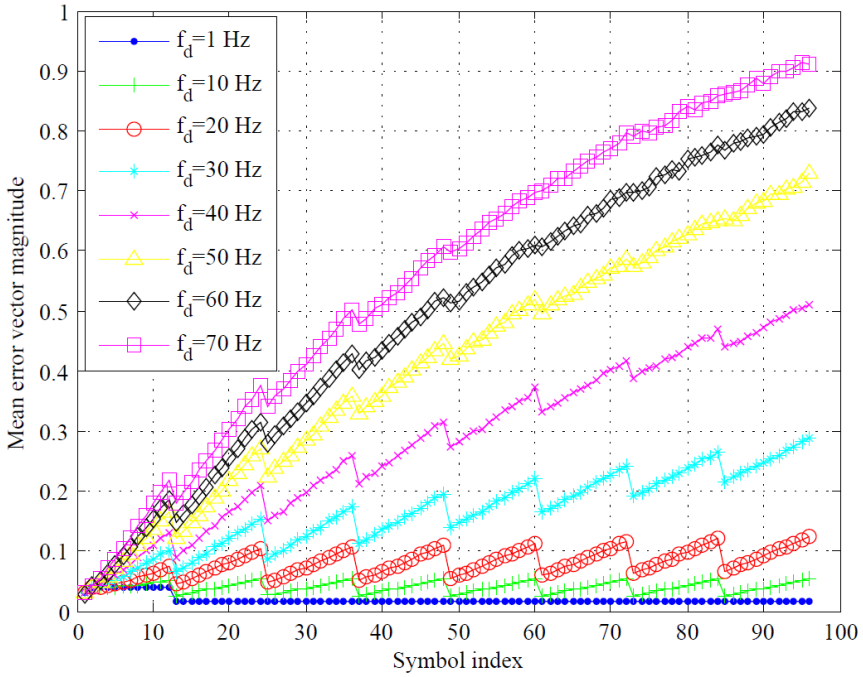

Figure 6.13: Performance of channel tracking for different maximum Doppler shifts (f_d)s in Hz

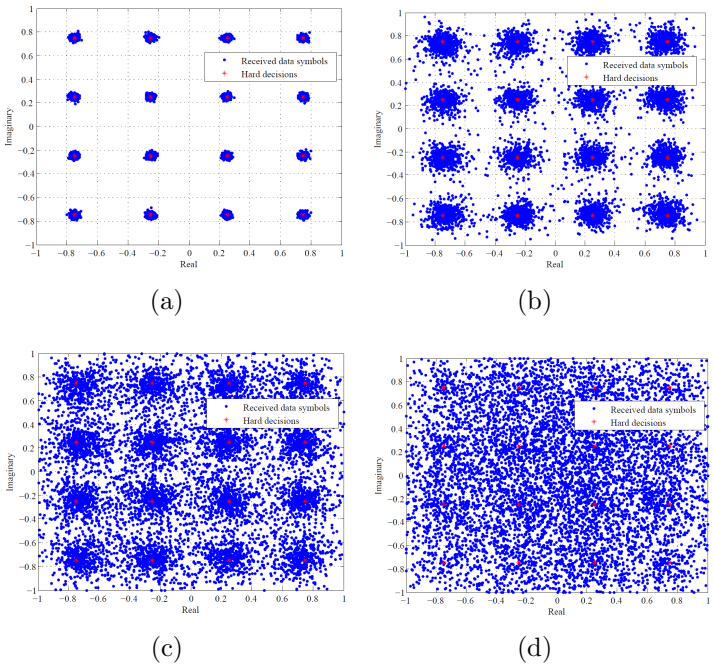

Figure 6.14: Signal constellations of received data and the hard-decision symbols for (a) $f_d = 1$ Hz (b) $f_d = 20$ Hz (c) $f_d = 30$ Hz (d) $f_d = 40$ Hz.

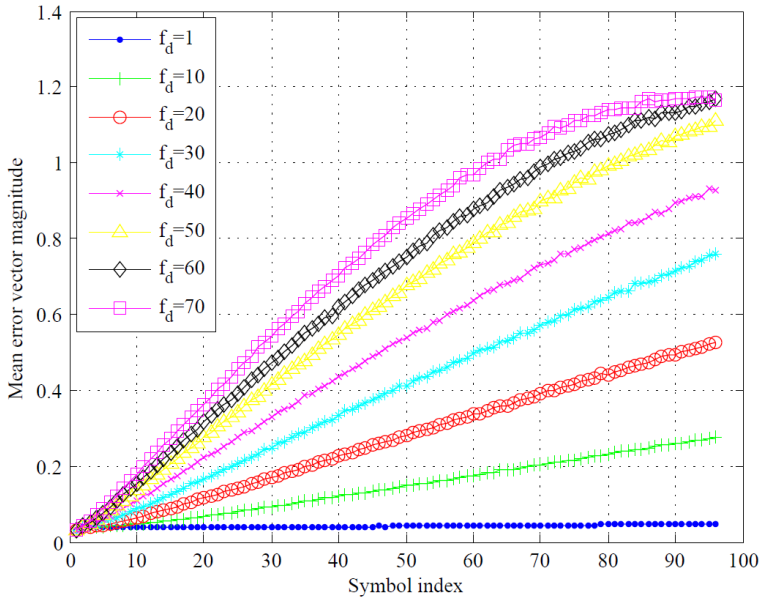

(a)

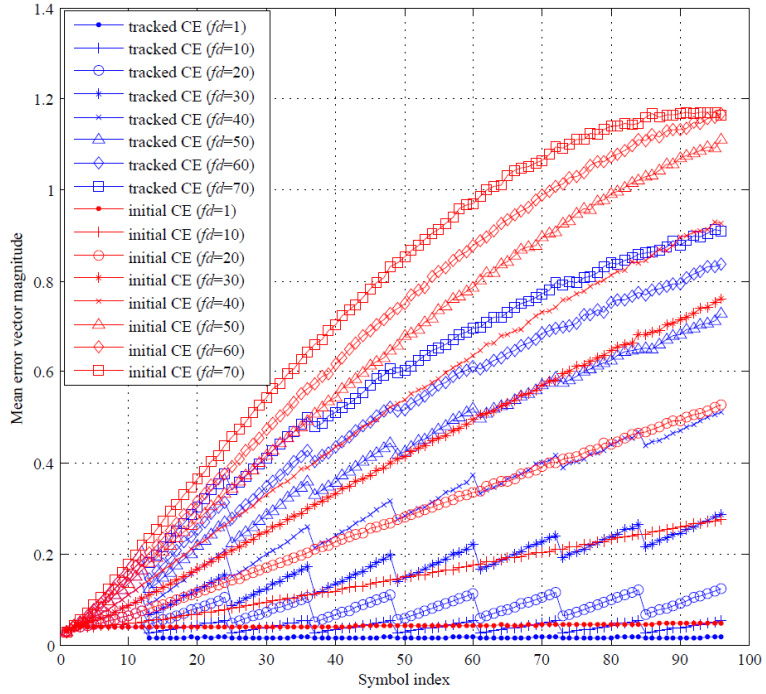

(b)

Figure 6.15: Performance of channel tracking for different maximum Doppler shifts (a) initial channel estimation (b) both methods.

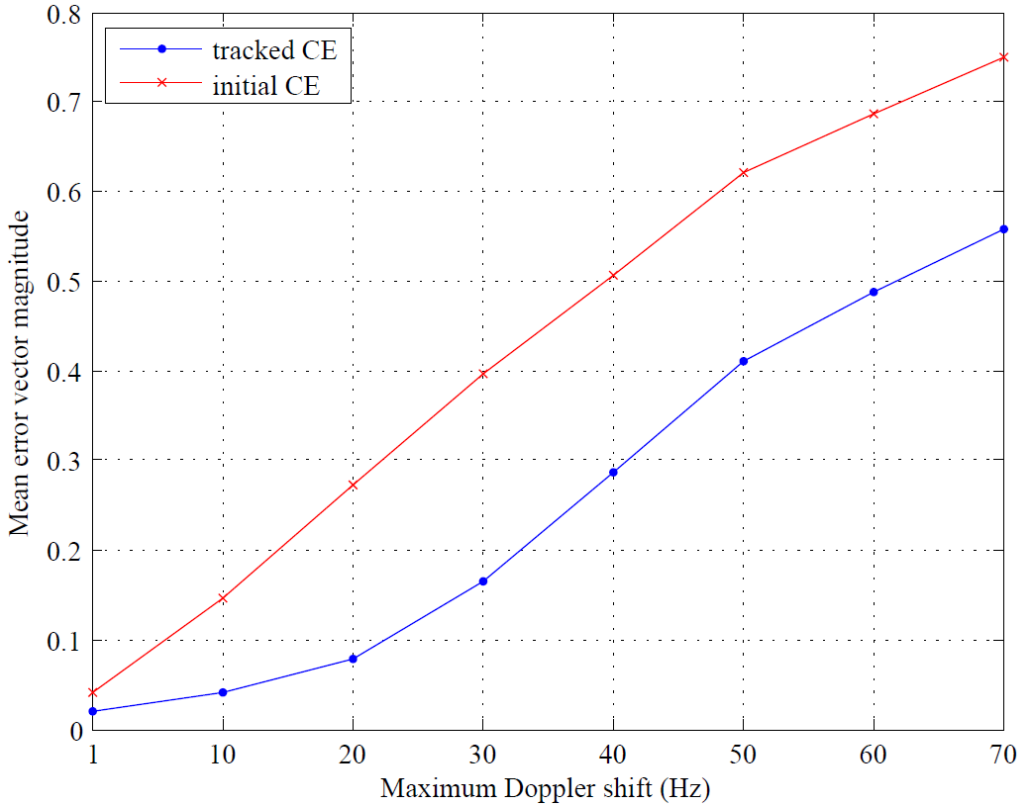

Figure 6.16: Mean EVM for the channel tracking method and the initial training-based channel estimation method versus maximum Doppler shifts.

Figure 6.16 shows the difference in mean EVM for the channel tracking method and the initial training-based channel estimation method versus f_d in Hz. The averages of the mean EVM for the tracking method and the initial channel estimation method are 0.4337 and 0.7475, respectively. This implies that, the average EVM for the tracking method is lower by 0.3138 compared to the training-based channel estimation method. Moreover, the mean EVM for the initial channel estimation method is always higher than the channel tracking method. Therefore, the novel channel tracking method performs better than the initial channel estimation method for all the considered f_ds. In this section, a detailed analysis of the performance of the proposed channel tracking method and the training-based initial channel estimation method with a range maximum Doppler shifts (f_ds) was discussed.

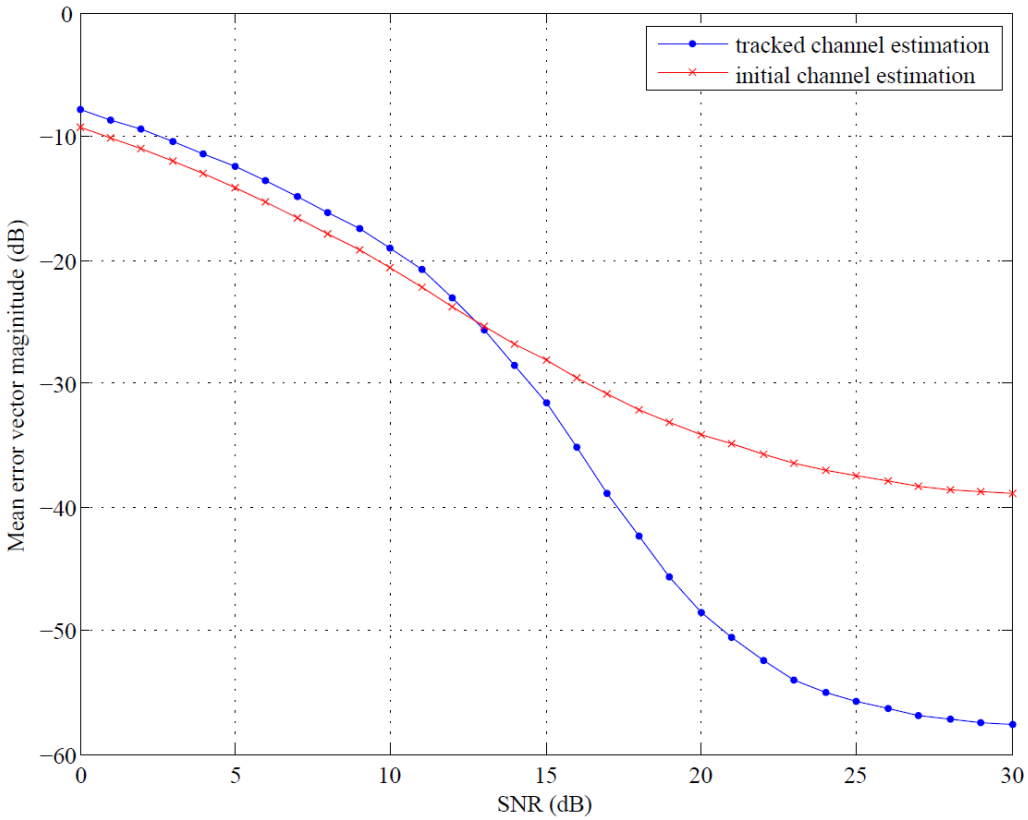

Figure 6.17: Sample performance of the channel tracking method and the initial channel estimation method against SNR.

6.3.4 SNR analysis

This section provides a detailed analysis of the performance of the proposed channel tracking method and the training-based initial channel estimation method for a range of SNR values with $f_d = 10$ Hz.

The performance of the novel channel tracking method with the initial channel estimates for a range of SNR values at $f_d = 10$ Hz is illustrated in Figure 6.17. The simulations are conducted for 100 EVM iterations and the performance is shown for the 48^{th} symbol averaged over all EVM iterations, all subcarriers and all MSs. The mean EVM decreases as SNR increases for both methods. The average EVM for the initial channel estimation is -1.5605 dB lower than that of the channel tracking method for SNR ranging from 0 dB to 13 dB. However, when the SNR increases beyond 13 dB, the proposed tracking method shows considerably lower mean EVM when compared with the initial channel estimates. For example, at an SNR of 30 dB, the mean EVM of the proposed tracking method is approximately

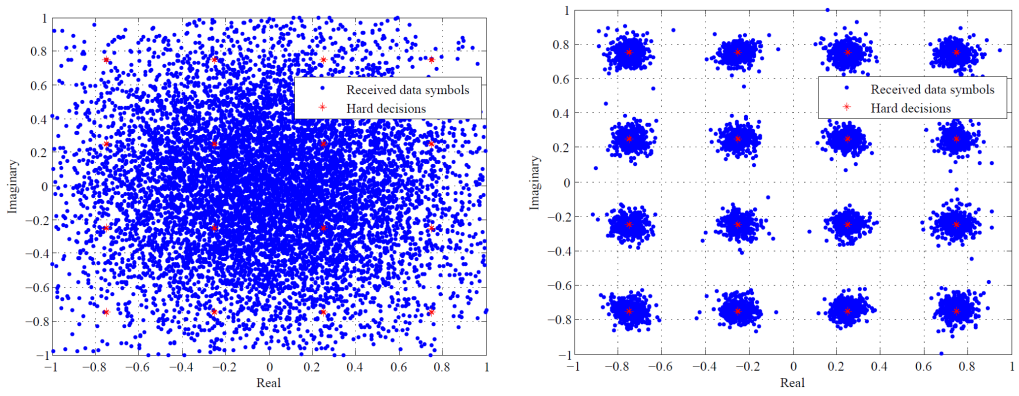

(a) (b)

Figure 6.18: Signal constellations of received data and hard-decision symbols for (a) SNR= 0 dB (b) SNR= 30 dB.

−73 dB while the mean EVM for the training based method is approximately −50 dB, which is a 23 dB loss in mean EVM for the proposed method. This implies that, when the SNR is more than 13 dB, the proposed channel tracking method performs better than the training based method. Figure 6.18 shows the signal constellations of the received data and the hard-decision symbols for SNR= 0 dB and SNR= 30 dB, respectively. When the SNR is 30 dB, the noise levels are lower and it makes the hard-decision process more effective, as the received data symbols in the signal constellation will be closer to the hard-decision red points. At low SNR levels, the received data symbols in blue will appear more spread out around the hard-decision red points, merging with the neighboring symbols, causing more errors. Because of that, the channel tracking method does not work well when the SNR is lower than 13 dB. At low SNR levels, the tracked channel estimates provides more errors than the initial channel estimation method. This is because, as shown in Figure 6.18, hard decisions provide erroneous outcomes at low SNR levels which are used in the tracking method. This could be addressed by employing an error correction method. However, this is out of the scope of this thesis and is left for future works.

Figure 6.19 illustrates the performance of the novel channel tracking method and initial training-based channel estimation method with the SNR and symbol index. The performance is shown for the fourth MS averaged over all EVM iterations and all subcarriers. In Figure 6.19(b), the mean EVM increases linearly with the time index, as the initial channel estimation method incorporates a single training

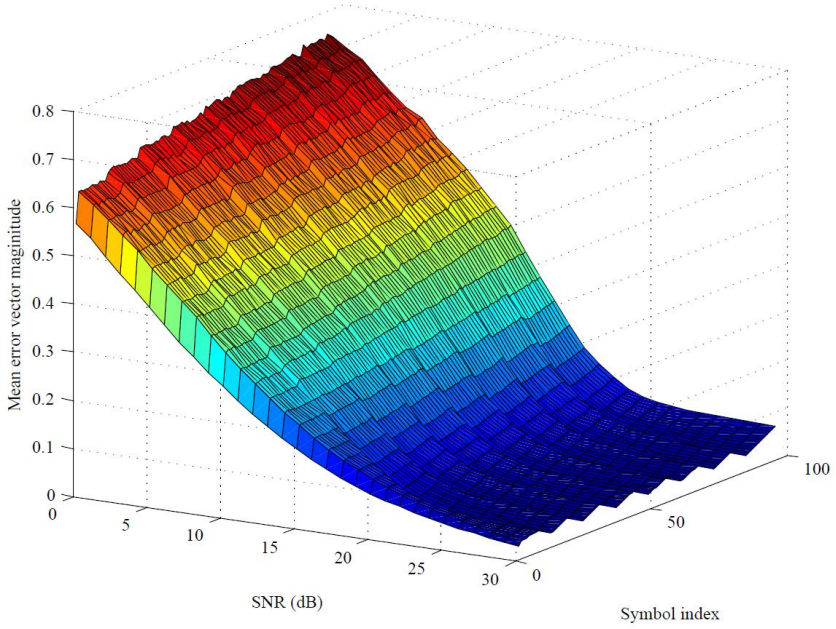

(a)

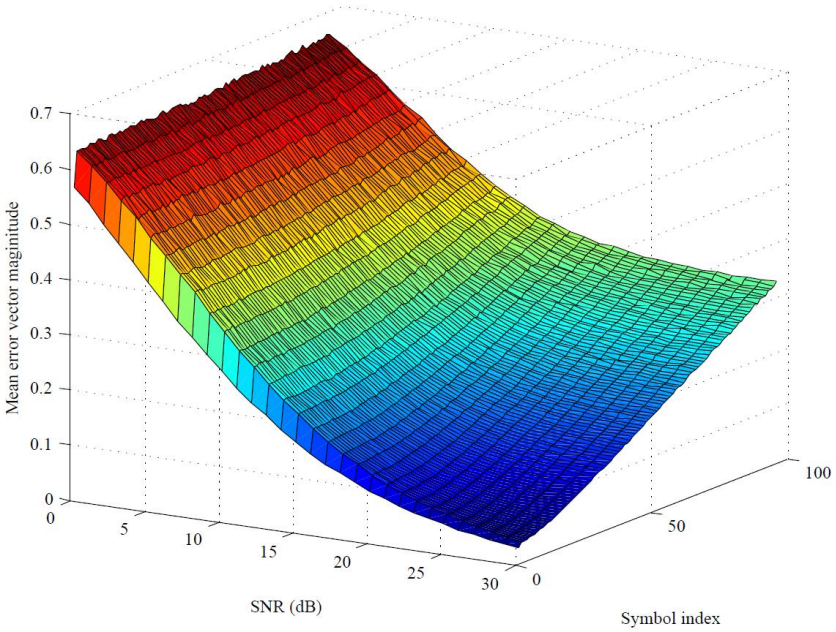

(b)

Figure 6.19: Performance of (a) channel tracking method; (b) initial channel estimation method with SNR and symbol index.

sequence for each transmitter to estimate the time-varying channel. In contrast, in Figure 6.19(a), the mean EVM remains at an average of 0.0478 for all OFDM symbols, which is significantly lower than the use of initial channel estimates, and do not require the use of additional training sequences, as the tracking method keeps updating the channel estimates by incorporating the hard-decision symbols. The mean EVM of both methods decreases as the SNR increases as explained in the previous paragraph.

6.4 Statistical analysis of the error vector magnitude

This section discusses the statistical analysis of the EVM of the novel channel tracking method in SDMA-based multi-user MIMO-OFDM systems. As explained in Chapter 4 (Section 4.6.1), the EVM is computed by comparing the recovered symbols ($\hat{\mathbf{X}}$) with the actual transmitted symbols ($\mathbf{X}$). The EVM is computed to obtain the magnitude and the complex numbers for different maximum Doppler shift values in a range of 1, 10, 20 and 30 Hz. The following section presents the results obtained in the simulations conducted to perform error and statistical analysis of the EVM for the novel channel tracking method. The simulations of a statistical analysis on the EVM variance is conducted.

6.4.1 Analysis on variance of EVM

This section presents an analysis conducted on the variance computed for the EVM. The variance of the EVM for different f_ds is illustrated in Figure 6.20. It can be seen that the variance of the EVM increases as f_d increases. For example, the variances of the EVM at symbol 96 for $f_d = 1$, 10, 20 and 30 Hz are 0.0002, 0.0019, 0.0139 and 0.0751, respectively. Because f_d increases the time variations of the channel, the variance of the EVM for $f_d = 20$ and 30 Hz increases as the symbol index increases. Since the tracking method incorporated the channel estimated by using training symbols during the first 12 symbols, it shows a very low EVM at the beginning of the OFDM symbol index (during the first 12 symbols) for all the f_ds. As explained in the previous section, the channel tracking method shows high mean EVM when f_d is larger than 30 Hz and the mean EVM increases as f_d increases. Therefore, statistical analysis of the EVM is carried out employing the data calculated for f_d up to 30 Hz.

The probability distribution functions (PDFs) for the EVM variance for different f_ds are calculated and are shown in Figures 6.21 and 6.22 for the real and imaginary

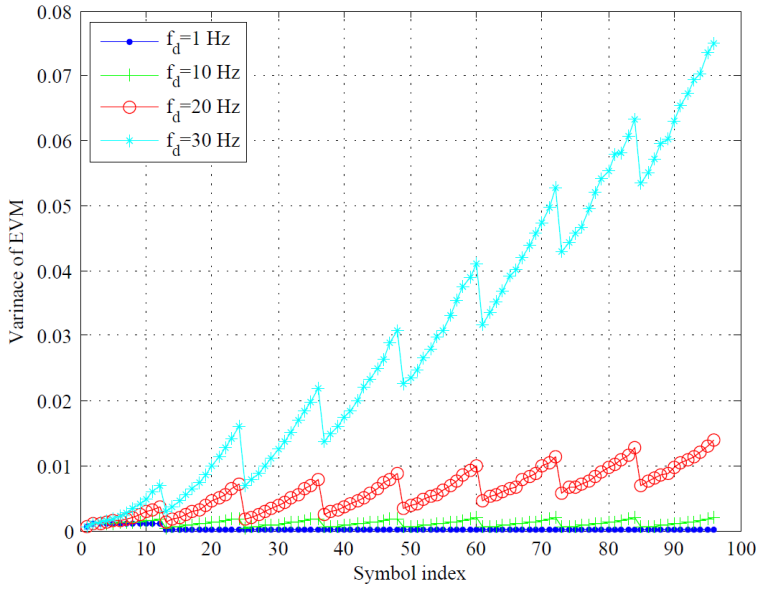

Figure 6.20: Variance of EVM for different maximum Doppler shifts (f_ds) in Hz.

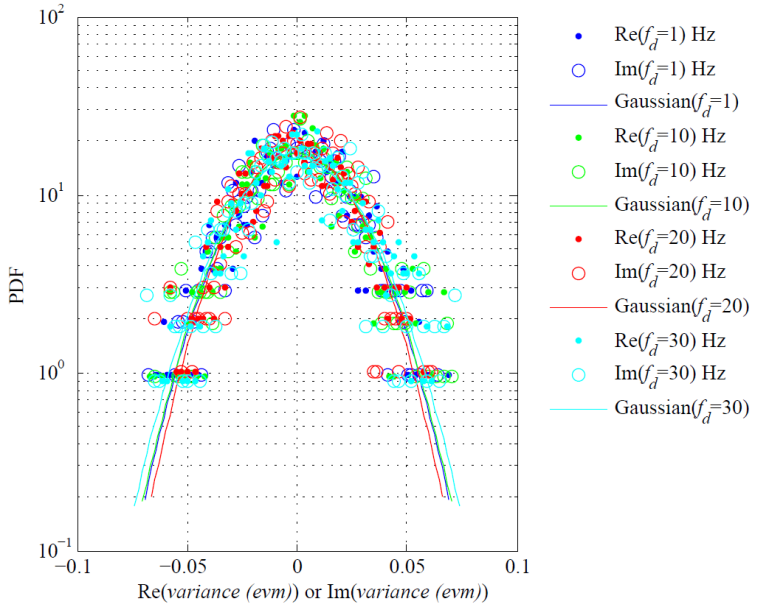

Figure 6.21: Probability distribution functions of the variance of the EVM for different maximum Doppler shifts (f_ds) in Hz.

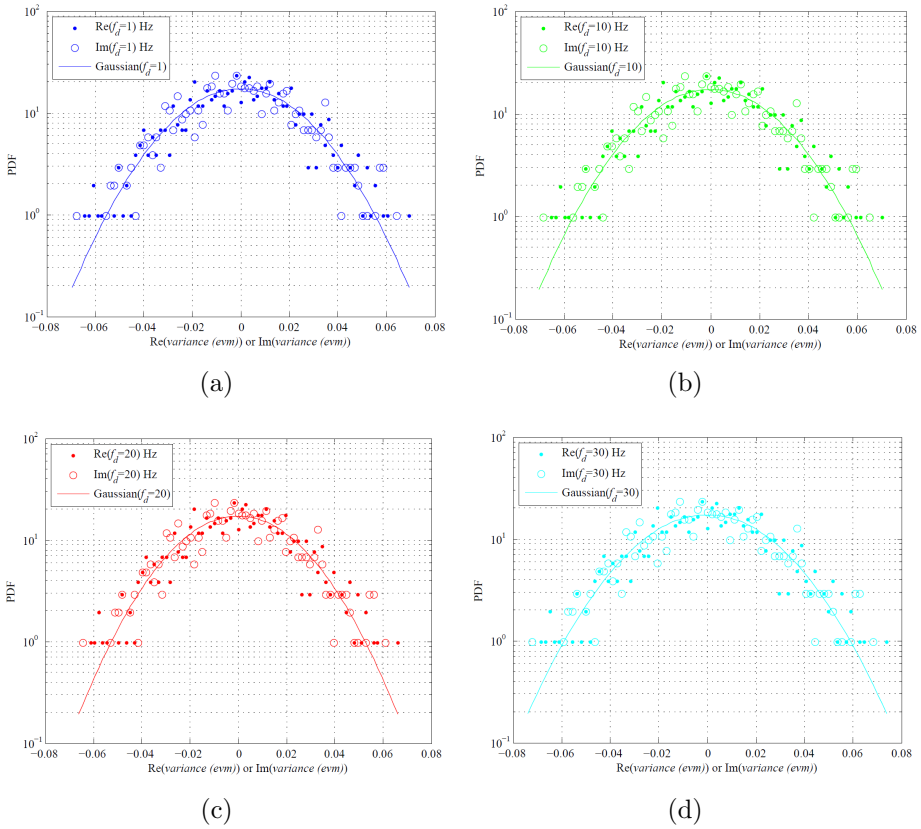

Figure 6.22: PDF of variance of EVM when (a) $f_d = 1$ Hz (b) $f_d = 10$ Hz (c) $f_d = 20$ Hz (d) $f_d = 30$ Hz.

values of EVM variance. The PDFs in Figure 6.21 is a sample for the first symbol and for the first subcarrier. There is no apparent difference between the PDFs of the EVM variance for different f_ds. It can be seen that all the PDFs follow a Gaussian distribution with zero mean for a range of f_ds.

The performance of the novel channel tracking algorithm in terms of symbol error probability (SEP) versus SNR in dB for f_d ranging from 1 to 30Hz is illustrated in Figure 6.23. The SEP is computed by averaging over all subcarriers, all channel realisations and all MSs and taking the corresponding values of the 25^{th} symbol. It can be seen that the SEP increases as f_d increases. For example, the SEP is 1.9×10^{-2}, 2.4×10^{-2}, 4.9×10^{-2}, and 9.2×10^{-2} for $f_d = 1$, 10, 20, and 30Hz, respectively. Moreover, it can be seen that, the SEP reduces as SNR increases. When f_d increases, the time variations in the multi-user MIMO channel increases and the SEP of the tracking algorithm increases with f_d. The demodulation process

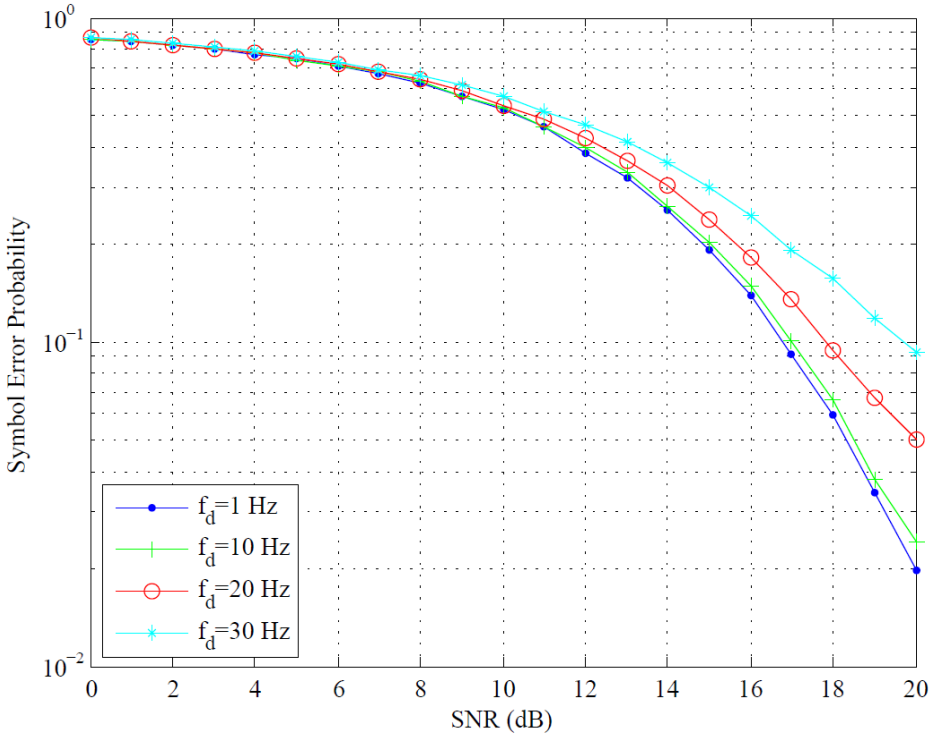

Figure 6.23: Symbol error probability versus SNR for a range of f_ds in Hz.

will have more errors as there is a shift in the carrier frequency.

6.5 Chapter summary

This chapter presents a novel and efficient channel tracking method for time-varying and frequency selective channels in SDMA-based multi-user MIMO-OFDM systems. The proposed method tracks the channel using hard-decision data symbols. One single-training sequence for each transmitter is employed to generate the initial channel estimates. The transmitted data are detected using zero-forcing to reduce the computational complexity and remove the effect of the channel's frequency selectivity. Subsequently, the channel estimates are updated using the detected data symbols.

A detailed analysis of the simulation results with error, channel matrix, maximum Doppler shift and SNR are presented. The results show that the proposed method performs better than the initial training sequence based method in time-varying, frequency selective, multi-path channels in SDMA-based multi-user MIMO-OFDM

systems. For example, the mean EVM for the proposed novel method is up to 79% lower than a training-based channel estimation method using a single-training sequence for each transmitter. Therefore, this novel channel tracking mechanism allows more efficient channel estimation without having to spend bandwidth in additional training sequences. It can be concluded that both magnitude error and variance of EVM increases as the maximum Doppler shift increases. Furthermore, the statistical analysis proves that the variance of the EVM follows a Gaussian distribution with zero mean.

Chapter 7

Conclusion

The results and contributions of this thesis are summarised in this final chapter. The first part of the thesis discussed the literature and established the ground work on adaptive channel equalization and novel channel tracking. Specifically, we concentrated on the development of a novel channel tracking algorithm in the uplink of SDMA-based multi-user MIMO-OFDM systems. A review of the theory on multi-path fading, MIMO and OFDM and the relevant literature review on channel tracking is also presented. The next section presents a chapter by chapter summary of the thesis.

A detailed overview of multipath fading and MIMO-OFDM wireless communications systems, presenting the necessary background to understand the succeeding research findings, is provided in Chapter 2. The importance of OFDM, MIMO and MIMO-OFDM systems is established through a thorough literature review and explanations of the basic theoretical concepts of these technologies. A comprehensive literature review is presented in Chapter 3, with a focus on the literature on existing adaptive equalization methods, channel estimation techniques and channel tracking algorithms that are employed in MIMO-OFDM systems. The foundation for formulating the scope, objectives and methodology of this thesis is built by idetifying the existing gaps in knowledge as revealed by the literature review.

The methodology for carrying out the research in five phases is discussed in Chapter 4. First, we constructed a time-varying, frequency selective, multi-user, MIMO channel. Next, we derived an efficient method to perform the initial channel estimation using a single-training sequence. Then, we developed adaptive equalization methods in the uplink of the SDMA-based multi-user MIMO-OFDM systems based on discussion of the theoretical concepts. Next, we developed a novel channel tracking algorithm in the uplink of the SDMA-based multi-user MIMO-OFDM systems. Finally, we conducted statistical analysis of the EVM.

Chapter 5 is dedicated to discussing the developed system model and presenting the simulation results of the proposed adaptive equalization methods for compen-

sating the channel impairments such as ISI produced by multi-path propagation. This chapter discussed the simulation results obtained for linear and DFE adaptive equalizers with LMS and RLS adaptive algorithms for both static and time-varying channels. The novel and efficient channel tracking method in time-varying and frequency selective channels for the SDMA-based multi-user MIMO-OFDM systems is presented in Chapter 6. The simulation results are discussed in four categories: 1) error analysis, 2) channel matrix analysis, 3) Doppler shift analysis, and 4) SNR analysis. Statistical analysis on the variance of the EVM is then presented. For this purpose, first, we computed the EVM and its variance. Then, the simulation results are produced to provide an analysis.

7.1 Summary of research findings and contributions

The research presented in this thesis first created a channel model for SDMA-based multi-user MIMO-OFDM systems to characterise the time-variations and frequency selectivity in the propagation environments in order for the adaptive equalization techniques and tracking algorithms to equalize and track a time-varying, and frequency selective channel, respectively. Then, the time-varying, frequency selective CSI is estimated at the receiver for SDMA-based multi-user MIMO-OFDM systems using a single-training sequence for each transmitter. Next, adaptive equalization mechanisms in SDMA-based MIMO-OFDM systems are developed to compensate the channel impairments caused by multi-path propagation and time-variations in the propagation environment. After that, the novel algorithm is developed to recursively track the time-varying, frequency selective, multi-user MIMO channels. Then, the effects of temporal variations in terms of the EVM between the recovered symbols and the transmitted symbols are measured.

The study in this thesis presented a novel and efficient channel tracking algorithm for time-varying and frequency selective channels in SDMA-based multi-user MIMO-OFDM systems. The proposed method tracks the channel using hard-decision data symbols. One single-training sequence for each transmitter is employed to generate the initial channel estimates. The transmitted data are detected using zero-forcing to reduce the computational complexity. Subsequently, the channel estimates are updated using the detected data symbols.

The tracked channel estimation provides a significantly lower EVM when used in SDMA-based multi-user MIMO-OFDM systems. For example, the value of the EVM for the proposed novel method is up to 79% lower than for a training-based

channel estimation method using a single-training sequence. Therefore, the novel channel tracking method offers a significant advantage of using a reduced amount of bandwidth when compared to the training-based channel estimation method. Moreover, the proposed method shows lower EVM values for lower Doppler shifts. For example, when f_d is less than 30 Hz, the EVM approximately remained under 0.2. Furthermore, there is no considerable difference in EVM for different Rician k-factors, making the performance of the novel proposed channel tracking method independent of the Rician k-factor. Since the proposed method used the hard-decisions, the noise can be efficiently removed from the tracked channel estimation. This shows the significance of the proposed novel channel tracking method in SDMA-based multi-user MIMO-OFDM systems, as it offers a more efficient use of bandwidth and performs accurate channel tracking for time-varying, frequency selective, multi-user, multi-path MIMO channels.

Since most of the channel estimation and tracking methods employ more than 20% of the OFDM transmission duration as training data, the scarce bandwidth that can be allocated for transmitting information is wasted. However, the novel channel tracking method presented in this thesis only uses single pilot data for each transmitter, saving valuable bandwidth in OFDM transmission. Moreover, this method does not depend on the number of users or the number of receiver antennas at the AP. Most of the channel estimation and tracking algorithms degrade in performance when the number of users or the number of receiver antennas is increased.

The study presented in this thesis considered the linear and DFE adaptive channel equalization using the LMS algorithm and the RLS algorithm for SDMA-based multi-user MIMO-OFDM wireless communications systems. The contribution of these techniques relates to the application of adaptive equalization methods to multi-user MIMO-OFDM systems using SDMA for the first time. Furthermore, this contribution consists of applying these techniques in both static and time-varying, frequency selective, SDMA-based multi-user, MIMO-OFDM channels. The channel impairments caused by multi-path propagation and time-variations in the propagation environments are compensated by the proposed adaptive equalization methods. The proposed DFE adaptive equaliser reached a BER of 10^{-3} at an SNR of 12 dB when using the RLS adaptive algorithm. In general, the adaptive equalization using the LMS and RLS algorithms are shown to be significantly beneficial for SDMA-based multi-user MIMO-OFDM systems.

7.2 Suggested future work

A number of valuable directions for future research work arise as a result of the work presented in this thesis. As we discussed in relation to the simulation results, the EVM increases with the f_d. Therefore, it would be worthwhile to incorporate an error correction method into the simulations of the channel tracking method in multi-user MIMO-OFDM systems to improve the EVM so that the accuracy of the novel channel tracking technique can be improved. Incorporating soft-decisions in the simulations of the tracking method to improve performance can also be suggested as an area of investigation in future work. In practical terms, the processing of the corresponding downlink MIMO channel needs to be implemented. For time division duplex systems, channel reciprocity may be employed to derive the downlink channel from the uplink channel (which may be tracked or predicted). Therefore, channel tracking in downlink channel processing can also be suggested as a worthwhile area of investigation for future work.

The proposed channel tracking method operates in quasi-static, frequency selective, multi-path, SDMA-based multi-user MIMO channels. It would be worthwhile to develop tracking and equalization methods for fast time-varying, frequency selective, multi-path, multi-user, MIMO channels. Moreover, a mechanism could be developed to estimate and track doubly-selective channels in vehicle-to-vehicle environments. Furthermore, it would be worthwhile to investigate the implementation of this method in a real-time multi-user MIMO-OFDM system. Narrowband MIMO channel has a very short time delay. Therefore, it can be modeled as dense channel model. In contrast, broadband channel model may be modelled as a sparse channel. Therefore, it would be interesting to explore and exploit MIMO channels inherent sparsity to estimate and track multi-user MIMO-OFDM channels.

7.2.1 Extensions

Some of the work presented in this thesis can be further extended. The availability of channel knowledge or the CSI at the transmitter (Tx) is the most common assumption in all of the recent research done on the subject of multi-user MIMO systems. There are several advantages of having CSI at the transmitter, such as achieving high SNR at the preferred receiver (Rx) and reducing the inter-user interference. Having CSI at the transmitter, a single-user MIMO system benefits either when $N_{Tx} > N_{Rx}$ antennas, or at low SNR. However, an AP transmitting to multiple users via the same channel will always benefit from CSI.

The CSI can be obtained at the transmitter by using two techniques. The first

method is to use the pilot or training data in the uplink for time division duplex systems. The second mechanism uses the feedback from the receivers channel estimate obtained by the training data in the downlink. The latter is suitable for frequency-division duplex transmission systems. In each scenario, it is not only a technical challenge, but also not economical to obtain the CSI at the transmitter. However, it is justifiable for multi-user channels [106]. Therefore, the CSI obtained by the tracking algorithm can be fed back to the transmitter by extending the work presented in this thesis.

Bibliography

[1] L. Jin and L. Xiaofeng, "Equalization in high-speed communication systems," *IEEE Circuits and Systems Magazine*, vol. 4, no. 2, pp. 4–17, Second quarter 2004.

[2] J. Stott, "The how and why of COFDM," *EBU Technical Review*, 1999.

[3] Orthogonal frequency division multiplexing. http://wiki.hsc.com/. Accessed: 05/06/2011.

[4] M. Jiang and L. Hanzo, "Multiuser MIMO-OFDM for next-generation wireless systems," *Proceedings of the IEEE*, vol. 95, no. 7, pp. 1430–1469, 2007.

[5] A. Goldsmith, *Multiuser Systems*. Cambridge, New York: Cambridge University Press, 2005.

[6] D. Gesbert, M. Shafi, S. Da-shan, P. J. Smith, and A. Naguib, "From theory to practice: an overview of MIMO space-time coded wireless systems," *IEEE Journal on Selected Areas in Communications*, vol. 21, no. 3, pp. 281–302, April 2003.

[7] F. Tufvesson and T. Maseng, "Pilot assisted channel estimation for OFDM in mobile cellular systems," in *Vehicular Technology Conference, 1997 IEEE 47th*, vol. 3, pp. 1639–1643 vol.3.

[8] F. Tavassoli and B. Abolhassani, "Comb-type pilot aided channel estimation for OFDM systems," in *International Symposium on Wireless Communications (ISWSN'05)*, 2005.

[9] T. Rappaport, *Wireless Communications Principles and Practice*, 2nd ed. Prentice Hall, Inc, 2002.

[10] "National broadband network implementation study," Australian Government, Tech. Rep., April 2009.

[11] I. B. Collings, H. Suzuki, and D. Robertson, "Ngara broadband access system for rural and regional areas," *Telecommunication Journal of Australia*, 2012.

[12] J. Cimini, L., "Analysis and simulation of a digital mobile channel using orthogonal frequency division multiplexing," *IEEE Transactions on Communications*, vol. 33, no. 7, pp. 665–675, July 1985.

[13] G. J. Foschini and M. J. Gans, "On limits of wireless communications in a fading environment when using multiple antennas," *Wireless Personal Communications*, vol. 6, no. 3, pp. 311–335, 1998.

[14] H. Sampath, S. Talwar, J. Tellado, V. Erceg, and A. Paulraj, "A fourth-generation MIMO-OFDM broadband wireless system: design, performance, and field trial results," *IEEE Communications Magazine*, vol. 40, no. 9, pp. 143–149, September 2002.

[15] H. Taewon, Y. Chenyang, W. Gang, L. Shaoqian, and G. Ye Li, "OFDM and its wireless applications: A survey," *IEEE Transactions on Vehicular Technology*, vol. 58, no. 4, pp. 1673–1694, May 2009.

[16] H. Suzuki, D. B. Hayman, J. Pathikulangara, I. B. Collings, C. Zhuo, and R. Kendall, "Design criteria of uniform circular array for multi-user MIMO in rural areas," in *Wireless Communications and Networking Conference (WCNC), 2010 IEEE*, 2010, pp. 1–6.

[17] H. Suzuki, D. Hayman, J. Pathikulangara, I. B. Collings, and Z. Chen, "Highly spectrum-efficient fixed wireless multiple access," Patent PCT/AU2009/101 022, August, 2009.

[18] ——, "Fixed multiple access wireless communication," Patent WO 2010/025 492 A1, March 11, 2010.

[19] H. Suzuki, D. Robertson, N. L. Ratnayake, and K. Ziri-Castro, "Prediction and measurement of multiuser MIMO-OFDM channel in rural australia," in *Vehicular Technology Conference (VTC Spring), 2012 IEEE 75th*, pp. 1–5.

[20] J. Proakis, *Digital communications*, 4th ed. Boston: McGraw-Hill Science/Engineering/Math, 2001.

[21] P. Hammarberg, F. Rusek, and O. Edfors, "Iterative receivers with channel estimation for multi-user MIMO-OFDM: complexity and performance," *EURASIP Journal on Wireless Communications and Networking*, 2012.

[22] F. Delestre and S. Yichuang, "MIMO-OFDM with pilot-aided channel estimation for wimax systems," in *Wireless and Mobile Computing, Networking*

and Communications (WiMob), 2010 IEEE 6th International Conference on, pp. 586–590.

[23] R. W. Lucky, "Techniques for adaptive equalization of digital communication systems," *The Bell System Technical Journal*, October 1966.

[24] E. Karami and M. Shiva, "Blind multi-input multi-output channel tracking using decision-directed maximum-likelihood estimation," *IEEE Transactions on Vehicular Technology*, vol. 56, no. 3, pp. 1447–1454, May 2007.

[25] G. L. Stuber, J. R. Barry, S. W. McLaughlin, L. Ye, M. A. Ingram, and T. G. Pratt, "Broadband MIMO-OFDM wireless communications," *Proceedings of the IEEE*, vol. 92, no. 2, pp. 271–294, February 2004.

[26] A. Goldsmith, S. A. Jafar, N. Jindal, and S. Vishwanath, "Capacity limits of MIMO channels," *IEEE Journal on Selected Areas in Communications*, vol. 21, no. 5, pp. 684–702, June 2003.

[27] Y. Qinghai, Z. Huamin, X. Shaoyi, and K. Kyung-Sup, "Centralized and decentralized channel estimation for multiuser MIMO-OFDM systems," in *Communications, 2006. APCC '06. Asia-Pacific Conference on*, pp. 1–5.

[28] T. Islam, I. Ahmed, S. Mallick, F. Alam, and M. S. Rahman, "Quasi-static channel estimation for multiuser STBC-OFDM systems," in *Electrical and Computer Engineering, 2006. ICECE '06. International Conference on*, pp. 68–71.

[29] M. A. Mohammadi, M. Ardabilipour, B. Moussakhani, and Z. Mobini, "Performance comparison of RLS and LMS channel estimation techniques with optimum training sequences for MIMO-OFDM systems," in *Wireless and Optical Communications Networks, 2008. WOCN '08. 5th IFIP International Conference on*, pp. 1–5.

[30] A. Goldsmith, *Statistical Multipath Channel Models*. Cambridge, New York: Cambridge University Press, 2005.

[31] L. Hanzo, M. Munster, B. J. Choi, and T. Keller, *OFDM and MC-CDMA for broadband multi-user communications, WLANs and broadcasting*. Wiley-IEEE Press, 2003.

[32] R. V. Nee and R. Prasad, *OFDM for Wireless Multimedia Communications*. London, U.K.: Artech House, 2000.

[33] J. A. C. Bingham, "Multicarrier modulation for data transmission: an idea whose time has come," *IEEE Communications Magazine*, vol. 28, no. 5, pp. 5–14, 1990.

[34] R. W. Chang, "Synthesis of band-limited orthogonal signals for multichannel data transmission," *Bell System Technical Journal*, vol. 45, pp. 1775–1796, August 1966.

[35] "Digital audio broadcasting (DAB), DAB to mobile, portable and fixed receivers," European Telecommunication Standard Institute, Tech. Rep., 1995.

[36] "Digital video broadcasting (DVB); framing structure, channel coding and modulation for digital terrestrial television (DVB-T)," European Telecommunication Standard Institute, Tech. Rep., 1997.

[37] "Digital video broadcasting (DVB); transmission system for handheld terminals (DVB-H)," European Telecommunication Standard Institute, Tech. Rep., 2004.

[38] "Radio equipment and systems (RES); high performance radio local area network (HIPERLAN) type 1; functional specification," European Telecommunication Standard Institute, Tech. Rep., 1996.

[39] *Broadband Radio Access Networks (BRAN); Inventory of Broadband Radio Technologies and Techniques*, European Telecommunication Standard Institute Std., May 1998.

[40] B. Das and S. Das, "Efficacy of multiband OFDM approach in high data rate ultra wideband wpan physical layer standard using realistic channel models," *International Journal of Computer Applications*, vol. 2, no. 2, May 2010.

[41] I. Koffman and V. Roman, "Broadband wireless access solutions based on OFDM access in IEEE 802.16," *IEEE Communications Magazine*, vol. 40, no. 4, pp. 96–103, April 2002.

[42] R. Laroia, S. Uppala, and L. Junyi, "Designing a mobile broadband wireless access network," *IEEE Signal Processing Magazine*, vol. 21, no. 5, pp. 20–28, September 2004.

[43] X. Pengfei, Z. Shengli, and G. B. Giannakis, "Bandwidth and power-efficient multicarrier multiple access," *IEEE Transactions on Communications*, vol. 51, no. 11, pp. 1828–1837, November 2003.

[44] C. Zhongren, U. Tureli, and Y. Yu-Dong, "Deterministic multiuser carrier-frequency offset estimation for interleaved OFDMA uplink," *IEEE Transactions on Communications*, vol. 52, no. 9, pp. 1585–1594, September 2004.

[45] A. Peled and A. Ruiz, "Frequency domain data transmission using reduced computational complexity algorithms," in *Acoustics, Speech, and Signal Processing, IEEE International Conference on ICASSP '80.*, vol. 5, pp. 964–967.

[46] T. May, H. Rohling, and V. Engels, "Performance analysis of viterbi decoding for 64-DAPSK and 64-QAM modulated OFDM signals," *IEEE Transactions on Communications*, vol. 46, no. 2, pp. 182–190, February 1998.

[47] L. Lin, L. J. Cimini, and J. C. I. Chuang, "Comparison of convolutional and turbo codes for OFDM with antenna diversity in high-bit-rate wireless applications," *IEEE Communications Letters*, vol. 4, no. 9, pp. 277–279, September 2000.

[48] B. Saltzberg, "Performance of an efficient parallel data transmission system," *IEEE Transactions on Communication Technology*, vol. 15, no. 6, pp. 805–811, December 1967.

[49] R. Chang and R. Gibby, "A theoretical study of performance of an orthogonal multiplexing data transmission scheme," *IEEE Transactions on Communication Technology*, vol. 16, no. 4, pp. 529–540, August 1968.

[50] R. W. Chang, "Orthogonal frequency division multiplexing," Patent US 3 488 445, Jan 06, 1970.

[51] S. Weinstein and P. Ebert, "Data transmission by frequency-division multiplexing using the Discrete Fourier Transform," *IEEE Transactions on Communication Technology*, vol. 19, no. 5, pp. 628–634, October 1971.

[52] B. Hirosaki, "An analysis of automatic equalizers for orthogonally multiplexed QAM systems," *IEEE Transactions on Communications*, vol. 28, no. 1, pp. 73–83, January 1980.

[53] W. E. Keasler, D. L. Bitzer, and P. T. Tucker, "High-speed modem suitable for operating with a switched network," Patent US 4 206 320, June 03, 1980.

[54] B. Hirosaki, "An orthogonally multiplexed QAM system using the discrete fourier transform," *IEEE Transactions on Communications*, vol. 29, no. 7, pp. 982–989, July 1981.

[55] L. J. Cimini, "Analysis and simulation of a digital mobile channel using orthogonal frequency division multiplexing," *IEEE Transactions on Communications*, vol. 33, no. 7, pp. 665–675, July 1985.

[56] B. Hirosaki, S. Hasegawa, and A. Sabato, "Advanced groupband data modem using orthogonally multiplexed QAM technique," *IEEE Transactions on Communications*, vol. 34, no. 6, pp. 587–592, July 1986.

[57] I. Kalet, "The multitone channel," *IEEE Transactions on Communications*, vol. 37, no. 2, pp. 119–124, February 1989.

[58] J. M. Cioffi, *A Multicarrier Primer*. Amati Communications Corporation and Stanford University, 1991.

[59] W. D. Warner and C. Leung, "OFDM/FM frame synchronization for mobile radio data communication," *IEEE Transactions on Vehicular Technology*, vol. 42, no. 3, pp. 302–313, August 1993.

[60] P. H. Moose, "A technique for orthogonal frequency division multiplexing frequency offset correction," *IEEE Transactions on Communications*, vol. 42, no. 10, pp. 2908–2914, October 1994.

[61] T. Pollet, M. Van Bladel, and M. Moeneclaey, "BER sensitivity of OFDM systems to carrier frequency offset and wiener phase noise," *IEEE Transactions on Communications*, vol. 43, no. 234, pp. 191–193, April 1995.

[62] A. E. Jones, T. A. Wilkinson, and S. K. Barton, "Block coding scheme for reduction of peak to mean envelope power ratio of multicarrier transmission schemes," *Electronics Letters*, vol. 30, no. 25, pp. 2098–2099, December 1994.

[63] S. J. Shepherd, P. W. J. Van Eetvelt, C. W. Wyatt-Millington, and S. K. Barton, "Simple coding scheme to reduce peak factor in QPSK multicarrier modulation," *Electronics Letters*, vol. 31, no. 14, pp. 1131–1132, July 1995.

[64] D. Wulich, "Reduction of peak to mean ratio of multicarrier modulation using cyclic coding," *Electronics Letters*, vol. 32, no. 5, p. 432, February 1996.

[65] D. Wulich, "Peak factor in orthogonal multicarrier modulation with variable levels," *Electronics Letters*, vol. 32, no. 20, pp. 1859–1861, September 1996.

[66] L. Xiaodong and L. J. Cimini, "Effects of clipping and filtering on the performance of OFDM," in *IEEE 47th Vehicular Technology Conference, 1997*, vol. 3, pp. 1634–1638 vol.3.

[67] L. Xiaodong and L. J. Cimini, "Effects of clipping and filtering on the performance of OFDM," *IEEE Communications Letters*, vol. 2, no. 5, pp. 131–133, May 1998.

[68] S. Hara and R. Prasad, "Overview of multicarrier CDMA," *IEEE Communications Magazine*, vol. 35, no. 12, pp. 126–133, December 1997.

[69] Y. Li, J. Cimini, L. J., and N. R. Sollenberger, "Robust channel estimation for OFDM systems with rapid dispersive fading channels," *IEEE Transactions on Communications*, vol. 46, no. 7, pp. 902–915, July 1998.

[70] L. Ye and N. R. Sollenberger, "Adaptive antenna arrays for OFDM systems with cochannel interference," *IEEE Transactions on Communications*, vol. 47, no. 2, pp. 217–229, February 1999.

[71] S. Armour, A. Nix, and D. Bull, "Pre-FFT equaliser design for OFDM," *Electronics Letters*, vol. 35, no. 7, pp. 539–540, April 1999.

[72] S. Armour, A. Nix, and D. Bull, "Performance analysis of a pre-FFT equalizer design for DVB-T," in *Consumer Electronics, 1999. ICCE. International Conference on*, pp. 72–73.

[73] S. Armour, A. Nix, and D. Bull, "Complexity evaluation for the implementation of a pre-FFT equalizer in an OFDM receiver," *IEEE Transactions on Consumer Electronics*, vol. 46, no. 3, pp. 428–437, August 2000.

[74] B. Y. Prasetyo and A. H. Aghvami, "Simplified frame structure for MMSE-based fast burst synchronisation in OFDM systems," *Electronics Letters*, vol. 35, no. 8, pp. 617–618, April 1999.

[75] B. Y. Prasetyo, F. Said, and A. H. Aghvami, "Fast burst synchronisation technique for OFDM-WLAN systems," *IEE Proceedings - Communications*, vol. 147, no. 5, pp. 292–298, October 2000.

[76] P. Cherriman, T. Keller, and L. Hanzo, "Orthogonal frequency-division multiplex transmission of H.263 encoded video over highly frequency-selective wireless networks," *IEEE Transactions on Circuits and Systems for Video Technology*, vol. 9, no. 5, pp. 701–712, August 1999.

[77] W. Cheong Yui, R. S. Cheng, K. B. Lataief, and R. D. Murch, "Multiuser OFDM with adaptive subcarrier, bit, and power allocation," *IEEE Journal on Selected Areas in Communications*, vol. 17, no. 10, pp. 1747–1758, October 1999.

[78] K. Fazel and S. Kaiser, *Multi-Carrier Spread-Spectrum and Related Topics*. MA, USA: Kluwer Academic Publishers Norwell, 2000.

[79] R. V. Nee and R. Prasad, *OFDM for Wireless Multimedia Communications*. Boston, London: Artech House, 2000.

[80] L. Chee-Siong, T. Keller, and L. Hanzo, "OFDM-based turbo-coded hierarchical and non-hierarchical terrestrial mobile digital video broadcasting," *IEEE Transactions on Broadcasting*, vol. 46, no. 1, pp. 1–22, March 2000.

[81] T. Keller and L. Hanzo, "Adaptive multicarrier modulation: a convenient framework for time-frequency processing in wireless communications," *Proceedings of the IEEE*, vol. 88, no. 5, pp. 611–640, May 2000.

[82] T. Keller and L. Hanzo, "Adaptive modulation techniques for duplex OFDM transmission," *IEEE Transactions on Vehicular Technology*, vol. 49, no. 5, pp. 1893–1906, September 2000.

[83] T. Keller, L. Piazzo, P. Mandarini, and L. Hanzo, "Orthogonal frequency division multiplex synchronization techniques for frequency-selective fading channels," *IEEE Journal on Selected Areas in Communications*, vol. 19, no. 6, pp. 999–1008, June 2001.

[84] B. Lu, W. Xiaodong, and K. R. Narayanan, "LDPC-based space-time coded OFDM systems over correlated fading channels: performance analysis and receiver design," in *Information Theory, 2001. Proceedings. 2001 IEEE International Symposium on*, p. 313.

[85] B. Lu, W. Xiaodong, and K. R. Narayanan, "LDPC-based space-time coded OFDM systems over correlated fading channels: Performance analysis and receiver design," *IEEE Transactions on Communications*, vol. 50, no. 1, pp. 74–88, January 2002.

[86] B. Lu, W. Xiaodong, and L. Ye, "Iterative receivers for space-time block coded OFDM systems in dispersive fading channels," in *Global Telecommunications Conference, 2001. GLOBECOM '01. IEEE*, vol. 1, pp. 514–518 vol.1.

[87] B. Lu, W. Xiaodong, and L. Ye, "Iterative receivers for space-time block-coded OFDM systems in dispersive fading channels," *IEEE Transactions on Wireless Communications*, vol. 1, no. 2, pp. 213–225, January 2002.

[88] O. Simeone, Y. Bar-Ness, and U. Spagnolini, "Pilot-based channel estimation for OFDM systems by tracking the delay-subspace," *IEEE Transactions on Wireless Communications*, vol. 3, no. 1, pp. 315–325, January 2004.

[89] J. Zhang, H. Rohling, and P. Zhang, "Analysis of ICI cancellation scheme in OFDM systems with phase noise," *IEEE Transactions on Broadcasting*, vol. 50, no. 2, pp. 97–106, June 2004.

[90] M. C. Necker and G. L. Stuber, "Totally blind channel estimation for OFDM on fast varying mobile radio channels," *IEEE Transactions on Wireless Communications*, vol. 3, no. 5, pp. 1514–1525, September 2004.

[91] A. Doufexi, S. Armour, A. Nix, P. Karlsson, and D. Bull, "Range and throughput enhancement of wireless local area networks using smart sectorised antennas," *IEEE Transactions on Wireless Communications*, vol. 3, no. 5, pp. 1437–1443, September 2004.

[92] E. Alsusa, Y. Lee, and S. McLaughlin, "Channel-adaptive sectored multicarrier packet based systems," *Electronics Letters*, vol. 40, no. 19, pp. 1194–1196, September 2004.

[93] C. Williams, M. A. Beach, and S. McLaughlin, "Robust OFDM timing synchronisation," in *Vehicular Technology Conference, 2006. VTC 2006-Spring. IEEE 63rd*, vol. 4, pp. 1947–1950.

[94] L. Hanzo and C. Byoung-Jo, "Near-instantaneously adaptive HSDPA-style OFDM versus MC-CDMA transceivers for WIFI, WIMAX, and next-generation cellular systems," *Proceedings of the IEEE*, vol. 95, no. 12, pp. 2368–2392, December 2007.

[95] R. F. H. Fischer and C. Siegl, "Performance of peak-to-average power ratio reduction in single- and multi-antenna OFDM via directed selected mapping," *IEEE Transactions on Communications*, vol. 57, no. 11, pp. 3205–3208, November 2009.

[96] G. Mileounis, N. Kalouptsidis, and P. Koukoulas, "Blind identification of hammerstein channels using QAM, PSK, and OFDM inputs," *IEEE Transactions on Communications*, vol. 57, no. 12, pp. 3653–3661, November 2009.

[97] H. Shih-Gu and H. Chien-Hwa, "Improvement of active interference cancellation: avoidance technique for OFDM cognitive radio," *IEEE Transactions on Wireless Communications*, vol. 8, no. 12, pp. 5928–5937, December 2009.

[98] C. Hou-Shin, G. Wen, and D. G. Daut, "Spectrum sensing for ofdm systems employing pilot tones," *IEEE Transactions on Wireless Communications*, vol. 8, no. 12, pp. 5862–5870, December 2009.

[99] S. Pengfei, M. Morelli, and Z. Li, "Carrier frequency offset tracking in the IEEE 802.16e OFDMA uplink," *IEEE Transactions on Wireless Communications*, vol. 9, no. 12, pp. 3613–3619, December 2010.

[100] W. Kuo-Guan and W. Jer-An, "Efficient decision-directed channel estimation for OFDM systems with transmit diversity," *IEEE Communications Letters*, vol. 15, no. 7, pp. 740–742, July 2011.

[101] G. Lu, J. Wang, C. Zhang, and Z. Wang, "Hard decision directed frequency tracking for OFDM on frequency selective channel," *Tsinghua Science and Technology*, vol. 17, no. 2, pp. 202–208, April 2012.

[102] Y. Mingchao and P. Sadeghi, "A study of pilot-assisted OFDM channel estimation methods with improvements for DVB-T2," *IEEE Transactions on Vehicular Technology*, vol. 61, no. 5, pp. 2400–2405, June 2012.

[103] C. E. Shannon, "A mathematical theory of communication (parts 1 and 2)," *The Bell System Technical Journal*, vol. 27, pp. 379–423, October 1948.

[104] N. Dutta. (March 2013) Can electromagnetic radiation from mobile towers harm you? Accessed: 30/06/2013. [Online]. Available: http://health.india.com/diseases-conditions/can-electromagnetic-radiation-from-mobile-towers-harm-you/

[105] E. Telatar, "Capacity of multi-antenna Gaussian channels," *European Transactions on Telecommunications*, vol. 10, no. 6, pp. 585–595, 1999.

[106] Q. H. Spencer, C. B. Peel, A. L. Swindlehurst, and M. Haardt, "An introduction to the multi-user MIMO downlink," *IEEE Communications Magazine*, vol. 42, no. 10, pp. 60–67, October 2004.

[107] P. Almers, E. Bonek, A. Burr, N. Czink, M. Debbah, V. Degli-Esposti, H. Hofstetter, P. Kyolsti, D. Laurenson, G. Matz, A. F. Molisch, C. Oestges, and H. Ozcelik, "Survey of channel and radio propagation models for wireless MIMO systems," *EURASIP Journal on Wireless Communications and Networking*, vol. 2007, no. 1, 2007.

[108] R. E. Jaramillo, O. Fernandez, and R. P. Torres, "Empirical analysis of a 2 x 2 MIMO channel in outdoor-indoor scenarios for BFWA applications," *IEEE*

Antennas and Propagation Magazine, vol. 48, no. 6, pp. 57–69, December 2006, 1045-9243.

[109] G. Raleigh and J. Cioffi, "Spatio-temporal coding for wireless communications," in *Global Telecommunications Conference, 1996. GLOBECOM '96. 'Communications: The Key to Global Prosperity*, vol. 3, 1996, pp. 1809–1814.

[110] G. C. Raleigh and J. M. Cioffi, "Spatio-temporal coding for wireless communication," *IEEE Transactions on Communications*, vol. 46, no. 3, pp. 357–366, March 1998.

[111] A. J. Paulraj, D. A. Gore, R. U. Nabar, and H. Bolcskei, "An overview of MIMO communications - a key to gigabit wireless," *Proceedings of the IEEE*, vol. 92, no. 2, pp. 198–218, February 2004.

[112] B. A. Bjerke and J. G. Proakis, "Multiple-antenna diversity techniques for transmission over fading channels," in *Wireless Communications and Networking Conference, 1999. WCNC. 1999 IEEE*, vol. 3, pp. 1038–1042.

[113] G. J. Foschini, "Layered space-time architecture for wireless communication in a fading environment when using multi-element antennas," *Bell Labs Technical Journal*, vol. 1, no. 2, pp. 41–59, Autumn 1996.

[114] M. Munster and L. Hanzo, "Parallel-interference-cancellation-assisted decision-directed channel estimation for OFDM systems using multiple transmit antennas," *IEEE Transactions on Wireless Communications*, vol. 4, no. 5, pp. 2148–2162, September 2005.

[115] S. M. Alamouti, "A simple transmit diversity technique for wireless communications," *IEEE Journal on Selected Areas in Communications*, vol. 16, no. 8, pp. 1451–1458, October 1998.

[116] L. Tong-Hooi and L. Hanzo, "Space-time trellis and space-time block coding versus adaptive modulation and coding aided OFDM for wideband channels," *IEEE Transactions on Vehicular Technology*, vol. 55, no. 1, pp. 173–187, January 2006.

[117] V. Tarokh, H. Jafarkhani, and A. R. Calderbank, "Space-time block codes from orthogonal designs," *IEEE Transactions on Information Theory*, vol. 45, no. 5, pp. 1456–1467, July 1999.

[118] L. Hanzo, T. H. Liew, and B. L. Yeap, *Turbo Coding, Turbo Equalisation and Space-Time Coding for Transmission Over Fading Channels.* Piscataway, NJ: IEEE Press/Wiley, 2002.

[119] V. Tarokh, N. Seshadri, and A. R. Calderbank, "Space-time codes for high data rate wireless communication: performance criterion and code construction," *IEEE Transactions on Information Theory*, vol. 44, no. 2, pp. 744–765, March 1998.

[120] L. Hanzo, L.-L. Yang, E.-L. Kuan, and K. Yen, *Single- and Multi-Carrier DS-CDMA: Multi-User Detection, Space-Time Spreading, Synchronisation and Standards.* Piscataway, NJ:: IEEE Press/Wiley, 2003.

[121] Y. Lie-Liang and L. Hanzo, "Performance of broadband multicarrier DS-CDMA using space-time spreading-assisted transmit diversity," *IEEE Transactions on Wireless Communications*, vol. 4, no. 3, pp. 885–894, May 2005.

[122] J. Blogh and L. Hanzo, *Third-Generation Systems and Intelligent Networking.* Piscataway, NJ: IEEE Press/Wiley, 2002.

[123] A. Paulraj, *Introduction to Space-Time Wireless Communications.* Cambridge University Press, 2003.

[124] P. W. Wolniansky, G. J. Foschini, G. D. Golden, and R. A. Valenzuela, "V-BLAST: an architecture for realizing very high data rates over the rich-scattering wireless channel," in *Signals, Systems, and Electronics, 1998. ISSSE 98. 1998 URSI International Symposium on*, pp. 295–300.

[125] G. D. Golden, C. J. Foschini, R. A. Valenzuela, and P. W. Wolniansky, "Detection algorithm and initial laboratory results using V-BLAST space-time communication architecture," *Electronics Letters*, vol. 35, no. 1, pp. 14–16, January 1999.

[126] G. B. Giannakis, Z. Liu, X. Ma, and S. Zhou, *Space-Time Coding for Broadband Wireless Communications.* John Wiley & Sons Inc, 2007.

[127] J. Winters, "Optimum combining in digital mobile radio with cochannel interference," *IEEE Journal on Selected Areas in Communications*, vol. 2, no. 4, pp. 528–539, July 1984.

[128] J. Winters, "On the capacity of radio communication systems with diversity in a rayleigh fading environment," *IEEE Journal on Selected Areas in Communications*, vol. 5, no. 5, pp. 871–878, June 1987.

[129] J. H. Winters, "Wireless PBX/LAN system with optimum combining," Patent 4 639 914, 01 27, 1987.

[130] J. H. Winters, "Optimum combining for indoor radio systems with multiple users," *IEEE Transactions on Communications*, vol. 35, no. 11, pp. 1222–1230, June 1987.

[131] J. Salz, "Digital transmission over cross-coupled linear channels," *AT&T Technical Journal*, vol. 64, pp. 1147–1159, Aug. 1985.

[132] A. Duel-Hallen, "Equalizers for multiple input/multiple output channels and PAM systems with cyclostationary input sequences," *IEEE Journal on Selected Areas in Communications*, vol. 10, no. 3, pp. 630–639, April 1992.

[133] R. Cheng and S. Verdu, "Gaussian multiaccess channels with ISI: capacity region and multiuser water-filling," *IEEE Transactions on Information Theory*, vol. 39, no. 3, pp. 773–785, May 1993.

[134] J. H. Winters, J. Salz, and R. D. Gitlin, "The impact of antenna diversity on the capacity of wireless communication systems," *IEEE Transactions on Communications*, vol. 42, no. 234, pp. 1740–1751, April 1994.

[135] J. Yang and S. Roy, "On joint transmitter and receiver optimization for multiple-input-multiple-output (MIMO) transmission systems," *IEEE Transactions on Communications*, vol. 42, no. 12, pp. 3221–3231, December 1994.

[136] J. Yang and S. Roy, "Joint transmitter-receiver optimization for multi-input multi-output systems with decision feedback," *IEEE Transactions on Information Theory,*, vol. 40, no. 5, pp. 1334–1347, September 1994.

[137] J. Winters and J. Salz, "Upper bounds on the bit error rate of optimum combining in wireless systems," in *Vehicular Technology Conference, 1994 IEEE 44th*, vol. 2, 1994, pp. 942–946.

[138] J. H. Winters, ""The diversity gain of transmit diversity in wireless systems with Rayleigh fading"," *IEEE Transactions on Vehicular Technology*, vol. 47, no. 1, pp. 119–123, February 1998.

[139] B. Lu and W. Xiaodong, "Iterative receivers for multiuser space-time coding systems," *IEEE Journal on Selected Areas in Communications*, vol. 18, no. 11, pp. 2322–2335, November 2000.

[140] K. Sun-Yuan, Y. Wu, and Z. Xinying, "Bezout space-time precoders and equalizers for MIMO channels," *IEEE Transactions on Signal Processing*, vol. 50, no. 10, pp. 2499–2514, October 2002.

[141] F. Petre, G. Leus, L. Deneire, M. Engels, M. Moonen, and H. De Man, "Space-time block coding for single-carrier block transmission DS-CDMA downlink," *IEEE Journal on Selected Areas in Communications*, vol. 21, no. 3, pp. 350–361, April 2003.

[142] Z. Lijun, G. Lin, Q. Yantao, and Z. Wenjun, "Obtaining diversity gain for DTV by using MIMO structure in SFN," *IEEE Transactions on Broadcasting*, vol. 50, no. 1, pp. 83–90, March 2004.

[143] Z. Xu and R. D. Murch, "Layered space-frequency equalization in a single-carrier MIMO system for frequency-selective channels," *IEEE Transactions on Wireless Communications*, vol. 3, no. 3, pp. 701–708, May 2004.

[144] M. R. McKay and I. B. Collings, "Capacity and performance of MIMO-BICM with zero-forcing receivers," *IEEE Transactions on Communications*, vol. 53, no. 1, pp. 74–83, January 2005.

[145] B. Balakumar, S. Shahbazpanahi, and T. Kirubarajan, "Joint MIMO channel tracking and symbol decoding using Kalman filtering," *IEEE Transactions on Signal Processing*, vol. 55, no. 12, pp. 5873–5879, December 2007.

[146] T. Koike-Akino, "Optimum-weighted RLS channel estimation for rapid fading MIMO channels," *IEEE Transactions on Wireless Communications 7(11)*, pp. 4248–4260, March 2008.

[147] K. Yau Hee and D. P. Taylor, "MIMO receiver using reduced complexity sequence estimation with channel estimation and tracking," *IEEE Transactions on Vehicular Technology*, vol. 58, no. 2, pp. 682–691, February 2009.

[148] C. Yen-Chih and Y.-T. Su, "MIMO channel estimation in correlated fading environments," *IEEE Transactions on Wireless Communications*, vol. 9, no. 3, pp. 1108–1119, March 2010.

[149] R. Arablouei and K. Dogancay, "Modified RLS algorithm with enhanced tracking capability for MIMO channel estimation," *Electronics Letters*, vol. 47, no. 19, pp. 1101–1103, September 2011.

[150] M. Rupp, "Robust design of adaptive equalizers," *IEEE Transactions on Signal Processing*, vol. 60, no. 4, pp. 1612–1626, April 2012.

[151] C. Dubuc, D. Starks, T. Creasy, and H. Yong, "A MIMO-OFDM prototype for next-generation wireless WANs," *IEEE Communications Magazine*, vol. 42, no. 12, pp. 82–87, December 2004.

[152] A. van Zelst and T. C. W. Schenk, "Implementation of a MIMO OFDM-based wireless LAN system," *IEEE Transactions on Signal Processing*, vol. 52, no. 2, pp. 483–494, February 2004.

[153] Y. Li, N. Seshadri, and S. Ariyavisitakul, "Channel estimation for OFDM systems with transmitter diversity in mobile wireless channels," *IEEE Journal on Selected Areas in Communications*, vol. 17, no. 3, pp. 461–471, March 1999.

[154] R. S. Blum, L. Ye, J. H. Winters, and Y. Qing, "Improved space-time coding for MIMO-OFDM wireless communications," *IEEE Transactions on Communications*, vol. 49, no. 11, pp. 1873–1878, November 2001.

[155] Y. Li, "Simplified channel estimation for OFDM systems with multiple transmit antennas," *IEEE Transactions on Wireless Communications*, vol. 1, no. 1, pp. 67–75, January 2002.

[156] H. Bolcskei, D. Gesbert, and A. J. Paulraj, "On the capacity of OFDM-based spatial multiplexing systems," *IEEE Transactions on Communications*, vol. 50, no. 2, pp. 225–234, February 2002.

[157] R. Piechocki, P. Fletcher, A. Nix, N. Canagarajah, and J. McGeehan, "A measurement based feasibility study of space-frequency MIMO detection and decoding techniques for next generation wireless LANs," *IEEE Transactions on Consumer Electronics*, vol. 48, no. 3, pp. 732–737, August 2002.

[158] A. Doufexi, M. Hunukumbure, A. Nix, M. Beach, and S. Armour, "COFDM performance evaluation in outdoor MIMO channels using space/ polarisation-time processing techniques," *Electronics Letters*, vol. 38, no. 25, pp. 1720–1721, July 2002.

[159] H. Bolcskei, M. Borgmann, and A. J. Paulraj, "Impact of the propagation environment on the performance of space-frequency coded MIMO-OFDM," *IEEE Journal on Selected Areas in Communications*, vol. 21, no. 3, pp. 427–439, April 2003.

[160] I. Barhumi, G. Leus, and M. Moonen, "Optimal training design for MIMO OFDM systems in mobile wireless channels," *IEEE Transactions on Signal Processing*, vol. 51, no. 6, pp. 1615–1624, June 2003.

[161] G. Leus and M. Moonen, "Per-tone equalization for MIMO OFDM systems," *IEEE Transactions on Signal Processing*, vol. 51, no. 11, pp. 2965–2975, November 2003.

[162] R. J. Piechocki, A. R. Nix, J. P. McGeehan, and S. M. D. Armour, "Joint blind and semi-blind detection and channel estimation," *IEE Proceedings - Communications*, vol. 150, no. 6, pp. 419–426, December 2003.

[163] S. Myeongchoel, L. Hakju, and L. Chungyong, "Enhanced channel-estimation technique for MIMO-OFDM systems," *IEEE Transactions on Vehicular Technology*, vol. 53, no. 1, pp. 261–265, January 2004.

[164] M. R. G. Butler and I. B. Collings, "A zero-forcing approximate log-likelihood receiver for MIMO bit-interleaved coded modulation," *IEEE Communications Letters*, vol. 8, no. 2, pp. 105–107, February 2004.

[165] Y. Zeng and T.-S. Ng, "A semi-blind channel estimation method for multiuser multiantenna OFDM systems," *IEEE Transactions on Signal Processing*, vol. 52, no. 5, pp. 1419–1429, May 2004.

[166] B. Myung-Sun, K. Mi-Jeong, Y. Young-Hwan, and S. Hyoung-Kyu, "Semi-blind channel estimation and PAR reduction for MIMO-OFDM system with multiple antennas," *IEEE Transactions on Broadcasting*, vol. 50, no. 4, pp. 414–424, December 2004.

[167] Y. Hongwei, "A road to future broadband wireless access: MIMO-OFDM-based air interface," *IEEE Communications Magazine*, vol. 43, no. 1, pp. 53–60, January 2005.

[168] X. Ma, O. Mi-Kyung, G. B. Giannakis, and P. Dong-Jo, "Hopping pilots for estimation of frequency-offset and multiantenna channels in MIMO-OFDM," *IEEE Transactions on Communications*, vol. 53, no. 1, pp. 162–172, January 2005.

[169] K. Kyeong Jin, Y. Jiang, R. A. Iltis, and J. D. Gibson, "A QRD-M/Kalman filter-based detection and channel estimation algorithm for MIMO-OFDM systems," *IEEE Transactions on Wireless Communications*, vol. 4, no. 2, pp. 710–721, March 2005.

[170] Q. Yantao, Y. Songyu, S. Pengcheng, and Z. Lijun, "Research on an iterative algorithm of LS channel estimation in MIMO OFDM systems," *IEEE Transactions on Broadcasting*, vol. 51, no. 1, pp. 149–153, March 2005.

[171] H. Bolcskei, "MIMO-OFDM wireless systems: basics, perspectives, and challenges," *IEEE Wireless Communications*, vol. 13, no. 4, pp. 31–37, August 2006.

[172] M. Cicerone, O. Simeone, and U. Spagnolini, "Channel estimation for MIMO-OFDM systems by modal analysis/filtering," *IEEE Transactions on Communications*, vol. 54, no. 11, pp. 2062–2074, November 2006.

[173] T. Kashima, K. Fukawa, and H. Suzuki, "Adaptive MAP receiver via the EM algorithm and message passings for MIMO-OFDM mobile communications," *IEEE Journal on Selected Areas in Communications*, vol. 24, no. 3, pp. 437–447, March 2006.

[174] L. Tingting, W. Mao, L. Yan, S. Feng, W. Jianxin, S. Weixin, and C. Qian, "A minimum-complexity high-performance channel estimator for MIMO-OFDM communications," *IEEE Transactions on Vehicular Technology*, vol. 59, no. 9, pp. 4634–4639, November 2010.

[175] Y. Daejung and M. Jaekyun, "Soft-decision-driven channel estimation for pipelined turbo receivers," *IEEE Transactions on Communications*, vol. 59, no. 8, pp. 2141–2151, August 2011.

[176] C. Bor-Sen, Y. Chang-Yi, and L. Wei-Ji, "Robust fast time-varying multipath fading channel estimation and equalization for MIMO-OFDM systems via a fuzzy method," *IEEE Transactions on Vehicular Technology*, vol. 61, no. 4, pp. 1599–1609, May 2012.

[177] S. A. Ramprashad and G. Caire, "Cellular vs. network MIMO: A comparison including the channel state information overhead," in *Personal, Indoor and Mobile Radio Communications, 2009 IEEE 20th International Symposium on*, pp. 878–884.

[178] G. J. Foschini, K. Karakayali, and R. A. Valenzuela, "Coordinating multiple antenna cellular networks to achieve enormous spectral efficiency," *IEE Proceedings - Communications*, vol. 153, no. 4, pp. 548–555, August 2006.

[179] D. Gesbert, M. Kountouris, R. W. Heath, C. byoung Chae, and T. Salzer, "From single user to multiuser communications: Shifting the MIMO paradigm," *IEEE Sig. Proc. Magazine*, 2007.

[180] M. Sann Maw and S. Iwao, "Efficient resource allocation for multiuser MIMO-OFDM uplink system to guarantee the proportional data rate fairness among

users in a system," in *Access Spaces (ISAS), 2011 1st International Symposium on*, pp. 132–137.

[181] P. Vandenameele, L. V. D. Perre, and M. Engels, *Space Division Multiple Access for Wireless Local Area Networks*. London, U.K.: Kluwer, 2001.

[182] I. P. Kovalyov, *SDMA for Multipath Wireless Channels: Limiting Characteristics and Stochastic Models*, 1st ed. Berlin, Germany: Springer-Verlag, 2004, vol. 3-540-40225-X.

[183] P. Vandenameele, L. Van der Perre, M. Engels, B. Gyselinckx, and H. De Man, "A novel class of uplink of OFDM/SDMA algorithms: a statistical performance analysis," in *Vehicular Technology Conference, 1999. VTC 1999 - Fall. IEEE VTS 50th*, vol. 1, pp. 324–328 vol.1.

[184] P. Vandenameele, L. Van der Perre, M. G. E. Engels, B. Gyselinckx, and H. J. De Man, "A combined OFDM/SDMA approach," *IEEE Journal on Selected Areas in Communications*, vol. 18, no. 11, pp. 2312–2321, November 2000.

[185] P. Salvo Rossi, "On throughput of MIMO-OFDM systems with joint iterative channel estimation and multiuser detection under different multiple access schemes," *IEEE Communications Letters*, vol. 15, no. 8, pp. 831–833, August 2011.

[186] S. Thoen, L. Deneire, L. Van der Perre, M. Engels, and H. De Man, "Constrained least squares detector for OFDM/SDMA-based wireless networks," *IEEE Transactions on Wireless Communications*, vol. 2, no. 1, pp. 129–140, January 2003.

[187] A. T. Alastalo and M. Kahola, "Smart-antenna operation for indoor wireless local-area networks using OFDM," *IEEE Transactions on Wireless Communications*, vol. 2, no. 2, pp. 392–399, March 2003.

[188] S. Chen, G. Dai, and H. Tang, "Low complexity DFE for OFDM systems over time-varying channels," *IEEE Transactions on Consumer Electronics*, vol. 53, no. 2, May 2007.

[189] D. Zheng, S. Xuegui, J. Cheng, and N. C. Beaulieu, "Maximum likelihood based channel estimation for macrocellular OFDM uplinks in dispersive time-varying channels," *IEEE Transactions on Wireless Communications*, vol. 10, no. 1, pp. 176–187, January 2011.

[190] M. Enescu, M. Sirbu, and V. Koivunen, "Recursive semi-blind equalizer for time-varying MIMO channels," in *Statistical Signal Processing, 2001. Proceedings of the 11th IEEE Signal Processing Workshop on*, 2001, pp. 289–292.

[191] L. Yongming, L. Hanwen, Y. Chongguang, and H. Jianguo, "Channel estimation using adaptive filters in MIMO-OFDM systems," in *Wireless Communications, Networking and Mobile Computing, 2006. WiCOM 2006.International Conference on*, pp. 1–4.

[192] B. Widrow and M. Hoff, *Adaptive switching circuits*. MIT Press, 1988, pp. 123–134.

[193] B. Farhang-Boroujeny, *Adaptive filters: theory and applications*. Chichester, England: John Wiley & Sons, 1999.

[194] Y. Yapici and A. O. Yilmaz, "Low-complexity iterative channel estimation and tracking for time-varying multi-antenna systems," in *Personal, Indoor and Mobile Radio Communications, 2009 IEEE 20th International Symposium on*, 2009, pp. 1317–1321.

[195] S. J. Orfanidis, *Optimum Signal Processing: An Introduction*. New York: Mc-Graw Hill, 1988.

[196] J. K. Cavers, "An analysis of pilot symbol assisted modulation for rayleigh fading channels [mobile radio]," *IEEE Transactions on Vehicular Technology*, vol. 40, no. 4, pp. 686–693, November 1991.

[197] L. Tong, B. M. Sadler, and M. Dong, "Pilot-assisted wireless transmissions: general model, design criteria, and signal processing," *IEEE Signal Processing Magazine*, vol. 21, no. 6, pp. 12–25, November 2004.

[198] B. Hassibi and B. M. Hochwald, "How much training is needed in multiple-antenna wireless links?" *IEEE Transactions on Information Theory*, vol. 49, no. 4, pp. 951–63, April 2003.

[199] B. Jong-Seob and S. Jong-Soo, "Efficient pilot patterns and channel estimations for MIMO-OFDM systems," *IEEE Transactions on Broadcasting*, vol. 58, no. 4, pp. 648–653, December 2012.

[200] J.-J. van de Beek, O. Edfors, M. Sandell, S. K. Wilson, and P. O. Borjesson, "On channel estimation in OFDM systems," in *Vehicular Technology Conference, 1995 IEEE 45th*, vol. 2, pp. 815–819 vol.2.

[201] O. Edfors, M. Sandell, J. J. van de Beek, S. K. Wilson, and P. O. Borjesson, "OFDM channel estimation by singular value decomposition," *IEEE Transactions on Communications*, vol. 46, no. 7, pp. 931–939, July 1998.

[202] H. Meng-Han and W. Che-Ho, "Channel estimation for OFDM systems based on comb-type pilot arrangement in frequency selective fading channels," *IEEE Transactions on Consumer Electronics*, vol. 44, no. 1, pp. 217–225, January 1998.

[203] H. Hailang and Z. Ying, "A simplified channel estimation method based on optimal pilots design for MIMO-OFDM systems," in *Computer and Information Technology (CIT), 2012 IEEE 12th International Conference on*, pp. 623–626.

[204] S. Coleri, M. Ergen, A. Puri, and A. Bahai, "Channel estimation techniques based on pilot arrangement in OFDM systems," *IEEE Transactions on Broadcasting*, vol. 48, no. 3, pp. 223–229, September 2002.

[205] N. Liu, Y. Yuan, K. Xia, and Z. Zhang, "Study on channel estimation technology in OFDM system," in *Artificial Intelligence, 2009. JCAI '09. International Joint Conference on*, pp. 773–776.

[206] F. Pena-Campos, R. Carrasco-Alvarez, O. Longoria-Gandara, and R. Parra-Michel, "Estimation of fast time-varying channels in OFDM systems using two-dimensional prolate," *IEEE Transactions on Wireless Communications*, vol. 12, no. 2, pp. 898–907, February 2013.

[207] W. G. Jeon, P. Kyung Hyun, and Y. S. Cho, "An efficient channel estimation technique for OFDM systems with transmitter diversity," in *Personal, Indoor and Mobile Radio Communications, 2000. PIMRC 2000. The 11th IEEE International Symposium on*, vol. 2, pp. 1246–1250 vol.2.

[208] S. Sumei, I. Wiemer, C. K. Ho, and T. T. Tjhung, "Training sequence assisted channel estimation for MIMO OFDM," in *Wireless Communications and Networking, 2003. WCNC 2003. 2003 IEEE*, vol. 1, pp. 38–43 vol.1.

[209] H. Die, Y. Luxi, and H. Zhenya, "Time-varying channel estimation for MIMO OFDM systems," in *Intelligent Multimedia, Video and Speech Processing, 2004. Proceedings of 2004 International Symposium on*, pp. 93–96.

[210] J. Gao, X. Zhu, Y. Wu, and A. K. Nandi, "Kalman smoothing-based adaptive frequency domain channel estimation for uplink multiple-input multiple-output

orthogonal frequency division multiple access systems," *Communications, IET*, vol. 5, no. 2, pp. 199–208, 2011.

[211] S. Borching and P. P. Vaidyanathan, "Generalized subspace-based algorithms for blind channel estimation in cyclic prefix systems," in *Signals, Systems and Computers, 2006. ACSSC '06. Fortieth Asilomar Conference on*, pp. 1796–1800.

[212] S. Yatawatta and A. P. Petropulu, "Blind channel estimation in MIMO OFDM systems with multiuser interference," *IEEE Transactions on Signal Processing*, vol. 54, no. 3, pp. 1054–1068, March 2006.

[213] S. Zhou and G. B. Giannakis, "Finite-alphabet based channel estimation for OFDM and related multicarrier systems," *IEEE Transactions on Communications*, vol. 49, no. 8, pp. 1402–1414, August 2001.

[214] C. Ning and G. T. Zhou, "A superimposed periodic pilot scheme for semi-blind channel estimation of OFDM systems," in *Digital Signal Processing Workshop, 2002 and the 2nd Signal Processing Education Workshop. Proceedings of 2002 IEEE 10th*, pp. 362–365.

[215] X. Changhui, L. Hong, and C. Shuai, "Semi-blind MIMO-OFDM channel estimation based on ICA and pilot carriers," in *Signal Processing, Communications and Computing (ICSPCC), 2011 IEEE International Conference on*, pp. 1–4.

[216] V. D. Luong, "Optimal training sequence design for MIMO-OFDM in spatially correlated fading environments," Master's thesis, University of New South Wales, Oct 2009.

[217] W. Kuo-Guan and W. Jer-An, "Efficient decision-directed channel estimation for OFDM systems with transmit diversity," *IEEE Communications Letters*, vol. 15, no. 7, pp. 740–742, July 2011.

[218] R.S.Ganesh and J. Kumari, "A survey on channel estimation techniques in MIMO-OFDM mobile communication systems," *International Journal of Scientific & Engineering Research*, vol. 4, no. 5, May 2013.

[219] M. Honglei and M. J. Juntti, "Space-time MMSE channel estimation for MIMO-OFDM system with spatial correlation," in *Vehicular Technology Conference, 2004. VTC 2004-Spring. 2004 IEEE 59th*, vol. 3, pp. 1806–1810 Vol.3.

[220] A. Gomaa, C. Yuejie, N. Al-Dhahir, and R. Calderbank, "On training signal design for multi-user MIMO-OFDM: Performance analysis and tradeoffs," in *Vehicular Technology Conference (VTC Fall), 2011 IEEE*, pp. 1–5.

[221] Z. Jiankang, L. Hanzo, and M. Xiaomin, "Joint decision-directed channel and noise-variance estimation for MIMO OFDM/SDMA systems based on expectation-conditional maximization," *IEEE Transactions on Vehicular Technology*, vol. 60, no. 5, pp. 2139–2151, June 2011.

[222] R. Hidayat, A. F. Isnawati, and B. Setiyanto, "Channel estimation in MIMO-OFDM spatial multiplexing using least square method," in *Intelligent Signal Processing and Communications Systems (ISPACS), 2011 International Symposium on*, pp. 1–5.

[223] M. Morelli and U. Mengali, "A comparison of pilot-aided channel estimation methods for OFDM systems," *IEEE Transactions on Signal Processing*, vol. 49, no. 12, pp. 3065–3073, December 2001.

[224] H. Krouma, M. Benslama, and F. Othmani-Marabout, "Low rank MMSE channel estimation in MIMO-OFDM systems," in *Innovative Computing Technology (INTECH), 2012 Second International Conference on*, pp. 279–284.

[225] R. Negi and J. Cioffi, "Pilot tone selection for channel estimation in a mobile OFDM system," *IEEE Transactions on Consumer Electronics*, vol. 44, no. 3, pp. 1122–1128, August 1998.

[226] T. Lang, "Blind sequence estimation," *IEEE Transactions on Communications*, vol. 43, no. 12, pp. 2986–2994, December 1995.

[227] A. Vosoughi and A. Scaglione, "Channel estimation for precoded MIMO systems," in *Statistical Signal Processing, 2003 IEEE Workshop on*, pp. 442–445.

[228] E. Karami and M. Shiva, "Maximum likelihood MIMO channel tracking," in *Vehicular Technology Conference, 2004. VTC 2004-Spring. 2004 IEEE 59th*, vol. 2, pp. 876–879 Vol.2.

[229] K. Molnar, G. Bottomley, and R. Ramesh, "Method and apparatus for channel tracking," Patent 6,084,929, 07 04, 2000.

[230] T. Chao-Cheng and B. Champagne, "Blind recursive subspace-based identification of time-varying wideband MIMO channels," *IEEE Transactions on Vehicular Technology*, vol. 61, no. 2, pp. 662–674, February 2012.

[231] E. Yakhnich, "Block based channel tracking using weighted recursive least squares," Patent US 7 050 513, 05 23, 2006.

[232] K. Hyosung and J. K. Tugnait, "Data detection for doubly-selective MIMO channels using decision-directed channel tracking and exponential basis models," in *Global Telecommunications Conference, 2008. IEEE GLOBECOM 2008. IEEE*, pp. 1–6.

[233] H. Hijazi, E. P. Simon, M. Lienard, and L. Ros, "Channel estimation for MIMO-OFDM systems in fast time-varying environments," in *Communications, Control & Signal Processing (ISCCSP), 2010 4th International Symposium on*, pp. 1–6.

[234] S. Gifford, C. Bergstrom, and S. Chuprun, "Adaptive and linear prediction channel tracking algorithms for mobile OFDM-MIMO applications," in *Military Communications Conference, 2005. MILCOM 2005. IEEE*, pp. 1298–1302 Vol. 2.

[235] H. Schmidt, V. Kühn, K.-D. Kammeyer, R. Rueckriem, and S. Fechtel, "Channel tracking in wireless OFDM systems," in *World Multiconference on Systemics, Cybernetics and Informatics (SCI 01)*. IIIS.

[236] W. H. Tranter, K. S. Shanmugan, T. S. Rappaport, and K. L. Kosbar, *Modeling and simulating time-varying systems*. Prentice Hall, 2003.

[237] Channel modeling and RF impairments. Accessed: 13/03/2013. [Online]. Available: http://www.mathworks.com.au/help/comm/ug/fading-channels.html

[238] P. F. Driessen, "Prediction of multipath delay profiles in mountainous terrain," *IEEE Journal on Selected Areas in Communications*, vol. 18, no. 3, pp. 336–346, March 2000.

[239] S. U. H. Qureshi, "Adaptive equalization," *Proceedings of the IEEE*, vol. 73, no. 9, pp. 1349–1387, 1985.

[240] N. W. K. Lo, D. D. Falconer, and A. U. H. Sheikh, "Adaptive equalizer MSE performance in the presence of multipath fading, interference and noise," in *Vehicular Technology Conference, 1995 IEEE 45th*, vol. 1, pp. 409–413 vol.1.

[241] B. Widrow, "Adaptive filter, 1: Fundamentals," Stanford Electronics Laboratory, Tech. Rep., 1966.

[242] S. Haykin, *Adaptive Filter Theory*. Englewood Cliffs, NJ, USA: Prentice-Hall, 1996.

[243] J. Proakis, *Digital Communications*. New York: McGraw-Hill, 1989.

Index